UNIVERSITY OF CALIFORNIA, SAN DIEGO

Overcoming Biological Barriers: Synthesis and Evaluation of Molecular Transporters

A dissertation submitted in partial satisfaction of the requirements for the degree Doctor of Philosophy

in

Chemistry

by

Kristina Moriah Hamill

Committee in Charge:

Professor Yitzhak Tor, Chair
Professor Jeffrey Esko
Professor Kamil Godula
Professor Andrew Kummel
Professor Jerry Yang

2016

The dissertation of Kristina Moriah Hamill is approved, and it is acceptable in quality and form for publication on microfilm and electronically:

Chair

University of California, San Diego

2016

DEDICATION

To my amazing parents, Wayne and Jan, and to my best friend & love of my life, Ryan.

TABLE OF CONTENTS

Signature Page iii

Dedication iv

Table of Contents v

List of Figures viii

List of Schemes x

List of Tables xi

List of Spectra xii

Acknowledgements xiii

Vita xv

Abstract of the Dissertation xvi

Chapter 1: Discovery and Development of Guanidinium-Rich Molecular Transporters 1

1.1 Introduction 1

1.2 The Discovery of Guanidinium-Rich Molecular Transporters 5

1.3 Interactions of the Guanidinium Group with the Cell Surface 7

1.4 Endocytosis Mechanisms of Guanidinium-Rich Transporters 11

1.5 Non-Peptidic Guanidinium-Rich Molecular Transporters 14

1.5.1 Linear Guanidinium-Rich Molecular Transporters 14

1.5.2 Branched Guanidinium-Rich Molecular Transporters 17

1.5.3 Guanidinoglycosides 18

1.5.4 Additional Carbohydrate-Based Guanidinium-Rich Molecular Transporters 21

1.5.5 Oligomerization-Based Guanidinium-Rich Molecular Transporters 25

1.6 Summary and Outlook 31

1.7 References 34

Chapter 2: Polymyxins Facilitate Entry into Mammalian Cells 44

2.1 Introduction 44

2.2 Results 46

2.3 Discussion 57

2.4 Conclusions 63

2.5 Experimental 64

2.6 References 86

Chapter 3: GNeo-Modified Liposomes Deliver Active Lysosomal Enzyme 91

3.1 Introduction 91

3.2 Results 93

3.3 Discussion 101

3.4 Conclusions 105

3.5 Experimental 106

3.6 References 118

Chapter 4: Length Matters: Effects of Linker on Cellular Uptake of Guanidinylated Neomycin 123

4.1 Introduction 123

4.2 Results and Discussion 125

4.3 Conclusions 130

4.4 Experimental 130

4.5 References 152

Chapter 5: Synthesis of Cell-Penetrating Guanidinylated Neomycin Oligomers via ROMP 155

5.1 Introduction 155

5.2 Results and Discussion 157

5.3 Conclusions and Outlook 166

5.4 Experimental 168

5.5 References 175

LIST OF FIGURES

Figure 1.1. Structures of guanidinium-rich peptides 7

Figure 1.2. A heparan sulfate octasaccharide subunit.....8

Figure 1.3. Interactions of guanidinium with cell surface components.....9

Figure 1.4. Mechanisms of cellular uptake.....12

Figure 1.5. Structures of linear, guanidinium-rich molecular transporters.....16

Figure 1.6. Examples of branched and dendrimeric guanidinium-rich transporters.....18

Figure 1.7. Representative structures of aminoglycosides (Tob and Neo) and guanidinoglycosides (GTob and GNeo) 19

Figure 1.8. Structures of various guanidinoneomycin derivatives 20

Figure 1.9. Representative *scyllo*-inositol transporter 22

Figure 1.10. Sorbitol-based transporters.....24

Figure 1.11. Disaccharide-based transporters.....25

Figure 1.12. Synthesis of guanidinium-rich transporters using ROMP.....27

Figure 1.13. Oxanorbornene-based guanidinium-rich transporters 28

Figure 1.14. Organocatalytic synthesis of guanidinium-rich transporters.....30

Figure 1.15. Poly(disulfide)-based transporters.....31

Figure 2.1. Structures of bTob and bGTob (a) bArg8 (b) and PMB and GPMB (c).....49

Figure 2.2. Cellular uptake and cell viability of bPMB and bGPMB.....51

Figure 2.3. Cellular uptake control with GPMB and PMB.....52

Figure 2.4. Cellular uptake and binding in wild-type and mutant CHO cells 53

Figure 2.5. Cellular uptake in the presence of inhibitors.....54

Figure 2.6. Intracellular localization of bGPMB and bPMB 55

Figure 2.7. Cellular uptake of ST-Cy5.....55

Figure 2.8. Delivery of saporin.....56

Figure 2.9. Cellular uptake of PMB and GPMB liposomes 57
Figure 2.10. Analytical HPLC trace for bArg8.....82
Figure 2.11. Analytical HPLC trace for PMB 82
Figure 2.12 Analytical HPLC trace for GPMB 82
Figure 3.1. Methods for incorporating GNeo into liposomes.....96
Figure 3.2. Characterization of GNeosomes.....97
Figure 3.3. Cellular uptake of Cy5-containing GNeosomes.....98
Figure 3.4. Liposomal delivery of IDUA.....100
Figure 3.5. Glycosaminoglycan turnover using IDUA-containing GNeosomes 101
Figure 3.6. Cy-5 encapsulation efficiency 116
Figure 3.7. Protein gel of IDUA-containing liposomes.....116
Figure 4.1. Structures of biotinylated-GNeo transporters.....125
Figure 4.2. HPLC traces of biotinylated GNeo transporters.....127
Figure 4.3. FPLC integrations of GNeo-biotin-ST conjugates 128
Figure 4.4. Cellular uptake of GNeo-biotin-ST conjugates.....130
Figure 4.5. FPLC chromatograms of GNeo-biotin-ST conjugates 151
Figure 5.1. ^{1}H NMR (500 MHz) of biotin-oligoGNeo in D_2O.....162
Figure 5.2. Structures of GNeo-monomers.....163
Figure 5.3. Cellular uptake and binding of biotin-GNeo monomer and oligomer 164
Figure 5.4. Cellular uptake of fluorescein-GNeo monomer and oligomer 165
Figure 5.5. Cellular binding of fluorescein-GNeo monomer and oligomer 166

LIST OF SCHEMES

Scheme 2.1. Retrosynthesis of biotinylated PMB and GPMB 47

Scheme 2.2. Synthesis of Boc-protected and Boc-guanidinylated PMBN 48

Scheme 2.3. Synthesis of biotinylated linker 48

Scheme 2.4. Synthesis of polymyxin and guanidinopolymyxin transporters 49

Scheme 2.5. Synthesis of bGTob and bTob 76

Scheme 3.1. Synthesis of GNeo-lipids 94

Scheme 3.2. Synthesis of GNeo-NHS 95

Scheme 3.3. Synthesis of oleyl-GNeo 107

Scheme 3.4. Synthesis of di-oleyl-GNeo 109

Scheme 3.5. Synthesis of NHS-N_3 linker and GNeo-NHS 111

Scheme 4.1. Combinatorial synthesis of biotinylated GNeo carriers 126

Scheme 4.2. Synthesis of diazide linker intermediates 131

Scheme 4.3. Synthesis of azide-amino linker intermediates 132

Scheme 4.4. Synthesis of biotin linkers 133

Scheme 4.5. Synthesis of BocNeo-alkyne intermediates 134

Scheme 4.6. Synthesis of Neo-alkyne intermediates 136

Scheme 4.7. Synthesis of BocGNeo-alkyne intermediates 137

Scheme 4.8. Synthesis of biotin-linker-GNeo derivatives 139

Scheme 4.9. Synthesis of GNeo-biotin with no linker 148

Scheme 5.1. Synthesis of norbornene-BocGNeo monomer 158

Scheme 5.2. Synthesis of biotin, FITC, and BODIPY-containing terminating agents 160

Scheme 5.3. Synthesis of azide, boc-hydroxylamine, and Cy3-containing terminating agents 160

Scheme 5.4. General synthesis of GNeo oligomers 161

LIST OF TABLES

Table 2.1. Physicochemical characterization of PMB and GPMB liposomes.....57

Table 5.1. ^{1}H NMR characterization of GNeo-oligomers 162

LIST OF SPECTRA

Spectrum 2.1. ^{1}H NMR of PMB-biotin 79

Spectrum 2.2. ^{13}C NMR of PMB-biotin 80

Spectrum 2.3. ^{1}H NMR of GPMB-biotin 81

Spectrum 2.4. ^{13}C NMR of GPMB-biotin 81

Spectrum 2.5. ^{1}H NMR of GPMB 83

ACKNOWLEDGEMENTS

I am very grateful for all the individuals who have helped me grow as a scientist and as a person throughout my graduate career. I would especially like to thank my advisor Professor Yitzhak Tor for his invaluable mentorship, support, and patience. He is an incredible teacher and has pushed me to become a critical, scientific thinker. Thank you for giving me the opportunity to work in your lab and the freedom to figure things out for myself.

I also want to thank all the many members of the Tor lab for being so helpful and supportive throughout my graduate career. I especially want to thank Dr. Dongwon Shin, Dr. Noam Freeman, and Dr. Ezequiel Wexselblatt for your guidance, helpful discussions, and always inviting me to join for coffee. I feel very fortunate to have shared a lab space with you all. I would also like to thank Dr. Ryan Weiss, Dr. Lisa McCoy, Patrycja Hopkins, and Dr. Rich Fair for being great labmates and even better friends. I don't know if I would have made it this far without our valuable lunch conversations.

I would like to thank and acknowledge Professor Jeffrey Esko for allowing me to work in his lab while I learned cell biology and for his guidance and mentorship. In his lab, Dr. Wenyong Tong was incredibly helpful and patient while teaching me cell biology and helping me with all the enzymatic assays.

I acknowledge Dr. Yongxuan Su (UCSD MS Facility) for his assistance with the mass spectrometry instruments and Dr. Anthony Mrse (UCSD NMR Facility) for always being available to assist with the NMR instruments or to talk about football.

I also want to thank my amazing network of family (especially Mom and Dad) and friends, both near (specifically Sara Bell for all of the things) and far (WT4life). Without your love and support, I would not be where I am today.

Chapter 2 is a full reprint from: Hamill, K. M.; McCoy, L. S.; Wexselblatt, E.; Esko, J. D.; Tor, Y. Polymyxins Facilitate Entry into Mammalian Cells. *Chem. Sci*., (2016), DOI:10.1039/c6sc00488a. The dissertation author is the primary author and researcher of this work.

Chapter 3 is currently being prepared for submission for publication: Hamill, K.M.; Wexselblatt, E., Tong, W.; Esko, J. E.; Tor, Y. The dissertation author is the main author and researcher of this work.

Chapter 4 is currently being prepared for submission for publication: Hamill, K.M.; Wexselblatt, E., Hadidi. K.; Esko, J. E.; Tor, Y. The dissertation author is the co-main author and researcher of this work.

VITA

2007–2009	Teaching Assistant, James Madison University
2009	B.S. in Chemistry, James Madison University
2009–2014	Teaching Assistant, University of California, San Diego
2011	M.S. in Chemistry, University of California, San Diego
2016	Ph.D. in Chemistry, University of California, San Diego

PUBLICATIONS

Hamill, K.M.; Wexselblatt, E.; Tong, W.; Esko, J. D.; Tor, Y. Delivery of an Active Lysosomal Eznyme Using GNeosomes. *Submitted*.

Hamill, K. M.; McCoy, L. S.; Wexselblatt, E.; Esko, J. D.; Tor, Y. Polymyxins Facilitate Entry into Mammalian Cells. *Chem. Sci*. **2016**, DOI:10.1039/c6sc00488a.

LaDow, J. E.; Warnock, D. C.; Hamill, K. M.; Simmons, K. L.; Davis, R. W.; Schwantes, C. R.; Flaherty, D. C.; Willcox, J. A. L.; Wilson-Henjum, K.; Caran, K. L.; Minbiole, K. P. C.; Seifert, K. "Bicephalic Amphiphile Architecture Affects Antibacterial Activity" *Eur. J. Med. Chem*. **2011**, *46*, 4219.

Roszak, K. Z.; Torcivia, S. L.; Hamill, K. M.; Hill, A. R.; Radloff, K. R.; Crizer, D. M.; Middleton, A. M.; Caran, K. L. "Biscationic Bicephalic (Double-Headed) Amphiphiles with an Aromatic Spacer and a Single Hydrophobic Tail" *J. Colloid Interface Sci.* **2009**, *331*, 560.

ABSTRACT OF THE DISSERTATION

Overcoming Biological Barriers: Synthesis and Evaluation of Molecular Transporters

by

Kristina Moriah Hamill

Doctor of Philosophy in Chemistry

University of California, San Diego, 2016

Professor Yitzhak Tor, Chair

High molecular weight and highly-charged biomolecules are emerging as drugs with high selectivity and efficacy; however, new strategies are needed to improve their efficiency and targeted delivery in biological systems. One potential solution is the conjugation or association of the biologic with a molecular transporter.

Inspired by proteins, such as HIV-Tat, with cellular translocation abilities, numerous guanidinium-rich molecular transporters have been synthesized from a diverse range of nonpeptidic scaffolds. While their repertoire has expanded tremendously in the past two decades, new transporters can provide unique intracellular distributions, targeting effects, or pharmacological properties.

Polymyxin B is a cyclic polypeptide antibiotic containing five primary amines and a hydrophobic tail that has not been exploited as a delivery module. Here, we synthesized functionalized derivatives of polymyxin and its per-guanidinylated derivative and evaluated their cellular uptake in mammalian cells. Both polymyxin and its guanidinylated form effectively enter mammalian cells at nanomolar concentrations and can facilitate the cellular delivery of large biomolecules and liposomal assemblies.

Guanidinoglycosides are a non-oligomeric class of molecular transporters developed in our lab that permeate the cell membrane through heparan sulfate-dependent pathways at low nanomolar concentrations. To further advance guanidinoglycosides as transporters, guanidinylated neomycin (GNeo) derivatives containing different fatty acids were synthesized and incorporated into liposomes. A small molecule dye or a lysosomal enzyme were encapsulated in the liposomes and delivered to Chinese hamster ovary cells or human fibroblasts, respectively. Incorporation of stearyl- or di-oleyl-GNeo lipids into liposomes resulted in the greatest enhancement of uptake. The delivery of α-L-iduronidase, a lysosomal enzyme, was able to restore enzyme function in fibroblasts lacking endogenous enzyme. As an alternative approach to enhance GNeo as a molecular transporter, oligomers of GNeo were synthesized using ring-opening metathesis polymerization. The synthesis of the reactive monomer, formation of GNeo oligomers, and preliminary cellular

uptake studies are presented. In addition to using GNeo for new delivery systems, we also sought to explore the effect the linker connecting the cargo to the carrier has on conjugation and uptake. Varying the length and hydrophobic properties of the linker joining GNeo to biotin resulted in diverse conjugation efficiencies to streptavidin and differences in cellular uptake, highlighting the importance of the linker when designing and studying new molecular transporters.

Chapter 1:

Discovery and Development of Guanidinium-Rich Molecular Transporters

1.1 Introduction

Several biological barriers stand between the administration of a therapeutic agent and its final cellular destination and function. Biological barriers were designed by nature to compartmentalize, protect against foreign material, and selectively control what goes in and out. These barriers can be divided into epithelial, endothelial, elimination, and target cell barriers.[1] Epithelial barriers serve as both physical and biochemical barriers that prevent a potential drug from accessing the systemic circulation. If a drug enters the blood circulation, either by passing the epithelial barrier or by being directly administered into the systemic circulation, the endothelium acts as a barrier between the blood vessel and the surrounding tissue.[1] One of the most significant and selective endothelial barriers is the blood brain barrier (BBB). The BBB is composed of special endothelial cells connected by tight junctions, lacks fenestrations, and has low levels of pinocytic uptake, thus making it poorly penetrable by both small- and large- molecule drugs.[2] Elimination barriers include the liver and kidneys that can remove the drug from circulation and excrete it in the bile or urine. Lastly, once the drug reaches the target tissue, it must cross the cell membrane and target the desired organelle or cytosol.

In designing new drug candidates, the ability to overcome these barriers has to be considered. For orally administered, small molecule drugs, Lipinski's rule of five was

developed to guide medicinal chemists during drug design.[3] Generally, this means a log P less than +5, molecular mass less than 500 Da, no more than 10 hydrogen bond acceptors, and no more than 5 hydrogen bond donors. Compounds that fall into this narrow range of criteria should be polar enough to traverse the extracellular milieu but small and lipophilic enough to diffuse through the nonpolar membrane of a cell. Potential small molecule drugs that fall outside of this range must be formulated with various solvent mixtures and excipients or chemically modified to enhance absorption, distribution, metabolism, and excretion.

Within the last decade, the pharmaceutical industry has become increasingly interested in utilizing large biologics, such as proteins (e.g., enzymes and antibiodies)[4,5] and oligonucleotides,[6] as drugs.[7-9] The advantage of such drugs is their specificity and efficacy, which reduces off-target side-effects frequently seen with small molecule drugs. Biologics also have the potential to treat a variety of conditions of significant unmet medical need such as Alzheimer's disease, multiple sclerosis, Crohn's disease, and arthritis.[2,9] However, high-molecular weight and highly charged biomolecules usually have poor bioavailability, short half-lives, and are unable to traverse cellular membranes.[10] The strategies employed in the development of low-molecular weight drugs cannot be applied to the development of biologics; therefore, new delivery strategies are necessary to enhance or enable the therapeutic performance of such biologics on intracellular targets.

A majority of clinically approved biological drugs are administered via intravenous (IV) infusion or subcutaneous (SC) or intramuscular (IM) injection to avoid initial degradation and poor absorption in the GI tract. However, these delivery routes can be invasive and inconvenient, limited to concentrations with low viscosity for administration,

and do not provide localized treatment. They are also rapidly cleared from the body, thus requiring frequent injections. New delivery systems using various materials and chemical strategies have been developed to address these limitations.[10-12]

Modifications to the macromolecule can be applied to reduce renal clearance. For example, chemical modification with hydrophilic polymers, such as polyethylene glycol (PEG), can increase the hydrodynamic radius of the biologic and extend its circulating half-life.[13] The advantages of conjugating other polymers such as sialic acid[14] and hyaluronic acid[15] are also being investigated. Genetic constructs or fusion approaches are another method for creating modified proteins with longer half-lives. Genetic fusion of a protein with the Fc region of immunoglobulin G (IgG) facilitated binding to the neonatal Fc receptor on the endothelium.[16] Receptor-bound fusion proteins are internalized via endocytosis then recycled back to the cell membrane and released back into the blood, resulting in prolonged circulation times. Similarly, proteins can be fused to albumin and take advantage of its extended circulating half-life.[17,18] Alternatives and improvements to protein modification and genetic engineering continue to be investigated.

Sustained release formulations improve the controlled release and delivery of biologics while avoiding any chemical or fusion modification of the macromolecule. The main systems include biodegradable microparticles based on polymers such as poly(lactic-co-glycolic acid) (PLGA)[19], liquid gelling or self-assembling systems,[20] nanoparticles based on biodegradable polymers or lipids[21,22], and depot injections[23]. Microparticles can be used to encapsulate a protein or peptide for long-term delivery (1 week or longer) with sustained release of the drug. The chemical functionalities of the polymer affect encapsulation, biocompatibility, and protein release from the microparticle. The use of

nanoparticles composed of materials such as polymers, lipids, and dendrimers, have been studied for the delivery of biomolecules in the clinical and preclinical stages.

While promising and widely used, the above mentioned methods still require injections which can be inconvenient and undesirable. Implantable pumps are one method to control the rates and duration of drug delivery. Although a successful method for the delivery of insulin, the implantation of pumps can also be invasive and susceptible to infection.[24] Liquid jet injectors are another needle-free route of administration. Liquid jet injections work with currently approved injectable formulations but can cause occasional pain at the site of injection and variations in the amount of protein that is delivered.[25] Other routes of administration have also been investigated as alternatives to injections including pulmonary[26], nasal[27], oral[28], and transdermal[29,30]. The main limitation to delivering biomolecules through these routes continues to be poor distribution across biological barriers. Novel approaches, therefore, continue to be developed to overcome these barriers.

One method to improve the drug delivery problem is to conjugate or associate the biomolecule with a molecular transporter. Molecular transporters can be either covalently attached or non-covalently associated with target cargo that will enhance or enable intracellular delivery of the cargo. The approach can be applied to several of the techniques described above to improve intracellular delivery of otherwise impermeable cargo. Guanidinium-rich transporters (GRTs) represent a large class of delivery vehicles with various scaffolds, decorated with guanidinium groups, that can facilitate translocation across cellular membranes.[31-34] GRTs have been shown to deliver cargos including small molecules, imaging agents, metals, quantum dots, proteins, plasmids, and RNA, among others, both *in vitro* and *in vivo*.

1.2 The Discovery of Guanidinium-Rich Molecular Transporters

In 1988, it was discovered that the 86-amino acid protein Tat encoded by human immunodeficiency virus type 1 (HIV-1) could penetrate cells when added exogenously.[35,36] This was surprising as polar molecules such as proteins and peptides are typically unable to cross non-polar cell membranes. Further studies found that the cell-penetrating function of the protein was due to the basic arginine-rich region (RKKRRQRRR),[37-39] often referred to as Tat_{49-57} or the Tat 9-mer (Figure 1.1).[40] Additionally, the 60-amino acid peptide Antennapedia from *Drosophila* was also shown to enter nerve cells and translocate to the nucleus when added exogenously.[41] Subsequent studies indicated a 16-amino acid region, derived from the third helix of the protein and rich in basic and hydrophobic residues, was critical for uptake and is now referred to as Penetratin.[42]

Early investigation into the ability of Tat to transport other macromolecules into cells used a truncated version, Tat_{37-72}, chemically cross-linked to different proteins – β-galactosidase, horseradish peroxidase, RNase A, and *Pseudomonas* exotoxin III.[39,43] Tat was able to mediate the cytoplasmic delivery of all proteins in tissue culture. Intravenous injection of Tat-β-galactosidase into the tail vein of mice resulted in delivery to several tissues including the heart, liver, and spleen, primarily targeting cells surrounding the blood vessels. Together, this suggested early on the ability of cell-penetrating peptides to mediate the therapeutic delivery of biomolecules into living cells. The Tat 9-mer was then utilized to deliver a variety of other proteins into cells including E2 repressor that inhibits human papillomavirus type 16,[38] ovalbumin,[44] $p27^{kip1}$ and $p16^{INK4a}$ Cdk inhibitor proteins,[45,46] casapase-3,[47] and β-galactosidase.[48]

The intriguing observation that these polar, water-soluble peptides could traverse the non-polar membrane prompted a thorough structure-function analysis by Rothbard and Wender to understand the requirements for the cellular uptake of the Tat peptide and develop improved molecular transporters.[40] Using flow cytometry, they showed that fluorescently tagged D-Tat_{49-57} isomer exhibits greater cellular uptake in Jurkat cells than L-Tat_{49-57} indicating the chirality of the peptide backbone is not critical for uptake and the D-isomer most likely has increased stability towards proteolysis.[40] Nine derivatives of Tat_{49-57} in which an alanine replaced one residue at a time in each (Ala scan), indicated all cationic residues of the Tat peptide are necessary for uptake. Furthermore, deletion of one arginine residue from the Tat peptide (Tat_{49-56} or Tat_{50-57}) reduced cellular uptake by 80%. An additional deletion of one arginine (Tat_{49-55}) further reduced uptake whereas, deletion of one lysine (Tat_{51-57}) had no affect on uptake, suggesting the importance of the guanidinium group.[40] To further probe the contribution of arginine, homo-oligomers of arginine (Arg5–Arg9) were synthesized and their uptake compared to Tat_{49-57} (Figure 1.1). Although the Tat peptide contains 8 cationic residues, its uptake was better than Arg6 but lower than Arg7–Arg9.[40] A related study showed oligomers of arginine had much higher cellular uptake than oligomers of lysine, ornithine, and histidine.[49] Since these early observations, further investigation into the role of the guanidinium group has been conducted and numerous guanidinium-rich molecular transporters of varying scaffolds have been described and exploited.

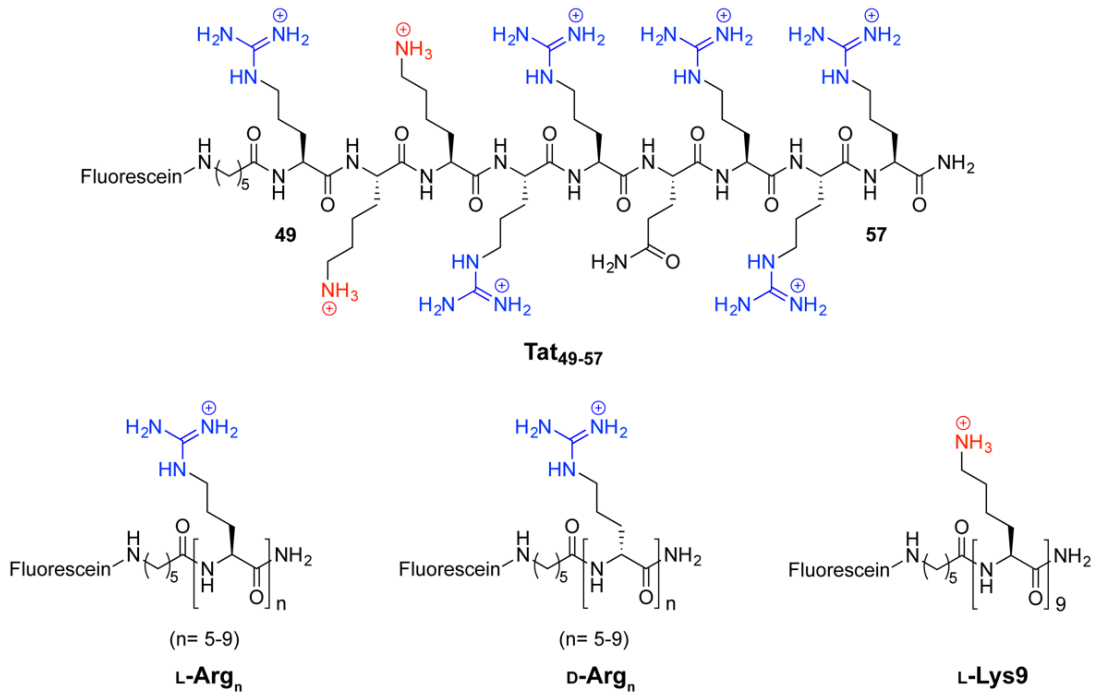

Figure 1.1. Structures of guanidinium-rich peptides. D-Tat_{49-57}, L-oligoarginine, D-oligoarginine, and oligolysine conjugated to fluorescein for structure-uptake activity studies.

1.3 Interactions of the Guanidinium Group with the Cell Surface

The first step in translocation of cell-penetrating peptides is most likely interaction of the guanidinium-rich transporter with the cell membrane. The cell membrane is predominantly composed of proteins embedded in a phospholipid-rich bilayer. Further, extracellular membrane proteins can consist of one or more covalently attached glycosaminoglycan chains forming a proteoglycan. Glycosaminoglycans are linear disaccharide units containing either an N-acetylated or N-sulfated hexosamine and either a uronic acid (heparan sulfate, chondroitin sulfate/dermatan sulfate) or a galactose (keratin sulfate), making these biomolecules highly heterogeneous and negatively charged (Figure 1.2).

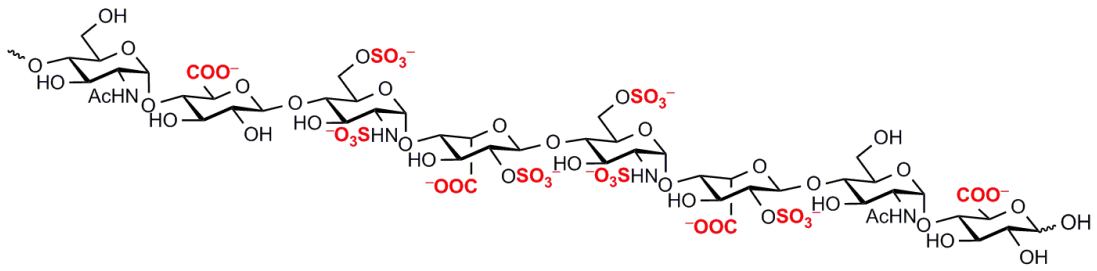

Figure 1.2. A heparan sulfate octasaccharide subunit. The anionic sulfate and carboxylate moieties are shown in red.

The guanidinium group appears to be unique in its ability to facilitate cellular uptake, for conversion of the Tat peptide to all lysine residues did not enhance uptake as did conversion to arginine amino acids.[40] At physiological pH, guanidine (pKa ~13.7) exists in its protonated form as the guanidinium cation. The delocalized positive charge is softer than the localized (hard) charge of an ammonium group, enhancing interactions with softer, anionic cell surface phosphates, carboxylates, and/or sulfates (Figure 1.3).[50] Furthermore, the planar, positively-charged guanidinium group, unlike an ammonium group, is well suited for forming a bidentate hydrogen bond with negatively-charged membrane constituents (Figure 1.3).

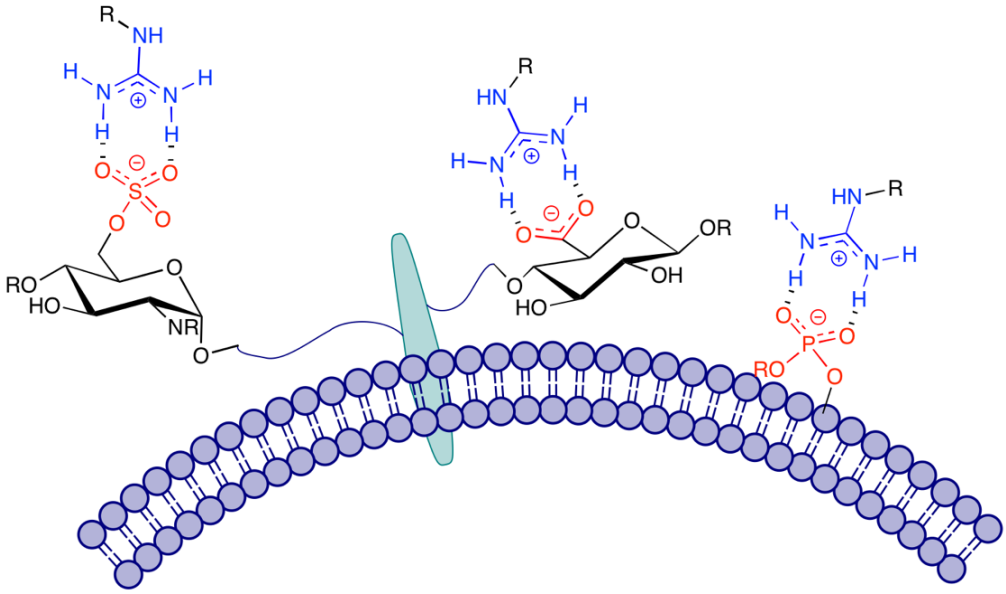

Figure 1.3. Interactions of guanidinium with cell surface components. An example of a bidentate hydrogen bond between the guanidinium functional group and either a sulfate, carboxylate, or phosphate.

To determine if the different physical properties of lysines and arginines contribute to the differences in uptake, Wender et al. replaced the hydrogens of the guanidinium groups in Arg_8 with one or two methyl groups to eliminate the hydrogen bonding ability while retaining the positive charge.[51] Increasing methylation decreased uptake, supporting the hypothesis that arginine's ability to form bidentate hyrodgen bonds contributes to the enhanced uptake of arginine-containing peptides. Additional evidence to support the role of hydrogen bonding arose from examining the partitioning of oligoarginine between octanol and water. Both a fluoresceinated arginine octamer and ornithine octamer, a non-proteogenic, cationic amino acid with one less methylene group in the side chain than lysine, partitioned in the water layer; however, when sodium laurate, a fatty acid salt, was added to the mixture, >95% of octaarginine partitioned in the octanol layer, whereas the ornithine oligomers preferentially stayed in the water layer.[51] This suggests that the

guanidinium groups can complex to counterions found on the cell surface and transform into a membrane soluble complex that can be driven into the cytosol of the cell. Likewise, the Matile group investigated the contribution of counteranions in the ability of oligo/poly-arginines and polylysine to transfer from an aqueous to a nonpolar environment.[52-55] In the presence of amphipathic anions such as sodium dodecyl sulfate (SDS), cholesterol sulfate, phosphatidylglycerol (PG) and pyrenebutyrate, poly-arginine and hexa-arginine are soluble in chloroform but poly-lysine is not.[52] Additional counterions with large, aromatic groups were also effective at activating oligoarginines across lipid membranes.[54] The authors conclude that in the presence of both hydrophilic and amphiphilic anions, arginine-rich peptides can be hydrophilic or lipophilic depending on the associated counterion.[52] Moreover, preincubation of cells with pyrenebutyrate results in direct membrane translocation and an increase in the cytosolic delivery of Arg8 peptide and enhanced green fluorescent protein (EGFP) containing an Arg8 segment in HeLa cells and primary cultured neurons.[54,55]

Other proposed mechanisms for the direct translocation of cell-penetrating peptides include inverted micelle formation,[56,57] pore formation,[58] and carpet-like model.[59] Direct-translocation mechanisms have been suggested for cell-penetrating peptides including Tat peptides[60], octa-arginine, and peptides containing hydrophobic residues such as penetratin[42]; however, the mechanism of uptake is highly dependent on cell-line, concentration of the peptide, and attached cargo. It would be applicable to cell-penetrating peptides conjugated to small molecular weight cargo and would likely compete with endocytotic mechanisms as cargo size increases.

1.4 Endocytosis Mechanisms of Guanidinium-Rich Transporters

Endocytosis is an energy-dependent process cells use to internalize macromolecules and particles from the extracellular environment.[61,62] The plasma membrane engulfs the material and buds off to form a vesicle inside the cell. Phagocytosis is the ingestion of large particles such as bacteria and pinocytosis is the ingestion of fluids or macromolecules. Pinocytosis can be categorized as either macropinocytosis, clathrin-dependent, or caveolin-dependent. Once internalized, the endocytic vesicles generally recycle the internalized cargo back to the cell surface or fuse with early endosomes to be sorted for transport to late endosomes/lysosomes (Figure 1.4).

Clathrin-mediated endocytosis is the most well-studied pathway and the primary method eukaryotic cells internalize receptors, nutrients, growth factors, etc. Clathrin polymerizes into triskelion, which consists of three heavy chains and three light chains and assembles into polyhedral lattices. Macromolecules to be internalized bind to specific cell surface receptors at specialized sites where clathrin-coated pits are formed (~100 nm in diameter) in order to concentrate surface proteins for internalization. With the help of other endocytotic regulatory proteins such as the GTPase dynamin, the pits pinch-off from the membrane to form the intracellular clathrin-coated vesicle.

The most well-studied clathrin-independent, lipid raft mediated forms of endocytosis are caveolin-dependent endocytosis and macropinocytosis. Caveolae are small invaginations of the plasma membrane rich in cholesterol and sphingolipids, signaling proteins, and clustered glycosyl phosphatidylinositol-anchored proteins.[63-65] The flask-shaped plasma membrane invaginations (50-80 nm in diameter) possess a coat

formed by the protein caveolin. The protein dynamin is also necessary for the fission of caveolae from the plasma membrane. Several bacterial toxins, such as cholera toxin,[66] and some viruses, such as SV40,[67] are internalized via caveolar endocytosis. Macropinocytosis is a less-specific, actin-dependent form of endocytosis. This mechanism is normally in response to growth factor stimulation and forms large, vesicles (0.2 – 5.0 μm in diameter) to internalize large amounts of fluid and macromolecules.[68]

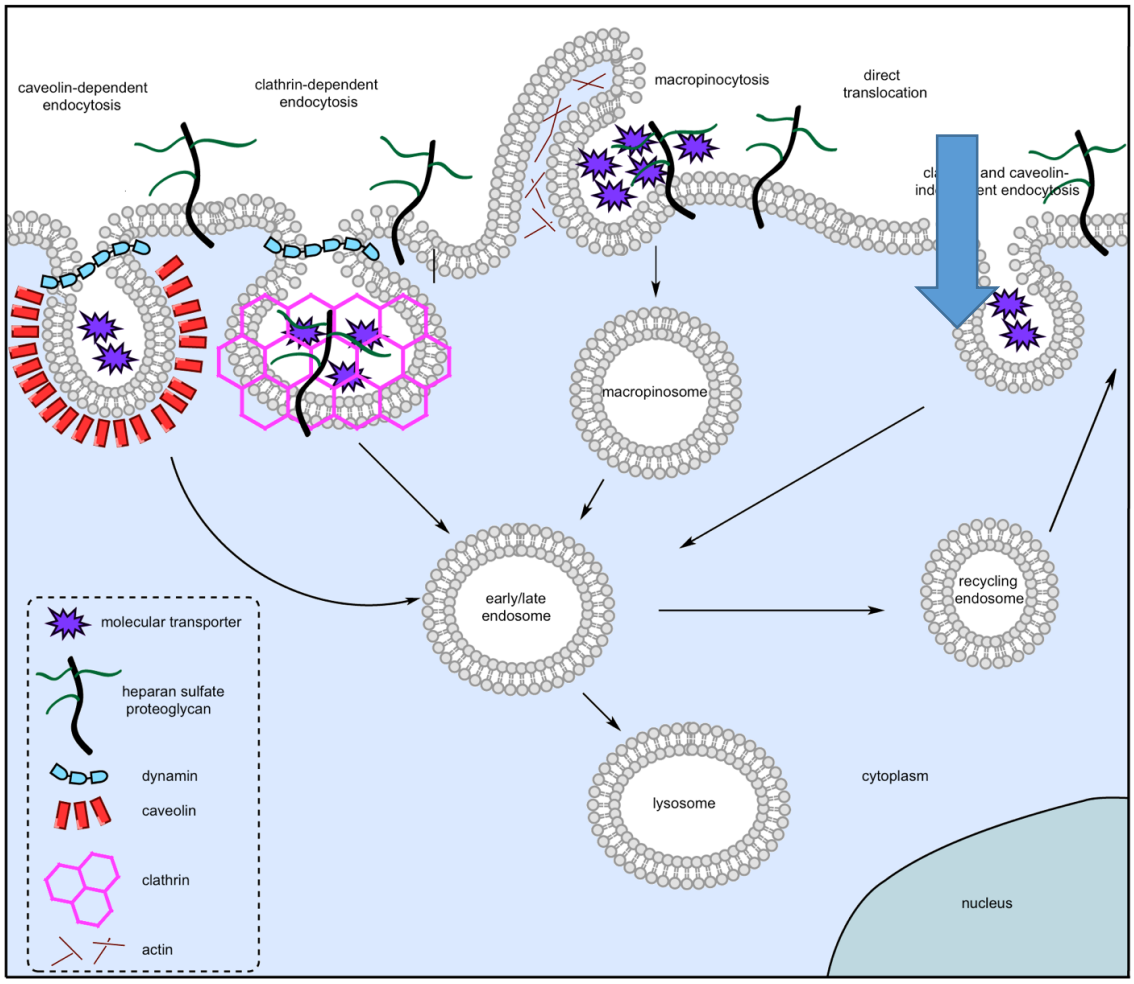

Figure 1.4. Mechanisms of cellular uptake. The different mechanisms of uptake suggested for guanidinium-rich transporters are shown in a schematic illustration of a section of a cell's plasma membrane.

The mechanism in which guanidinium-rich transporters are internalized remains unclear, most likely involves multiple pathways, and varies with different transporters. The degree to which the different pathways are utilized can also be dependent on the size and charge of the cargo attached and can differ from the uptake mechanism of the free peptide.[69,70] Clathrin-mediated uptake of arginine-rich transporters has been proposed by several groups as the primary uptake mechanism. Reports show that the Tat peptide-fluorophore conjugate colocalizes with transferrin, a marker of receptor-mediated endocytosis.[71,72] Additionally, the use of inhibitors of clathrin-mediated endocytosis reduced uptake of the Tat peptide,[73-75] whereas, caveolae-mediated endocytosis inhibitors had no affect on uptake.[73] However, other authors have reported that Tat and Arg8 do not colocalize with transferrin, but with cholera toxin,[76] suggesting caveolae-dependent uptake. Tat-fusion proteins were also shown to internalize through caveolar endocytosis.[77,78] A combination of clathrin- and caveolae-mediated uptake mechamisms has also been suggested.[75]

A number of groups have also proposed macropinocytosis as the mechanism of uptake for arginine-rich peptides.[79-81] The contribution of macropinocytosis in the uptake of oligoarginine peptides was found to be dependent on the length of the peptide.[79] Additionally, interaction of Arg8 and Tat with cell surface proteoglycans is important for activation of the Rac protein, actin organization and their macropinocytic uptake.[82] The Tat peptide was more dependent on heparan sulfate proteoglycans than the Arg8 peptide, possibly due to charge density. In a related study, it was found that the uptake mechanism of Arg8-modified liposomes containing a rhodamine dye shifted from clathrin-mediated endocytosis to macropinocytosis as the density of Arg8 increased.[83] Using a Tat-Cre

recombinase reporter assay, the Dowdy group found that Tat-fusion proteins, as well as the Tat-peptide, were internalized by macropinocytosis and independent of dynamin, caveolae and clathrin endocytosis.[80,84] In contrast to the results of Futaki and coworkers, the Dowdy group found that uptake of Tat-peptide and Tat-fusion proteins were not dependent on cell-surface proteoglycans.[85] Duchardt, et. al. demonstrated that macropinocytosis is the primary mechanism of uptake for Arg9 and Tat peptides at concentrations less than 10 μM, whereas, clathrin-mediated, caveolae-mediated, and macropinocytosis all occur at higher peptide concentrations.

As mentioned, the uptake of different guanidinium-rich transporters is dependent on a variety of factors that could effect the mechanism of uptake. Furthermore, the use of different cell lines and methods for analyzing endocytosis are not universal between labs. The use of chemical inhibitors or detecting colocalization with protein markers can have side effects, for example, blocking one route of entry might up regulate another pathway. These methods can also have poor specificity, high dependence on the cell line used, and affect cell viability;[86,87] therefore, a universal internalization mechanism for guanidinium-rich transporters is unlikely and must be taken into consideration when analyzing and developing new transporters.

1.5 Non-Peptidic Guanidinium-Rich Molecular Transporters

1.5.1 Linear Guanidinium-Rich Molecular Transporters

Since early structure-activity studies suggest the presence of guanidinium groups plays a greater role than charge or backbone in facilitating translocation of peptides, Wender et al. synthesized a family of polyguanidine peptoid derivatives.[40] These oligo-

peptoids (**1.1**) maintain the 1,4-backbone spacing of peptide side chains but lack stereogenic centers, are more resistant to proteolysis, and are easier to synthesize. The uptake of fluorescently labeled polyguanidine peptoids was comparable to corresponding D-arginine peptides. More flexible peptoids in which alkyl spacers were introduced between the guanidino head groups show improved uptake compared to Arg9, suggesting the peptide backbone is not critical for cell entry. Additionally, peptides containing seven arginine residues and one or more aminocaproic acid groups or other spacers integrated in various positions (**1.2**) were synthesized and evaluated for uptake.[88] The spaced oligomers showed more efficient uptake than heptaarginine itself, further indicating that increased flexibility leads to enhanced cellular uptake.

β-peptides, which contain one additional methylene unit between guanidinium containing side chains (**1.3**), also show similar uptake efficiency as α-peptides but are more resistant to enzymatic degradation and can be designed to form secondary structures. Gellman and coworkers showed a β-peptide TAT analogue is internalized as well as the natural $TAT_{49\text{-}57}$ and uptake of the β-peptide remains dependent on the presence of charged groups.[89] The Seebach group also investigated the uptake of β-peptides and found that β-oligoarginine outperformed β-oligolysine.[90] Additionally, arginine-rich β-peptides that form a stable helix in aqueous solution in which the guanidinium groups are grouped to one side, exhibit enhanced uptake.[91] Similarly, cell-penetrating peptides derived from a polyproline helix (**1.4**) were designed to have a well-folded secondary structure in which the cationic modifications are on one side and a hydrophobic region on the other face of the helix.[92] The amine-containing compounds showed minimal uptake and little difference

between the flexible and rigid structures; however, when the polyproline helix is modified with six guanidinium groups, an 8-fold increase in uptake compared to Arg6 is observed and an order of magnitude higher uptake compared to the Tat peptide. The organization of the hydrophobic and hydrophilic groups proved to be important, as scrambled versions of the transporters, with hydrophobic and cationic groups on all faces of the helix, were less effective.[92]

The importance of the peptide backbone and spacing was further challenged by replacing the amide bond with a carbamate backbone (**1.5**). The carbamate guanidinium 9-mer translocated into cells 2.3 times faster than D-arg9, which is 100 times faster than Tat_{49-57}, whereas, the ammonium carbamate 9-mer showed poor uptake.[93] The extensive work on linear guanidinium-rich molecular transporters with various backbone structures, spacing modifications, and even secondary structures (Figure 1.5) suggest that effective molecular transporters can go beyond flexible, linear arrangements and additional three-dimensional structures should be considered.

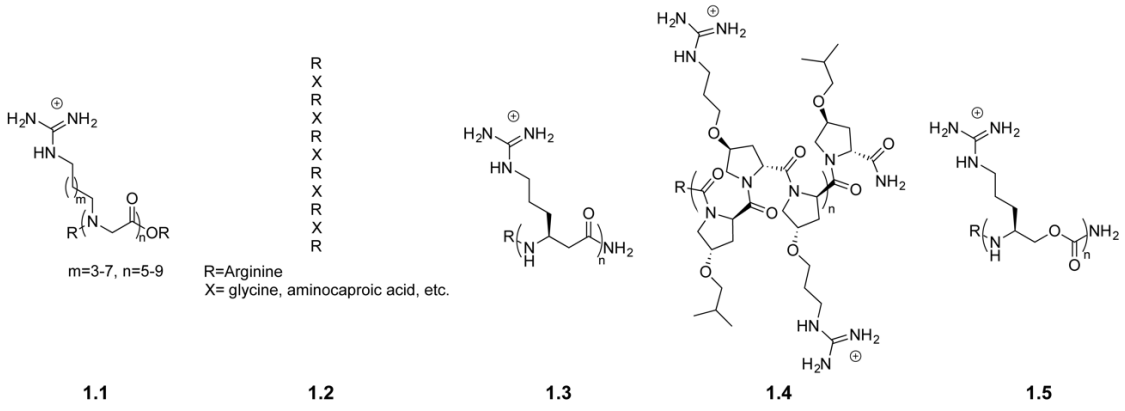

Figure 1.5. Structures of linear, guanidinium-rich molecular transporters.

1.5.2 Branched Guanidinium-Rich Molecular Transporters

Guanidinium-rich molecular transporters based on branched scaffolds, such as dendrimers, were synthesized and their cellular uptake was analyzed to determine the effect of branching on cellular uptake (Figure 1.6). Futaki and coworkers were the first to show that branched arginine-rich peptides ($(R_2)_4$) (**1.6**) have translocation efficiencies comparable to linear peptides (Arg8);[94] therefore, a linear structure is not necessary for translocation. Further, as seen with linear transporters, uptake was dependent on the number of guanidinium groups but the optimal location and spacing of the guanidinium groups is flexibile.[94]

Shortly after, Goodman et al. synthesized nonpeptidic dendritic compounds bearing 3, 6, 9, or 12 guanidinium moieties (**1.7**) conjugated to fluorescein or to green fluorescent protein (GFP) and found them to exhibit comparable cellular uptake to Tat_{49-57}.[95] Additional investigations found that a series of dendrimers displaying 8-guanidinium groups but with different chain-length spaces between the groups (**1.8**) exhibit various degrees of uptake.[96] Generally, the longer, more flexible chain lengths led to better uptake, analogous to what was observed for arginine-rich peptoids with varying hydrocarbon side chains.[40,96]

Other branched guanidinium-rich transporters have been synthesized from poly-(propylene imine),[97] Newkome-type,[98] and polyamidoamine (PAMAM)[99] dendrimer scaffolds. Similarly, the results obtained indicated the number of guanidinium groups,[97] the length of the backbone spacers,[98] and the presence of guanidinium groups, not overall charge,[99] effect cellular uptake of the dendritic transporters. The diversity of linear and branched guanidinium-rich transporters suggests that a variety of other scaffolds, if

properly functionalized with guanidinium groups, could also be utilized to control intracellular delivery.

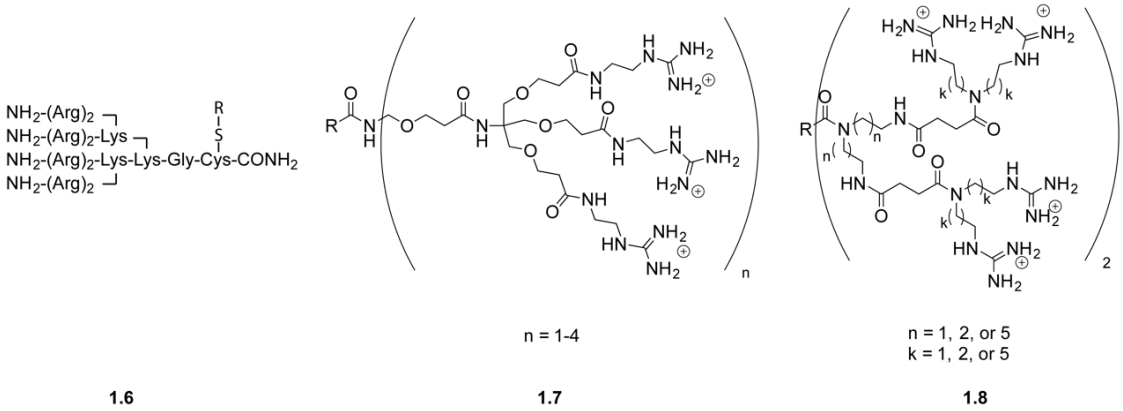

Figure 1.6. Examples of branched and dendrimeric guanidinium-rich transporters.

1.5.3 Guanidinoglycosides

Aminoglycosides are an important class of naturally occurring antibiotics. When the ammonium groups of aminoglycosides are converted to guanidinium groups, termed guanidinoglycosides (Figure 1.7), cellular uptake in eukaryotic cells is dramatically enhanced.[100] Cellular uptake of BODIPY-tagged tobramycin, neomycin B, and their guanidinylated derivatives were compared to Arg9 in two different eukaryotic cell lines. While the aminoglycosides exhibited poor uptake, guanidinylated tobramycin (GTob) and guanidinylated neomycin B (GNeo, **1.9**) showed uptake efficiencies similar or better than Arg9, respectively, despite having fewer guanidinium groups.[100] Furthermore, inhibition of Arg9 uptake by GNeo suggests a common internalization pathway.[101]

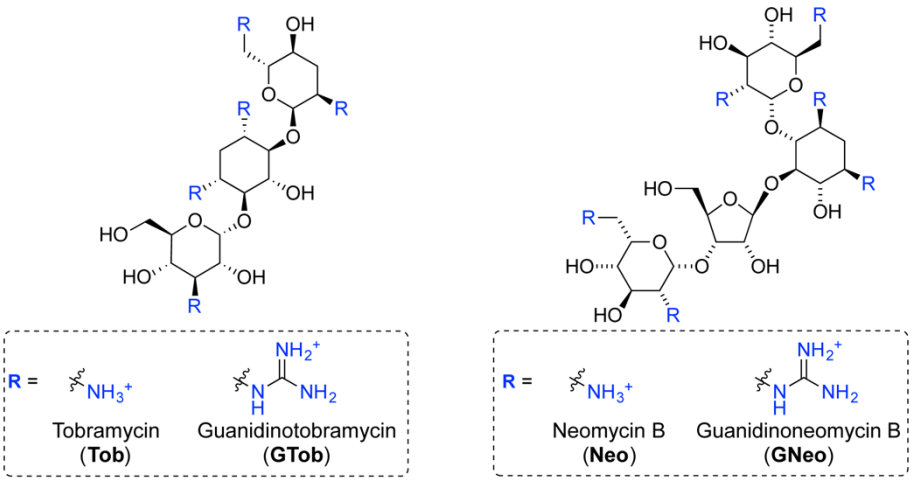

Figure 1.7. Representative structures of aminoglycosides (Tob and Neo) and guanidinoglycosides (GTob and GNeo).

Additional studies on guanidinoglycosides were performed to further investigate the mechanism of uptake and their ability to transport high molecular weight cargo into cells. Biotinylated-GNeo (**1.10**) was synthesized and conjugated to the fluorescently tagged protein streptavidin and studied in several wild-type and mutant eukaryotic cells lines.[101] At low nanomolar concentrations, GNeo was found to deliver the fluorescent protein into cells and its uptake depended exclusively on cell surface heparan sulfate, a negatively charged polysaccharide found on the surface of all mammalian cells, rather than other negatively charged glycans such as chondroitin sulfate.[101] The role of heparan sulfate (HS) in the uptake of guanidinoglycosides was further investigated by synthesizing monomeric and dimeric transporters and examining their uptake in wild-type CHO cells or mutant CHO cells void of HS or displaying HS with altered sulfation patterns.[102] All derivatives showed minimal uptake in cells lacking HS. Monomeric guanidinoglycosides also showed reduced uptake in cells having lower levels of sulfation, whereas, dimeric guanidinoglycoside conjugates could overcome HS deficiency and maintain high levels of

cellular uptake. The cooperative response observed with dimeric guanidinoglycosides show that increasing the valency of the transporter affects uptake efficiency. The HS–GNeo interactions were further studied using binding and FRET studies to show that the multi-valent GNeo-biotin-streptavidin complex can induce HS-proteoglycan aggregation on the cell surface which then leads to endocytic entry into cells.[103] The clustering of HSPG can be altered by modifying the GNeo transporter with a long, alkyl chain.[104] Derivatives with longer alkyl chains showed greater uptake but did not induce HSPG clustering, suggesting the hydrophobic interactions with the membrane assist in uptake, offering a different internalization pathway.[104]

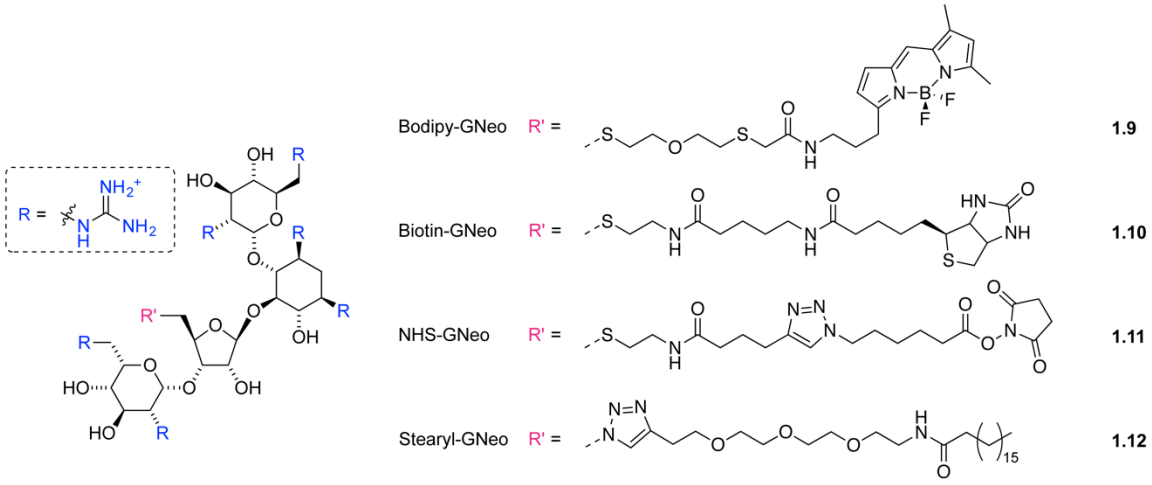

Figure 1.8. Structures of various guanidinoneomcyin derivatives.

GNeo has been shown to deliver a variety of large, bioactive cargo into cells. GNeo-biotin (**1.10**) facilitated the uptake of streptavidin-coated quantum dots while retaining HS selectivity.[105] Microscopy images demonstrated that ~90% of internalized GNeo-conjugated quantum dots colocalized with lysosomes. To prepare a more generalized protein transporter, an activated ester of GNeo was synthesized (GNeo-NHS, **1.11**) and conjugated to the lysines of two lysosomal enzymes, β-D-glucuronidase and α-

L-iduronidase. Conjugation did not interfere with enzyme activity and facilitated sufficient delivery of the enzyme to restore normal glycosaminoglycan turnover in patient cells lacking the endogenous enzyme.[105] More recently, a stearyl-GNeo derivative (**1.12**) was incorporated into liposomes.[106] These "GNeosomes", were able to deliver small molecules and high molecular weight proteins to the lysosomes of mammalian cells. Together, these studies suggest the therapeutic potential of designing novel, multivalent transporters to enhance lysosomal delivery of biomolecules.

1.5.4 Additional Carbohydrate-Based Guanidinium-Rich Molecular Transporters

Guanidinylation of carbohydrate scaffolds based on *myo*- and *scyllo*- inositol dimers (Figure 1.9) were prepared and studied by Chung and coworkers.[107] Inositol structures are naturally occurring carbohydrates thus mostly nontoxic and have a high density of functionality with diverse stereochemical possibilities. Initial studies found that the amide-linked *scyllo*-inositol dimer containing 8 guanidinium moieties (G8), with a seven carbon spacer from the ring, (**1.13**) outperformed the Arg8 transporter three-fold.[107] Uptake efficiency correlated with an increase in the linker length between the guanidinium groups and inositol. Microscopy studies indicated a clathrin-independent uptake mechanism different from that of the Tat peptide. Furthermore, while the Tat peptide generally accumulates in the liver, kidney, and spleen, in vivo studies showed higher distributions of the inositol transporter in the heart, lung, and brain tissue. The delivery of a doxorubicin-transporter conjugate to the brain further shows the ability of these transporters to cross the highly exclusive BBB.[107] To further investigate the structural properties driving the organellar and tissue selectivity, the effect of the scaffold

stereochemistry was evaluated using monomeric *myo*- and *scyllo*-inositol and other monosaccharide-based G8 molecular transporters.[108] *Myo*-inositol transporters with *para*-like substitution were found to target mitochondria, whereas, *scyllo*-inositol transporters with *para*- or *ortho*-like substitutions did not show affinity for mitochondria or clear localization.[108] Moreover, G8-D-glucose transporters show higher colocalization with mitochondria than G8-mannose, -allose, or –galactose based transporters in which only one stereochemical variation occurs between each and which localized more in lysosomes.[109] All transporters maintained the ability to cross the mouse BBB. Despite having the same number of guanidinium groups and similar structures, these results suggest minor differences in scaffold stereochemistry play a role in the uptake and organellar affinity of carbohydrate-based transporters.

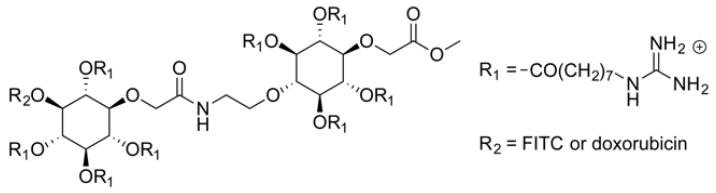

1.13

Figure 1.9. Representative *scyllo*-inositol transporter. Amide-linked dimeric *scyllo*-inositol transporter containing eight guanidinium groups.

To further explore the idea of utilizing different scaffolds to selectively target intracellular organelles or specific tissues, transporters based on the sugar alcohol sorbitol were designed and synthesized (Figure 1.10).[110] Sorbitol transporters were modified using branched linkers to have eight guanidinium residues with different types of branch chains and varying chain lengths. The most promising transporters in the series were found to selectively localize in the mitochondria. As with the inositol transporters, the sorbitol

transporters were found predominantly in the heart muscle and brain tissue of mice.[110] The ability of the G8-sorbital transporter to traverse the BBB opens up the potential to treat a variety of diseases that affect the brain and in which current therapeutics are unable to achieve. Derivatives of the G8-sorbitol molecular transporter have been successfully employed to deliver 3'-azido-3'-deoxythymidine (AZT) (**1.14**) ,[111] a nucleoside reverse transcriptase inhibitor used in the treatment of acquired immunodeficiency syndrome (AIDS), 5-fluorouracil (5-FU) (**1.15**),[112] an anticancer drug, and paclitaxel (**1.16**),[113] an anti-tumor agent, to brain tissue in vivo. Delivery of 5-FU resulted in a more cytotoxic agent against two multidrug-resistant cancer cell lines then 5-FU alone[112] and transport of paclitaxel led to enhanced anti-tumor effects in a mouse model of glioblastoma.[113] Additionally, a lipidated derivative of the sorbitol transporter was utilized in nonviral gene and siRNA delivery.[114] Derivatives with short hydrophobic chains (C12) more successfully condensed DNA/RNA, whereas, compounds with longer lipid chains (C30) were more effective at transfection when used to modify the surface of nucleic acid containing lipid nanoparticles. Furthermore, a biotin-derivative of the G8-sorbitol transporter was able to internalize quantum dots coated with streptavidin.[115] The larger cargo resulted in slower uptake kinetics but is ultimately internalized through macropinocytosis and resides in the cytoplasm. Despite the large cargo size, the quantum dot-conjugate is able to traverse the BBB when injected intravenously into mice.[115]

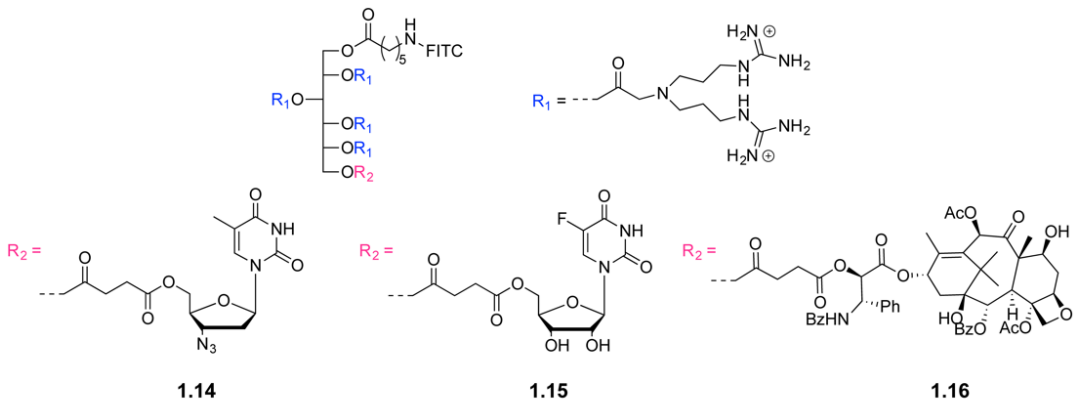

Figure 1.10. Sorbitol-based transporters. Sorbitol-based carriers conjugated to either AZT (**1.14**), 5-FU (**1.15**), or paclitaxel (**1.16**).

The success obtained from inositol and sorbitol based transporters led to the synthesis and uptake of transporters based on the disaccharides lactose,[116] sucrose,[117] and trehalose (Figure 1.11).[118] The lactose-based transporters were found to localize in the brain, liver, and spleen and target either the mitochondria or the endosomes depending on linker length.[116] Sucrose-based transporters, functionalized with seven guanidinium groups, also showed localization depends on linker length as well as the nature of the fluorescent dye attached to the transporter.[117] Similarly, trehalose-derived transporters, displaying either six (G6) or eight (G8) guanidinium groups, are predominantly found in the brain tissue and show high colocalization with mitochondria.[118] Trehalose has been reported to inhibit polyQ aggregates involved in Huntington's disease (HD) and show neuroprotective effects;[119] however, cellular uptake of trehalose in mammalian cells is very limited.[120] The BBB permeable G6-trehalose derivative was able to reduce the aggregation of polyQ in vitro and when orally administered to HD mice, an increased life span, improved motor skills, and a reduction in the inclusion bodies in the brain and liver were observed.[118]

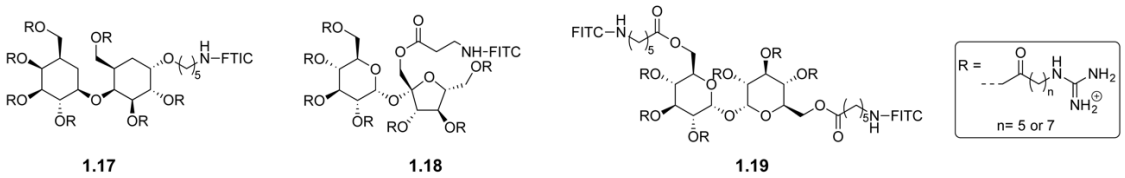

Figure 1.11. Disaccharide-based transporters. Lactose (**1.17**), sucrose (**1.18**), and trehalose (**1.19**) based transporters conjugated to fluorescein.

1.5.5. Oligomerizaton-Based Guanidinium-Rich Molecular Transporters

The structural diversity of guanidinium-rich transporters indicated variations in backbone could lead to different uptake and *in vivo* properties. The synthesis of previously reported transporters required several synthetic steps. Even the synthesis of octa-arginine required 16 steps when prepared via solid-phase peptide synthesis; therefore, synthetic strategies to improve step economy and design novel transporters were explored. The growing field of polymer chemistry found various ways to synthesize polymers with well-defined architectures and lengths termed "controlled polymerization".[121] The narrow polydispersity is a result of polymerization reactions without chain transfer or termination, a rate of initiation greater than the rate of propagation, and irreversible addition of each monomer. Moreover, these methods allow the addition of a second monomer (or a third, etc.) after the first is consumed to generate well-defined block copolymers.[122] The molecular weight or degree of polymerization can be controlled by adjusting the ratio of initiator to monomer.[123] Additionally, this method allows for control over end groups and a variety of functionalities can be incorporated at the polymer termini. Applying this strategy to assemble multiple guanidinium groups reduces the step count to two (oligomerization and deprotection); therefore, different length transporters can easily be obtained without an increase in the number of synthetic steps.

In 2008, the Kiessling lab utilized living ring opening metathesis polymerization (ROMP) to form succinimidyl ester-substituted oligomers terminated with a ketone (**1.21**) for further functionalization (Figure 1.12).[124] The oligomers had narrow polydispersities and average length of ten monomer units. The active esters were reacted with an amine-linked to the guanidinium groups and a rhodamine B derivative was introduced via an oxime linkage (**1.22**). Cellular uptake was evaluated using live cell confocal microscopy and showed uptake of the guanidinium-rich oligomer in punctate vesicles and throughout the cytoplasm through an energy-dependent pathway. Longer polymers with an average length of 25 units were internalized less efficiently and were more cytotoxic. The idea was extended to form block copolymers which contained two different activated monomers and a terminal ketone (**1.24**).[125] The succinimidyl esters were again replaced with guanidinium groups, the chloroacetamide-functionalized second block was substituted by mercaptoethanol, and the ketone was reacted with a rhodamine B derivative (**1.25**). The guanidinium-rich block copolymer was internalized in mammalian cells and localized predominantly in the cytoplasm.

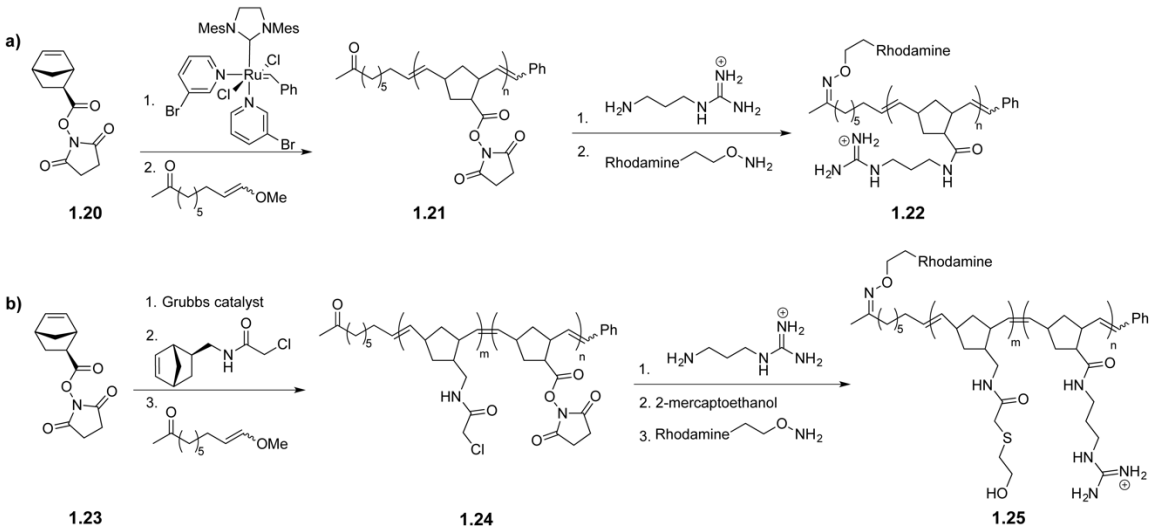

Figure 1.12. Synthesis of guanidinium-rich transporters using ROMP. Representative polymers (a) and block copolymers (b) synthesized via ROMP.

In related work, the Tew research group used ROMP to synthesize guanidinium-rich transporters with an oxanorbornene scaffold containing a protected guanidinium moiety (Figure 1.13). Initial studies looked at transporter efficiencies with respect to polymer length, hydrophobicity, pH, membrane fluidity and membrane potentials as well as antimicrobial activity.[126] This polymer (**1.27**) was found to be strongly antibacterial against gram-negative and gram-positive bacteria as well as low hemolytic activity against human red blood cell, whereas previously studied poly-ammonium oxanorbonene species were either inactive or toxic.[127] The uptake activity of the oxanorbornene-derived transporters was assessed in mammalian cells to evaluate the effects of polymer length and guanidinium density,[128] aromaticity and hydrophobicity,[129] and aromatic -interactions.[130] The transporters were then used to deliver small interfering RNAs (siRNA) into T-cells.[131] Copolymers consisting of guanidinium and hydrophobic groups (**1.28**) outperformed homopolymers containing only the guanidinium monomer when in the presence of

serum.[131] Additional studies to optimize the oxanorbornene transporters for siRNA delivery found an optimal cationic charge of 40 and again, block copolymers outperformed homopolymers.[132] The optimized transporter was able to knockdown target protein expression in T cells up to 80%.[132] The synthetic accessibility to a variety of guanidinium-rich polymers and copolymers was key to understanding and optimizing the uptake of these novel transporters.

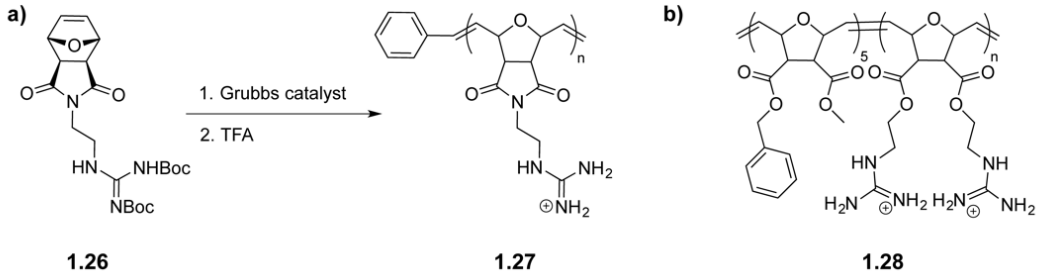

Figure 1.13. Oxanorbornene-based guanidinium-rich transporters. (a) Synthesis of homopolymers via ROMP. (b) Block copolymer structure used for intracellular delivery.

The Wender group took an organocatalytic approach, and utilized a ring-opening polymerization of cyclic carbonates modified with a guanidinium side chain (**1.29**) to synthesize a new class of transporters (**1.30**).[133] Oligomers of various lengths were obtained by varying the ratio of monomer to initiator with narrow polydispersities. This method offers several advantages over other oligomerization strategies including the metal-free nature of the catalyst, a stable backbone in powder form but a non-toxic degradable backbone under physiological conditions, and the opportunity to initiate synthesis from a functional probe or drug (Figure 1.14). The dansyl-terminated guanidinium-rich oligocarbonate transporters exhibited efficient cellular uptake similar to an octa-arginine control. The transporters were also able to deliver and release luciferin in cells with a slower release rate than octa-arginine.[133] Block copolymers containing the guanidinium

side chains mixed with hydrophobic side chains (**1.31**) were investigated for their ability to complex small interfering RNAs (siRNA) and facilitate uptake.[134] The oligomerization strategy allows easy access to test numerous hydrophobic side chains, different ratios of the two monomers and different oligomer lengths without lengthy syntheses. The best amphipathic co-oligomers were able to noncovalently complex and deliver siRNA into cells, resulting in up to 90% knockdown of target protein synthesis.[134] A second generation oligocarbonate delivery system was derived from 1,3-glycerol carbonate monomers (**1.32**) to enhance biocompatibility and stability.[135] The aliphatic oligocarbonates containing the ether linkage at C2 (**1.33**) maintained high levels of target protein suppression and exhibited enhanced siRNA/co-oligomer complex stabilization. The release of siRNA could be controlled by modifying the monomers and using mixtures of the glycerol-derived monomer with the previously reported methyl(trimethylene)carbonate-derived monomers.[135] A third-generation of organocatalytic ring-opening polymers were formed from cyclic phospholane monomers (**1.34**).[136] The transporters were initiated from fluorophore directly or with a reactive thiol, which could then be reacted with a fluorophore or the cancer drug paclitaxel, and released intracellularly upon exposure to glutathione. Oligophosphoesters (**1.35**) exhibited increased water solubility, hydrolytic stability, and ultimately better cellular uptake than peptide or oligocarbonate transporters.[136]

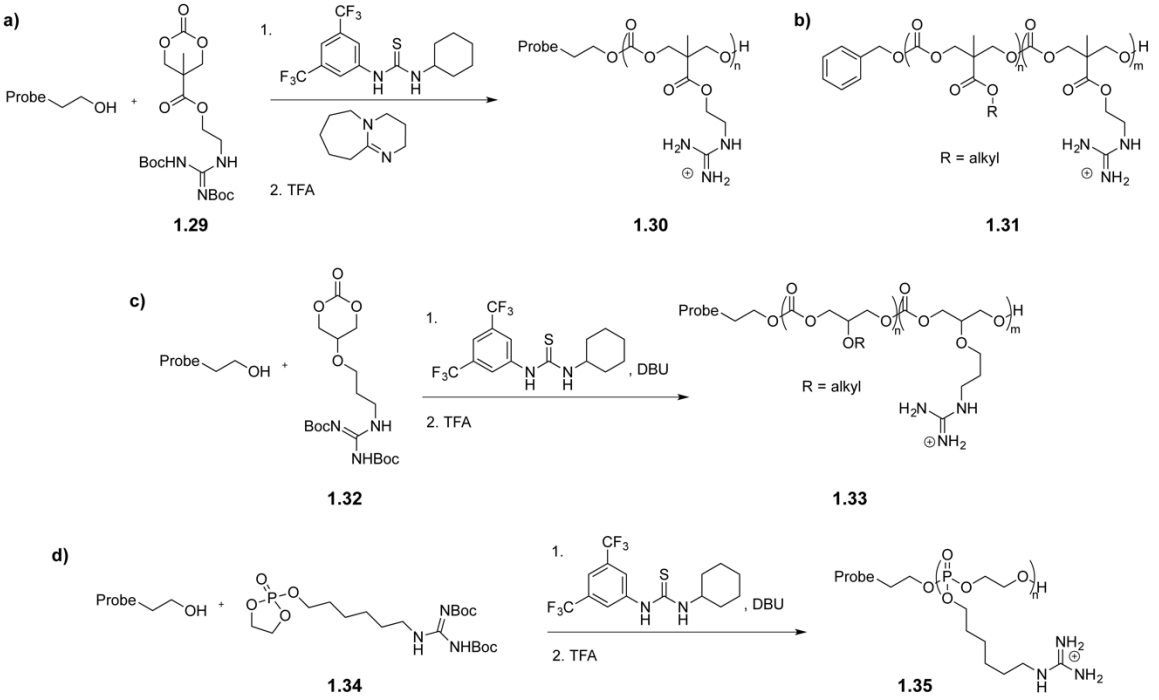

Figure 1.14. Organocatalytic synthesis of guanidinium-rich transporters. (a) Methyl(trimethylene)carbonate (MTC) scaffold, (b) amphipathic block MTC co-oligomers, (c) 1,3-glycerol carbonate scaffold, and (d) phosphoester scaffold.

Poly(disulfide)s have been developed for gene delivery systems due to their low toxicity and their ability to release cargo in the presence of intracellular reducing agents such as glutathione.[137] Ammonium or guanidinium residues have been incorporated to enhance cellular translocation.[138-141] These poly(disulfide) transporters rely on noncovalent association of the cargo; therefore, Matile and coworkers developed a method for synthesizing cell penetrating poly(disulfide)s with covalently attached cargo (Figure 1.15).[142] Probes or drugs containing a thiol group can initiate a ring-opening disulfide-exchange polymerization of guanidinium-containing propagators (**1.36**). Guanidinium-rich poly(disulfide)s (**1.37**) grown on a fluorescent substrate were able to reach the cytosol and release the substrate in HeLa cells within 5 min.[143] Co-polymerization with hydrophobic monomers results in a high accumulation in endosomes, whereas more

hydrophilic polymers reside in the cytosol.[143,144] The uptake mechanism was independent of cargo, however, altering the length of the polymer can be used to control their intracellular destination. For example, increasing the length of the guanidinium-containing poly(disulfide)s results in a higher accumulation in the cytsol over endosomes.[145] Even longer polymers, however, exhibit slower depolymerization kinetics and proceed into the nucleus. Guanidinium-rich poly(disulfide)s were also shown to facilitate the intracellular delivery of proteins to the nucleoli, further demonstrating the cargo-independent ability of these transporters to translocate the membrane.[146]

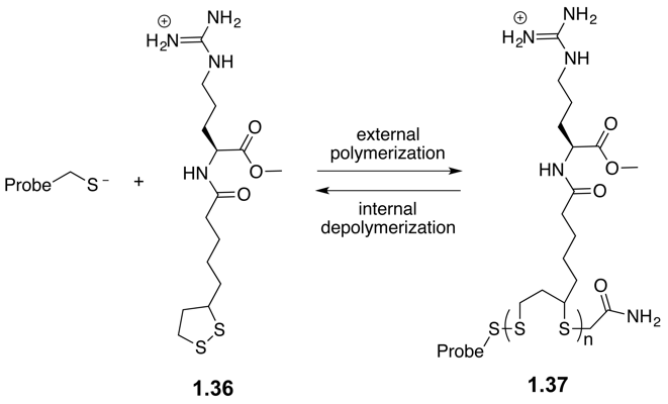

Figure 1.15. Poly(disulfide)-based transporters. Synthesis of substrate-initiated cell-penetrating poly(disulfide)s which undergo intracellular depolymerization to minimize toxicity and release the substrate/probe.

1.6 Summary and Outlook

The discovery that certain proteins, such as HIV Tat, are able to cross biological barriers due to a basic, guanidinium-rich segment, led to the development of several classes of guanidinium-rich transporters. These molecular transporters offer a method for delivering both polar and nonpolar agents such as biologics or drugs that would otherwise be impermeable to the cell membrane. The efficacy of guanidinium-rich transporters based

on various scaffolds indicates the requirements for transporter uptake are quite general and are effective in a variety of cell lines. Guanidinium groups generally show enhanced uptake compared to their ammonium counterparts and multiple guanidinium groups are necessary for uptake, with an optimum number between 5 and 15.

Although the collection of guanidinium-rich transporters has increased tremendously in the past twenty years, very few have moved forward clinically. The design and development of new transporters can lead to unique intracellular distributions, targeting effects, and pharmacology. In our recent work, described in detail in Chapter 2, we guanidinylated polymyxin B, a cyclic, polypeptide antibiotic containing five primary amines, and evaluated its uptake properties in mammalian cells. Interestingly, unlike previously described transporters, conversion of the ammonium groups to guanidinium groups did not enhance uptake of the parent antibiotic. Both the ammonium and guanidinium derivatives showed comparable uptake to a control transporter with five guanidinium groups. Additionally, their mechanism of uptake, localization in cells, and ability to deliver cargo to the cytosol were also evaluated. Polymyxin was also shown to enhance intracellular delivery of lipid vesicles. In addition to developing a novel, synthetically accessible transporter, these findings suggest the cyclic portion of polymyxin can facilitate uptake in mammalian cells which could help explain the observed toxicity of the antibiotic.

Guanidinoglycosides have been extensively developed and utilized in our lab over the past thirteen years to transport various cargo into mammalian cells.[100] It has been shown that guanidinylated neomycin (GNeo) selectively delivers cargo to the lysosomes.[105] The lysosomes are known to be involved in a variety of diseases including

lysosomal storage disorders, neurodegenerative disorders, cancer, and cardiovascular diseases;[147] therefore, establishing a lysosomotropic molecular transporter would be useful in delivering medicinal agents for therapeutic treatments. Of particular interest is the delivery of lysosomal enzymes for the treatment of lysosomal storage disorders. Recently, we showed liposomes modified with GNeo, termed GNeosomes, could efficiently deliver various cargo into the lysosomes of cells without chemical modification of the cargo.[106] In Chapter 3, we aimed to improve the delivery of liposomes by incorporating different GNeo-lipids. The optimized system was then used to deliver therapeutic quantities of lysosomal enzymes to fibroblasts cultured from patients with a lysosomal storage disorder. The versatility of GNeosomes to encapsulate different cargos suggests that this system might be useful for treatment of other lysosome-involved diseases.

As mentioned previously, the cellular uptake mechanism of guanidinium-rich transporters is complex and somewhat controversial. It is also evident that cargo-type, cell-line, and transporter can have an affect on overall cellular uptake as well as the mechanism of uptake. Furthermore, contributions from the linker connecting the cargo and carrier are often overlooked. Therefore, to probe the role the linker plays in the uptake of our GNeo transporter, we synthesized linkers with different lengths and polarities and evaluated their effects on conjugation of the transporter to a model protein and its cellular uptake efficiency. Chapter 4 outlines the synthesis of seventeen GNeo derivatives, their conjugation to streptavidin, and their cellular uptake.

In collaboration with the Esko lab, it was discovered early on that guanidinoglycosides depend on heparan sulfate for their cellular uptake.[101] To further study the heparan sulfate – guanidinoglycoside interactions, dimeric compounds were

synthesized and tested in several under-sulfated cell lines.[102] These multivalent transporters exhibited a cooperative response to these mutant cell lines. In addition, it was recently shown that guanidinoglycosides can cluster heparan sulfate on the cell surface.[103] To further exploit this multivalent – heparan sulfate interaction, oligomers of GNeo were synthesized from a norbornene-GNeo monomer that could undergo ring-opening metathesis polymerization (ROMP). In Chapter 5, the synthesis of the reactive monomer, formation of GNeo oligomers, and preliminary cellular uptake studies are presented. While we have increased the number of examples of transporters effectively delivering various cargo to cells and displaying great therapeutic potential, future studies should focus on testing transporters *in vivo* for eventual treatment in humans.

1.7 References

(1) Borchardt, R. T.; Smith, P. L.; Wilson, G. *Models for Assessing Drug Absorption and Metabolism*; Springer US, 2013.

(2) Pardridge, W. M. *NeuroRx* **2005**, *2*, 3.

(3) Lipinski, C. A.; Lombardo, F.; Dominy, B. W.; Feeney, P. J. *Adv. Drug Del. Rev.* **1997**, *23*, 3.

(4) Leader, B.; Baca, Q. J.; Golan, D. E. *Nat. Rev. Drug Discov.* **2008**, *7*, 21.

(5) Nelson, A. L.; Dhimolea, E.; Reichert, J. M. *Nat. Rev. Drug Discov.* **2010**, *9*, 767.

(6) Eckstein, F. *Expert opinion on biological therapy* **2007**, *7*, 1021.

(7) Carton, J. M.; Strohl, W. R. In *Introduction to Biological and Small Molecule Drug Research and Development*; Jefferis, S. R., Ed.; Elsevier: Oxford, 2013, p 127.

(8) Kling, J. *Nat. Biotechnol.* **2012**, *30*, 128.

(9) Ho, R. J.; Chien, J. Y. *J. Pharm. Sci.* **2012**, *101*, 2668.

(10) Škalko-Basnet, N. *Biologics : Targets & Therapy* **2014**, *8*, 107.

(11) Mitragotri, S.; Burke, P. A.; Langer, R. *Nat. Rev. Drug Discov.* **2014**, *13*, 655.

(12) Tibbitt, M. W.; Dahlman, J. E.; Langer, R. *J. Am. Chem. Soc.* **2016**, *138*, 704.

(13) Pasut, G.; Veronese, F. M. *Journal of controlled release : official journal of the Controlled Release Society* **2012**, *161*, 461.

(14) Constantinou, A.; Epenetos, A. A.; Hreczuk-Hirst, D.; Jain, S.; Wright, M.; Chester, K. A.; Deonarain, M. P. *Bioconjug Chem* **2009**, *20*, 924.

(15) Mero, A.; Pasqualin, M.; Campisi, M.; Renier, D.; Pasut, G. *Carbohydrate polymers* **2013**, *92*, 2163.

(16) Suzuki, T.; Ishii-Watabe, A.; Tada, M.; Kobayashi, T.; Kanayasu-Toyoda, T.; Kawanishi, T.; Yamaguchi, T. *J. Immunol.* **2010**, *184*, 1968.

(17) Syed, S.; Schuyler, P. D.; Kulczycky, M.; Sheffield, W. P. *Blood* **1997**, *89*, 3243.

(18) Sleep, D.; Cameron, J.; Evans, L. R. *Biochim. Biophys. Acta* **2013**, *1830*, 5526.

(19) Cohen, S.; Yoshioka, T.; Lucarelli, M.; Hwang, L. H.; Langer, R. *Pharmaceutical research* **1991**, *8*, 713.

(20) Van Tomme, S. R.; Storm, G.; Hennink, W. E. *Int. J. Pharm.* **2008**, *355*, 1.

(21) Blanco, E.; Shen, H.; Ferrari, M. *Nat Biotech* **2015**, *33*, 941.

(22) Leleux, J.; Roy, K. *Advanced healthcare materials* **2013**, *2*, 72.

(23) Jiskoot, W.; Randolph, T. W.; Volkin, D. B.; Middaugh, C. R.; Schoneich, C.; Winter, G.; Friess, W.; Crommelin, D. J.; Carpenter, J. F. *J. Pharm. Sci.* **2012**, *101*, 946.

(24) Schaepelynck, P.; Darmon, P.; Molines, L.; Jannot-Lamotte, M. F.; Treglia, C.; Raccah, D. *Diabetes & metabolism* **2011**, *37 Suppl 4*, S85.

(25) Baxter, J.; Mitragotri, S. *Expert review of medical devices* **2006**, *3*, 565.

(26) Edwards, D. A.; Hanes, J.; Caponetti, G.; Hrkach, J.; Ben-Jebria, A.; Eskew, M. L.; Mintzes, J.; Deaver, D.; Lotan, N.; Langer, R. *Science* **1997**, *276*, 1868.

(27) Illum, L. *Journal of controlled release : official journal of the Controlled Release Society* **2003**, *87*, 187.

(28) Whitehead, K.; Shen, Z.; Mitragotri, S. *Journal of controlled release : official journal of the Controlled Release Society* **2004**, *98*, 37.

(29) Mitragotri, S.; Blankschtein, D.; Langer, R. *Science* **1995**, *269*, 850.

(30) Schuetz, Y. B.; Naik, A.; Guy, R. H.; Kalia, Y. N. *Expert opinion on drug delivery* **2005**, *2*, 533.

(31) Wender, P. A.; Cooley, C. B.; Geihe, E. I. *Drug Discovery Today: Technologies* **2012**, *9*, e49.

(32) Bechara, C.; Sagan, S. *FEBS Lett.* **2013**, *587*, 1693.

(33) Stanzl, E. G.; Trantow, B. M.; Vargas, J. R.; Wender, P. A. *Accounts of Chemical Research* **2013**, *46*, 2944.

(34) Wexselblatt, E.; Esko, J. D.; Tor, Y. *The Journal of Organic Chemistry* **2014**, *79*, 6766.

(35) Frankel, A. D.; Pabo, C. O. *Cell* **1988**, *55*, 1189.

(36) Green, M.; Loewenstein, P. M. *Cell* **1988**, *55*, 1179.

(37) Vives, E.; Brodin, P.; Lebleu, B. *J. Biol. Chem.* **1997**, *272*, 16010.

(38) Pepinsky, R. B.; Androphy, E. J.; Corina, K.; Brown, R.; Barsoum, J. *DNA Cell Biol.* **1994**, *13*, 1011.

(39) Fawell, S.; Seery, J.; Daikh, Y.; Moore, C.; Chen, L. L.; Pepinsky, B.; Barsoum, J. *Proceedings of the National Academy of Sciences of the United States of America* **1994**, *91*, 664.

(40) Wender, P. A.; Mitchell, D. J.; Pattabiraman, K.; Pelkey, E. T.; Steinman, L.; Rothbard, J. B. *Proc. Natl. Acad. Sci. USA* **2000**, *97*, 13003.

(41) Joliot, A.; Pernelle, C.; Deagostini-Bazin, H.; Prochiantz, A. *Proc. Natl. Acad. Sci. USA* **1991**, *88*, 1864.

(42) Derossi, D.; Joliot, A. H.; Chassaing, G.; Prochiantz, A. *J. Biol. Chem.* **1994**, *269*, 10444.

(43) Anderson, D. C.; Nichols, E.; Manger, R.; Woodle, D.; Barry, M.; Fritzberg, A. R. *Biochem. Biophys. Res. Commun.* **1993**, *194*, 876.

(44) Kim, D. T.; Mitchell, D. J.; Brockstedt, D. G.; Fong, L.; Nolan, G. P.; Fathman, C. G.; Engleman, E. G.; Rothbard, J. B. *J. Immunol.* **1997**, *159*, 1666.

(45) Nagahara, H.; Vocero-Akbani, A. M.; Snyder, E. L.; Ho, A.; Latham, D. G.; Lissy, N. A.; Becker-Hapak, M.; Ezhevsky, S. A.; Dowdy, S. F. *Nat. Med.* **1998**, *4*, 1449.

(46) Gius, D. R.; Ezhevsky, S. A.; Becker-Hapak, M.; Nagahara, H.; Wei, M. C.; Dowdy, S. F. *Cancer Res.* **1999**, *59*, 2577.

(47) Vocero-Akbani, A. M.; Heyden, N. V.; Lissy, N. A.; Ratner, L.; Dowdy, S. F. *Nat. Med.* **1999**, *5*, 29.

(48) Schwarze, S. R.; Ho, A.; Vocero-Akbani, A.; Dowdy, S. F. *Science* **1999**, *285*, 1569.

(49) Mitchell, D. J.; Steinman, L.; Kim, D. T.; Fathman, C. G.; Rothbard, J. B. *J. Pept. Res.* **2000**, *56*, 318.

(50) Fromm, J. R.; Hileman, R. E.; Caldwell, E. E.; Weiler, J. M.; Linhardt, R. J. *Archives of biochemistry and biophysics* **1995**, *323*, 279.

(51) Rothbard, J. B.; Jessop, T. C.; Lewis, R. S.; Murray, B. A.; Wender, P. A. *J. Am. Chem. Soc.* **2004**, *126*, 9506.

(52) Sakai, N.; Matile, S. *J. Am. Chem. Soc.* **2003**, *125*, 14348.

(53) Sakai, N.; Takeuchi, T.; Futaki, S.; Matile, S. *ChemBioChem* **2005**, *6*, 114.

(54) Perret, F.; Nishihara, M.; Takeuchi, T.; Futaki, S.; Lazar, A. N.; Coleman, A. W.; Sakai, N.; Matile, S. *J. Am. Chem. Soc.* **2005**, *127*, 1114.

(55) Takeuchi, T.; Kosuge, M.; Tadokoro, A.; Sugiura, Y.; Nishi, M.; Kawata, M.; Sakai, N.; Matile, S.; Futaki, S. *ACS Chem. Biol.* **2006**, *1*, 299.

(56) Derossi, D.; Joliot, A. H.; Chassaing, G.; Prochiantz, A. *J. Biol. Chem.* **1994**, *269*, 10444.

(57) Derossi, D.; Chassaing, G.; Prochiantz, A. *Trends Cell Biol.* **1998**, *8*, 84.

(58) Matsuzaki, K.; Yoneyama, S.; Murase, O.; Miyajima, K. *Biochemistry* **1996**, *35*, 8450.

(59) Pouny, Y.; Rapaport, D.; Mor, A.; Nicolas, P.; Shai, Y. *Biochemistry* **1992**, *31*, 12416.

(60) Ter-Avetisyan, G.; Tunnemann, G.; Nowak, D.; Nitschke, M.; Herrmann, A.; Drab, M.; Cardoso, M. C. *J. Biol. Chem.* **2009**, *284*, 3370.

(61) GM, C. In *The Cell: A Molecular Approach*; 2nd ed.; Sinauer Associates: Sunderland, MA, 2000.

(62) Doherty, G. J.; McMahon, H. T. *Annu. Rev. Biochem.* **2009**, *78*, 857.

(63) Matveev, S.; Li, X.; Everson, W.; Smart, E. J. *Adv. Drug Del. Rev.* **2001**, *49*, 237.

(64) Mayor, S.; Pagano, R. E. *Nat. Rev. Mol. Cell Biol.* **2007**, *8*, 603.

(65) Anderson, R. G. W. *Annu. Rev. Biochem.* **1998**, *67*, 199.

(66) Orlandi, P. A.; Fishman, P. H. *J. Cell Biol.* **1998**, *141*, 905.

(67) Pelkmans, L.; Kartenbeck, J.; Helenius, A. *Nat. Cell Biol.* **2001**, *3*, 473.

(68) Lim, J. P.; Gleeson, P. A. *Immunol. Cell Biol.* **2011**, *89*, 836.

(69) El-Andaloussi, S.; Järver, P.; Johansson, Henrik J.; Langel, Ü. *Biochem. J.* **2007**, *407*, 285.

(70) Jiao, C.-Y.; Delaroche, D.; Burlina, F.; Alves, I. D.; Chassaing, G.; Sagan, S. *J. Biol. Chem.* **2009**, *284*, 33957.

(71) Richard, J. P.; Melikov, K.; Vives, E.; Ramos, C.; Verbeure, B.; Gait, M. J.; Chernomordik, L. V.; Lebleu, B. *J. Biol. Chem.* **2003**, *278*, 585.

(72) Potocky, T. B.; Menon, A. K.; Gellman, S. H. *J. Biol. Chem.* **2003**, *278*, 50188.

(73) Richard, J. P.; Melikov, K.; Brooks, H.; Prevot, P.; Lebleu, B.; Chernomordik, L. V. *J. Biol. Chem.* **2005**, *280*, 15300.

(74) Vendeville, A.; Rayne, F.; Bonhoure, A.; Bettache, N.; Montcourrier, P.; Beaumelle, B. *Molecular biology of the cell* **2004**, *15*, 2347.

(75) Saalik, P.; Elmquist, A.; Hansen, M.; Padari, K.; Saar, K.; Viht, K.; Langel, U.; Pooga, M. *Bioconjug Chem* **2004**, *15*, 1246.

(76) Jones, S. W.; Christison, R.; Bundell, K.; Voyce, C. J.; Brockbank, S. M. V.; Newham, P.; Lindsay, M. A. *Br. J. Pharmacol.* **2005**, *145*, 1093.

(77) Fittipaldi, A.; Ferrari, A.; Zoppe, M.; Arcangeli, C.; Pellegrini, V.; Beltram, F.; Giacca, M. *J. Biol. Chem.* **2003**, *278*, 34141.

(78) Ferrari, A.; Pellegrini, V.; Arcangeli, C.; Fittipaldi, A.; Giacca, M.; Beltram, F. *Mol. Ther.* **2003**, *8*, 284.

(79) Nakase, I.; Niwa, M.; Takeuchi, T.; Sonomura, K.; Kawabata, N.; Koike, Y.; Takehashi, M.; Tanaka, S.; Ueda, K.; Simpson, J. C.; Jones, A. T.; Sugiura, Y.; Futaki, S. *Mol. Ther.* **2004**, *10*, 1011.

(80) Wadia, J. S.; Stan, R. V.; Dowdy, S. F. *Nat. Med.* **2004**, *10*, 310.

(81) Duchardt, F.; Fotin-Mleczek, M.; Schwarz, H.; Fischer, R.; Brock, R. *Traffic* **2007**, *8*, 848.

(82) Nakase, I.; Tadokoro, A.; Kawabata, N.; Takeuchi, T.; Katoh, H.; Hiramoto, K.; Negishi, M.; Nomizu, M.; Sugiura, Y.; Futaki, S. *Biochemistry* **2007**, *46*, 492.

(83) Khalil, I. A.; Kogure, K.; Futaki, S.; Harashima, H. *J. Biol. Chem.* **2006**, *281*, 3544.

(84) Kaplan, I. M.; Wadia, J. S.; Dowdy, S. F. *Journal of controlled release : official journal of the Controlled Release Society* **2005**, *102*, 247.

(85) Gump, J. M.; June, R. K.; Dowdy, S. F. *J. Biol. Chem.* **2010**, *285*, 1500.

(86) Ivanov, A. I. In *Exocytosis and Endocytosis*; Ivanov, A. I., Ed.; Humana Press: Totowa, NJ, 2008, p 15.

(87) Vercauteren, D.; Vandenbroucke, R. E.; Jones, A. T.; Rejman, J.; Demeester, J.; De Smedt, S. C.; Sanders, N. N.; Braeckmans, K. *Mol. Ther.* **2010**, *18*, 561.

(88) Rothbard, J. B.; Kreider, E.; VanDeusen, C. L.; Wright, L.; Wylie, B. L.; Wender, P. A. *J. Med. Chem.* **2002**, *45*, 3612.

(89) Umezawa, N.; Gelman, M. A.; Haigis, M. C.; Raines, R. T.; Gellman, S. H. *J. Am. Chem. Soc.* **2002**, *124*, 368.

(90) Rueping, M.; Mahajan, Y.; Sauer, M.; Seebach, D. *ChemBioChem* **2002**, *3*, 257.

(91) Potocky, T. B.; Menon, A. K.; Gellman, S. H. *J. Am. Chem. Soc.* **2005**, *127*, 3686.

(92) Fillon, Y. A.; Anderson, J. P.; Chmielewski, J. *J. Am. Chem. Soc.* **2005**, *127*, 11798.

(93) Wender, P. A.; Rothbard, J. B.; Jessop, T. C.; Kreider, E. L.; Wylie, B. L. *J. Am. Chem. Soc.* **2002**, *124*, 13382.

(94) Futaki, S.; Nakase, I.; Suzuki, T.; Zhang; Sugiura, Y. *Biochemistry* **2002**, *41*, 7925.

(95) Chung, H. H.; Harms, G.; Seong, C. M.; Choi, B. H.; Min, C.; Taulane, J. P.; Goodman, M. *Biopolymers* **2004**, *76*, 83.

(96) Wender, P. A.; Kreider, E.; Pelkey, E. T.; Rothbard, J.; VanDeusen, C. L. *Organic Letters* **2005**, *7*, 4815.

(97) Tsogas, I.; Sideratou, Z.; Tsiourvas, D.; Theodossiou, T. A.; Paleos, C. M. *ChemBioChem* **2007**, *8*, 1865.

(98) Huang, K.; Voss, B.; Kumar, D.; Hamm, H. E.; Harth, E. *Bioconj. Chem.* **2007**, *18*, 403.

(99) Choi, J. S.; Nam, K.; Park, J. Y.; Kim, J. B.; Lee, J. K.; Park, J. S. *Journal of controlled release : official journal of the Controlled Release Society* **2004**, *99*, 445.

(100) Luedtke, N. W.; Carmichael, P.; Tor, Y. *J. Am. Chem. Soc.* **2003**, *125*, 12374.

(101) Elson-Schwab, L.; Garner, O. B.; Schuksz, M.; Crawford, B. E.; Esko, J. D.; Tor, Y. *J. Biol. Chem.* **2007**, *282*, 13585.

(102) Dix, A. V.; Fischer, L.; Sarrazin, S.; Redgate, C. P. H.; Esko, J. D.; Tor, Y. *ChemBioChem* **2010**, *11*, 2302.

(103) Inoue, M.; Tong, W.; Esko, J. D.; Tor, Y. *ACS Chemical Biology* **2013**, *8*, 1383.

(104) Inoue, M.; Wexselblatt, E.; Esko, J. D.; Tor, Y. *ChemBioChem* **2014**, *15*, 676.

(105) Sarrazin, S.; Wilson, B.; Sly, W. S.; Tor, Y.; Esko, J. D. *Mol. Ther.* **2010**, *18*, 1268.

(106) Wexselblatt, E.; Esko, J. D.; Tor, Y. *ACS Nano* **2015**, *9*, 3961.

(107) Maiti, K. K.; Jeon, O.-Y.; Lee, W. S.; Kim, D.-C.; Kim, K.-T.; Takeuchi, T.; Futaki, S.; Chung, S.-K. *Angewandte Chemie International Edition* **2006**, *45*, 2907.

(108) Ghosh, S. C.; Kim, B.; Im, J.; Lee, W. S.; Im, C.-N.; Chang, Y.-T.; Kim, W.; Kim, K.-T.; Chung, S.-K. *Bull. Korean Chem. Soc.* **2010**, *31*, 3623.

(109) Lee, W. S.; Kim, W.; Kim, K.-T.; Chung, S.-K. *Bull. Korean Chem. Soc.* **2011**, *32*, 2286.

(110) Maiti, K. K.; Lee, W. S.; Takeuchi, T.; Watkins, C.; Fretz, M.; Kim, D.-C.; Futaki, S.; Jones, A.; Kim, K.-T.; Chung, S.-K. *Angewandte Chemie International Edition* **2007**, *46*, 5880.

(111) Im, J.; Kim, W.; Kim, K. T.; Chung, S. K. *Chemical communications (Cambridge, England)* **2009**, 4669.

(112) Im, J.; Biswas, G.; Kim, W.; Kim, K.-T.; Chung, S.-K. *Bull. Korean Chem. Soc.* **2011**, *32*, 873.

(113) Jin, J.; Lee, W. S.; Joo, K. M.; Maiti, K. K.; Biswas, G.; Kim, W.; Kim, K.-T.; Lee, S. J.; Kim, K.-H.; Nam, D.-H.; Chung, S.-K. *MedChemComm* **2011**, *2*, 270.

(114) Higashi, T.; Khalil, I. A.; Maiti, K. K.; Lee, W. S.; Akita, H.; Harashima, H.; Chung, S. K. *Journal of controlled release : official journal of the Controlled Release Society* **2009**, *136*, 140.

(115) Im, J.; Maiti, K. K.; Kim, W.; Kim, K.-T.; Chung, S.-K. *Bull. Korean Chem. Soc.* **2011**, *32*, 1282.

(116) Biswas, G.; Jeon, O.-Y.; Lee, W. S.; Kim, D.-C.; Kim, K.-T.; Lee, S.; Chang, S.; Chung, S.-K. *Chemistry – A European Journal* **2008**, *14*, 9161.

(117) Lee, W. S.; Im, C. N.; Teng, Q. Y.; Chang, Y. T.; Kim, D. C.; Kim, K. T.; Chung, S. K. *Molecular bioSystems* **2009**, *5*, 822.

(118) Im, J.; Kim, S.; Jeong, Y.-H.; Kim, W.; Lee, D.; Lee, W. S.; Chang, Y.-T.; Kim, K.-T.; Chung, S.-K. *MedChemComm* **2013**, *4*, 310.

(119) Tanaka, M.; Machida, Y.; Niu, S.; Ikeda, T.; Jana, N. R.; Doi, H.; Kurosawa, M.; Nekooki, M.; Nukina, N. *Nat. Med.* **2004**, *10*, 148.

(120) Kikawada, T.; Saito, A.; Kanamori, Y.; Nakahara, Y.; Iwata, K.; Tanaka, D.; Watanabe, M.; Okuda, T. *Proceedings of the National Academy of Sciences of the United States of America* **2007**, *104*, 11585.

(121) Szwarc, M. *Nature* **1956**, *178*, 1168.

(122) Szwarc, M.; Levy, M.; Milkovich, R. *J. Am. Chem. Soc.* **1956**, *78*, 2656.

(123) Waack, R.; Rembaum, A.; Coombes, J. D.; Szwarc, M. *J. Am. Chem. Soc.* **1957**, *79*, 2026.

(124) Kolonko, E. M.; Kiessling, L. L. *J. Am. Chem. Soc.* **2008**, *130*, 5626.

(125) Kolonko, E. M.; Pontrello, J. K.; Mangold, S. L.; Kiessling, L. L. *J. Am. Chem. Soc.* **2009**, *131*, 7327.

(126) Hennig, A.; Gabriel, G. J.; Tew, G. N.; Matile, S. *J. Am. Chem. Soc.* **2008**, *130*, 10338.

(127) Gabriel, G. J.; Madkour, A. E.; Dabkowski, J. M.; Nelson, C. F.; Nüsslein, K.; Tew, G. N. *Biomacromolecules* **2008**, *9*, 2980.

(128) Tezgel, A. Ö.; Telfer, J. C.; Tew, G. N. *Biomacromolecules* **2011**, *12*, 3078.

(129) Som, A.; Reuter, A.; Tew, G. N. *Angewandte Chemie International Edition* **2012**, *51*, 980.

(130) deRonde, B. M.; Birke, A.; Tew, G. N. *Chemistry – A European Journal* **2015**, *21*, 3013.

(131) Tezgel, A. O.; Gonzalez-Perez, G.; Telfer, J. C.; Osborne, B. A.; Minter, L. M.; Tew, G. N. *Mol. Ther.* **2013**, *21*, 201.

(132) deRonde, B. M.; Torres, J. A.; Minter, L. M.; Tew, G. N. *Biomacromolecules* **2015**, *16*, 3172.

(133) Cooley, C. B.; Trantow, B. M.; Nederberg, F.; Kiesewetter, M. K.; Hedrick, J. L.; Waymouth, R. M.; Wender, P. A. *J. Am. Chem. Soc.* **2009**, *131*, 16401.

(134) Geihe, E. I.; Cooley, C. B.; Simon, J. R.; Kiesewetter, M. K.; Edward, J. A.; Hickerson, R. P.; Kaspar, R. L.; Hedrick, J. L.; Waymouth, R. M.; Wender, P. A. *Proc. Natl. Acad. Sci. USA* **2012**, *109*, 13171.

(135) Wender, P. A.; Huttner, M. A.; Staveness, D.; Vargas, J. R.; Xu, A. F. *Mol. Pharm.* **2015**, *12*, 742.

(136) McKinlay, C. J.; Waymouth, R. M.; Wender, P. A. *J. Am. Chem. Soc.* **2016**, *138*, 3510.

(137) Kim, T.-i.; Kim, S. W. *React. Funct. Polym.* **2011**, *71*, 344.

(138) Lin, C.; Zhong, Z.; Lok, M. C.; Jiang, X.; Hennink, W. E.; Feijen, J.; Engbersen, J. F. J. *Bioconjugate Chem.* **2007**, *18*, 138.

(139) Kim, T.-i.; Lee, M.; Kim, S. W. *Biomaterials* **2010**, *31*, 1798.

(140) Kim, T.-i.; Ou, M.; Lee, M.; Kim, S. W. *Biomaterials* **2009**, *30*, 658.

(141) Kim, S. H.; Jeong, J. H.; Kim, T.-i.; Kim, S. W.; Bull, D. A. *Mol. Pharmaceutics* **2009**, *6*, 718.

(142) Bang, E.-K.; Gasparini, G.; Molinard, G.; Roux, A.; Sakai, N.; Matile, S. *J. Am. Chem. Soc.* **2013**, *135*, 2088.

(143) Gasparini, G.; Bang, E.-K.; Molinard, G.; Tulumello, D. V.; Ward, S.; Kelley, S. O.; Roux, A.; Sakai, N.; Matile, S. *J. Am. Chem. Soc.* **2014**, *136*, 6069.

(144) Bang, E.-K.; Ward, S.; Gasparini, G.; Sakai, N.; Matile, S. *Polym. Chem.* **2014**, *5*, 2433.

(145) Chuard, N.; Gasparini, G.; Roux, A.; Sakai, N.; Matile, S. *Org. Biomol. Chem.* **2015**, *13*, 64.

(146) Gasparini, G.; Matile, S. *Chem. Commun.* **2015**, *51*, 17160.

(147) Appelqvist, H.; Wäster, P.; Kågedal, K.; Öllinger, K. *J. Mol. Cell Biol.* **2013**, *5*, 214.

Chapter 2:

Polymyxins Facilitate Entry into Mammalian Cells

2.1 Introduction

Several biological barriers stand between exogenous agents and their entry to cells and tissues. These barriers hamper the administration of therapeutic agents, limiting their delivery and therapeutic utility. For example, high molecular weight and highly charged biomolecules such as proteins and oligonucleotides display therapeutic potential but have limited cellular uptake.[1] Thus, great interest exists in developing molecular transporters as tools for exploring cell entry pathways and for facilitating the delivery of impermeable agents.

Certain natural macromolecules, for example the HIV-1 Tat protein, exhibit cellular uptake.[2-4] When added exogenously, Tat efficiently crosses cell membranes and can facilitate the uptake of conjugated or fused cargo.[4-7] The basic, arginine rich region of the protein is critical for uptake, mediated to a large extent through interaction with cell surface proteoglycans.[8-10] Since these early observations, numerous guanidinium-rich molecular transporters of varying scaffolds have been described and exploited,[11-13] and recent reports have shown that cyclic guanidinium-rich peptides have enhanced cellular uptake compared to linear peptides.[14-18]

Guanidinoglycosides constitute a distinct non-oligomeric, but multivalent, family of low MW cell penetrating scaffolds.[19] Guanidinoglycosides are derived from the naturally occurring aminoglycosides by converting the ammonium groups to guanidinium groups. They display unique uptake features when compared to other

guanidinium-rich transporters by their activity at nanomolar concentrations and dependence on cell surface heparan sulfate proteoglycans for cellular entry. A variety of analogs derived from different aminoglycosides enable uptake of large, bioactive cargo into cells.[20-23]

Recent observations suggesting similarities between aminoglycosides and polymyxins,[24] in addition to their analogous self-promoted uptake mechanisms in bacterial cells,[25-27] have provoked a hypothesis that guanidinylated derivatives of the latter may display useful cellular entry features in mammalian cells. Here we explore the cellular delivery and internalization mechanism of high molecular weight biomolecules and nano-assemblies using polymyxin (PMB) and guanidinopolymyxin (GPMB) derivatives as carriers. Unlike the guanidinoglycosides that show substantially enhanced cellular uptake, when compared to their parent aminoglycoside precursors, both PMB and GPMB display highly competent uptake in mammalian cells. Intriguingly, while the cellular uptake of PMB and GPMB remains highly dependent on cell surface heparan sulfate, a fine mechanistic analysis suggests unique internalization pathways and more efficient cytosolic delivery than other well-studied molecular transporters. Our major conclusions include: (1) polymyxin and its guanidinylated form effectively enter mammalian cells, (2) the cyclic peptide and not the hydrophobic tail is the entry-facilitating module, and (3) these molecules can facilitate the cellular delivery of large biomolecules and liposomal assemblies. We further speculate that the effective entry of parent natural antibiotics into mammalian cells, coupled to earlier observations indicating their ability to interfere with eukaryotic translation,[24] may

contribute to their adverse cytotoxic effects in mammals. These observations, in addition to enriching the repertoire of cellular delivery vehicles, illustrate the wide landscape and potential utility of new ammonium and guanidinium rich transporters.

2.2. Results

Synthetic strategy

We envisioned a convergent synthesis, wherein the PMB molecular transporters were made via amide formation from two fragments, a biotinylated linker and the PMB core (Scheme 2.1). Relying on steric hindrance of the primary amine of Thr2, the primary amines on Dab residues of the polymyxin core could be tetra-Boc protected[28] or guanidinylated. Instead of synthesizing these PMB derivatives de novo, enzymatic hydrolysis of the fatty acyl chain-Dab1 portion of the commercially available PMB can generate the polymyxin B nonapeptide (PMBN).[29-31] The linker can be formed by a 1,3-dipolar cycloaddition of an alkyne portion and an azide-containing biotinylated linker.[21] The enzymatically cleaved Dab residue can be reintroduced as part of the linker by amide bond formation to hexynoic acid so the final product will be similar to the natural PMB scaffold containing five Dab moieties (and the same number of primary amines).

Synthesis of transporters

The fatty acid chain and Dab1 residue on PMB (**2.1**) were cleaved with Ficin to generate PMBN (**2.2**).[29-31] PMBN (**2.2**) was subsequently tetra-Boc-protected[28] using Boc-ON or Boc-guanidinylated using *N*,*N*′-Di-Boc-1*H*-pyrazole-1-carboxamidine to afford **2.3a** and **2.3b**, respectively (Scheme 2.2).

5-Hexynoic acid (**2.4**) was first coupled to H-Dab(Boc)-OMe (**2.5**) to yield **2.6a**. Deprotection and guanidinylation of **2.6a** provided **2.6b**. A copper catalyzed 1,3-dipolar cycloaddition of **2.6a** or **2.6b** with an azide-terminated biotin-PEG_3 fragment (**2.7**) previously used in our lab,[21] yielded compounds **2.8a** and **2.8b**, with subsequent hydrolysis providing **2.9a** and **2.9b** (Scheme 2.3).

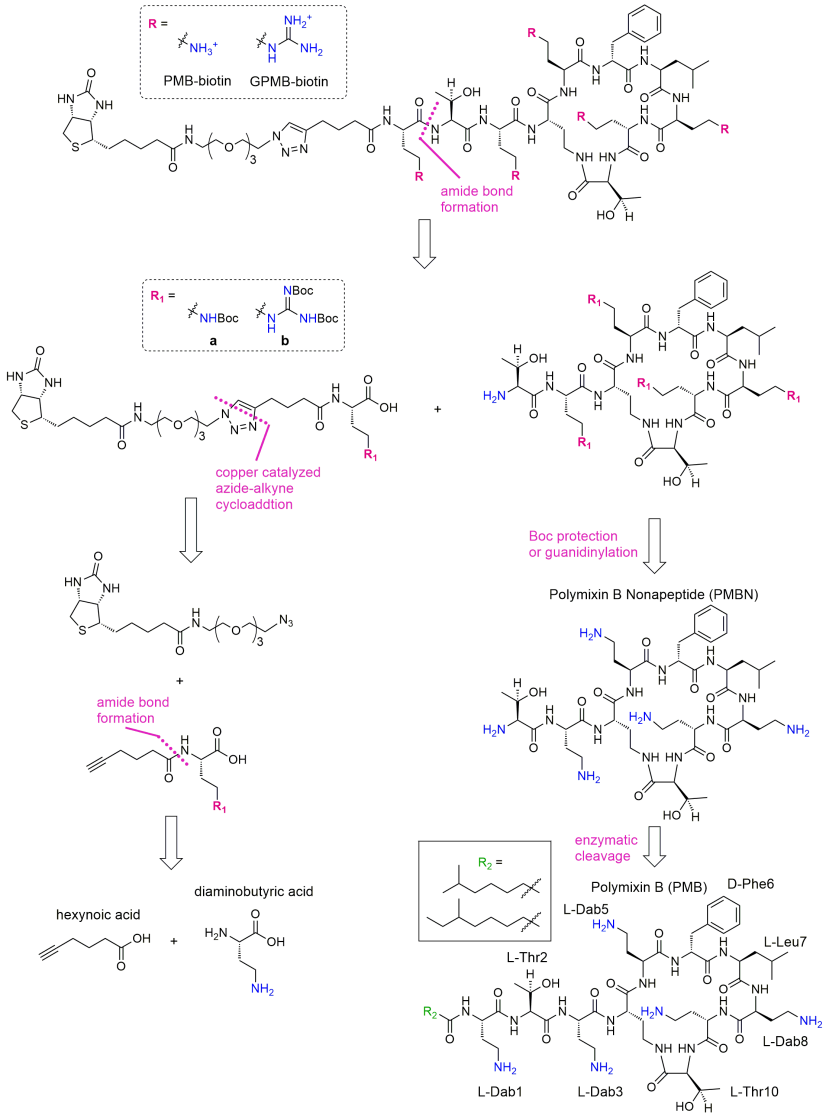

Scheme 2.1 Retrosynthesis of biotinylated PMB and GPMB.

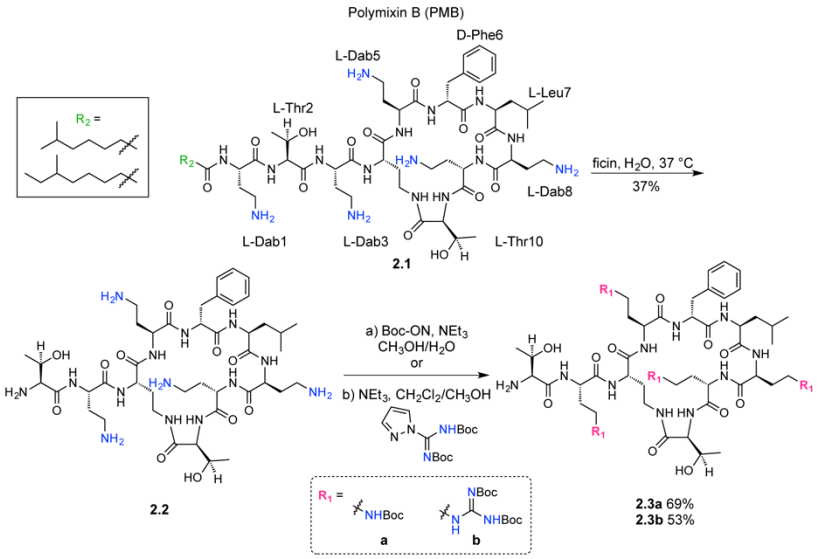

Scheme 2.2. Synthesis of Boc-protected PMBN and Boc-guanidinylated PMBN.

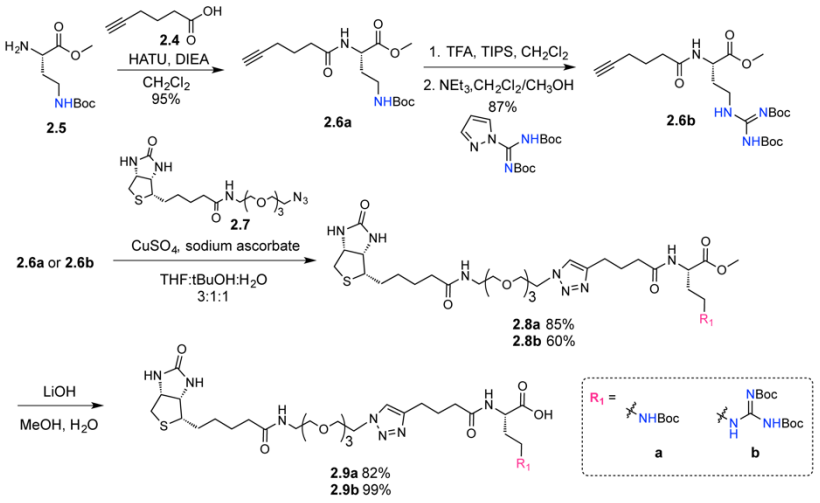

Scheme 2.3. Synthesis of biotinylated linker.

The biotinylated Dab linker (**2.9a** or **2.9b**) was then coupled to Boc-protected PMBN (**2.3a**) or Boc-protected guanidinylated PMBN (**2.3b**), and subsequently deprotected using trifluoroacetic acid (TFA) in dichloromethane and tri-iso-propyl silane (TIPS) as a scavenger. HPLC purification afforded the analytically pure bPMB (**2.10a**) and bGPMB (**2.10b**) (Scheme 2.4).

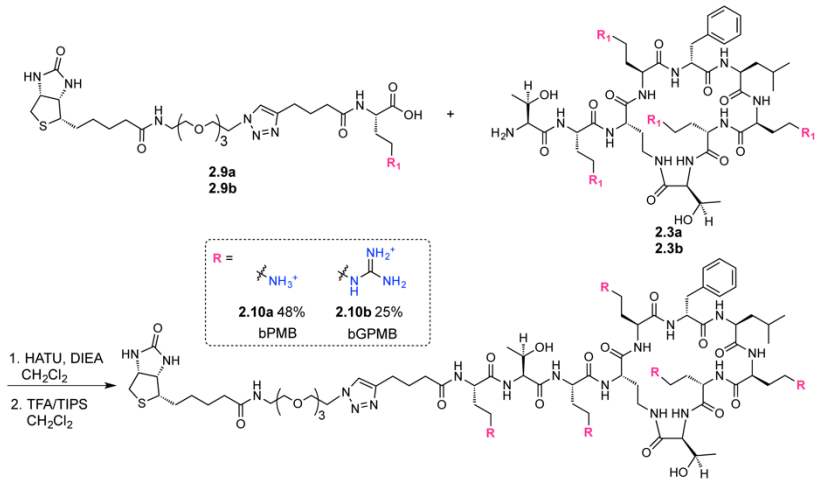

Scheme 2.4. Synthesis of polymyxin and guanidinopolymyxin transporters.

The same azide-terminated biotin linker **2.7** was clicked to the previously reported alkyne-tobramycin or alkyne-guanidinotobramycin[21] derivatives to yield biotinylated tobramycin (bTob) and guanidinotobramycin (bGTob) (Figure 2.1a and Scheme 2.5). For comparison, biotinylated octaarginine (bArg8, Figure 2.1b) was synthesized using standard solid phase peptide synthesis protocols. An aminohexanoic acid spacer was introduced at the N-terminus and coupled to biotin-NHS.

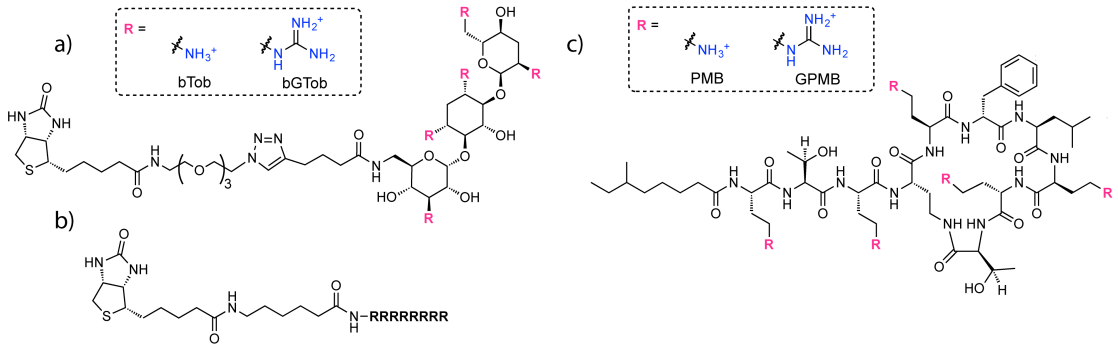

Figure 2.1. Structures of bTob and bGTob (a) bArg8 (b) and PMB and GPMB (c).

To obtain the PMB and GPMB transporters (Figure 2.1c), commercially available PMB was HPLC purified to isolate PMB terminated with 6-

methyloctanoic acid. Purified PMB was then guanidinylated using *N*,*N*′-Di-Boc-1*H*-pyrazole-1-carboxamidine followed by TFA deprotection to yield GPMB.

Formation of biotin-streptavidin complexes

Biotinylated transporters allow conjugation of the carriers to fluorescent proteins and the ability to test a variety of analogs in different assays. Biotinylated carriers were incubated in a 5:1 molar ratio with streptavidin derivatives for 20 min at room temperature. Conjugates were then diluted in culture medium to the final streptavidin concentration. Streptavidin conjugated to R-phycoerythrin (PE) coupled to the cyanine dye Cy5 (ST-PE-Cy5) was used as a high molecular weight model protein (MW = 300 kDa), streptavidin-Cy5 (ST-Cy5) was used for microscopy experiments, and streptavidin-saporin was used to analyze cytosolic delivery.

Cellular uptake and cell surface binding in wild type and heparan sulfate-deficient CHO cells

Wild type CHO-K1 cells were incubated with the carrier-ST-PE-Cy5 conjugate for 1 h at 37 °C, detached with trypsin/EDTA, and analyzed by flow cytometry. Uptake of the fluorescent conjugate occurred at concentrations as low as 2 nM and increased in a dose dependent manner (Figure 2.2a). bGTob showed uptake behavior similar to bPMB and bGPMB whereas bTob exhibited a ten-fold reduction in uptake. bArg8 showed approximately two- to three-fold higher uptake than bPMB and bGPMB. Similar uptake patterns for bPMB and bGPMB were also observed in the human embryonic kidney cell line HEK-293 and the human hepatocyte cell line HEP-3B (Figure 2.2b). CellTiter-Blue assays indicate that

bPMB and bGPMB showed no cytotoxicity when incubated with either CHO-K1 or HEK-293 cell lines for 72 h at concentrations as high as 0.5 μM (Figure 2.2c&d). To demonstrate that the formation of a stable biotin-streptavidin complex is necessary for cellular delivery, ST-PE-Cy5 was incubated with PMB and GPMB, which do not contain the biotin moiety. Figure 2.3 shows no enhanced uptake of ST-PE-Cy5 in the absence of the biotin-linked transporter.

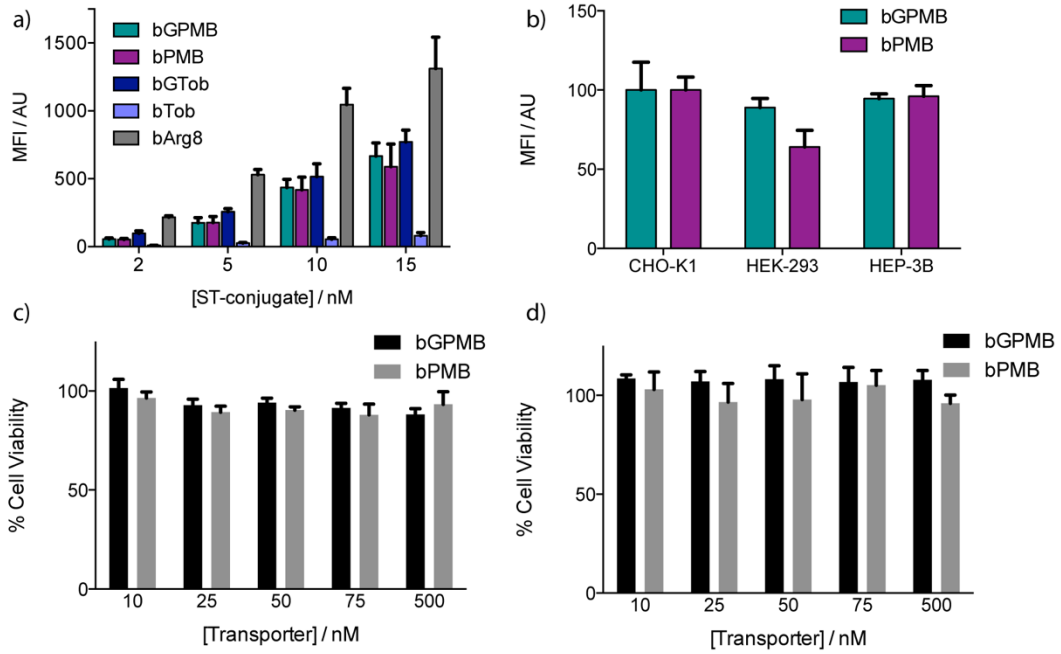

Figure 2.2. Cellular uptake and cell viability of bPMB and bGPMB. Mean fluorescence intensity (MFI) was measured by flow cytometry. The background signal from untreated cells was subtracted. a) Cellular uptake of biotinylated guanidinopolymyxin (bGPMB), polymyxin (bPMB), guanidinotobramycin (bGTob), tobramycin (bTob), and octarginine (bArg8) conjugated to ST-PE-Cy5. CHO-K1 cells were incubated with the conjugates at the indicated concentrations at 37 °C for 1 h and lifted with EDTA/trypsin. b) Cellular uptake of bGPMB and bPMB conjugated to ST-PE-Cy5. CHO-K1, HEK-293, and HEP-3B cells were incubated with conjugate (5nM) at 37 °C for 1 h. CHO-K1 cells (c) and HEK-293 cells (d) were incubated with various concentrations of GPMB-biotin or PMB-biotin in complete media for 72 hours in a 96-well plate. Cell titer blue was added and incubated an additional 4 hours. Cell viability was calculated by measuring the fluorescence intensity at 560/590 and comparing the signal to untreated cells.

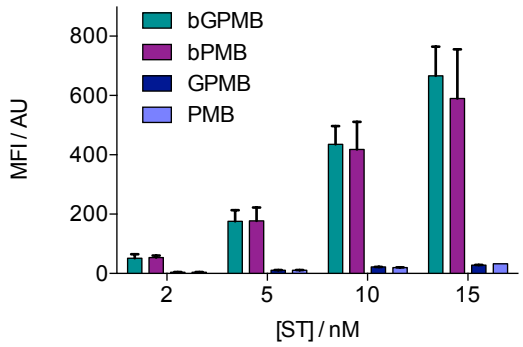

Figure 2.3. Cellular uptake control with GPMB and PMB. ST-PE-Cy5 was incubated with biotinylated compounds bPMB or bGPMB, or with non-biotinylated compounds PMB or GPMB, then diluted to the desired final ST-PE-Cy5 concentrations. The mixtures were then added to CHO-K1 cells and incubated at 37 °C for 1 h. Mean fluorescence intensity was measured by flow cytometry and the background signal from untreated cells was subtracted.

The dependence of bPMB and bGPMB on cell surface heparan sulfate (HS) proteoglycans for cellular entry was evaluated using two mutant CHO cell lines, pgsA-745 which does not express neither HS nor chondroitin sulfate/dermatan sulfate (CS/DS), and pgsD-677 which does not express HS but expresses 2 to 3-fold higher levels of CS/DS. Figure 2.4a shows uptake in HS-deficient cell lines was reduced to <20% of that observed in wild-type cells.

To investigate cell-surface binding, CHO-K1 cells were incubated for 1 h with the fluorescent conjugates at 37 °C and harvested using EDTA to prevent cleavage of cell-surface bound compounds. The fluorescence signal was compared to that observed when cells were lifted with EDTA/trypsin, which removes cell surface proteoglycans. Figure 2.4b shows that for both bPMB and bGPMB, binding accounts for about 15% of the signal. Greater binding was observed in CHO-K1 cells compared to mutant pgsA-745 cells for both transporters (Figure 2.4b).

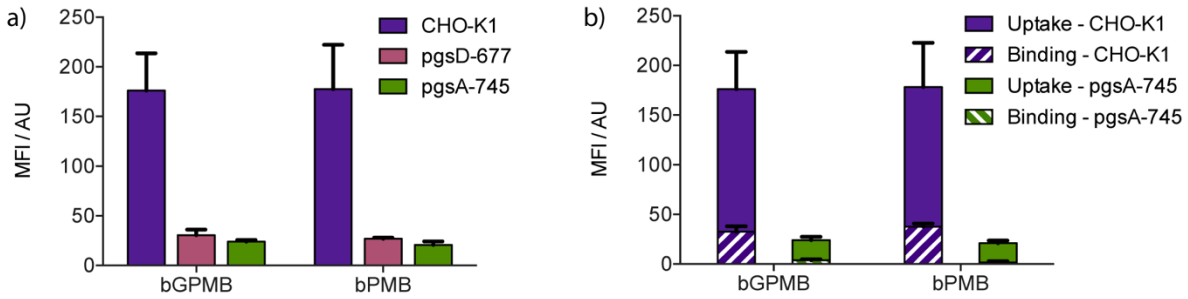

Figure 2.4 Cellular uptake and binding in wild-type and mutant CHO cells. Mean fluorescence intensity (MFI) was measured by flow cytometry.[29] The background signal from untreated cells was subtracted. a) bGPMB and bPMB streptavidin-PE-Cy5 conjugates (5 nM) were incubated with WT and mutant CHO cell lines for 1 h at 37 °C then lifted with EDTA/trypsin. b) CHO-K1 and pgsA-745 cells were incubated with bGPMB and bPMB streptavidin-PE-Cy5 conjugates (5 nM) for 1 h at 37 °C. Cells were lifted with EDTA only (binding+uptake) or EDTA/trypsin (uptake). Binding values were determined by subtracting the MFI values obtained for cells lifted with EDTA/trypsin from those obtained for cells lifted with EDTA only.

Mechanism(s) of uptake

To shed light on the internalization mechanism(s), the contribution of various endocytotic pathways was evaluated pharmacologically. CHO-K1 cells were incubated with the fluorescent bPMB or bGPMB conjugates at 4 °C to assess the contribution of energy-dependent processes. Further, uptake was evaluated in cells pretreated with inhibitors of macropinocytosis (amiloride), clathrin-mediated endocytosis (sucrose and chlorpromazine) or caveolae-mediated endocytosis (genistein and nystatin) (Figure 2.5). Their inhibitory effect on the uptake of bGTob was also evaluated for comparison. While low temperature practically abolished internalization, treatment with amiloride, sucrose or chlorpromazine did not affect the cellular uptake of bPMB or bGPMB high MW conjugates. However, in cells treated with either genistein or nystatin, cellular uptake was reduced by ~50–60%, indicating that bPMB and bGPMB conjugates internalize through energy-dependent processes, presumably through caveolae-mediated pathways. bGTob, on the other

hand, showed reduced uptake in the presence of sucrose, chlorpromazine and genistein and no change in uptake when cells were treated with amiloride or nystatin (Figure 2.5), indicating a different mechanism of uptake.

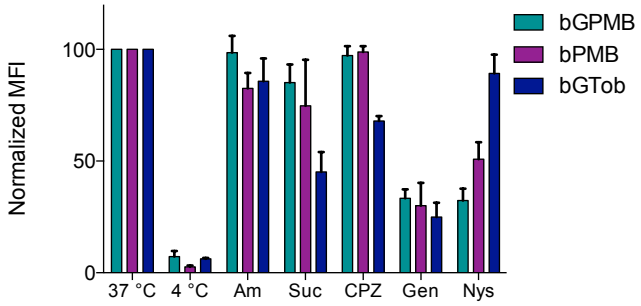

Figure 2.5. Cellular uptake in the presence of inhibitors. CHO-K1 cells were incubated with bGPMB, bPMB, or bTob conjugated to streptavidin-PE-Cy5 (5 nM) for 1 h at 37 °C or 4 °C. For inhibition experiments, cells were pretreated with amiloride (Am, 10 min, 5 mM), sucrose (Suc, 30 min, 400 mM), chlorpromazine (CPZ, 30 min, 20 μM), genistein (Gen, 30 min, 200 μM), or nystatin (Nys, 30 min, 5 μM) at 37 °C prior to incubation with the conjugate (5 nM).

Intracellular localization

To learn about the intracellular localization of these transporters, wild type CHO-K1 cells were incubated with the carrier–ST-Cy5 conjugates (20 nM) for 1 h at 37 °C and imaged using confocal laser scanning microscopy (CLSM). Cells were further treated with the nuclear stain Hoechst 33342 and the lysosomal marker LysoTracker Green DND-26 (Figure 2.6). The images show transporter accumulation in punctate vesicles. Overlaying the images from the green and far red (pseudo-colored in red) channels reveals a moderate degree of co-localization for the conjugates and LysoTracker-stained compartments, resulting in a Pearson's correlation of 0.62 for both bPMB and bGPMB (Figure 2.6). FACS analyses of carrier-ST-Cy5 conjugates up to 20 nM (Figure 2.7) were consistent with ST-PE-Cy5 delivery.

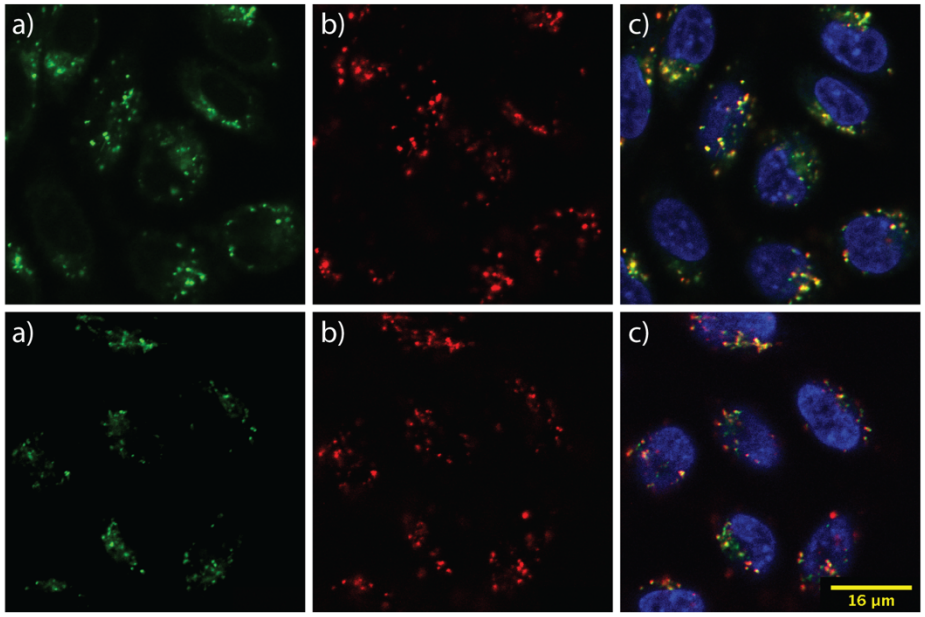

Figure 2.6. Intracellular localization of bGPMB and bPMB. Confocal microscopy images of CHO K1 cells incubated for 1 h at 37 °C with bGPMB (upper panels) or bPMB (lower panels) conjugated to streptavidin-Cy5 (20 nM) (a) LysoTracker Green (b) ST-Cy5 conjugate (c) merged images with nuclear Hoechst Dye.

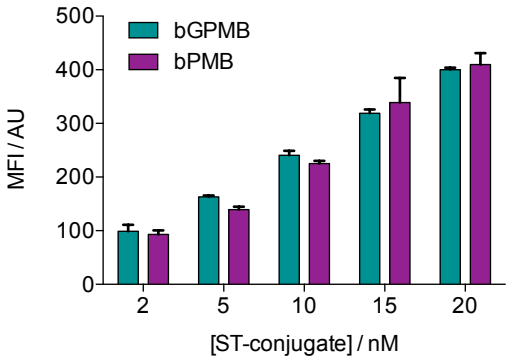

Figure 2.7. Cellular uptake of ST-Cy5. CHO-K1 cells were incubated with bPMB or bGPMB conjugated to streptavidin-PE-Cy5 at various concentrations for 1 h at 37 °C. Mean fluorescence intensity was measured and the background signal from untreated cells was subtracted.

Cytoplasmic delivery

The ability of bPMB and bGPMB to deliver cargo to the cytosol was evaluated by conjugating the transporter to a ribosome-inactivating toxin, streptavidin-saporin (ST-SAP), and incubating the conjugate with CHO-K1 or pgsA cells at various concentrations. After four days, the CellTiter-Blue assay was used to asses the number of viable cells.

Figure 2.8a shows bPMB and bGPMB have LD_{50} values of 3.1 nM and 3.3 nM respectively. bGTob has an LD_{50} value of 13.2 nM and bArg8 of 3.1 nM. Additionally, ST-SAP without transporter or saporin without streptavidin incubated with bPMB and bGPMB were unable to induce cell death (Figure 2.8b) indicating the need of forming the biotin-ST complex. ST-SAP-transporter conjugates showed no toxicity in pgsA cells (Figure 2.8c).

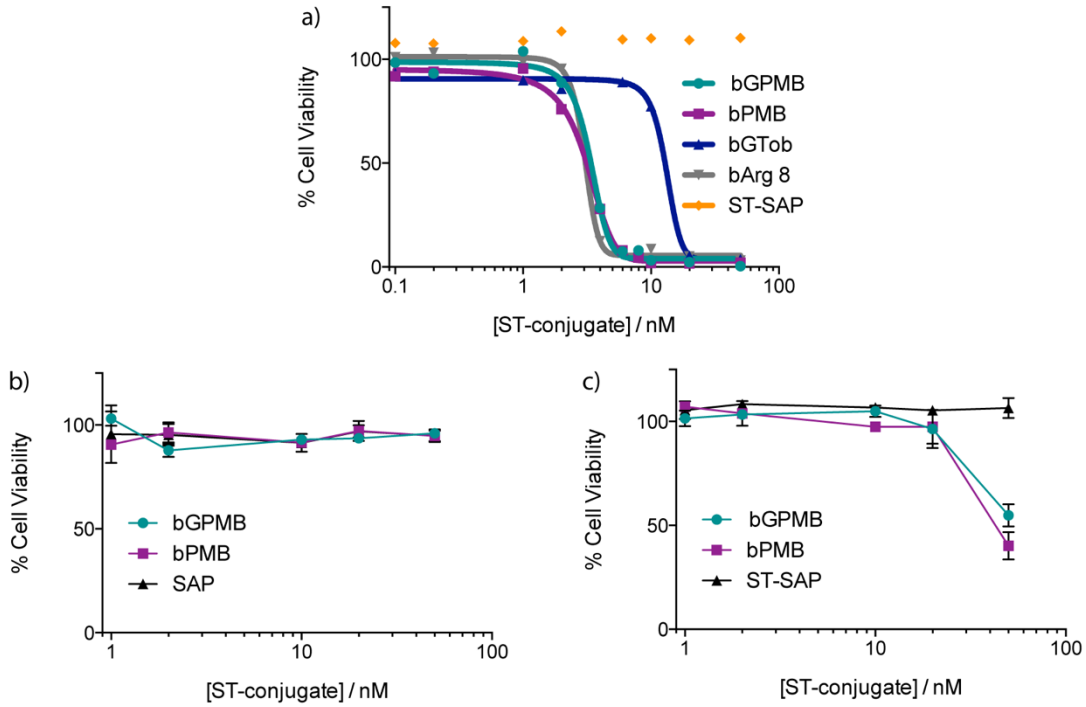

Figure 2.8. Delivery of saporin. a) CHO-K1 cells were incubated with transporter-streptavidin-saporin conjugates at 37 °C. b) Saporin (no streptavidin) was incubated with bPMB or bGPMB for 20 min then dliuted to final saporin concentrations and added to CHO-K1 cells. c) pgsA cells were incubated with transporter-streptavidin-saporin conjugates at 37 °C. In all cases, the number of viable cells was determined after four days using CellTiter-Blue and measuring fluorescence intensity at 560/590.

Cellular uptake of PMB and GPMB modified liposomes

To examine the significance of the cyclic peptide as a delivery module, rather than the lipophilic tail, and the versatility of PMB and GPMB as transporters, liposomes containing the fluorescent Cy5 dye were mixed with 10 mol% PMB or

GPMB. Uptake was evaluated using flow cytometry and the size and zeta potential of the liposomes were measured using dynamic light scattering (DLS) and are reported in Table 2.1. Both carriers showed the ability to enhance delivery of cargo containing liposomes into wild-type CHO cells with similar efficacy (Figure 2.9).

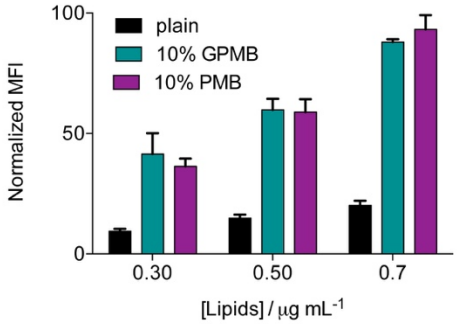

Figure 2.9. Cellular uptake of PMB and GPMB liposomes**.** CHO-K1 cells were incubated with plain and PMB or GPMB decorated liposomes at the indicated concentration for 1h at 37 °C. The background signal from untreated cells was subtracted and the MFI was normalized.

Table 2.1. Physicochemical characterization of PMB and GPMB liposomes. Size, polydispersity, and zeta-potential of evaluated liposomes. Plain liposomes were compared to liposomes mixed with 10 mol% GPMB or 10 mol% PMB.

	Z-average (± SD) / nm	PDI (± SD)	Z-potential (± SD) / mV
Plain liposomes	143.9 (4.0)	0.122 (.039)	3.78 (0.09)
GPMB liposomes	138.2 (1.9)	0.166 (0.021)	26.9 (0.70)
PMB liposomes	139.7 (1.7)	0.164 (0.056)	22.0 (0.70)

2.3 Discussion

Polymyxin B is a cyclic polypeptide antibiotic containing five primary amines and an eight carbon fatty acid chain, used against Gram-negative bacteria.[32]. The proposed antibacterial mechanism of action first involves electrostatic interactions between the positively charged 2,4-diaminobutyric acid (Dab) residues

with the negatively charged bacterial lipopolysaccharide phosphate groups.[33-36] This interaction facilitates insertion of the lipophilic moieties and disruption of the outer membrane.[33-37] Internalized polymyxin, through self-promoted uptake, can then interact with the cytoplasmic membrane, a pathway that remains poorly characterized.[33,34] Clinical use of polymyxin has diminished due to observed neurotoxicity and nephrotoxicity.[38] Recently, however, with the increase in resistant gram-negative infections, the clinical use of polymyxins has been resurrected.[39-42]

Interestingly, the cellular uptake of polymyxins in eukaryotic cells has predominantly been studied in renal tubular cells in order to better understand their observed nephrotoxicity.[43-47] While the entry pathway in renal cells is still not completely known, it has been suggested that at low micromolar concentrations it is carrier-mediated, possibly by the multiligand receptor megalin, and is similar to the uptake mechanism of aminoglycoside antibiotics.[43,44] As mentioned previously, guanidinylation of aminoglycosides transforms these potent antibiotics into a family of highly efficient eukaryotic cell-transporters.[19,20] Their unique 3D display of guanidinium groups has proven to be key to their cellular uptake,[20,21] and their multivalency has been linked to cell surface aggregation of heparan sulfate proteoglycans leading to endocytosis.[23] Cargo–carrier complexes accumulate in the lysosomes through this endocytotic heparan sulfate-dependent uptake pathway, providing useful transporters for lysosomal delivery.[22,48] Inspired by the observed similarities between aminoglycosides and polymyxins,[24-27] we synthesized both polymyxin and guanidinylated polymyxin derived transporters and investigated their uptake in CHO cells.

To evaluate the ability of PMB and GPMB to deliver large, bioactive cargo into mammalian cells, biotinylated derivatives were synthesized and conjugated to streptavidin-PE-Cy5, a fluorescently tagged, high molecular weight protein (MW 300 kDa). Uptake of bPMB and bGPMB in wild-type CHO cells was observed at low nanomolar transporter concentrations. While conversion of ammonium groups to guanidinium groups generally enhances cellular uptake rather dramatically,[10,49] as seen with the conversion of bTob to bGTob (Figure 2.2a) and after guanidinylation of other aminoglycosides,[19,20] bPMB and bGPMB exhibit comparable cellular uptake (Figure 2.2a). This surprising observation suggests that both bPMB and bGPMB are able to form related interactions with the extracellular components that facilitate their internalization. When compared to bGTob, which has five guanidinium groups, these novel polymyxin-based carriers show the same cellular uptake efficiencies. Furthermore, similar uptake patterns were observed in two human cell lines, HEK-293 and HEP-3B, suggesting that this phenomenon is cell-type independent. Of significance for potential applications as a cellular delivery tool, we showed that bPMB and bGPMB are nontoxic to mammalian cells at sub-micromolar concentrations using the CellTiter-Blue assay (Figure S2.2c and 2.2d). Treated cells were >90% viable compared to untreated control cells after incubation for 72 h at concentrations as high as 0.5 μM, six-fold higher than the highest concentrations used in uptake assays. This is not necessarily unexpected, as previous studies have shown that polymyxin analogs lacking the fatty acid tail, for example PMBN, have less acute toxicity and reduced nephrotoxicity.[29,50-52] This

suggests that the cyclic peptide core can potentially serve as a non-toxic transporting module.

To investigate the involvement of cell surface glycosaminoglycans in the cellular uptake of these transporters, two mutant CHO cell lines were used, pgsA-745 and pgsD-677.[53,54] The former does not produce heparan sulfate (HS) or chondroitin sulfate (CS) while the latter does not express HS and expresses elevated levels of CS. The cellular uptake of bPMB and bGPMB is significantly diminished in the absence of HS by about seven-fold (Figure 2.4a). These experiments imply that the internalization of both bPMB and bGPMB rely on the presence of HS on the cell surface. The polycationic scaffold must therefore preferentially bind HS over other negatively charged cell surface glycans.

To examine cell-surface binding, cells were incubated with the fluorescent conjugates and harvested using only EDTA to prevent cleavage of cell-surface bound compounds. The fluorescence signal was compared to that arising from cells lifted with EDTA/trypsin, which effectively cleaves the cell surface bound components and represents only internalized conjugate. Figure 2.4b shows that although surface binding is observed (ca. 15% of the signal), these conjugates are efficiently internalized into wild type cells. bPMB and bGPMB derivatives display a comparable ratio between cellular uptake and surface binding. Additionally, greater binding was observed in CHO-K1 cells compared to mutant pgsA-745 cells for both transporters (Figure 2.4b). This is consistent with the observation that bPMB and bGPMB rely on interactions with cell surface heparan sulfate proteoglycans for internalization.

To gain insight into the potential internalization pathway(s) of these transporters, various endocytosis mechanisms were probed. Cellular uptake at low temperatures was initially evaluated to determine the contribution of energy-dependent processes. Minimal uptake of bPMB and bGPMB at low temperatures suggests endocytosis as the predominant mode of uptake. Known inhibitors of various endocytotic pathways were then used to analyze the uptake mechanisms of the high MW bPMB or bGPMB conjugates, including amiloride, sucrose, chlorpromazine, genistein and nystatin. Amiloride inhibits macropinocytosis by impairing Na+/H+ exchange.[55,56] Hypertonic sucrose and chlorpromazine are known inhibitors of clathrin-mediated endocytosis through dissociation of clathrin lattices on the plasma membrane and inhibition of clathrin-coated pit formation, respectively.[57,58] Genistein and nystatin were used to investigate caveolin-dependent endocytosis. Genistein is a tyrosine kinase inhibitor that inhibits caveolar endocytosis by preventing vesicle fusion.[59-61] Nystatin sequesters membrane cholesterol and inhibits lipid raft/caveolae mediated uptake.[62,63] Treatment of cells with amiloride, surcrose, or chlorpromazine resulted in little to no effect on uptake, whereas genistein and nystatin reduced cellular uptake of bPMB and bGPMB conjugates by over 50% compared to untreated cells (Figure 2.5). Taken together, these results suggest that bPMB and bGPMB conjugates internalize predominantly through caveolae-mediated pathways.

Although bGTob has five guanidinium groups and shows similar uptake to bPMB and bGPMB, the mechanisms of its cellular uptake differ. bGTob is also internalized through energy-dependent processes but uptake is inhibited by clathrin-

dependent-endocytocis inhibitors sucrose and chlorpromazine (Figure 2.5). The cellular uptake of bGTob is also reduced in the presence of genistein, suggesting bGTob is internalized through both clathrin-dependent and –independent endocytosis. Imaging studies (Figure 2.6) further support that bPMB and bGPMB are internalized through endocytosis.

To establish whether bPMB and bGPMB can deliver cargo to the cytosol, ST-SAP conjugated bPMB and bGPMB were added to CHO K1 or pgsA cells and cell death was monitored using the CellTiter-Blue assay. Saporin, a Type I ribosome-inactivating protein from *Saponaria officinalis* seeds, is an ideal candidate for evaluating cytosol delivery because it exhibits minimal cellular uptake on its own and needs to reach its cytosolic targets (ribosomal RNA) to exert its cytotoxic activity.[64] As shown in Figure 2.8, both bPMB- and bGPMB-saporin complexes killed CHO-K1 cells with an LD_{50} of ~ 3 nM. Although bGTob shows similar uptake efficiency as bPMB and bGPMB, its LD_{50} is almost seven-fold higher. Likewise, bArg8 showed three-fold higher uptake but a similar LD_{50} as bPMB and bGPMB suggesting a higher ability of bPMB and bGPMB to escape the endosomal uptake pathway and deliver a bioactive protein to the cytosol. The resistance of pgsA cells to transporter–toxin conjugates (Figure 2.8c) once again confirms the role of heparan sulfate in the uptake of bPMB and bGPMB.

The versatility of PMB and GPMB as transporters was further illustrated by incorporating these amphiphiles into preformed, cargo-containing liposomes. The hydrophobic tail of PMB is known to interact with phospholipids;[65,66] therefore, we used a post-insertion method to incorporate PMB or GPMB into premade and

preloaded liposomes. Figure 2.9 shows that compared to unmodified liposomes, PMB and GPMB-containing liposomes exhibit enhanced cellular uptake. As with the chemically conjugated cargo, no difference between PMB and GPMB was observed.

Lipid vesicles have previously been modified with cell-penetrating peptides and used to improve delivery of various drugs and cargo while avoiding covalent modification of the cargo.[67-73] The unique angle presented here is that we exploit the innate amphiphilic feature of PMB and its ability to act as a molecular transporter to assemble a novel delivery system utilizing a commercially available transporter. Unlike other transporter-modified liposomes, synthesis of a carrier-lipid or covalent modification of the liposome surface is not required. Furthermore, our observations with the decorated lipososmes further corroborate that the cyclic, polycationic portion of PMB is able to facilitate its entry into mammalian cells despite the hydrophobic tail. These observations may prove useful in advancing the understanding of the nephrotoxic effects impart by PMB and perhaps lead to novel safer polymyxins analogs with potent antibacterial features and minimal accumulation in human cells.

2.4 Conclusions

In summary, we have synthesized two new transporter modules derived from polymyxin B that can internalize and deliver large biomolecules, such as proteins, into mammalian cells via interactions with cell surface heparan sulfate. Inhibition studies indicate that these transporters are internalized through endocytosis,

primarily caveolae-mediated mechanisms, and predominantly localize in the lysosomes. Delivery of a ribosome-inactivating toxin demonstrates higher endosomal escape of these transporters when compared to bGTob or bArg8, which exhibit equal or greater overall uptake respectively. Furthermore, the natural polymyxin scaffold can spontaneously be incorporated into liposomes and substantially enhance their intracellular uptake. This suggests the potential for PMB and GPMB to expand our ability to selectively deliver bioactive cargo to intracellular targets and organelles. Additionally, the effective cellular uptake of the polymyxin-based transporter in eukaryotic cells presented here could help explain the observed human toxicity of the parent antibiotic.

2.5 Experimental

Materials

Materials obtained from commercial suppliers were used without further purification. Polymyxin B and tobramycin were purchased from TCI America. H-Dab(Boc)-OMe was purchased from Chem Impex International. Ficin was purchased from MP Biomedicals. Deuterated NMR solvents were purchased from Cambridge Isotope Laboratories. Amiloride, sucrose, and genistein were purchased from Sigma-Aldrich. Nystatin and EDTA/Trypsin were purchased from VWR and chlorpromazine was purchased from Fisher. Steptavidin-PE-Cy5 was purchased from Biolegend. PBS, F-12 media, Versene, streptavidin Cy-5, LysoTracker Green, and Hoescht dye were purchased from Life Technologies. Streptavidin saporin was purchased from Advanced Targeting Systems. 35 mm glass bottom culture dishes

were purchased from MatTek. CellTiter-Blue was purchased from Promega. DOPC (1,2-dioleoyl-snglycero-3-phosphocholine), DOPE (1,2-dioleoyl-sn-glycero-3-phospho-ethanolamine), and cholesterol were purchased from Avanti Polar Lipids.

Instrumentation

NMR spectra were recorded on a Varian VX 500 MHz spectrometer or a Varian 400 MHz spectrometer. Mass spectra were recorded at UCSD Chemistry and Biochemistry Mass Spectrometry Facility utilizing an Agilent 6230 HR-ESI-TOF mass spectrometer. Reverse-phase HPLC purification (CLIPEUS, C18, 5μm, 10x250 mm, Higgins analytical) and analysis (Eclipse, XDB-C18, 5μm, 4.6x150 mm) were carried out on an Agilent 1200 series instrument or Beckman Coulter System Gold 127P Solvent Module. Flow cytometry studies were performed on a BD FACSCalibur. Confocal laser scanning microscopy was performed using a Nikon A1R inverted fluorescence microscope with z-stepping motor. Particle size, polydispersity, and surface charge of the lipid vesicles were measured by dynamic light scattering on a Zetasizer Nano ZS (model ZEN3600 from Malvern Instruments).

Synthesis

PMBN (2.2). PMB (**2.1**, 2.0 g, 1.4 mmol) was dissolved in 50 mL of H_2O. Then 42 mg of dithiothreitrol and 450 mg of ficin (320-500 milk clotting units/mg) were added and the reaction was heated to 37 °C and stirred overnight. When all PMB was consumed and only PMBN was detected by HPLC, the reaction was heated to reflux to denature the enzyme. After cooling, the precipitate was filtered off and the mother liqueur was evaporated under reduced pressure. The product was purified by automated flash

chromatography Teledyne Isco Redisep Rf C18 30g gold column using a gradient of 0 – 15% ACN (0.1 % TFA) in H_2O (0.1% TFA), resulting in the TFA salt of **2.2** as a beige solid (1.5 g, 1.0 mmol, 72% yield). ^{1}H NMR (400 MHz, D_2O) δ 7.41 – 7.28 (m, 3H), 7.24 (d, *J* = 7.6 Hz, 2H), 4.58 – 4.45 (m, 3H), 4.32 – 4.12 (m, 7H), 3.95 (d, *J* = 5.5 Hz, 1H), 3.38 – 3.25 (m, 1H), 3.21 – 2.96 (m, 9H), 2.93 – 2.74 (m, 2H), 2.29 – 1.77 (m, 10H), 1.50 – 1.23 (m, 5H), 1.17 (d, *J* = 6.3 Hz, 3H), 0.77 – 0.59 (m, 7H). ^{13}C NMR (126 MHz, D_2O) δ 174.99, 173.33, 173.30, 172.72, 172.68, 171.94, 171.59, 171.39, 168.13, 163.29, 163.01, 162.73, 162.44, 135.41, 128.93, 127.37, 119.73, 117.41, 115.09, 112.77, 66.18, 66.01, 59.44, 58.16, 55.76, 52.85, 51.84, 51.72, 51.67, 51.19, 50.38, 39.04, 36.78, 36.38, 36.33, 36.08, 35.85, 30.51, 29.65, 28.61, 28.13, 27.76, 23.37, 22.28, 20.21, 19.05, 18.49. HR-ESI-MS calculated for $C_{43}H_{74}N_{14}O_{11}$ $[M+H]^+$ 963.5733, found 963.5734.

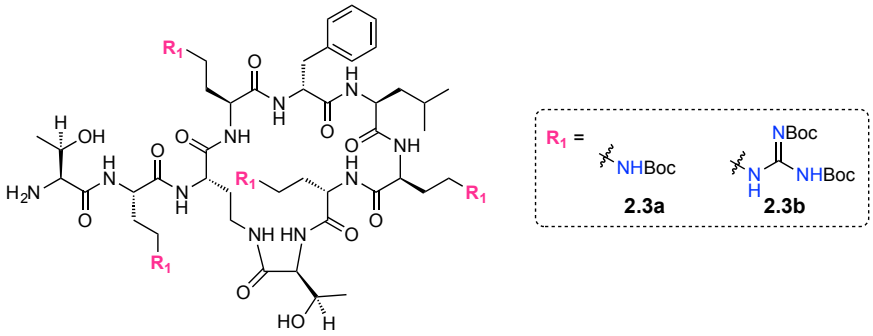

Compound 2.3a. In a 10 mL flask was added the TFA salt of PMBN (**2.2**, 104 mg, 0.0678 mmol), 2 mL MeOH, 1 mL H_2O, and NEt_3 (110 mg, 1.02 mmol, 140 µL). Then Boc-ON (67 mg, 0.27 mmol) was added and the reaction was stirred for 24 hours. The reaction was evaporated under reduced pressure and CH_2Cl_2 was added and washed with saturated $NaHCO_3$. The organic layer was dried over $MgSO_4$, filtered, and evaporated under reduced pressure. The product was isolated by automated flash chromatography (0 -

20% MeOH in CH_2Cl_2 over 18 mins) to afford the product **2.3a** as a white solid (63.8 mg, 0.039 mmol, 69% yield). ^{1}H NMR (500 MHz, CD_3OD) δ 7.34 – 7.20 (m, 5H), 4.49 – 4.37 (m, 2H), 4.36 – 4.21 (m, 4H), 4.15 – 4.04 (m, 3H), 4.01 (d, *J* = 3.7 Hz, 1H), 3.60 – 3.49 (m, 1H), 3.25 – 2.90 (m, 11H), 2.25 – 2.14 (m, 1H), 2.08 – 1.71 (m, 10H), 1.50 – 1.15 (m, 44H), 0.93 – 0.83 (m, 1H), 0.71 (s, 3H), 0.65 (s, 3H). ^{13}C NMR (126 MHz, CD_3OD) δ 175.41, 175.20, 174.17, 174.05, 173.74, 173.35, 172.71, 158.74, 158.39, 137.42, 130.40, 129.72, 128.06, 80.37, 80.14, 69.45, 67.28, 61.50, 61.09, 58.29, 54.82, 54.08, 52.91, 52.19, 52.07, 51.80, 40.49, 38.03, 37.79, 37.53, 36.75, 34.18, 33.24, 32.81, 32.28, 31.55, 30.81, 28.82, 28.40, 24.78, 23.80, 21.38, 20.82, 19.70. HR-ESI-MS calculated for $C_{63}H_{106}N_{14}O_{19}$ $[M+Na]^+$ 1385.7651, found 1385.7640.

Compound 2.3b. In a 10 mL flask was added the TFA salt of PMBN (**2.2**, 112 mg, 0.0728 mmol), 2 mL MeOH, 2 mL CH_2Cl_2, and NEt_3 (110 mg, 1.09 mmol, 152 μL). Then *N,N′*-Di-Boc-1*H*-pyrazole-1-carboxamidine (88 mg, 0.284 mmol) was added and the reaction was stirred for 24 hours. The reaction was evaporated under reduced pressure and CH_2Cl_2 was added and washed with saturated $NaHCO_3$. The organic layer was dried over $MgSO_4$, filtered, and evaporated under reduced pressure. The product was isolated by automated flash chromatography (0 - 10% MeOH in CH_2Cl_2 over 22 mins) to afford the product **2.3b** as a white solid (75 mg, 0.039 mmol, 53% yield). ^{1}H NMR (500 MHz, CD_3OD) δ 7.34 – 7.13 (m, 5H), 4.60 – 4.43 (m, 2H), 4.40 (t, *J* = 8.1 Hz, 1H), 4.31 – 4.16 (m, 5H), 4.14 – 4.01 (m, 1H), 3.95 (d, *J* = 4.8 Hz, 1H), 3.72 – 3.35 (m, 9H), 3.27 – 2.94 (m, 4H), 2.29 – 1.74 (m, 10H), 1.61 – 1.15 (m, 80H), 0.94 – 0.42 (m, 1H), 0.73 (dd, *J* = 15.8, 5.8 Hz, 6H). ^{13}C NMR (126 MHz, CD_3OD) δ 175.02, 173.95, 173.65, 173.50, 172.52,

164.59, 164.47, 157.85, 157.62, 153.99, 153.90, 150.97, 137.71, 130.29, 129.69, 128.03, 84.42, 84.35, 84.28, 84.22, 80.45, 80.41, 69.52, 67.23, 61.94, 61.16, 58.18, 57.47, 54.12, 53.62, 52.82, 52.37, 52.29, 51.91, 40.45, 38.86, 38.61, 38.57, 37.82, 37.70, 36.79, 33.39, 32.90, 32.43, 32.35, 31.98, 31.13, 30.78, 30.75, 28.74, 28.71, 28.69, 28.65, 28.35, 25.00, 23.81, 21.52, 20.93, 19.78. HR-ESI-MS calculated for $C_{87}H_{146}N_{22}O_{27}$ $[M+Na]^+$ 1954.0620, found 1954.0622.

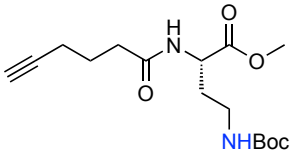

2.6a

Compound 2.6a. 5-hexynoic acid (257 µL, 262 mg, 2.33 mmol), 1.1 mL of DIEA (804 mg, 6.22 mmol), and 8.6 mL DMF (filtered through silica), and HATU (887 mg, 2.33 mmol) were added to a 50 mL round bottom flask and allowed to stir for 10 min to give a yellow solution. Next, H-Dab(Boc)-OMe·HCl (418 mg, 1.56 mmol) was added and the reaction was stirred overnight. To the reaction was added CH_2Cl_2, which was washed with 2% citric acid and then sat. $NaHCO_3$. The organic layer was dried, filtered, and evaporated under reduced pressure. The product was isolated by automated flash chromatography (20 - 90% EtOAc in hexanes over 15 mins) to afford the product as a viscous oil (467 mg, 1.43 mmol, 92% yield). ^{1}H NMR (500 MHz, $CDCl_3$): δ 6.48 (d, J = 7.4 Hz, 1NH), 5.19 – 5.13 (m, 1NH), 4.67 (td, J = 8.5, 4.5 Hz, 1H), 3.48 – 3.34 (m, 1H), 3.00 – 2.85 (m, J = 13.4, 9.2, 4.9 Hz, 1H), 2.40 (t, J = 7.4 Hz, 2H), 2.26 (td, J = 6.9, 2.6 Hz, 2H), 2.08 – 2.00 (m, 1H), 1.98 (t, J = 2.7 Hz, 1H), 1.90 – 1.83 (m, 2H), 1.80 – 1.71 (m, 1H), 1.42 (s, 9H). ^{13}C NMR (126 MHz, $CDCl_3$) δ 173.05, 172.80, 156.23, 83.42, 79.56, 77.41, 77.16, 76.91, 69.45,

52.77, 49.67, 36.51, 34.96, 33.17, 28.52, 24.12, 17.92. HR-ESI-MS calculated for $C_{16}H_{26}N_2O_5$ $[M+Na]^+$ 349.1734, found 349.1735.

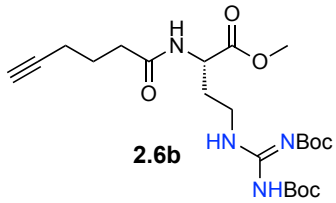

2.6b

Compound 2.6b. In a 25 mL flask was added BDabyne-OMe (**2.6a**, 212 mg, 0.629 mmol), CH_2Cl_2, triisopropylsilane (57 µL) and trifluoroacetic acid (1 mL). The solution was stirred for one hour and evaporated under reduced pressure. The residue was redissolved in CH_2Cl_2 (2 mL) and NEt_3 (1 mL). Then *N,N'*-Di-Boc-1*H*-pyrazole-1-carboxamidine (403 mg, 1.30 mmol) was added and the reaction was stirred overnight. The reaction was diluted with CH_2Cl_2 and washed with saturated $NaHCO_3$. The organic layer was dried over $MgSO_4$, filtered, and evaporated under reduced pressure. The product was isolated by automated flash chromatography (20 - 60% EtOAc in hexanes over 19 mins) to afford the product **2.6b** as an oil. ^{1}H NMR (400 MHz, CD_3OD) δ4.49 (dd, J = 8.5, 5.1 Hz, 1H), 3.71 (s, 3H), 3.54 (m, 1H), 3.38 (m, 1H), 2.41 (t, J = 7.4 Hz, 2H), 2.28 – 2.21 (m, 3H), 2.12 – 1.95 (m, 2H), 1.83 (p, J = 7.3 Hz, 2H), 1.53 (s, 9H), 1.49 (s, 9H). ^{13}C NMR (126 MHz, CD_3OD) δ 175.53, 173.71, 164.47, 157.75, 154.01, 84.49, 84.16, 80.50, 70.25, 52.84, 51.54, 38.22, 35.59, 31.73, 28.61, 28.23, 25.77, 18.60. HR-ESI-MS calculated for $C_{22}H_{37}N_4O_7$ $[M+H]^+$ 469.2657, found 469.2658.

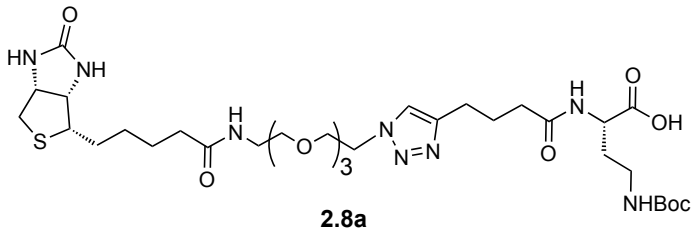

2.8a

Compound 2.8a. BDabyneOMe (**2.6a**, 28.5 mg, 0.064 mmol) and biotin-PEG-N_3 (**2.7**, 30.0 mg, .064 mmol) with a 1 mL 3:1:1 mixture of THF, t-BuOH, and H_2O was were added to a 10 mL round bottom flask and purged with argon for 10 min. Next, 35 µL of a freshly prepared 1M of a sodium ascorbate and then a 28 µL of 7.5% solution of $CuSO_4 \cdot 5H_2O$, both prepared in degassed water, were added. The reaction was stirred overnight. The reaction was evaporated under reduced pressure. The product was isolated by automated flash chromatography (2 - 17% MeOH in CH_2Cl_2 over 18 mins) to afford the product as a white solid (49.8 mg, 0.080 mmol, 85% yield). ^{1}H NMR (500 MHz, $CDCl_3$) δ 7.57 (s, 1H), 7.43 (d, *J* = 7.9 Hz, 1NH), 6.94 (brs, 1NH), 6.27 (brd, *J* = 22.5 Hz, 1NH), 5.40 (brd, *J* = 23.1 Hz, 1NH), 5.24 (brs, 1NH), 4.62 (td, *J* = 8.5, 4.5 Hz, 1H), 4.54 – 4.48 (m, 3H), 4.35 – 4.30 (m, 1H), 3.88 (t, *J* = 5.1 Hz, 2H), 3.72 (s, 3H), 3.64 – 3.56 (m, 8H), 3.54 (t, *J* = 5.1 Hz, 2H), 3.48 – 3.31 (m, 3H), 3.14 (td, *J* = 7.3, 4.8 Hz, 1H), 3.00 (dt, *J* = 13.5, 5.7 Hz, 1H), 2.90 (dd, *J* = 12.8, 4.9 Hz, 1H), 2.77 (t, *J* = 7.4 Hz, 2H), 2.73 (d, *J* = 12.8 Hz, 1H), 2.33 (t, *J* = 7.4 Hz, 2H), 2.24 – 2.13 (m, 2H), 2.08 – 1.96 (m, 4H), 1.86 – 1.57 (m, 5H), 1.42 (s, 10H). ^{13}C NMR (126 MHz, $CDCl_3$) δ173.65, 173.52, 173.50, 163.87, 156.21, 147.29, 122.54, 79.49, 70.61, 70.52, 70.49, 70.15, 70.06, 69.64, 61.96, 60.21, 55.73, 52.68, 50.22, 49.86, 40.70, 39.24, 36.78, 35.82, 35.36, 32.54, 28.56, 28.25, 28.17, 25.69, 25.49, 24.86. HR-ESI-MS calculated for $C_{34}H_{58}N_8O_{10}S$ $[M+Na]^+$ 793.3889, found 793.3885.

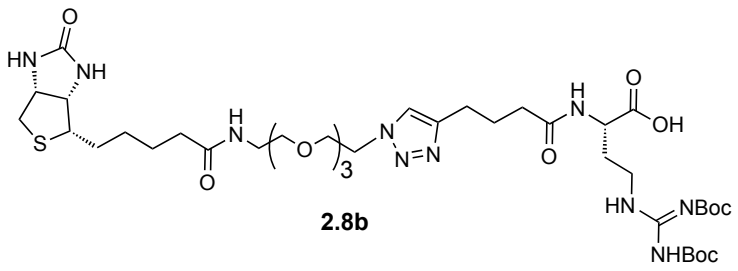

2.8b

Compound 2.8b. BGuanDabyneOMe (**2.6b**, 28.5 mg, 0.064 mmol) and biotin-PEG-N_3 (**2.7**, 30.0 mg, 0.064 mmol) with a 1 mL 3:1:1 mixture of THF, t-BuOH, and H_2O was added to a 10 mL round bottom flask and purged with argon for 10 min. Next, 35 µL of a freshly prepared 1M of a sodium ascorbate and then a 28 µL of 7.5% solution of $CuSO_4 \cdot 5H_2O$, both prepared in degassed water, were added. The reaction was stirred overnight. The reaction was evaporated under reduced pressure. The product was isolated by automated flash chromatography (5 - 12% MeOH in CH_2Cl_2 over 19 mins) to afford the product as a white solid (49.8 mg, 0.080 mmol, 85% yield). ^{1}H NMR (500 MHz, CD_3OD): δ 7.85 (s, 1H), 4.55 (t, J = 5.1 Hz, 2H), 4.52 – 4.47 (m, 2H), 4.31 (dd, J_1 = 8, 4.5 Hz, 1H), 3.89 (t, J = 5 Hz, 2H), 3.72 (s, 3H), 3.61 – 3.52 (m, 11H), 3.39 (q, J = 7 Hz, 1H), 3.35 (q, J = 5.5 Hz, 2H), 3.22 – 3.18 (m, 1H), 2.93 (dd, J_1 = 12.5, 5 Hz, 1H), 2.75 (dd, J_1 = 8.5, 7.3 Hz, 2H), 2.70 (d, J = 13 Hz, 1H), 2.37 – 2.34 (m, 2H), 2.21 (t, J = 7.3 Hz, 2H), 2.10 – 2.05 (m, 1H), 2.03 – 1.96 (m, 3H), 1.77– 1.39 (m, 26H); ^{13}C NMR (126 MHz, CD_3OD): δ 176.17, 176.08, 175.63, 173.75, 166.09, 164.47, 157.74, 153.99, 124.26, 84.49, 80.49, 71.56, 71.49, 71.43, 71.26, 70.57, 70.41, 63.35, 61.60, 57.03, 52.89, 51.54, 51.34, 41.08, 40.47, 40.34, 38.24, 36.77, 36.72, 35.99, 31.79, 29.78, 29.50, 28.61, 28.23, 26.87, 26.57, 25.68. HR-ESI-MS calculated for $C_{40}H_{68}N_{10}O_{12}S$ $[M+H]^+$ 913.4812, found 913.4811.

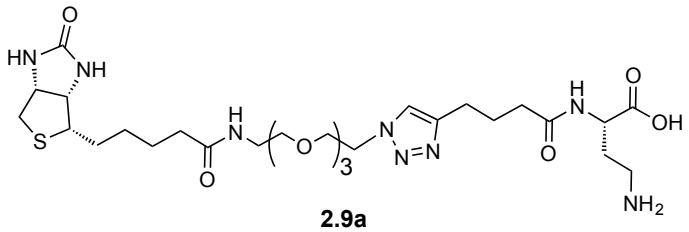

2.9a

Compound 2.9a. BDabOMeBiotin (**2.8a**, 27 mg, 0.035 mmol), 1.25 mL of MeOH, and 0.42 mL of 0.1 M LiOH solution in water (1 mg, .042 mmol) were added to a 10 mL round bottom flask and stirred overnight. The compound was desalted on a C-18 sep-pak (waters) to provide the product **2.9a** as a white solid (22 mg, 0.029 mmol, 82% yield). ^{1}H NMR (500 MHz, CD_3OD) δ 7.87 (s, 1H), 4.57 – 4.53 (m, 2H), 4.49 (ddd, *J* = 7.9, 4.9, 0.7 Hz, 1H), 4.33 – 4.27 (m, 2H), 3.91 – 3.87 (m, 2H), 3.63 – 3.56 (m, 10H), 3.53 (t, *J* = 5.5 Hz, 2H), 3.35 (t, *J* = 5.5 Hz, 2H), 3.19 (tt, *J* = 3.6, 3.2 Hz, 2H), 3.06 – 2.98 (m, 1H), 2.92 (dd, *J* = 12.7, 5.0 Hz, 1H), 2.75 (t, *J* = 7.6 Hz, 2H), 2.70 (d, *J* = 12.7 Hz, 1H), 2.32 (t, *J* = 7.5 Hz, 2H), 2.21 (t, *J* = 7.4 Hz, 2H), 2.07 – 1.94 (m, 4H), 1.78 – 1.54 (m, 6H), 1.45 – 1.40 (m, 11H).; ^{13}C NMR (126 MHz, CD_3OD): δ 176.17, 176.08, 175.63, 173.75, 166.09, 164.47, 157.74, 153.99, 124.26, 84.49, 80.49, 71.56, 71.49, 71.43, 71.26, 70.57, 70.41, 63.35, 61.60, 57.03, 52.89, 51.54, 51.34, 41.08, 40.47, 40.34, 38.24, 36.77, 36.72, 35.99, 31.79, 29.78, 29.50, 28.61, 28.23, 26.87, 26.57, 25.68; HR-ESI-MS calculated for $C_{33}H_{56}N_8O_{10}S$ $[M+Na]^+$ 779.3737, found 779.3732.

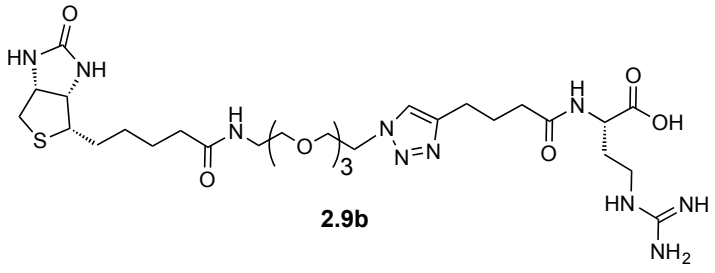

2.9b

Compound 2.9b. BGDabOMeBiotin (**2.8b**, 27 mg, 0.035 mmol), 1.25 mL of MeOH, and 0.42 mL of 0.1 M LiOH solution in water (1 mg, .042 mmol) were added to a 10 mL round bottom flask and stirred overnight. The compound was desalted on a C-18 sep-pak (waters) to provide the product **2.9b** as a white solid (22 mg, 0.029 mmol, 82% yield). ^{1}H NMR (500 MHz, CD_3OD) δ 7.87 (s, 1H), 4.55 (t, *J* = 5.0 Hz, 2H), 4.49 (dd, *J* = 7.8, 4.8 Hz, 1H), 4.33 – 4.27 (m, 2H), 3.89 (t, *J* = 5.1 Hz, 2H), 3.62 – 3.54 (m, 8H), 3.53 (t, *J* = 5.5 Hz, 2H), 3.35 (t, *J* = 5.4 Hz, 2H), 3.30 – 3.24 (m, 1H), 3.22 – 3.17 (m, 1H), 2.92 (dd, *J* = 12.7, 5.0 Hz, 1H), 2.75 (t, *J* = 7.6 Hz, 2H), 2.70 (d, *J* = 12.7 Hz, 1H), 2.35 (t, *J* = 7.3 Hz, 2H), 2.21 (t, *J* = 7.4 Hz, 2H), 2.17 – 2.09 (m, 1H), 2.04 – 1.96 (m, 2H), 1.88 – 1.78 (m, 1H), 1.77 – 1.55 (m, 5H), 1.52 (s, 9H), 1.48 – 1.39 (m, 11H).; ^{13}C NMR (126 MHz, CD_3OD) δ 178.59, 176.14, 174.91, 166.13, 158.21, 149.44, 148.27, 124.30, 79.84, 71.57, 71.50, 71.45, 71.27, 70.55, 70.42, 63.36, 61.61, 57.03, 53.91, 51.31, 41.07, 40.36, 38.43, 36.73, 36.36, 34.47, 29.78, 29.51, 28.80, 26.87, 26.71, 25.80. HR-ESI-MS calculated for $C_{39}H_{66}N_{10}O_{12}S$ $[M+H]^+$ 899.4655, found 899.4653.

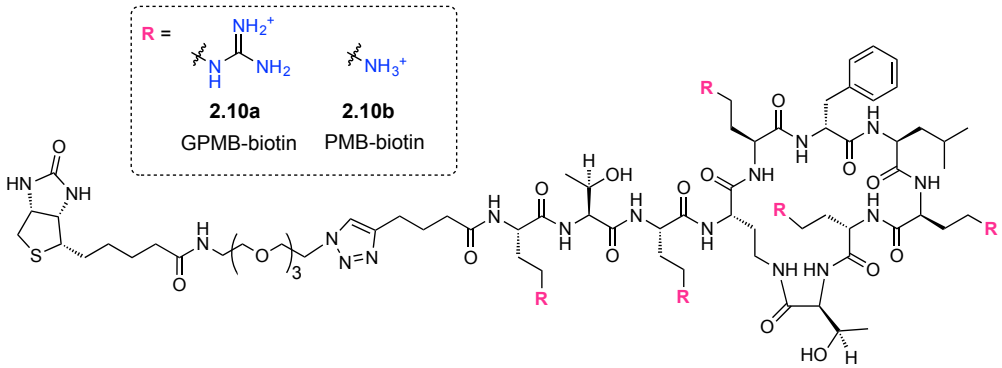

bPMB (2.10a). BiotinBDabOH (**2.9a**, 20.6 mg, 0.0258 mmol), DIEA (8.6 mg, 0.067 mmol, 11.6 µL), HATU (10.2 mg, 0.027 mmol) and DMF (1 mL) were added to a 10 mL flask and stirred for 10 min. Then Boc-PMBN (**2.3a**, 30.4 mg, 0.022 mmol) was

added to the reaction and stirred overnight. The reaction was diluted with CH_2Cl_2 and washed with 5% citric acid and then saturated $NaHCO_3$. The organic layer was then dried using $MgSO_4$, filtered, and evaporated under reduced pressure. The residue was then taken up in CH_2Cl_2/TFA (1:1, 1 mL) containing triisopropylsilane (10 μL) and stirred for 2 hours. The reaction was evaporated under reduced pressure the product was isolated by automated reverse phase flash chromatography using a Teledyne Isco Redisep Rf C18 5.5 g Gold column [5 - 30% ACN (0.1% TFA) in H_2O (0.1% TFA) over 14 mins]. The fractions containing the desired product were lyophilized to provide **2.10a** as a white solid as the TFA salt (19.9 mg, 0.0092 mmol, 48% yield). ^{1}H NMR (500 MHz, D_2O) δ 7.89 (dd, *J* = 10.2, 1.9 Hz, 1H), 7.34 – 7.22 (m, 3H), 7.17 (d, *J* = 5.2 Hz, 2H), 4.58 – 4.34 (m, 8H), 4.34 – 4.29 (m, 1H), 4.29 – 4.25 (m, 1H), 4.24 – 4.08 (m, 7H), 3.93 – 3.87 (m, 2H), 3.61 – 3.48 (m, 9H), 3.33 – 3.18 (m, 4H), 3.12 – 2.93 (m, 10H), 2.92 – 2.85 (m, 1H), 2.84 – 2.75 (m, 1H), 2.75 – 2.63 (m, 4H), 2.33 – 2.26 (m, 2H), 2.23 – 1.74 (m, 17H), 1.68 – 1.24 (m, 10H), 1.16 – 1.07 (m, 5H), 0.64 (d, *J* = 37.2 Hz, 7H). ^{13}C NMR (126 MHz, D_2O) δ 176.73, 176.24, 174.90, 173.25, 173.18, 173.09, 172.89, 172.67, 172.62, 172.54, 172.47, 172.27, 172.21, 171.86, 171.61, 171.47, 171.28, 171.24, 165.17, 163.24, 162.82 (TFA, q, *J* = 35.7 Hz), 146.46, 135.32, 128.83, 127.27, 124.28, 124.15, 116.23 (TFA, q, *J* = 292.1 Hz), 69.43, 69.29, 69.26, 68.67, 68.43, 68.39, 66.89, 66.66, 66.08, 61.92, 60.08, 59.32, 58.93, 58.79, 55.62, 55.21, 52.66, 52.57, 51.74, 51.64, 51.55, 51.39, 51.25, 51.05, 50.92, 50.36, 50.24, 39.54, 38.94, 38.74, 36.69, 36.27, 36.19, 36.10, 35.94, 35.80, 35.70, 35.27, 34.22, 30.43, 30.31, 29.59, 29.54, 28.67, 28.48, 28.34, 28.09, 27.71, 27.60, 27.54, 25.00, 24.50, 24.44, 23.52, 23.42, 23.30, 22.18, 20.11, 18.95, 18.73, 18.58, 16.13. HR-ESI-MS calculated for $C_{71}H_{120}N_{22}O_{18}S$ $[M+Na]^+$ 1623.8764, found 1623.8766.

bGPMB (2.10b). BiotinBGDabOH (**2.9b**, 20.2 mg, 0.0223 mmol), DIEA (12.02 mg, 0.093 mmol, 16.2 μL), PyBrop (10.4 mg, 0.0223 mmol) and DMF (1 mL) were added to a 10 mL flask and stirred for 10 min. Then BocGuan-PMBN (**2.3b**, 36.0 mg, 0.0186 mmol) was added to the reaction and stirred overnight. The reaction was diluted with CH_2Cl_2 and washed with 5% citric acid and then saturated $NaHCO_3$. The organic layer was then dried using $MgSO_4$, filtered, and evaporated under reduced pressure. The residue was then taken up in CH_2Cl_2/TFA (1:1, 1 mL) containing triisopropylsilane (10 μL) and stirred for 2 hours. The reaction was evaporated under reduced pressure the product was isolated by automated reverse phase flash chromatography using a C18 5.5 g Gold column [15 - 35% ACN (0.1% TFA) in H_2O (0.1% TFA) over 15 mins]. The fractions were lyophilized to provide **2.10b** as a white solid as the TFA salt (19.9 mg, 0.0092 mmol, 25% yield). ^{1}H NMR (500 MHz, D_2O) δ 7.89 – 7.86 (m, 1H), 7.44 – 7.33 (m, 3H), 7.30 – 7.26 (m, 2H), 4.65 – 4.54 (m, 4H), 4.51 – 4.39 (m, 5H), 4.36 – 4.18 (m, 9H), 4.02 – 3.97 (m, 2H), 3.71 – 3.59 (m, 11H), 3.42 – 3.25 (m, 13H), 3.23 – 2.96 (m, 7H), 2.81 – 2.71 (m, 3H), 2.44 – 2.35 (m, 2H), 2.27 (td, J = 7.3, 1.8 Hz, 3H), 2.24 – 2.10 (m, 6H), 2.23 – 1.30 (m, 28H), 1.27 – 1.18 (m, 6H), 0.89 – 0.70 (m, 7H). ^{13}C NMR (126 MHz, D_2O) δ 75, 176.59, 176.38, 175.00, 174.28, 173.96, 173.87, 173.83, 173.38, 173.32, 172.93, 172.63, 172.25, 172.25, 172.00, 171.67, 171.48, 171.43, 165.24, 163.35, 163.07, 162.79, 162.50 (TFA, q, J = 35.7 Hz), 156.77, 156.68, 156.64, 156.54, 147.26, 135.40, 128.91, 127.37, 123.55, 117.43, 115.11 (TFA, q, J = 291.5 Hz), 69.57, 69.52, 69.39, 68.78, 68.72, 66.85, 66.54, 66.06, 62.01, 60.19, 59.48, 59.29, 59.04, 55.86, 55.30, 52.59, 51.95, 51.70, 51.50, 51.18, 50.53, 49.84, 39.64, 39.04, 38.85, 37.83, 37.76, 37.39, 36.77, 35.39, 34.47, 34.38, 30.80, 29.76, 29.19,

27.84, 27.66, 25.10, 24.82, 23.95, 23.47, 22.29, 20.21, 19.09, 18.86, 18.72. HR-ESI-MS calculated for $C_{76}H_{130}N_{32}O_{18}S$ $[M+3H]^{3+}$ 604.6727, found 604.6722.

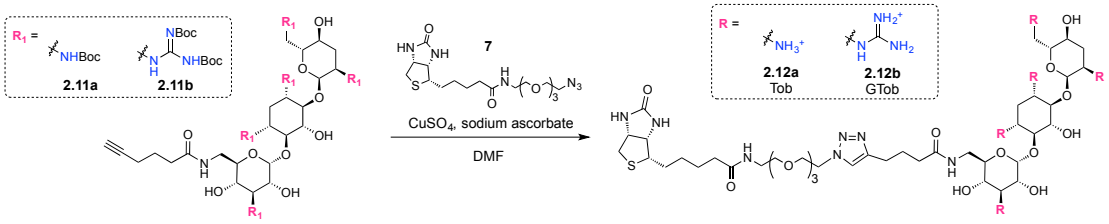

Scheme 2.5. Synthesis of bGTob and bTob.

Synthesis of alkyne-boc-tobramycin (**2.11a**), alkyne-boc-guan-tobramycin (**2.11b**) and GTob-biotin (**2.12b)** were prepared according to literature procedures.[21]

bTob (2.12a). Alkyne-Boc-Tob (**2.11a**, 25mg, 0.024 mmol) and biotin-PEG-N_3 (**2.7,** 16 mg, 0.035 mmol) were dissolved in DMF (500 uL) and treated with 0.2M solution of sodium ascorbate in H_2O (25 µL) and 0.2M solution of $CuSO_4 \cdot 5H_2O$ (25 µl). The reaction was stirred overnight at room temperature under argon. The reaction was evaporated under reduced pressure. The crude product was dissolved in CH_2Cl_2 and washed with aqueous KCN solution, EDTA (0.3 M, pH 8) and brine. The organic layer was then dried using $MgSO_4$, filtered and evaporated under reduced pressure. The residue was then dissolved in CH_2Cl_2/TFA (1:1, 1 mL) containing triisopropylsilane (10 µL) and stirred for 2 hours. The reaction was evaporated under reduced pressure and the product was purified by HPLC using a semiprep RP-C18 column [5 – 30% ACN (0.1% TFA) in H_2O (0.1% TFA) over 12 min]. The fractions containing the desired product were lyophilized to provide the product as a white solid, (20 mg, 0.013 mmol, 54% yield). ^{1}H NMR (500 MHz, D_2O): δ 7.80 (s, 1H), 5.70 (s, 1H), 4.96 (s, 1H), 4.50 (m, 3H), 4.30 (m, 1H), 3.91-3.80 (m, 6H), 3.73 (m, 1H), 3.66 (m, 2H), 3.60-3.40 (m, 16H), 3.38-3.27 (m,

3H), 3.26 (s, 2H), 3.19 (m, 2H), 2.88 (m, 1H), 2.65 (m, 3H), 2.45 (d, 1H, *J*=12.3 Hz), 2.22 (m, 3H), 2.13 (m, 2H), 1.96-1.83 (m, 4H), 1.62-1.40 (m, 4H), 1.28 (s, 2H). ^{13}C NMR (126 MHz, D_2O): δ 176.82, 165.28, 163.30, 163.02, 162.74, 162.45, 146.91, 123.97, 119.77, 117.44, 115.12, 112.80, 100.86, 94.10, 83.56, 77.32, 74.12, 70.92, 70.31, 69.58, 69.53, 69.40, 69.38, 68.78, 68.60, 68.00, 66.48, 64.32, 62.02, 60.20, 55.30, 54.62, 50.15, 49.72, 48.31, 47.70, 39.74, 39.63, 38.94, 38.86, 35.38, 34.86, 29.25, 27.81, 27.71, 27.64, 25.09, 24.93, 23.78. HR-ESI-MS calculated for $C_{42}H_{77}N_{12}O_{14}S$ $[M+H]^+$ 1005.5397, found 1005.5400.

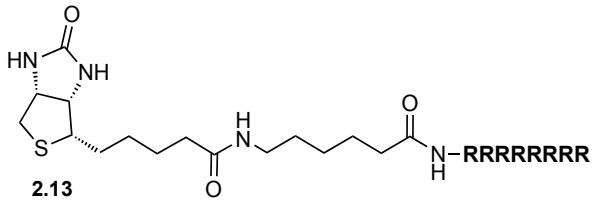

2.13

Octaarginine (bArg8). bArg8 was synthesized using standard solid phase peptide synthesis protocols (Rink amide resin). An aminohexanoic acid (Ahx) spacer was introduced in the N-terminus and biotin-NHS (4 eq) was coupled to the peptide's N-terminus over 1 h at rt in DMF containing DIEA (8 eq). The peptide was cleaved from the resin using TFA/TIS/water (95:2.5:2.5) at rt for 3h. The resin was filtered off and the peptide precipitated by the addition of cold ether and further standing at 4 degrees overnight. The crude was purified by HPLC using a semiprep RP-C18 column [5 – 60% ACN (0.1% TFA) in H_2O (0.1% TFA) over 9 min]. HRMS of the isolated peack confirms the identity of the biotinylated peptide. Purity was confirmed by analytical HPLC. HR-ESI-MS calculated for $C_{64}H_{124}N_{36}O_{11}S$ $[M+2H]^{2+}$ 926.4376, found 926.4374.

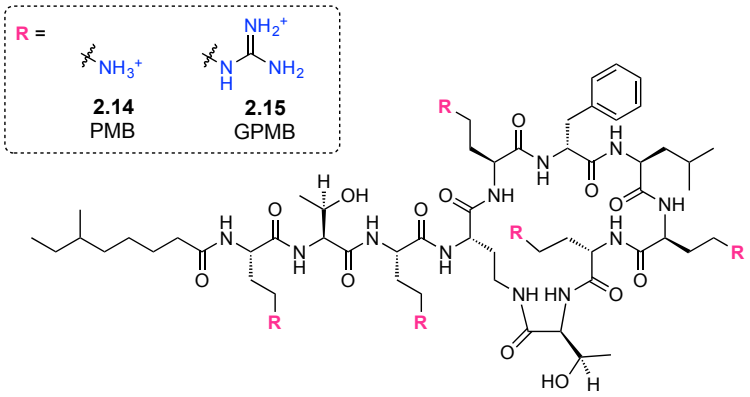

PMB (2.14). PMB was isolated from the mixture of isomers by HPLC using a RP-C18 column [5 – 50% ACN (0.1% TFA) in H_2O (0.1% TFA) over 40 mins]. Purity was confirmed by analytical HPLC. HR-ESI-MS calculated for $C_{56}H_{98}N_{16}O_{13}$ $[M+Na]^+$ 1225.7397, found 1225.7395.

GPMB (2.15). MeOH (15 mL) and NEt_3 (239 mg, 2.36 mmol, 329 µL) were added to **2.14** (226 mg, 0.157 mmol) followed by *N,N'*-Di-Boc-1*H*-pyrazole-1-carboxamidine (195 mg, 0.142 mmol) and stirred overnight. The reaction was evaporated under reduced pressure and CH_2Cl_2 was added and washed with saturated $NaHCO_3$. The organic layer was dried over $MgSO_4$, filtered, and evaporated under reduced pressure. The residue was then dissolved in CH_2Cl_2/TFA (1:1, 4 mL) containing triisopropylsilane (44 µL) and stirred for 2 hours. The reaction was diluted with 5 mL of CH_2Cl_2 and extracted with 10 mL of H_2O. The water was evaporated under reduced pressure and the product was isolated by HPLC using a RP-C18 column [5-50% ACN (0.1% TFA) in H_2O (0.1% TFA) over 40 mins]. The fractions containing the desired product were lyophilized to provide the TFA salt of GPMB as a white solid, (74.7 mg, 0.0378 mmol, 24% yield). ^{1}H NMR (400 MHz, D_2O): δ 7.42 – 7.29 (m, 3H), 7.26 (d, J = 6.9 Hz, 2H), 4.56 – 4.50 (m, 1H), 4.45 (ddd, J = 17.2, 8.7, 5.3 Hz, 3H), 4.35 – 4.21 (m, 6H), 4.20 – 4.14 (m, 2H), 3.43 – 2.98 (m, 14H),

2.33 (t, J = 7.2 Hz, 2H), 2.22 – 1.74 (m, 12H), 1.67 – 1.03 (m, 17H), 0.82 (t, J = 6.8 Hz, 6H), 0.75 (s, 3H), 0.68 (s, 3H). HR-ESI-MS calculated for $C_{61}H_{108}N_{26}O_{13}$ $[M+2H]^{2+}$ 707.4367, found 707.4351.

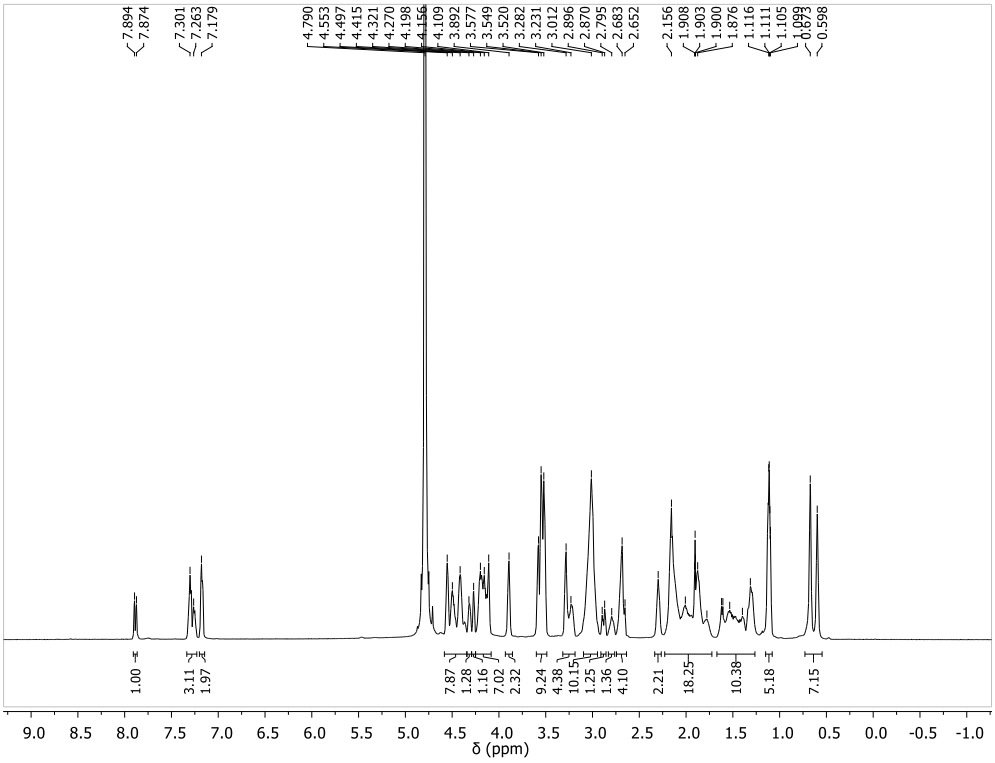

Spectrum 2.1. ^{1}H NMR of PMB-biotin (**2.10a,** D_2O, 500 MHz).

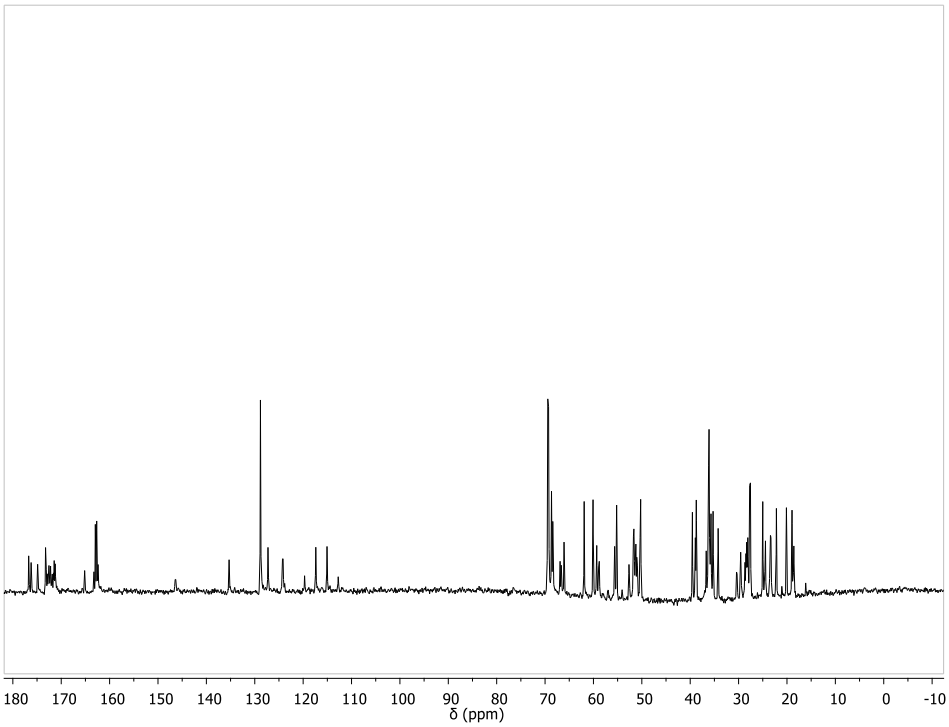

Spectrum 2.2. ^{13}C NMR of PMB-biotin (**2.10a,** D_2O, 126 MHz).

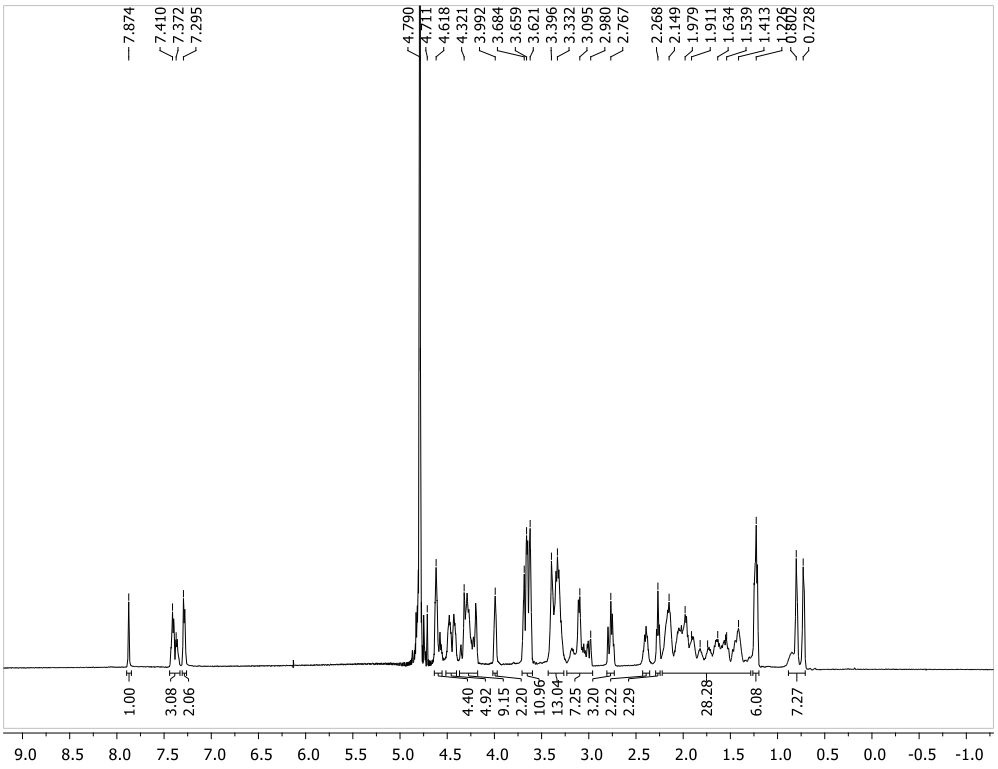

Spectrum 2.3. ^{1}H NMR of GPMB-biotin (**2.10b,** D_2O, 500 MHz).

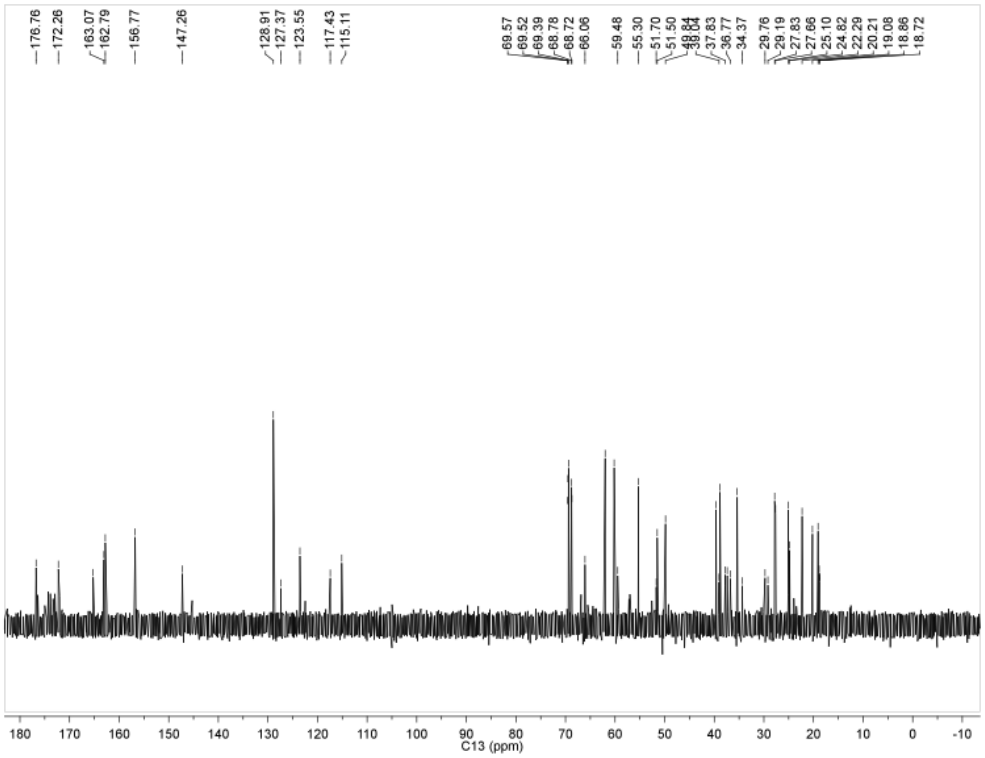

Spectrum 2.4. ^{13}C NMR of GPMB-biotin (**2.10b,** D_2O, 126 MHz)

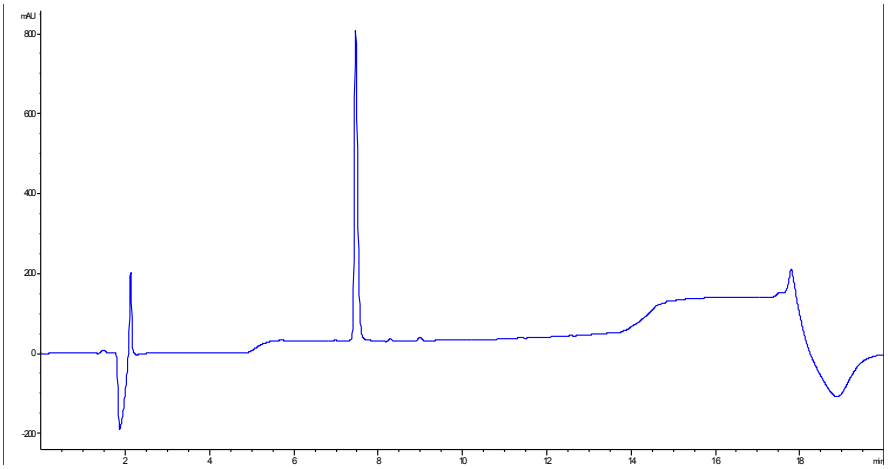

Figure 2.10. Analytical HPLC trace for bArg8. [RP-C18, 5 – 60% ACN (0.1% TFA) in H_2O (0.1% TFA) over 9 min]

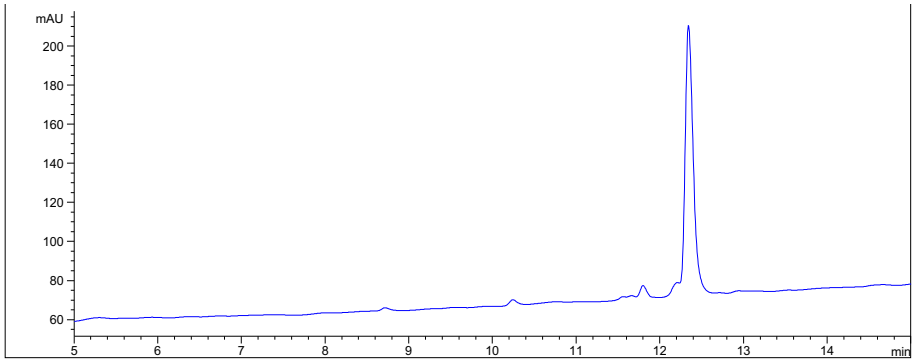

Figure 2.11. Analytical HPLC trace for PMB. [RP-C18 column, 5 – 50% ACN (0.1% TFA) in H_2O (0.1% TFA) over 15 mins].

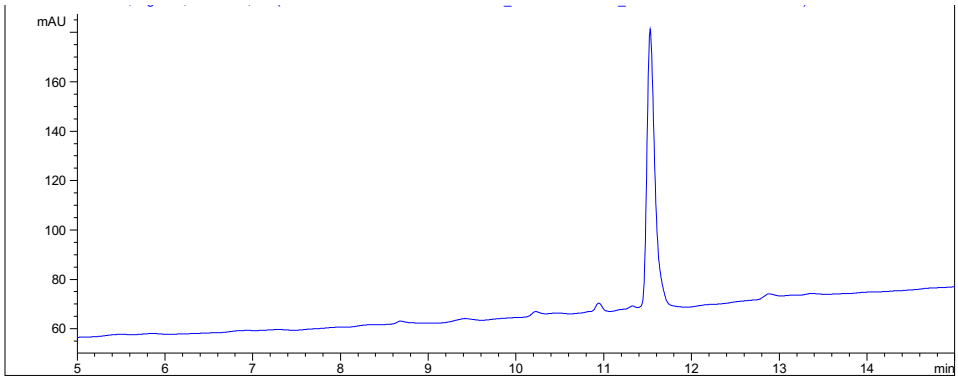

Figure 2.12. Analytical HPLC trace for GPMB. [RP-C18 column, 5 – 50% ACN (0.1% TFA) in H_2O (0.1% TFA) over 15 mins].

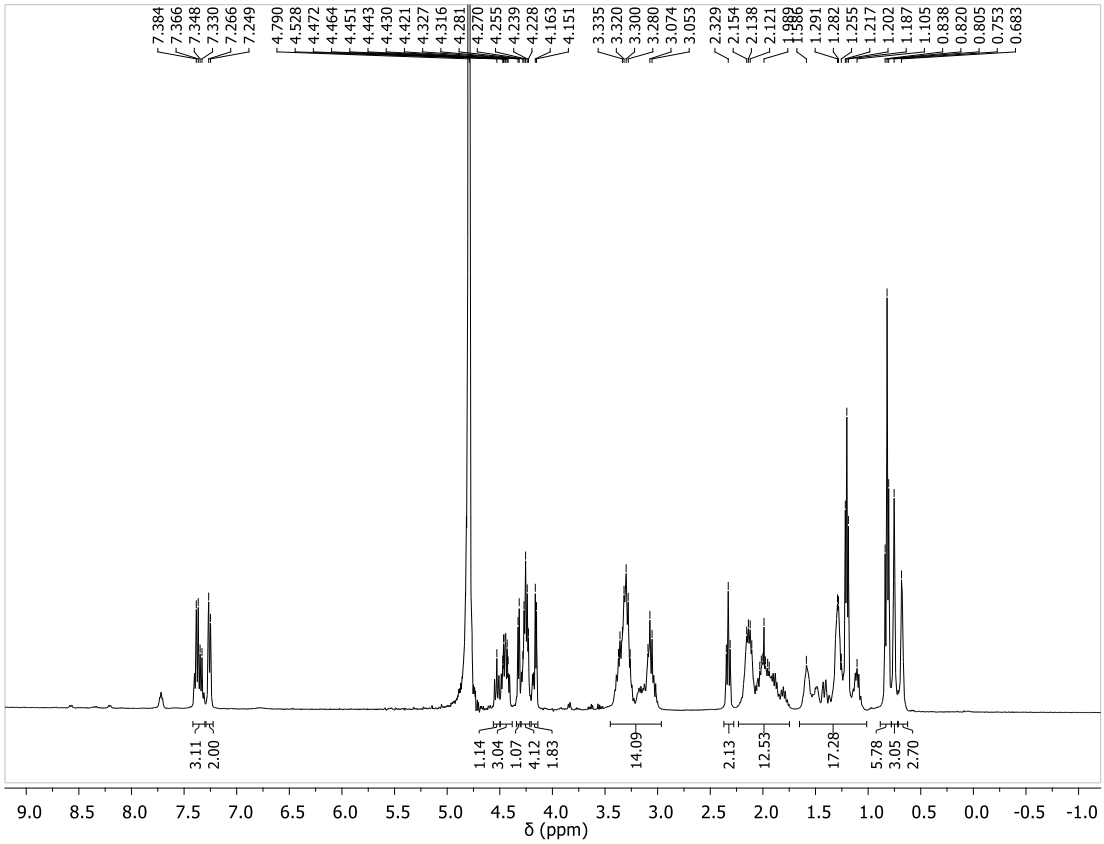

Spectrum 2.5. ^{1}H NMR of GPMB (**D_2O**, 500 MHz).

Cell culture

Wild-type Chinese hamster ovary cells (CHO-K1) were obtained from the American Type Culture Collection (CCL-61). Mutant pgsA745 and pgsD677 were described previously.41,42 All cells were grown under an atmosphere of 5% CO2 in air and 100% relative humidity. CHO-K1, pgsA, and pgsD cells were grown in F-12 medium (Life Technologies) supplemented with fetal bovine serum (10% v/v, Gemini Bio-Products) and penicillin/streptomycin solution (1% v/v). The Hep3B cell line was obtained from ATCC (HB-8064) and cultured in MEM (Invitrogen) supplemented with 10% fetal bovine serum, nonessential amino acids, and 1% penicillin/streptomycin. HEK293T cells were obtained from ATCC and maintained

in Dulbecco's modified Eagle medium (DMEM) supplemented with 10% fetal bovine serum and 1% penicillin/streptomycin.

Quantifying cellular uptake/binding

The polymyxin derivatives (2.5 μM in PBS) were incubated with ST-PE-Cy5 (0.5 μM in PBS) for 20 min at ambient temperature then diluted with F-12 cell culture medium to give final conjugate solutions.

Cells were plated onto 24-well plates (100 000 cells/well) and grown for 24 h to about 80% confluence. Cells were washed with PBS and incubated with 300 μL of the corresponding conjugate for 1 h at 37 °C under an atmosphere of 5% CO2. Cells were washed twice with PBS, detached with 50 μL of trypsin-EDTA for uptake studies or 100 μL Versene (EDTA) for binding studies, diluted with PBS containing 0.1% BSA, and analyzed by FACS. Cellular uptake was quantified by the mean fluorescence intensity; raw data was interpreted by using FlowJo v8.8.6.

Evaluation of uptake dependency on temperature

Cells were grown for 24 h in 24-well plates as described above. Cells were incubated at 4 °C for 15 min in F-12, washed with cold PBS, then incubated with the precooled conjugate solution for 30 min at 4 °C. Cells were washed, detached with trypsin-EDTA, and analyzed as described above.

Evaluation of endocytosis mechanisms

Cells were grown for 24 h in 24-well plates as described above, washed with PBS, and incubated with 5mM amiloride for 10 min or 400 mM sucrose, 20 μM chlorpromazine, 200 μM genistein, or 5 μM nystatin for 30 min at 37 °C. Cells were

then washed with PBS and treated with the conjugate solution in F-12 for the cells pretreated with amiloride, or the conjugate solution in the presence of the inhibitor, using the same concentration used for pretreatment, for 1 h at 37 °C under an atmosphere of 5% CO2. Cells were washed, detached with trypsin-EDTA, and analyzed as described above.

Fluorescence microscopy

CHO-K1 cells were grown for 24 h in 35 mm dishes equipped with a glass bottom coverslip coated with poly-D-lysine. Cells were washed with PBS, treated with 1.5 mL of transporter conjugated to ST-Cy5 (20 nM) and incubated at 37 °C for 1 h under an atmosphere of 5% CO2. Cells were washed with PBS and stained with Hoescht stain and LysoTracker. Images were processed and analyzed using Nikon Imaging Software Elements and ImageJ. Pearson's correlations were calculated for individual cells in three separate images from two different experiments and then averaged (n=30).

Saporin delivery

The biotinylated transporters were incubated with ST-Sap in a 5:1 molar ratio for 20 min at ambient temperature then diluted with F-12 cell culture medium to give final conjugate solutions. CHO-K1 and pgsA cells were incubated with 100 μL of the corresponding conjugate for 4 days at 37 °C under an atmosphere of 5% CO2. CellTiter-Blue (20 μL) was added to the medium and incubated for an additional 4 h to measure viability.

Preparation of liposomes

A mixture (30 mg total) of DOPC, DOPE, and cholesterol (73:11:16) was dissolved in chloroform to a final volume of 1 mL and evaporated in a round flask and further dried under high vacuum overnight to form a thin lipid layer. The resulting film was hydrated for 15 min at 37 °C with 1 mL of PBS containing 100 μM Cy5. The mixture was sonicated for 30 s, subjected to six freeze/thaw cycles using a dry ice/acetone bath and a water bath at 37 °C. Lastly, the suspension was extruded 17 times through a polycarbonate membrane (pore size 100 nm) at room temperature. Non-encapsulated dye was removed by gravitational gel filtration (Sephadex G-50). Lipid concentration was determined adapting the Stewart method.[74] Plain liposomes were diluted to 3mg/mL and mixed with 10 mol% PMB or GPMB for 1 h at room temperature. Unincorporated PMB or GPMB was removed via centrifuge gel filtration (Sephadex G-50).[75]

Acknowledgements

Chapter 2 is a full reprint from: Hamill, K. M.; McCoy, L. S.; Wexselblatt, E.; Esko, J. D.; Tor, Y. Polymyxins Facilitate Entry into Mammalian Cells. *Chem. Sci*. **2016**, DOI:10.1039/c6sc00488a. The dissertation author is the main author and researcher of this work.

2.6 References

(1) Ho, R. J. Y.; Chien, J. Y. *J. Pharm. Sci.* **2012**, *101*, 2668.

(2) Ryser, H. J. *Science* **1968**, *159*, 390.

(3) Green, M.; Loewenstein, P. M. *Cell* **1988**, *55*, 1179.

(4) Frankel, A. D.; Pabo, C. O. *Cell* **1988**, *55*, 1189.

(5) Mann, D. A.; Frankel, A. D. *The EMBO Journal* **1991**, *10*, 1733.

(6) Fawell, S.; Seery, J.; Daikh, Y.; Moore, C.; Chen, L. L.; Pepinsky, B.; Barsoum, J. *Proc. Natl. Acad. Sci. U. S. A.* **1994**, *91*, 664.

(7) Pepinsky, R. B.; Androphy, E. J.; Corina, K.; Brown, R.; Barsoum, J. *DNA Cell Biol.* **1994**, *13*, 1011.

(8) Vivès, E.; Granier, C.; Prevot, P.; Lebleu, B. *Letters in Peptide Science* **1997**, *4*, 429.

(9) Vivès, E.; Brodin, P.; Lebleu, B. *J. Biol. Chem.* **1997**, *272*, 16010.

(10) Wender, P. A.; Mitchell, D. J.; Pattabiraman, K.; Pelkey, E. T.; Steinman, L.; Rothbard, J. B. *Proc. Natl. Acad. Sci. U. S. A.* **2000**, *97*, 13003.

(11) Stanzl, E. G.; Trantow, B. M.; Vargas, J. R.; Wender, P. A. *Acc. Chem. Res.* **2013**, *46*, 2944.

(12) Chugh, A.; Eudes, F.; Shim, Y.-S. *IUBMB Life* **2010**, *62*, 183.

(13) Wexselblatt, E.; Esko, J. D.; Tor, Y. *J. Org. Chem.* **2014**, *79*, 6766.

(14) Mandal, D.; Nasrolahi Shirazi, A.; Parang, K. *Angewandte Chemie International Edition* **2011**, *50*, 9633.

(15) Qian, Z.; Liu, T.; Liu, Y.-Y.; Briesewitz, R.; Barrios, A. M.; Jhiang, S. M.; Pei, D. *ACS Chem. Biol.* **2013**, *8*, 423.

(16) Lättig-Tünnemann, G.; Prinz, M.; Hoffmann, D.; Behlke, J.; Palm-Apergi, C.; Morano, I.; Herce, H. D.; Cardoso, M. C. *Nat Commun* **2011**, *2*, 453.

(17) Nischan, N.; Herce, H. D.; Natale, F.; Bohlke, N.; Budisa, N.; Cardoso, M. C.; Hackenberger, C. P. R. *Angewandte Chemie International Edition* **2015**, *54*, 1950.

(18) Li, M.; Ehlers, M.; Schlesiger, S.; Zellermann, E.; Knauer, S. K.; Schmuck, C. *Angewandte Chemie International Edition* **2016**, *55*, 598.

(19) Luedtke, N. W.; Carmichael, P.; Tor, Y. *J. Am. Chem. Soc.* **2003**, *125*, 12374.

(20) Elson-Schwab, L.; Garner, O. B.; Schuksz, M.; Crawford, B. E.; Esko, J. D.; Tor, Y. *J. Biol. Chem.* **2007**, *282*, 13585.

(21) Dix, A. V.; Fischer, L.; Sarrazin, S.; Redgate, C. P. H.; Esko, J. D.; Tor, Y. *Chembiochem* **2010**, *11*, 2302.

(22) Sarrazin, S.; Wilson, B.; Sly, W. S.; Tor, Y.; Esko, J. D. *Mol. Ther.* **2010**, *18*, 1268.

(23) Inoue, M.; Tong, W. Y.; Esko, J. D.; Tor, Y. *ACS Chem. Biol.* **2013**, *8*, 1383.

(24) McCoy, L. S.; Roberts, K. D.; Nation, R. L.; Thompson, P. E.; Velkov, T.; Li, J.; Tor, Y. *Chembiochem* **2013**, *14*, 2083.

(25) Hancock, R. E. W. *J. Antimicrob. Chemother.* **1981**, *8*, 429.

(26) Hancock, R. E.; Raffle, V. J.; Nicas, T. I. *Antimicrob. Agents Chemother.* **1981**, *19*, 777.

(27) Nikaido, H. *Microbiol. Mol. Biol. Rev.* **2003**, *67*, 593.

(28) O'Dowd, H.; Kim, B.; Margolis, P.; Wang, W.; Wu, C.; Lopez, S. L.; Blais, J. *Tetrahedron Lett.* **2007**, *48*, 2003.

(29) Danner, R. L.; Joiner, K. A.; Rubin, M.; Patterson, W. H.; Johnson, N.; Ayers, K. M.; Parrillo, J. E. *Antimicrob. Agents Chemother.* **1989**, *33*, 1428.

(30) Chihara, S.; Ito, A.; Yahata, M.; Tobita, T.; Koyama, Y. *Agric. Biol. Chem.* **1974**, *38*, 521.

(31) Chihara, S.; Tobita, T.; Yahata, M.; Ito, A.; Koyama, Y. *Agric. Biol. Chem.* **1973**, *37*, 2455.

(32) Storm, D. R.; Rosenthal, K. S.; Swanson, P. E. *Annu. Rev. Biochem.* **1977**, *46*, 723.

(33) Velkov, T.; Thompson, P. E.; Nation, R. L.; Li, J. *J. Med. Chem.* **2010**, *53*, 1898.

(34) Clausell, A.; Garcia-Subirats, M.; Pujol, M.; Busquets, M. A.; Rabanal, F.; Cajal, Y. *J. Phys. Chem. B* **2007**, *111*, 551.

(35) Wu, M.; Maier, E.; Benz, R.; Hancock, R. E. *Biochemistry* **1999**, *38*, 7235.

(36) Pristovsek, P.; Kidric, J. *J. Med. Chem.* **1999**, *42*, 4604.

(37) Vaara, M. *Microbiol. Rev.* **1992**, *56*, 395.

(38) Falagas, M. E.; Kasiakou, S. K. *Crit. Care* **2006**, *10*, R27.

(39) Yahav, D.; Farbman, L.; Leibovici, L.; Paul, M. *Clin. Microbiol. Infect.* **2012**, *18*, 18.

(40) Falagas, M. E.; Kasiakou, S. K. *Clin. Infect. Dis.* **2005**, *40*, 1333.

(41) Kadar, B.; Kocsis, B.; Nagy, K.; Szabo, D. *Curr. Med. Chem.* **2013**, *20*, 3759.

(42) Nation, R. L.; Li, J. *Curr. Opin. Infect. Dis.* **2009**, *22*, 535.

(43) Abdelraouf, K.; Chang, K. T.; Yin, T. J.; Hu, M.; Tam, V. H. *Antimicrob. Agents Chemother.* **2014**, *58*, 4200.

(44) Moestrup, S. K.; Cui, S.; Vorum, H.; Bregeng; xE; rd, C.; Bj; xF; rn, S. E.; Norris, K.; Gliemann, J.; Christensen, E. I. *The Journal of Clinical Investigation* **1995**, *96*, 1404.

(45) Azad, M. A. K.; Roberts, K. D.; Yu, H. H.; Liu, B.; Schofield, A. V.; James, S. A.; Howard, D. L.; Nation, R. L.; Rogers, K.; de Jonge, M. D.; Thompson, P. E.; Fu, J.; Velkov, T.; Li, J. *Anal. Chem.* **2015**, *87*, 1590.

(46) Azad, M. A. K.; Yun, B.; Roberts, K. D.; Nation, R. L.; Thompson, P. E.; Velkov, T.; Li, J. *Antimicrob. Agents Chemother.* **2014**, *58*, 6337.

(47) Mingeot-Leclercq, M. P.; Tulkens, P. M.; Denamur, S.; Vaara, T.; Vaara, M. *Peptides* **2012**, *35*, 248.

(48) Wexselblatt, E.; Esko, J. D.; Tor, Y. *ACS Nano* **2015**, *9*, 3961.

(49) Mitchell, D. J.; Kim, D. T.; Steinman, L.; Fathman, C. G.; Rothbard, J. B. *J. Pept. Res.* **2000**, *56*, 318.

(50) Viljanen, P.; Vaara, M. *Antimicrob. Agents Chemother.* **1984**, *25*, 701.

(51) Vingsbo Lundberg, C.; Vaara, T.; Frimodt-Moller, N.; Vaara, M. *J. Antimicrob. Chemother.* **2010**, *65*, 981.

(52) Vaara, M.; Vaara, T. *Nature* **1983**, *303*, 526.

(53) Esko, J. D.; Stewart, T. E.; Taylor, W. H. *Proc. Natl. Acad. Sci. U. S. A.* **1985**, *82*, 3197.

(54) Lidholt, K.; Weinke, J. L.; Kiser, C. S.; Lugemwa, F. N.; Bame, K. J.; Cheifetz, S.; Massague, J.; Lindahl, U.; Esko, J. D. *Proc. Natl. Acad. Sci. U. S. A.* **1992**, *89*, 2267.

(55) West, M. A.; Bretscher, M. S.; Watts, C. *J. Cell Biol.* **1989**, *109*, 2731.

(56) Koivusalo, M.; Welch, C.; Hayashi, H.; Scott, C. C.; Kim, M.; Alexander, T.; Touret, N.; Hahn, K. M.; Grinstein, S. *J. Cell Biol.* **2010**, *188*, 547.

(57) Daukas, G.; Zigmond, S. H. *J. Cell Biol.* **1985**, *101*, 1673.

(58) Wang, L. H.; Rothberg, K. G.; Anderson, R. G. *J. Cell Biol.* **1993**, *123*, 1107.

(59) Dangoria, N. S.; Breau, W. C.; Anderson, H. A.; Cishek, D. M.; Norkin, L. C. *J. Gen. Virol.* **1996**, *77 (Pt 9)*, 2173.

(60) Chen, Y.; Norkin, L. C. *Exp. Cell Res.* **1999**, *246*, 83.

(61) Pelkmans, L.; Puntener, D.; Helenius, A. *Science* **2002**, *296*, 535.

(62) Rothberg, K. G.; Ying, Y. S.; Kamen, B. A.; Anderson, R. G. *J. Cell Biol.* **1990**, *111*, 2931.

(63) Ros-Baro, A.; Lopez-Iglesias, C.; Peiro, S.; Bellido, D.; Palacin, M.; Zorzano, A.; Camps, M. *Proc. Natl. Acad. Sci. U. S. A.* **2001**, *98*, 12050.

(64) Flavell, D. J. *Curr. Top. Microbiol. Immunol.* **1998**, *234*, 57.

(65) Imai, M.; Inoue, K.; Nojima, S. *Biochim. Biophys. Acta* **1975**, *375*, 130.

(66) HsuChen, C. C.; Feingold, D. S. *Biochemistry* **1973**, *12*, 2105.

(67) Torchilin, V. P. *Biopolymers* **2008**, *90*, 604.

(68) Marty, C.; Meylan, C.; Schott, H.; Ballmer-Hofer, K.; Schwendener, R. A. *Cell. Mol. Life Sci.* **2004**, *61*, 1785.

(69) Furuhata, M.; Kawakami, H.; Toma, K.; Hattori, Y.; Maitani, Y. *Bioconjug. Chem.* **2006**, *17*, 935.

(70) Tseng, Y. L.; Liu, J. J.; Hong, R. L. *Mol. Pharmacol.* **2002**, *62*, 864.

(71) Torchilin, V. P.; Rammohan, R.; Weissig, V.; Levchenko, T. S. *Proc. Natl. Acad. Sci. U. S. A.* **2001**, *98*, 8786.

(72) Fretz, M. M.; Koning, G. A.; Mastrobattista, E.; Jiskoot, W.; Storm, G. *Biochimica et Biophysica Acta (BBA) - Biomembranes* **2004**, *1665*, 48.

(73) Cryan, S.-A.; Devocelle, M.; Moran, P. J.; Hickey, A. J.; Kelly, J. G. *Mol. Pharm.* **2006**, *3*, 104.

(74) Stewart, J. C. *Anal. Biochem.* **1980**, *104*, 10.

(75) Fry, D. W.; White, J. C.; Goldman, I. D. *Anal. Biochem.* **1978**, *90*, 809.

Chapter 3:

GNeo-Modified Liposomes Deliver Active Lysosomal Enzyme

3.1 Introduction

Lysosomes are important for the degradation of intra- and extracellular material through the action of over 50 acid hydrolases and membrane proteins.[1-3] The absence or low activity of a particular lysosomal hydrolase enzyme leads to accumulation of its substrate(s) which causes damage in various tissues, organs, and in some cases, the central nervous system (CNS). These enzyme deficiencies are classified as approximately 50 recessively inherited lysosomal storage disorders (LSDs). LSDs are individually rare, however, their combined prevalence is about 1 in 8,000 births.[4-6]

The predominant treatment of LSDs is enzyme replacement therapy (ERT), where intravenously administered enzyme is taken up by cells through a mannose-6-phosphate mediated pathway.[6-9] Although ERT has been successful in treating several LSDs, it is limited, does not treat the CNS, and is a very expensive treatment mostly due to the short half life of the enzyme, thus requiring high doses and repeated administration.[7-9] Therapeutic limitations of ERT include inactivation of enzyme and low cellular uptake. Additionally, administration of exogenous enzyme into the bloodstream might trigger an immune response, reducing the safety and efficacy of ERT.[8,9]

In the 1970s, it was found that enzymes could be encapsulated in lipid vesicles.[10] Delivery of lysosomal enzymes encapsulated in liposomes protects the enzyme from degradation, has enhanced immune tolerance, and increases delivery of the enzyme to the lysosomes of cells *in vitro* and *in vivo*.[11-13] α-Glucosidase-, β-fructofuranosidase-, α-

mannosidase- β-glucuronidase- and neuraminidase-loaded liposomes all showed increase accumulation of the enzyme in liver and spleen of rats compared to unpackaged enzymes, with a majority of the delivered enzyme localizing in the lysosomes.[14-18] Modifying the surface of liposomes with ligands was also investigated early on as a method to improve overall uptake and cell selectivity.[19] Aggregated IgG-coated liposomes delivered more hexosaminidase A than uncoated liposomes to cells isolated from Tay-Sachs patients.[20] Recent efforts have focused on attaching other targeting ligands, such as low molecular weight ligands (*e.g.*, rhodamine B and mannose-6-phosphate) or high molecular weight proteins (*e.g.*, transferrin), to the surface of liposomes to improve their lysosomal delivery.[21-26]

A more general approach to improving the cellular delivery of biomolecules has been to conjugate the cargo to a molecular transporter. Certain peptides rich in basic amino acids, such as the TAT peptide and oligo-arginine, have repeatedly been shown to traverse the plasma membrane and facilitate the intracellular delivery of various cargo.[27-31] Numerous other guanidinium-rich molecular transporters based on diverse scaffolds have also been used to deliver a variety of cargo into cells through covalent attachment or noncovalent association.[32-34] Guanidinium-rich transporters have also been used to improve the intracellular delivery of liposomes that encapsulate the desired cargo.[24,35-41]

Guanidinoglycosides have been developed as a unique class of molecular transporters capable of delivering high-molecular weight, bioactive cargo into the lysosomes of cells through heparan sulfate exclusive pathways.[42-46] For example, guanidinylated neomycin (GNeo), containing 6 positively charged guanidinium groups,

was conjugated to the lysines of lysosomal enzymes responsible for breaking down glycosaminoglycans.[45] The GNeo-enzyme was internalized and able to restore normal glycosaminoglycan turnover in cells deficient in these enzymes. More recently, we reported on the assembly and cellular uptake of GNeosomes, lipid vesicles decorated with GNeo that maintain selectivity for heparan sulfate and demonstrate high cellular uptake and specificity for the lysosomes.[24] GNeosomes protect cargo from degradation and unfavorable reactions in biological systems and avoid modification of the cargo, which could alter its properties and lead to reduced activity. In addition to the general benefits of liposomes, modifying the surface with GNeo significantly increases the uptake and lysosomal delivery of diverse cargo compared to unmodified liposomes.[24]

In the present study, we report the synthesis of novel GNeo–lipid derivatives and compare different methods for incorporating GNeo into liposomes. The cellular uptake of the different derivatives and preparations were initially evaluated by their ability to deliver a fluorescent dye. All liposomes modified with GNeo showed enhanced uptake compared to the unmodified liposomes. The GNeosome preparations with the highest uptake efficiency were also evaluated for their ability to deliver the lysosomal enzyme α-L-iduronidase. GNeosomes increased the overall uptake of the enzyme compared to plain liposomes and a sufficient amount of enzyme was delivered to restore the normal turnover of glycosaminoglycans in MPS I cells, which lack endogenous enzyme. We conclude that GNeosomes can potentially be used to deliver therapeutic amounts of active enzyme to the lysosomes in cells for the treatment of lysosomal storage disorders.

3.2 Results

Synthesis of Guanidinoneomycin Derivatives

Three GNeo–lipid derivatives were synthesized as outlined in Scheme 3.1. Briefly, the fatty acid (**3.1, 3.2** or **3.3)** was coupled to the amino group of an amino-alkyne-functionalized triethylene glycol (**3.4**). The resulting compounds (**3.5, 3.6,** and **3.7**) underwent a 1,3-dipolar cycloaddition with **3.8** followed by acidic deprotection of the Boc-guanidinium groups to yield stearyl-GNeo (**3.9**), oleyl-GNeo (**3.10**), and di-oleyl-GNeo (**3.11**). In addition to the GNeo-lipids that can be directly incorporated in the liposomal bilayer, GNeo-NHS (**3.14)** was synthesized by clicking a previously reported alkyne-BocGNeo derivative (**3.12**) to an azide-NHS-functionalized triethylene glycol linker (**3.13**) to evaluate post-modification of liposomes (Scheme 3.2).

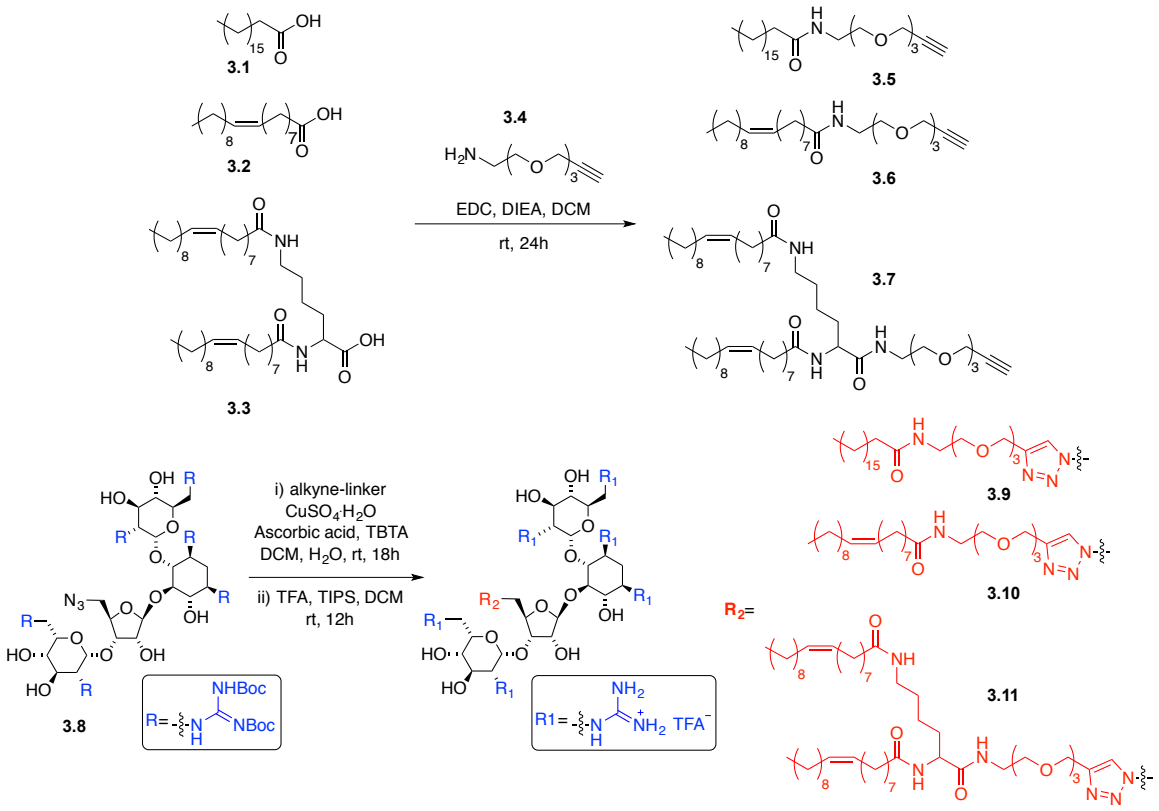

Scheme 3.1. Synthesis of GNeo-lipids.

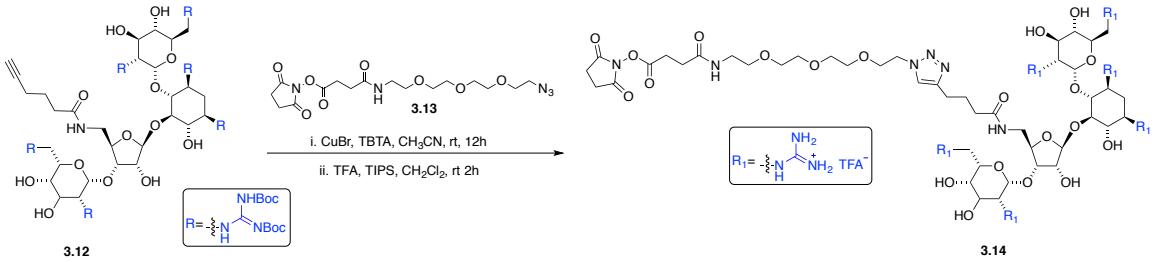

Scheme 3.2. Synthesis of GNeo-NHS.

Preparation and Characterization of Cy5-containing Lipid Vesicles

Liposomes were prepared by pre-inserted, post-inserted, or post-modification techniques (Figure 1). To evaluate the differences in cellular uptake between the different preparation methods and lipid derivatives, a fluorescent dye, Cy5, was encapsulated as low MW cargo mimic.

Pre-inserted liposomes were prepared by rehydrating a lipid film consisting of DOPC, DOPE, and cholesterol (73:11:16 mol %) with phosphate buffered saline (pH 7.4) containing 100 μM Cy5 and the GNeo–lipid derivative (0.9 mol %). The lipid suspension was subjected to sonication, freeze and thaw cycles, extrusion through a 100 nm polycarbonate membrane, and size exclusion chromatography (SEC) to remove unencapsulated dye and GNeo-lipid.[47]

Plain liposomes were prepared by rehydrating a lipid film consisting of DOPC, DOPE, and cholesterol (73:11:16 mol %) with phosphate buffered saline (pH 7.4) containing 100 μM Cy5. The lipid suspension was subjected to sonication, freeze and thaw cycles, extrusion through a 100 nm polycarbonate membrane, and SEC.[47] Plain liposomes were then modified either by post-insertion of the GNeo-lipid or post-modification of DOPE with GNeo-NHS. For post-inserted liposomes, plain liposomes were mixed for 1 h

at room temperature with the GNeo–lipid derivative (0.9 or 1.8 mol %). For post-modification, plain liposomes were mixed for 1 h at room temperature with GNeo-NHS (10 or 20 mol %). Unencapsulated GNeo-lipid or unreacted GNeo-NHS were removed by SEC.

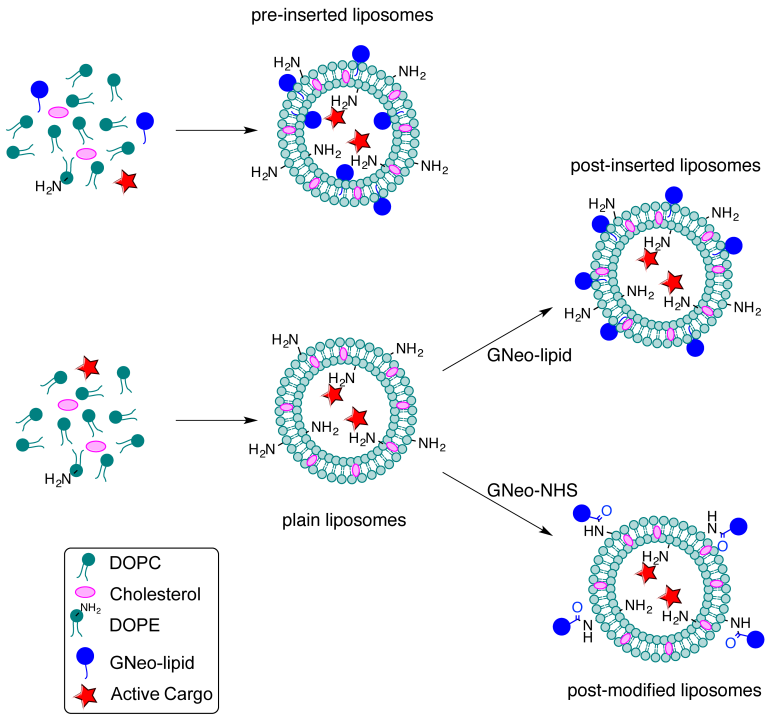

Figure 3.1. Methods for incorporating GNeo into liposomes. Schematic representation of the three different methods used for preparing GNeosomes.

All liposomes were then characterized by dynamic light scattering (DLS) to measure size and zeta-potential (Figure 3.2). The addition of GNeo did not affect the average size of the liposomes (Figure 3.2a). However, GNeosomes exhibited a positive increase in zeta potential compared to plain liposomes (Figure 3.2b). The zeta potentials of the pre-inserted liposomes using 0.9% GNeo-lipid are lower than the post-inserted liposomes modified. The zeta potential generally increases with an increase in GNeo-lipid

with the exception of liposomes post-modified with di-oleyl-GNeo. An increase in zeta potential is also observed when a higher concentration of GNeo-NHS is used (Figure 3.2b).

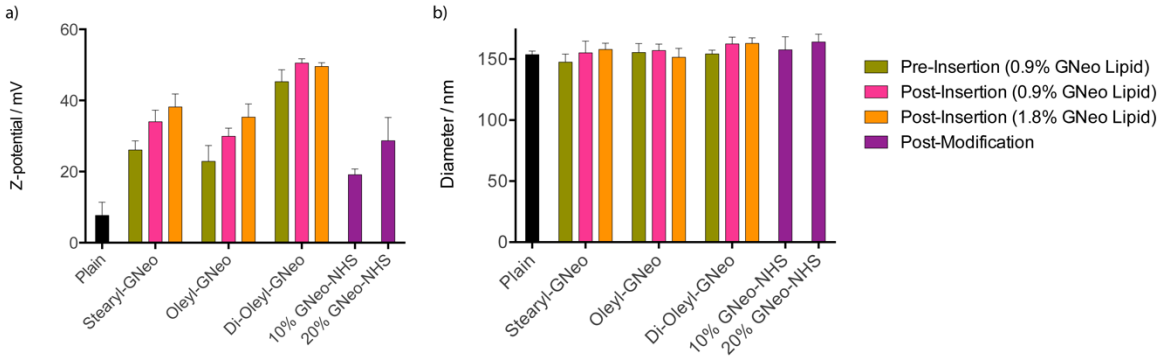

Figure 3.2. Characterization of liposomes. (a) Zeta potential of the evaluated liposomes. (b) Average diameter of the evaluated liposomes. Four different batches of liposomes were each measured in triplicate.

Cellular Uptake of Cy5-containing Liposomes

To compare the cellular uptake of the different GNeosomes, a water-soluble cyanine dye was encapsulated and uptake was evaluated in wild-type CHO-K1 cells. The cells were then incubated with liposomes at 37 °C for 1 h and analyzed by flow cytometry. In all cases, cells treated with GNeosomes showed higher mean fluorescence intensity (MFI) than cells treated with plain liposomes (Figure 3.3). For stearyl-GNeosomes, uptake for post-inserted liposomes was higher than pre-inserted ones and a higher concentration of stearyl-GNeo resulted in a two-fold increase in uptake. Oleyl-GNeosomes had the lowest overall uptake. Pre-inserted and post-inserted liposomes exhibited similar uptake but an increase in oleyl-GNeo concentration during post-insertion resulted in better uptake. Di-oleyl-GNeosomes showed the highest overall uptake and a difference in uptake was not observed between post-inserted and pre-inserted liposomes. Increasing the concentration of di-oleyl-GNeo resulted in a lower encapsulation of Cy5 (Figure 3.6, Experimental

Section); therefore, a lower amount of Cy5 was delivered to cells. For GNeo-NHS modified liposomes, uptake increased with an increase in GNeo-NHS.

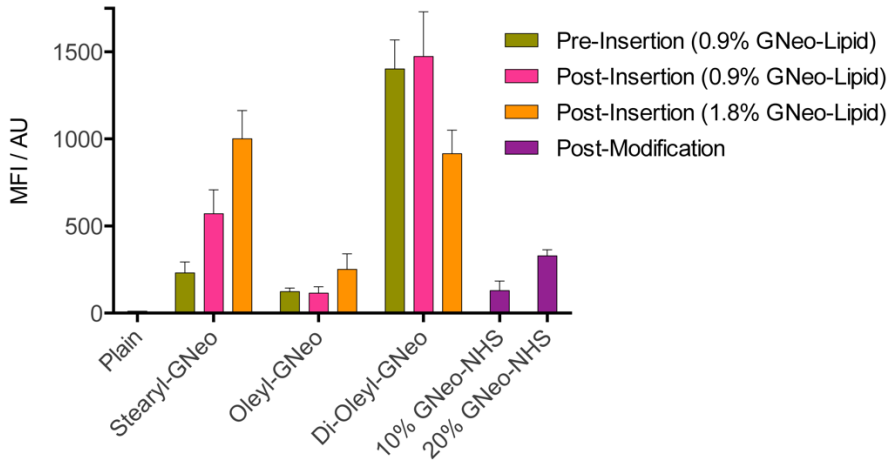

Figure 3.3. Cellular uptake of Cy5-containing GNeosomes. Wild-type CHO-K1 cells were incubated for 1 h at 37°C with 300 μg mL^{-1} Cy5-containing plain and GNeo-decorated liposomes prepared with the indicated concentrations and methods. Mean fluorescence intensity (MFI) was measured by flow cytometry. The background signal from untreated cells was subtracted. The experiment was performed three times in triplicate.

Preparation and Characterization of Liposomes Encapsulating a Lysosomal Enzyme

Based on their ability to internalize Cy5, the four liposome preparations with the most efficient uptake (0.9% and 1.8% stearyl-GNeo post inserted, 0.9% di-oleyl-GNeo post-inserted, and 0.9% di-oleyl-GNeo pre-inserted) were tested for their ability to deliver the lysosomal enzyme, α-L-Iduronidase (IDUA, Aldurazyme). Lipid films were rehydrated with PBS containing 5 mg/mL IDUA and liposomes were prepared the same way as described above for Cy5-containing liposomes. Liposomes were purified on a Sepharose size exclusion column to remove unencapsulated enzyme. To determine the amount of enzyme encapsulated, the liposomes were lysed using 10% Tween 20 and analyzed for enzyme concentration on an SDS-PAGE protein gel (Figure 3.7, Experimental Section)

and for enzyme activity using a fluorescent enzyme activity assay.[48] All of the preparations tested resulted in a 5% enzyme encapsulation efficiency (Figure 3.7, Experimental Section).

Delivery of IDUA by GNeosomes

To evaluate whether IDUA-containing liposomes and GNeosomes were taken up by IDUA-deficient cells, MPS I fibroblasts were incubated with plain liposomes or GNeosomes for 1 h at 37 °C. The cells were then lysed and analyzed for IDUA activity by measuring the conversion of 4-methylumbelliferyl α-L-iduronide into the fluorochrome 4-methylumbelliferone (4-MU).[48] Cells incubated with plain liposomes showed very little enzyme activity, whereas cells incubated with GNeosomes contained active enzyme (Figure 3.4). Relative uptake efficiencies were comparable to those seen with Cy5-containing liposomes. GNeosomes with 1.8% stearyl-GNeo showed higher enzyme activity in cells than GNeosomes with 0.9% stearyl-GNeo. Cells incubated with 1.8 % stearyl-, 0.9% di-oleyl-post-, or 0.9% di-oleyl-pre-GNeosomes all showed similar enzyme activity (Figure 3.4).

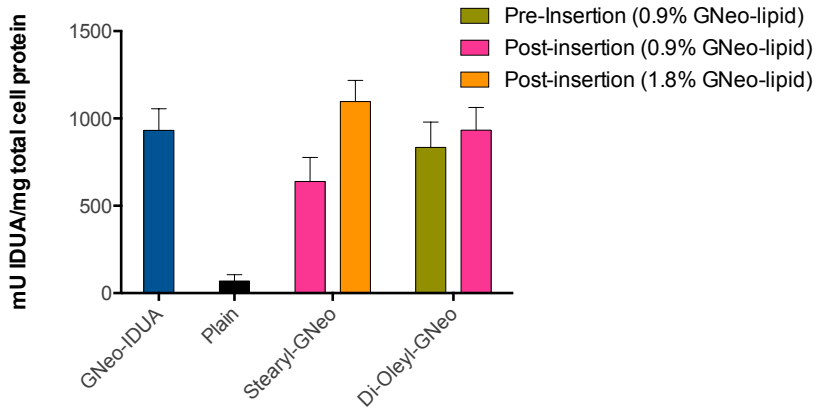

Figure 3.4. Liposomal delivery of IDUA. (a) MPS I fibroblasts were treated for 1 h at 37°C with 500 μg mL^{-1} plain or GNeo-decorated liposomes containing 2.5 μg mL^{-1} IDUA. The cells were washed, trypsin treated, sedimented by centrifugation, washed, lysed, and assays for IDUA activity. Cells were also treated with of 2.5 μg mL^{-1} GNeo-conjugated IDUA (G-IDUA) for comparison. The experiment was performed twice (with different batches of liposomes) in triplicate. Analysis of variance showed that the differences between plain liposomes and GNeosomes were significant (P = 0.007 — <0.0001).

GNeosomes Restore Normal Glycosaminoglycan Turnover

To determine whether GNeosomes were delivering active IDUA to the lysosomes, a label-chase experiment was performed. MPS I or wild-type fibroblast cells were incubated with ^{35}S-labeled sulfate for 48 h to radiolabel sulfated glycosaminoglycans. The cells were then incubated with plain liposomes or GNeosomes for 1h at 37 °C, washed, incubated with fresh medium for another 24 hours, then analyzed for the amount of [^{35}S]glycosaminoglycans associated with the cells. As shown in Figure 3.5, MPS I fibroblasts store [^{35}S]glycosaminoglycans resulting in higher liquid scintillation counts; whereas, wild-type HFF cells have regular turnover of glycosaminoglycans and lower counts per minute (cpm). GNeosomes containing IDUA were able to restore turnover to that of wild-type cells. Plain liposomes showed a two-fold higher storage of [^{35}S]glycosaminoglycans.

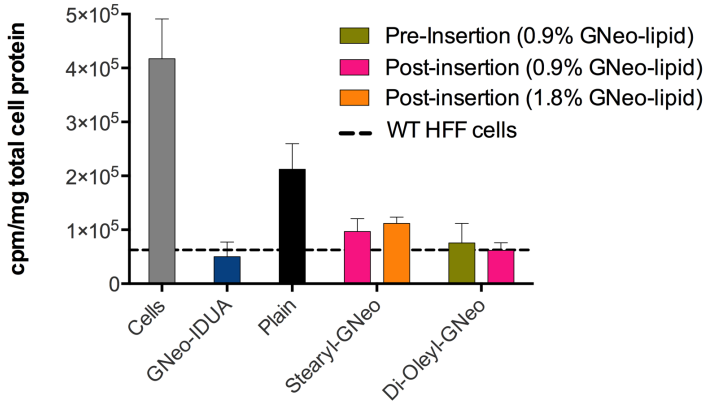

Figure 3.5. Glycosaminoglycan turnover using IDUA-containing GNeosomes. MPS I fibroblasts were radiolabeled with $^{35}SO_4$ and chased for 24 hours with 100 μg mL^{-1} plain or GNeo-decorated liposomes containing 0.2 μg mL^{-1} IDUA. The amount of [^{35}S]glycosaminoglycan remaining was measured (Experimental Section). Cells were also treated with 0.2 μg mL^{-1} of GNeo-conjugated IDUA (G-IDUA) for comparison. The dotted line represents the amount of [^{35}S]glycosaminoglycan remaining in wild-type fibroblasts (HFF) radiolabeled with $^{35}SO_4$ and chased for 24 hours without enzyme supplementation. The experiment was performed twice (with different batches of liposomes) in triplicate. Analysis of variance showed that the differences between plain liposomes and GNeosomes were significant ($P < 0.0005$). The difference between untreated MPS I cells and plain liposomes was also significant ($P = 0.0002$).

3.3 Discussion

As biomolecules gain prominence as potential therapeutics, the intracellular delivery of these molecules remains one of the key problems in drug development.[49-51] Arginine-rich transduction domains represent a promising method for facilitating intracellular delivery of impermeable cargo; however, their internalization mechanisms remain controversial, likely involve multiple pathways, and are dependent on other factors such as cargo size and cell type.[52,53] Guanidinoglycosides, in which the ammonium groups of aminoglycosides are converted to guanidinium groups, can deliver high molecular weight cargo into cells at low nanomolar carrier concentrations.[42,43] The uptake of guanidinoglycosides has consistently been shown to depend exclusively on cell-surface heparan sulfate proteoglycans.[43-46]

We previously demonstrated that liposomes incorporating a stearyl-guanidinylated neomycin (stearyl-GNeo) derivative specifically target the lysosomes and allow for increased delivery of liposome-entrapped material, including fluorescent proteins and small molecules.[24] The increase in cellular uptake of GNeosomes is not simply a result of an overall increase in net positive charge, as liposomes bearing the same positive charge showed lower uptake.[24] This suggests the spatial arrangement and presentation of the guanidinium-groups on GNeo contribute to its superior uptake ability. In the current study, we sought to explore the ability of other GNeo-lipids to further enhance the uptake of liposomes. We then evaluate the cellular delivery of a liposome-encapsulated lysosomal enzyme and the ability to restore normal glycosaminoglycan turnover in enzyme-deficient cells.

Three GNeo-lipids were synthesized from stearic acid, oleic acid, and a dimeric oleic acid tail (Scheme 3.1). The GNeo-lipids were incorporated into liposomes by either pre-insertion or post-insertion (Figure 3.1). Additionally, the primary amines on the surface of preformed liposomes containing 1,2-dioleoyl-*sn*-glycero-3-phosphoethanolamine (DOPE) were modified with GNeo-NHS and evaluated for uptake (Figure 3.1). The surface charge of the different GNeosomes was evaluated by measuring the zeta potential (Figure 3.2). Post-insertion of the GNeo-lipids resulted in a higher zeta potential than pre-insertion. This is not surprising because while the same amount of GNeo-lipid is added, the GNeo can position itself on both the inside and outside of the liposome when added during liposome formation (pre-insertion). During post-insertion, the GNeo-lipid can only insert into the outside liposomal membrane and it is unlikely it will flip to the inside since the GNeo moiety is highly charged. Furthermore, an increase

in the concentration of stearyl-GNeo, oleyl-GNeo, or GNeo-NHS leads to higher zeta potential, indicating a higher degree of insertion or modification. Increasing the concentration of post-inserted di-oleyl-GNeo from 0.9% to 1.8% did not increase the surface charge suggesting that 0.9% di-oleyl-GNeo is the optimal concentration and any additional di-oleyl-GNeo remains extravesicular. Di-oleyl-GNeosomes had the highest zeta potentials suggesting di-oleyl-GNeo inserts into the liposome membrane more efficiently than the GNeo-lipids with a single hydrophobic tail.

To evaluate the uptake of the different preparation methods, a fluorescent cyanine dye, Cy5, was encapsulated in the liposomes. Uptake was evaluated in wild-type CHO-K1 cells and analyzed by flow cytometry. As shown in Figure 3.3, the mean fluorescence intensity (MFI) of cells treated with GNeosomes is significantly higher than cells treated with plain liposomes. Generally, di-oleyl-GNeosomes exhibited the highest uptake, followed by stearyl-GNeosomes. This is consistent with the trend seen for the zeta potentials, and taken together, suggests these lipids insert better into the liposome membrane leading to an increase in GNeo on the surface and higher uptake. Oleyl-GNeosomes and GNeo-NHS modified GNeosomes had the lowest zeta potentials and also the lowest cellular uptake suggesting a lower degree of GNeo modification. The decrease in uptake when a higher concentration of di-oleyl-GNeo was used is attributed to a lower dye encapsulation efficiency (EE). Increasing the concentration of di-oleyl-GNeo to 1.8% resulted in a lower encapsulation of Cy5; whereas all the other methods resulted in similar EE (Figure 3.6). This suggests that the higher concentration of di-oleyl-GNeo results in leaky liposomes since the concentration before adding GNeo is the same for all the post-inserted liposomes. Moreover, the zeta potential remains unchanged when increased di-

oleyl-GNeo concentrations are used; therefore, it is unlikely that uptake would increase, regardless of the lower EE.

To investigate whether GNeosomes can deliver an active enzyme to the lysosomes, α-L-iduronidase (IDUA) was encapsulated in liposomes. IDUA is a lysosomal enzyme responsible for hydrolyzing the terminal α-L-iduronic acid residues in heparan sulfate (HS) and dermatan sulfate (DS). A deficiency in IDUA leads to the accumulation of HS and DS in the lysosomes and is responsible for the lysosomal storage disease mucopolysaccharidoses I (MPS I; Hurler, Hurler-Scheie, and Scheie syndromes).[54] The enzyme was stable to liposome preparation and uptake could be assessed in IDUA-deficient MPS I fibroblasts. MPS I cells have essentially no IDUA activity; therefore, they provide a low background when monitoring uptake. Low enzyme activity was observed in cells treated with plain liposomes; on the other hand, cells treated with GNeosomes show more than ten-fold higher enzyme activity (Figure 3.4). Liposomes post-inserted with 1.8% stearyl-GNeo delivered almost twice as much active enzyme to cells than liposomes post-inserted with 0.9% stearyl-GNeo, similar to the uptake of Cy5. The di-oleyl-GNeosomes also exhibited an uptake pattern similar to the delivery of Cy5 with the pre-inserted and post-inserted liposomes behaving similarly. However, unlike the delivery of Cy5, stearyl-GNeosomes outperformed the di-oleyl-GNeosomes in delivering IDUA.

The capability of GNeosomes to deliver functional enzyme to the lysosomes of MPS I cells was assessed by measuring the turnover of radiolabeled glycosaminoglycans (GAGs). Untreated MPS I cells deficient in IDUA store [^{35}S]-sulfated GAGs. Plain liposomes lower the amount of stored GAGs by about 50%, whereas GNeosomes return

the turnover of GAGs to a level comparable to that found in normal HFF cells (Figure 3.5). These results indicate that GNeosomes are taken up by IDUA-deficient fibroblasts, that they reach the lysosomal compartment, and that the cargo (IDUA) is efficiently released such that IDUA activity is restored.

Uptake was also compared to the conjugated GNeo-IDUA enzyme. GNeo-IDUA has previously been shown to have enhanced uptake and activity compared to Aldurazyme, the high-uptake form currently in clinical use for treatment of MPS I patients.[45] Maintaining this high uptake due to GNeo while encapsulating the enzyme in liposomes could have additional benefits for *in vivo* applications, including improved stability typically seen with liposome delivery systems.[55-58] Additional studies are needed to determine the plasma clearance and tissue specificity for GNeosomes.

3.4 Conclusions

In conclusion, we have demonstrated that introduction of GNeo to the surface of liposomes results in superior uptake in wild-type CHO cells and MPS I human fibroblasts compared to unmodified liposomes. These GNeosomes were demonstrated to be able to deliver and release a small molecule and an active enzyme to the lysosomes. The advantages of using GNeo to enhance cellular uptake and liposomes as delivery vehicles results in an improved lysosomal delivery system. Because virtually all mammalian cells express heparan sulfate, GNeosomes could be ideal for improving the enzymatic treatment of lysosomal storage disorders that affect all tissues. Furthermore, lipid vesicles avoid direct modification of enzymes and can be used to entrap other lysosomal enzymes whose activity might be affected by direct conjugation. The use of liposomes also allows for

further modification in addition to GNeo to potentially target specific tissues, such as the brain or cancer cells, [59-62] or to further stabilize the delivery system, by incorporating PEGylated-lipids for example.[63-65]

3.5 Experimental

Materials

Materials obtained from commercial suppliers were used without further purification. Chemicals and reagents were purchased from Sigma Aldrich. Deuterated NMR solvents were purchased from Cambridge Isotope Laboratories. DOPC (1,2-dioleoyl-*sn*-glycero-3-phosphocholine), DOPE (1,2-dioleoyl-*sn*-glycero-3-phospho-ethanolamine), and cholesterol were purchased from Avanti Polar Lipids. PBS (Dulbecco's phosphate buffered saline), F-12 Nutrient Mixture (Ham), DMEM, and F12/DMEM were purchased from Thermo Scientific. Trypsin/EDTA was purchased from VWR. α-L-Iduronidase (Aldurazyme) was obtained from BioMarin Pharmaceuticals and purified via FPLC on a heparin column prior to use.

Instrumentation

NMR spectra were recorded on either a Varian 400 MHz or 500 MHz spectrometers. Mass spectra were recorded at UCSD Chemistry and Biochemistry Mass Spectrometry Facility utilizing an Agilent 6230 HR-ESI-TOF mass spectrometer. Reverse-phase HPLC purification (CLIPEUS, C18, 5μm, 10x250 mm, Higgins analytical) and analysis (Eclipse, XDB-C18, 5μm, 4.6x150 mm) were carried out on an Agilent 1200 series instrument. Fluorescence spectroscopy measurements were performed using a Horiba fluorimeter. Particle size, polydispersity, and surface charge of the lipid vesicles

were measured by dynamic light scattering on a Zetasizer Nano ZS (model ZEN3600 from Malvern Instruments). Flow cytometry studies were performed on a BD FACSCalibur.

Synthesis of Lipid-GNeo Derivatives

Stearyl-GNeo (**3.1**), amino-alkyne linker (**3.4**), and N_3-BocGNeo (**3.8**) were synthesized according to previously published procedures.[24]

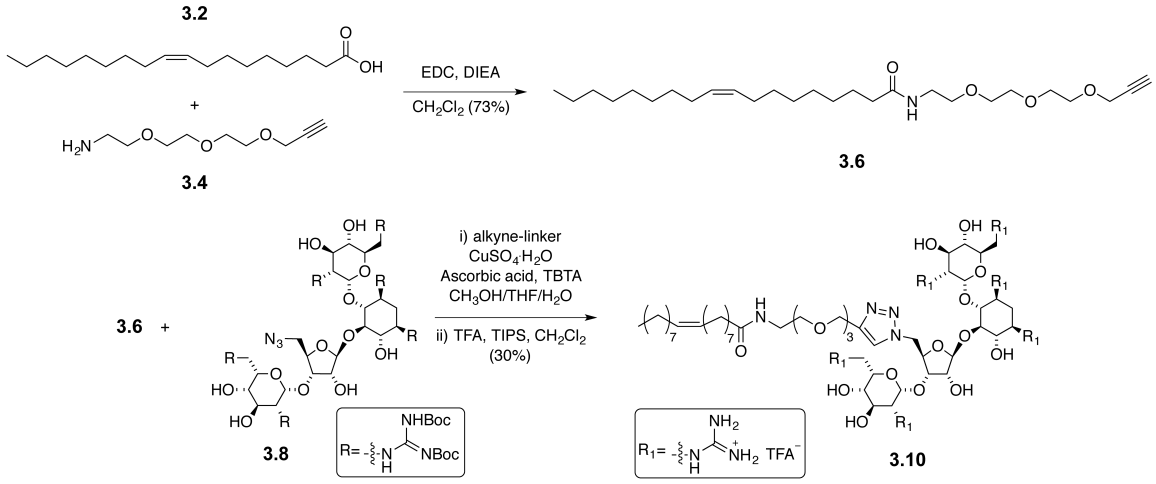

Scheme 3.3. Synthesis of oleyl-GNeo.

Oleyl-alkyne linker (3.6). To a solution of oleic acid (424 mg, 1.5 mmol) in dichloromethane, was added *N*-ethyl-*N*-(3-dimethylaminopropyl)carbodiimide hydrochloride (EDC) (370 mg, 2 mmol) and the solution was stirred at room temperature for 30 min. Compound **3.4** (187 mg, 1.0 mmol) and DIEA (178 μL, 1 mmol) were dissolved in CH_2Cl_2 and added to the reaction. After stirring overnight at room temperature, the reaction was diluted with CH_2Cl_2 and washed with aqueous citric acid (5%) and brine. The organic phase was dried over sodium sulfate and evaporated. The residue was purified by flash chromatography to afford the desired compound (340 mg, 0.75 mmol, 73% yield).). ^{1}H NMR (500 MHz, $CDCl_3$) δ: 6.12 (s, 1H), 5.3 (m, 2H), 4.21 (d, J = 2.4 Hz, 2H), 3.71–3.64 (m, 8H), 3.56 (t, J = 4.8 Hz, 2H), 3.45 (q, J = 5.1 Hz, 2H),

2.44 (t, J = 2.4 Hz, 1H), 2.18 (t, J = 7.5 Hz, 2H), 2.00 (m, 4H), 1.63 (m, 2H), 1.35–1.25 (m, 24H), 0.87 (t, J = 6.8 Hz, 3H). ^{13}C NMR (125 MHz, $CDCl_3$) δ: 173.32, 129.96, 129.74, 79.47, 74.64, 70.50, 70.34, 70.16, 69.95, 69.09, 58.41, 39.13, 36.70, 31.89, 29.75, 29.72, 29.51, 29.30, 29.16, 27.21, 27.18, 25.74, 22.66, 14.10. ESI-HR-MS calculated $[M+H]^+$ 452.3734, found 452.3735.

Oleyl-GNeo (3.10). Compounds **3.6** (2 eq) and **3.8** (1 eq) were dissolved in methanol/tetrahydrofuran/water (2:1:0.3, 3.3 mL/0.1 mmol). $CuSO_4 \cdot 5H_2O$ (2 eq) and sodium ascorbate (2 eq) were dissolved in water and added to the organic solution. The mixture was sonicated for 30 min then diluted with CH_2Cl_2 (40 mL) and washed twice with with EDTA (0.1 M, 50 mL), aqueous KCN (5%, 50 mL), and brine (50 mL). The organic phase was dried over Na_2SO_4 and evaporated. The residue was dissolved in CH_2Cl_2 (2 mL) and triisopropylsilane (100 μL) and trifluoroacetic acid (2 mL) were added. The reaction was stirred 12 h at room temperature, concentrated under vacuum and coevaporated with toluene (3×). The residue was dissolved in 5% aqueous acetonitrile and purified on reverse phase HPLC to obtain the desired compound as an amorphous fluffy white powder (30% yield). ^{1}H NMR (500 MHz, D_2O) δ: 7.90 (s, 1H), 5.63 (s, 1H), 5.28 (m, 2H), 4.97 (s, 2H), 4.34 (m, 1H), 4.26 (m, 2H, 4.03 (m, 2H), 3.68-3.38 (m, 26H), 3.26 (m, 2H), 2.10 (m, 3H), 1.89 (m, 4H), 1.45 (m, 3H), 1.14 (m, 22H), 0.74 (m, 3H). ^{13}C NMR (125 MHz, D_2O) δ: 176.66, 163.20, 162.92, 162.64, 162.36, 157.68, 157.26, 157.17, 157.03, 156.46, 143.70, 130.53, 130.20, 125.59, 119.81, 117.48, 115.16, 112.84, 111.37, 97.73, 95.81, 85.21, 78.82, 77.68, 77.21, 74.40, 72.78, 72.61, 71.87, 70.87, 69.60, 69.46, 69.26, 69.12, 68.92, 66.71, 63.14, 55.39, 53.29, 51.94, 50.43, 41.85, 41.69, 38.82, 35.79, 32.08, 32.06, 31.47,

29.12, 28.88, 28.78, 28.67, 28.54, 28.35, 26.68, 25.46, 22.24, 22.21. ESI-HR-MS calculated $[M+2H]^{2+}$ 672.4151, found 672.4149.

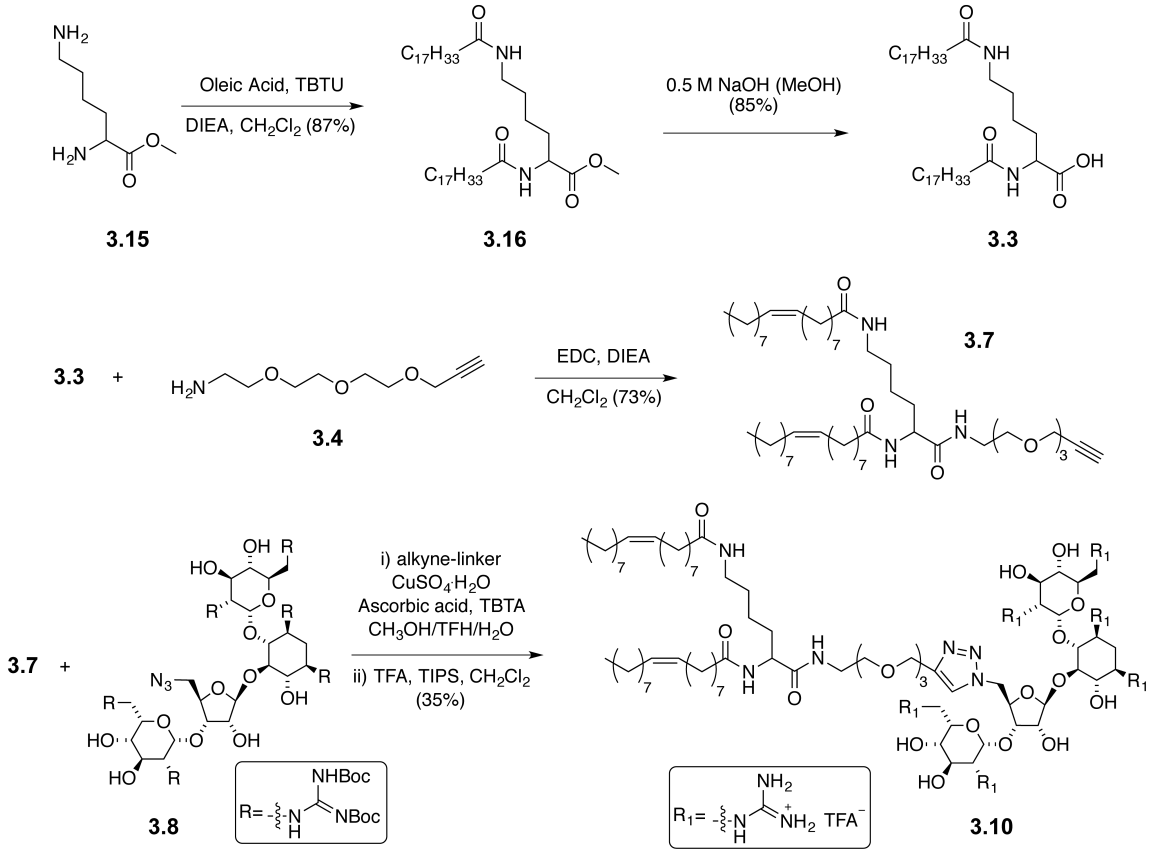

Scheme 3.4. Synthesis of di-oleyl-GNeo.

Di-oleyl-ester (**3.16**) and Di-oleyl-acid (**3.3**) were prepared according to literature procedures.[66]

Di-oleyl-alkyne linker (3.7). To a solution of **3.3** (152 mg, 0.225 mmol) in dichloromethane, was added EDC (56 mg, 0.3 mmol) and the solution was stirred at room temperature for 30 min. Compound **3.4** (28 mg, 0.15 mmol) and DIEA (27 μL, 0.15 mmol) were dissolved in CH_2Cl_2 and added to the reaction. After stirring overnight at room

temperature, the reaction was diluted with CH_2Cl_2 and washed with aqueous citric acid (5%) and brine. The organic phase was dried over sodium sulfate and evaporated. The residue was purified by flash chromatography to afford the desired compound (90 mg, 0.11 mmol, 73% yield). ^{1}H NMR (500 MHz, $CDCl_3$) δ: 6.97 (s, 1H), 6.57 (s, 1H), 6.23 (s, 1H), 5.34 (m, 4H), 4.42 (m 1H), 4.22 (d, J = 2.4 Hz, 2H), 3.75–3.68 (m, 5H), 3.64 (m, 4H), 3.56 (m, 2H), 3.46 (m, 2H), 3.25 (m, 2H), 2.49 (t, J = 2.4 Hz, 1H), 2.21 (m, 4H), 2.01 (m, 8H), 1.80 (m, 1H), 1.62 (m, 8H), 1.24–1.27 (m, 42H), 0.88 (t, J = 6.8 Hz, 6H). ^{13}C NMR (125 MHz, $CDCl_3$) δ: 174.64, 174.40, 174.27, 130.01, 129.70, 129.67, 52.10, 38.79, 36.68, 36.40, 31.92, 31.18, 29.77, 29.55, 29.34, 29.31, 29.22, 29.20, 28.96, 27.23, 25.84, 25.71, 22.70, 21.97, 14.15. ESI-HR-MS calculated $[M+H]^+$ 844.7137, found 844.7132.

Di-oleyl-GNeo (3.10). Compounds **3.6** (2 eq) and **3.8** (1 eq) were dissolved in methanol/tetrahydrofuran/water (2:1:0.3, 3.3 mL/0.1 mmol). $CuSO_4 \cdot 5H_2O$ (2 eq) and sodium ascorbate (2 eq) were dissolved in water and added to the organic solution. The mixture was sonicated for 30 min then diluted with CH_2Cl_2 (40 mL) and washed twice with with EDTA (0.1 M, 50 mL), aqueous KCN (5%, 50 mL), and brine (50 mL). The organic phase was dried over Na_2SO_4 and evaporated. The residue was dissolved in CH_2Cl_2 (2 mL) and triisopropylsilane (100 μL) and trifluoroacetic acid (2 mL) were added. The reaction was stirred 12 h at room temperature, concentrated under vacuum and coevaporated with toluene (3×). The residue was dissolved in 5% aqueous acetonitrile and purified on reverse phase HPLC to obtain the desired compound as an amorphous fluffy white powder (35% yield). ^{1}H NMR (500 MHz, $CDCl_3$) δ: 8.01 (s, 1H), 5.90 (d, J = 3.6 Hz, 1H), 5.35 (t, J = 5 Hz, 2H), 5.13 (s, 1H), 5.10 (m, 1H), 5.07 (s, 1H), 4.70 (m, 7H), 4.40 (m, 1H), 4.26 (m, 4H),

4.12 (m, 1H), 4.01 (m, 1H), 3.75–3.52 (m, 38H), 3.42-3.35 (m, 8H), 3.16 (m, 3H), 2.27 (m, 2H), 2.18 (t, J = 7.5 Hz, 2H), 2.04 (m, 6H), 1.70-1.51 (m, 16H), 1.39-1.27 (m, 50H), 0.91 (t, J = 6.6 Hz, 3H). ^{13}C NMR (125 MHz, $CDCl_3$) δ: 175.10, 174.90, 173.48, 161.70, 158.21, 157.89, 157.79, 157.67, 157.10, 144.03, 129.49, 129.33, 125.37, 111.91, 97.73, 95.57, 85.93, 79.97, 70.01, 77.65, 76.39, 74.97, 73.05, 72.76, 72.68, 70.61, 69.94, 69.89, 69.79, 69.71, 69.47, 69.07, 67.48, 63.46, 55.56, 53.91, 53.58, 53.54, 52.44, 51.58, 50.26, 42.17, 41.75, 38.89, 38.54, 35.81, 35.46, 33.31, 32.21, 31.65, 31.55, 31.19, 29.43, 29.20, 29.03, 29.00, 28.94, 28.89, 28.85, 28.68, 26.73, 25.71, 25.57, 24.69, 22.86, 22.32, 13.04. ESI-HR-MS calculated $[M+3H]^{3+}$ 579.3926, found 579.3925.

Synthesis of GNeo-NHS

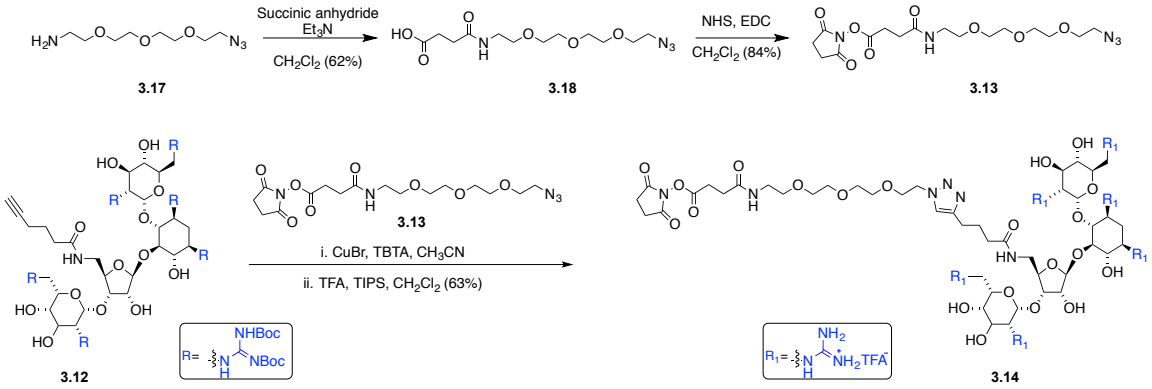

Scheme 3.5. Synthesis of NHS-N_3-linker and GNeo-NHS.

Alkyne-BocGNeo (**3.12**) was prepared according to a previously published procedure.[44]

Acid-N3-Linker (3.18). Succinic anhydride (110 mg, 1.1 mmol) and triethylamine (153 µL, 1.1 mmol) were added to a solution of 11-azido-3,6,9-trioxaundecan-1-amine (200 mg, 0.92 mmol) in dichloromethane (1 mL). The reaction was allowed to stir for 12

hours at room temperature. The reaction was diluted in CH_2Cl_2, washed with 0.1N HCl and brine. The organic layer was dried over sodium sulfate, concentrated under reduced pressure and further purified by flash chromatography (9% CH_3OH in CH_2Cl_2) to afford an oil (180mg, 62%). ^{1}H NMR (500 MHz, $CDCl_3$) δ: 6.57 (broad, 1H), 3.71–3.66 (m, 8H), 3.63(m, 2H), 3.55 (t, *J* = 5.2 Hz, 2H), 3.46 (m, 2H), 3.39 (t, *J* = 4.9 Hz, 2H) 2.69 (t, *J* = 6.2 Hz, 2H), 2.52 (t, *J* = 6.3 Hz, 2H); ^{13}C NMR (125 MHz, $CDCl_3$) δ: 174.48, 172.65, 70.75, 70.57, 70.44, 70.18, 69.95, 69.52, 50.66, 39.53, 31.09, 30.44. ESI-HRMS: calculated $[M+Na]^+$ 341.1432, found: 341.1434.

NHS-N_3-Linker (3.13). N-hydroxysuccinimde (32 mg, 0.232 mmol) and **3.18** (75 mg, 0.23 mmol) were dissolved in dichloromethane (2 mL) and treated with *N*-ethyl-*N*-(3-dimethylaminopropyl)carbodiimide hydrochloride (32 mg, 0.28 mmol). The reaction was stirred at room temperature for 12 hours. The reaction was diluted with CH_2Cl_2 and washed with water, brine, and dried over sodium sulfate. The organic layer was concentrated under reduced pressure and further purified by flash chromatography (4% CH_3OH in CH_2Cl_2) providing the product as an oil (57mg, 84%). ^{1}H NMR (500 MHz, $CDCl_3$) δ: 6.37 (s, 1H), 3.68–3.64 (m, 8H), 3.62 (m, 2H), 3.56 (t, *J* = 4.9 Hz, 2H), 3.46 (m, 2H), 3.39 (t, *J* = 5.1 Hz, 2H), 2.98 (t, *J* = 7.3 Hz, 2H), 2.82 (s, 4H), 2.60 (t, *J* = 7.3 Hz, 2H); ^{13}C NMR (125 MHz, $CDCl_3$) δ: 170.13, 169.09, 168.35, 70.80, 70.73, 70.65, 70.35, 70.14, 69.83, 50.81, 39.58, 30.66, 26.90, 25.71. ESI-HRMS: calculated $[M+Na]^+$ 438.1595, found: 438.1597.

GNeo-NHS (3.14). Compounds **3.12** (200 mg, 0.0925 mmol) and **3.13** (57 mg, 0.139 mmol) were dissolved in acetonitrile (2 mL). 20 mol % CuBr (462 μL of 0.04 M solution in acetonitrile) and 20 mol % *tris*[(1-benzyl-1*H*-1,2,3-triazol-4yl)methyl]amine (462 μL of 0.04 M solution in acetonitrile) were added to the reaction mixture. The reaction

was allowed to stir at room temperature under argon for 24 hours. The solvent was concentrated in vacuo. The residue was dissolved in CH_2Cl_2 and washed with aqueous KCN (5%) and EDTA (0.1 M). The organic layer was dried over sodium sulfate and concentrated under reduced pressure followed by flash chromatography purification (3% CH_3OH in CH_2Cl_2) to afford a white solid. The compound was then dissolved in CH_2Cl_2 (2 mL) and treated with triisopropylsilane (20 μL) and trifluoroacetic acid (2 mL) and stirred for 2 hours at room temperature. The reaction was concentrated in vacuo and coevaporated with toluene (3×) to remove the trifluoroacetic acid. The residue was dissolved in cold water, filtered, and lyophilized to afford a white solid (119 mg, 63%). ^{1}H NMR (500 MHz, DMSO–d_6) δ: 8.14 (b, 1H), 8.04 (m, 2H), 7.80 (s, 1H), 7.61 (b, 1H), 7.57–7.04 (m, 26H), 6.90 (d, J = 8.9 Hz, 1H) 5.93 (b, 1H), 5.77 (b, 1H), 5.61 (d, J = 3.6 Hz, 1H), 5.41 (b, 2H), 4.96 (s, 1H), 4.82 (s, 1H), 4.46 (t, J = 5.3 Hz, 2H), 4.19 (b, 1H), 4.08 (t, J = 5.8 Hz, 1H), 3.90 (t, J = 6.8 Hz, 1H), 3.85 (b, 1H), 3.79 (t, J = 5.4 Hz, 2H), 3.72 (m, 1H), 3.64 (m, 1H), 3.60–3.55 (m, 2H), 3.54–3.42 (m, 12H), 3.41–3.30 (m, 7H), 3.30–3.10 (m, 4H), 2.85 (t, J = 6.9 Hz, 1H), 2.79 (s, 4H), 2.49–2.30 (m, 3H), 2.20 (t, J = 7.3 Hz, 2H), 1.96 (m, 1H), 1.82 (m, 3H), 1.60–1.48 (m, 2H). ^{13}C NMR (125 MHz, DMSO–d_6) δ: 173.10, 171.08, 170.78, 170.11, 169.78, 168.63, 159.13, 158.86, 158.60, 158.33, 157.63, 157.45, 157.15, 157.06, 156.71, 146.30, 122.20, 110.41, 97.79, 95.45, 85.37, 79.20, 78.77, 75.88, 74.28, 73.03, 72.13, 70.08, 69.89, 69.60, 69.54, 69.50, 69.45, 69.05, 69.00, 68.75, 66.51, 55.22, 53.16, 51.65, 51.26, 50.09, 49.21, 41.40, 34.87, 29.91, 29.72, 29.15, 29,11, 28.76, 27.95, 25.90, 25.22, 25.10, 24.60. ESI-HRMS: calculated $[M+2H]^{2+}$ 688.3429 found: 688.3408.

Preparation of liposomes

Lipid films were prepared from DOPC (1,2-dioleoyl-*sn*-glycero-3-phosphocholine), DOPE (1,2-dioleoyl-*sn*-glycero-3-phosphoethanolamine), and cholesterol (73:11:16) dissolved in chloroform. The solvent was evaporated and further dried under high vacuum to form a lipid film. The resulting film was rehydrated with phosphate buffered saline (PBS, pH 7.4) containing the cargo to be encapsulated (either 100 μM Cy5 or 5mg/ml α-L-iduronidase). The lipid suspension was subjected to sonication, freeze and thaw cycles, and extrusion 17 times through 100 nm polycarbonate membranes. Extravesicular cargo was removed by gravitational gel filtration (Sephadex G-50 for small molecules or Sepharose 4B for enzyme), eluting with PBS. Lipid concentration was determined by adapting the Stewart method.[67]

Preparation of GNeo-liposomes: Pre-inserted

Liposomes were prepared as described above except the lipid film was rehydrated with PBS containing 0.9 mol % lipid-GNeo and the cargo to be encapsulated.

Preparation of GNeo-liposomes: Post-inserted

Unmodified liposomes, as described above, were stirred for 1 h at room temperature with the lipid-GNeo derivative (0.9 or 1.8 mol %). Unincorporated lipid-GNeo was removed via centrifuge gel filtration (Sephadex G-50).

Preparation of GNeo-liposomes: Post-modification

Unmodified liposomes, as described above, were stirred for 1 h at room temperature with GNeo-NHS (10 or 20 mol %). Remaining GNeo-NHS was removed via centrifuge gel filtration (Sephadex G-50).

Determination of lipid concentration in liposomal suspension

Lipid concentration was determined by adapting the Stewart method.[67] Briefly, diluted liposomes (50 μL) were vortexed with chloroform (1.5 mL) for 10 s. Ammonium ferrothiocyanate (1.5 mL, 0.1 M) was added and the biphasic systems was vortexed for 15 s then centrifuged for 1 min. The optical density of the organic phase was measured at 480 nm against chloroform as a blank. The amount of lipids present was estimated by comparison to a calibration curve generated using liposomal suspensions with a known lipid content.

Enzyme activity assay

α-L-Iduronidase activity was measured by assaying the conversion of 4-methylumbelliferyl α-L-iduronide (Carbosynth, Belkshire, UK) into the fluorochrome 4-methylumbelliferone (4-MU). The assay was performed in 96-well plates, using sodium citrate buffer (80 μL of 0.1 M, 150 mM NaCl, pH 4.5), substrate (50 nmol) substrate, and enzyme (10 μL). After 1 h at 37 °C, fluorescent product was measured (Ex/Em 340 and 485 nm, respectively) and quantified using a standard curve of 4-MU. One unit (U) of activity is defined as the liberation of 1 μg 4-MU per hour at pH 4.5, 37 °C.

Cy5 encapsulation efficiency

To estimate the encapsulation efficiency of Cy5, the fluorescence intensity (640/672) of the liposome solution was measured in 1 mL 0.075 N HCl in isopropanol:water (9:1) before and after size exclusion purification.

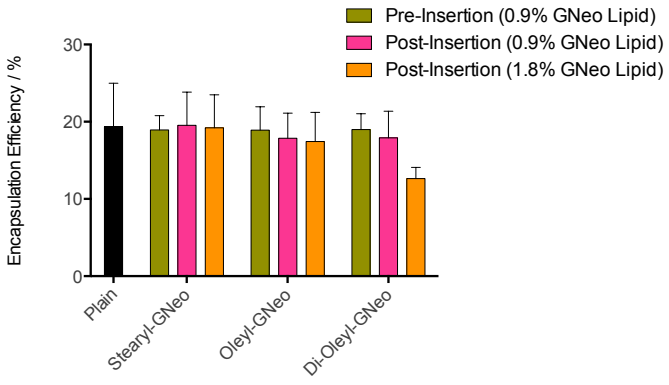

Figure 3.6. Cy5-encapsulation efficiency.

Enzyme encapsulation efficiency

To estimate the amount of enzyme encapsulated, liposomes were lysed with 3% Tween 20 and analyzed for enzyme concentration by protein gel and for enzyme activity using the fluorescent 4-MU-α-L-iduronide substrate. Protein gel was run on a NuPage 4-12% Bis-Tris gel (Novex by Life Technologies) for 35 min at 200 V with MES buffer. Protein bands were visualized on an Odyssey Infrared imaging system (Li-Cor Biosciences) and quantitated by densitometry. Enzyme encapsulation efficiency was calculated as the ratio of IDUA before and after SEC.

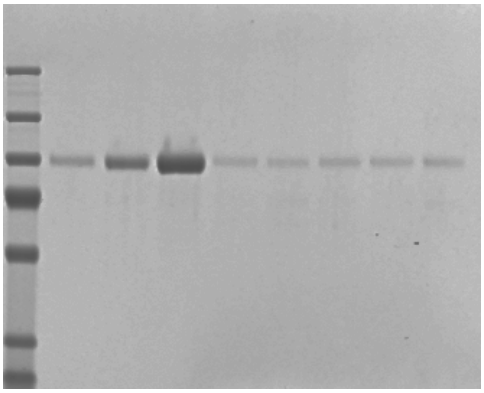

Figure 3.7. Protein gel of IDUA-containing liposome. Opened liposomes and known concentrations of IDUA were loaded onto NuPage 4-12% Bis-Tris gel and run for 35 min at 200 V with MES buffer. Protein bands were imaged on an Odyssey Infrared imaging system. Lane 1: PageRuler Plus Prestained Protein Ladder (Life Technologies). Lane 2-4: 500, 100, and 50 ng IDUA. Lane 5: Plain liposomes.

Lane 6: 0.9% stearyl-GNeo post-inserted. Lane 7: 1.8% stearyl-GNeo post-inserted. Lane 8: 0.9% di-oleyl-GNeo post-inserted. Lane 9: 0.9% di-oleyl-GNeo pre-inserted.

Cell culture

All cells were grown at 37 °C under an atmosphere of 5% CO_2 in air and 100% relative humidity. Wild-type Chinese hamster ovary cells (CHO-K1) were obtained from the American Type Culture Collection (CCL-61). CHO-K1 cells were grown in F-12 medium supplemented with fetal bovine serum (10% v/v), penicillin/streptomycin. HFF and fibroblasts from MPS I patients were obtained from Coriell (GM00200 and GM00338) and grown in Dulbecco's modified Eagle medium (DMEM) supplemented with 10% FBS, penicillin/streptomycin, sodium pyruvate, and glutamine.

Cellular uptake of Cy5-containing liposomes

Wild-type CHO-K1 cells were seeded onto 24-well tissue culture plates (100,000 cells/well, 0.4 mL) and grown for 24 h to about 80% confluence. Cells were washed with PBS and incubated with 300 μL of the liposomal suspension diluted in F-12 growth medium to 300 μg/mL at 37 °C for 1 h. Cells were washed twice with PBS, detached with trypsin/EDTA, diluted with PBS containing 0.1% BSA and analyzed by flow cytometry.

Cellular uptake of IDUA-containing liposomes

Normal HFF and MPS I fibroblasts were seeded onto 24-well plates (80,000 cells/well, 0.4 mL) and grown for 48 h. Cells were washed with PBS and incubated with liposome suspensions diluted in DMEM growth medium at the concentrations indicated. The cells were incubated at 37 °C for 1 h, washed twice with PBS, treated with trypsin/EDTA, and then combined with complete medium to inhibit the trypsin. Cells were sedimented by centrifugation, washed with PBS, and resuspended in 30 μL of RIPA lysis

buffer. Enzyme activity in the cell extracts was measured as described above in triplicate using 10 μL of cell lysate. Total protein concentration in the cell lysate was determined using the Pierce BCA Protein Assay Kit (Thermo Scientific).

Turnover of [^{35}S]glycosaminoglycans

Normal and MPS fibroblasts were seeded in 12-well plates, and at confluence 50 μCi of $H_2[^{35}S]O_4$ (PerkinElmer) was added in 1 mL DMEM/F12 medium supplemented with 10% fetal bovine serum. After 48 hours, the MPS I cells were washed with PBS and incubated with IDUA-containing liposomes or GNeo-IDUA at 37 °C for 1 h. All cells were then washed twice with PBS and chased for 24 h with 1 mL fresh DMEM/F12. Cells were harvested with trypsin, centrifuged (2400 rpm, 5 min), and washed once with PBS. The sedimented cells were then lysed with 0.1 M NaOH and purified over DEAE column. Total [^{35}S]glycosaminoglycan was counted by liquid scintillation spectroscopy using Scintillator Ultima Gold XR (PerkinElmer).

Acknowledgements

Chapter 3 is in full currently being submitted for publication: Hamill, K.M.; Wexselblatt, E.; Tong, W.; Esko, J. E.; Tor, Y. The dissertation author is the main author and researcher of this work.

3.6 References

(1) Luzio, J. P.; Pryor, P. R.; Bright, N. A. *Nat Rev Mol Cell Biol* **2007**, *8*, 622.

(2) Braulke, T.; Bonifacino, J. S. *Biochim. Biophys. Acta - Molecular Cell Research* **2009**, *1793*, 605.

(3) Appelqvist, H.; Waster, P.; Kagedal, K.; Ollinger, K. *J Mol Cell Biol* **2013**, *5*, 214.

(4) Neufeld, E. F. *Ann. Rev. Biochem* **1991**, *60*, 257.

(5) Winchester, B.; Vellodi, A.; Young, E. *Biochem Soc Trans* **2000**, *28*, 150.

(6) Richard III, C. W. In *Introduction to Biological and Small Molecule Drug Research and Development*; Jefferis, S. R., Ed.; Elsevier: Oxford, 2013, p 327.

(7) Grabowski, G. A.; Hopkin, R. J. *Annu Rev Genomics Hum Genet* **2003**, *4*, 403.

(8) Beck, M. *IUBMB Life* **2010**, *62*, 33.

(9) Martin-Banderas, L.; Holgado, M. A.; Duran-Lobato, M.; Infante, J. J.; Alvarez-Fuentes, J.; Fernandez-Arevalo, M. *Curr Med Chem* **2016**, *23*, 929.

(10) Sessa, G.; Weissmann, G. *J Biol Chem* **1970**, *245*, 3295.

(11) Gregoriadis, G.; Buckland, R. A. *Nature* **1973**, *244*, 170.

(12) Finkelstein, M.; Weissmann, G. *J Lipid Res* **1978**, *19*, 289.

(13) Gregoriadis, G. *Nature* **1978**, *275*, 695.

(14) Gregoriadis, G.; Ryman, B. E. *Eur J Biochem* **1972**, *24*, 485.

(15) Gregoriadis, G.; Ryman, B. E. *Biochem J* **1972**, *129*, 123.

(16) Patel, H. M.; Ryman, B. E. *Biochem. Soc. Trans.* **1974**, *2*, 1014.

(17) Steger, L. D.; Desnick, R. J. *Biochim. Biophys. Acta - Biomembranes* **1977**, *464*, 530.

(18) Gregoriadis, G.; Putman, D.; Louis, L.; Neerunjun, D. *Biochem J* **1974**, *140*, 323.

(19) Gregoriadis, G. *Biochem Soc Trans* **1975**, *3*, 613.

(20) Cohen, C. M.; Weissmann, G.; Hoffstein, S.; Awasthi, Y. C.; Srivastava, S. K. *Biochemistry* **1976**, *15*, 452.

(21) Koshkaryev, A.; Thekkedath, R.; Pagano, C.; Meerovich, I.; Torchilin, V. P. *J Drug Target* **2011**, *19*, 606.

(22) Thekkedath, R.; Koshkaryev, A.; Torchilin, V. P. *Nanomedicine* **2013**, *8*, 1055.

(23) Crucianelli, E.; Bruni, P.; Frontini, A.; Massaccesi, L.; Pisani, M.; Smorlesi, A.; Mobbili, G. *RSC Advances* **2014**, *4*, 58204.

(24) Wexselblatt, E.; Esko, J. D.; Tor, Y. *ACS Nano* **2015**, *9*, 3961.

(25) Koshkaryev, A.; Piroyan, A.; Torchilin, V. P. *Cancer Biol Ther* **2012**, *13*, 50.

(26) Muro, S.; Schuchman, E. H.; Muzykantov, V. R. *Mol Ther* **2006**, *13*, 135.

(27) Vives, E.; Brodin, P.; Lebleu, B. *J Biol Chem* **1997**, *272*, 16010.

(28) Pepinsky, R. B.; Androphy, E. J.; Corina, K.; Brown, R.; Barsoum, J. *DNA Cell Biol* **1994**, *13*, 1011.

(29) Fawell, S.; Seery, J.; Daikh, Y.; Moore, C.; Chen, L. L.; Pepinsky, B.; Barsoum, J. *Proc Natl Acad Sci U S A* **1994**, *91*, 664.

(30) Wender, P. A.; Mitchell, D. J.; Pattabiraman, K.; Pelkey, E. T.; Steinman, L.; Rothbard, J. B. *Proc. Natl. Acad. Sci. U.S.A.* **2000**, *97*, 13003.

(31) Bechara, C.; Sagan, S. *FEBS Lett.* **2013**, *587*, 1693.

(32) Stanzl, E. G.; Trantow, B. M.; Vargas, J. R.; Wender, P. A. *Acc. Chem. Res.* **2013**, *46*, 2944.

(33) Wexselblatt, E.; Esko, J. D.; Tor, Y. *J. Org. Chem.* **2014**, *79*, 6766.

(34) Chung, S.-K.; Maiti, K. K.; Lee, W. S. *Int. J. Pharm.* **2008**, *354*, 16.

(35) Torchilin, V. P. *Biopolymers* **2008**, *90*, 604.

(36) Torchilin, V. P.; Rammohan, R.; Weissig, V.; Levchenko, T. S. *Proc. Natl. Acad. Sci. U.S.A.* **2001**, *98*, 8786.

(37) Marty, C.; Meylan, C.; Schott, H.; Ballmer-Hofer, K.; Schwendener, R. A. *Cell Mol Life Sci* **2004**, *61*, 1785.

(38) Tseng, Y. L.; Liu, J. J.; Hong, R. L. *Mol Pharmacol* **2002**, *62*, 864.

(39) Fretz, M. M.; Koning, G. A.; Mastrobattista, E.; Jiskoot, W.; Storm, G. *Biochim. Biophys. Acta - Biomembranes* **2004**, *1665*, 48.

(40) Furuhata, M.; Kawakami, H.; Toma, K.; Hattori, Y.; Maitani, Y. *Bioconjug Chem* **2006**, *17*, 935.

(41) Cryan, S.-A.; Devocelle, M.; Moran, P. J.; Hickey, A. J.; Kelly, J. G. *Mol. Pharm.* **2006**, *3*, 104.

(42) Luedtke, N. W.; Carmichael, P.; Tor, Y. *J. Am. Chem. Soc.* **2003**, *125*, 12374.

(43) Elson-Schwab, L.; Garner, O. B.; Schuksz, M.; Crawford, B. E.; Esko, J. D.; Tor, Y. *J Biol Chem* **2007**, *282*, 13585.

(44) Dix, A. V.; Fischer, L.; Sarrazin, S.; Redgate, C. P. H.; Esko, J. D.; Tor, Y. *ChemBioChem* **2010**, *11*, 2302.

(45) Sarrazin, S.; Wilson, B.; Sly, W. S.; Tor, Y.; Esko, J. D. *Mol Ther* **2010**, *18*, 1268.

(46) Inoue, M.; Tong, W.; Esko, J. D.; Tor, Y. *ACS Chem. Biol.* **2013**, *8*, 1383.

(47) Mayer, L. D.; Hope, M. J.; Cullis, P. R. *Biochim Biophys Acta* **1986**, *858*, 161.

(48) Hopwood, J. J.; Muller, V.; Smithson, A.; Baggett, N. *Clinica Chimica Acta* **1979**, *92*, 257.

(49) Kling, J. *Nat Biotechnol* **2012**, *30*, 128.

(50) Ho, R. J.; Chien, J. Y. *J Pharm Sci* **2012**, *101*, 2668.

(51) Škalko-Basnet, N. *Biologics : Targets & Therapy* **2014**, *8*, 107.

(52) Wender, P. A.; Galliher, W. C.; Goun, E. A.; Jones, L. R.; Pillow, T. H. *Adv. Drug Delivery Rev.* **2008**, *60*, 452.

(53) Schmidt, N.; Mishra, A.; Lai, G. H.; Wong, G. C. L. *FEBS Lett.* **2010**, *584*, 1806.

(54) Bach, G.; Friedman, R.; Weissmann, B.; Neufeld, E. F. *Proc Natl Acad Sci U S A* **1972**, *69*, 2048.

(55) Mayhew, E.; Papahadjopoulos, D.; Rustum, Y. M.; Dave, C. *Cancer Res* **1976**, *36*, 4406.

(56) Chang, H.-I.; Yeh, M.-K. *Int. J. Nanomedicine* **2012**, *7*, 49.

(57) Allen, T. M.; Cullis, P. R. *Adv. Drug Delivery Rev.* **2013**, *65*, 36.

(58) Pattni, B. S.; Chupin, V. V.; Torchilin, V. P. *Chem Rev.* **2015**, *115*, 10938.

(59) Schnyder, A.; Huwyler, J. *NeuroRX*, *2*, 99.

(60) Matsumura, Y.; Gotoh, M.; Muro, K.; Yamada, Y.; Shirao, K.; Shimada, Y.; Okuwa, M.; Matsumoto, S.; Miyata, Y.; Ohkura, H.; Chin, K.; Baba, S.; Yamao, T.; Kannami, A.; Takamatsu, Y.; Ito, K.; Takahashi, K. *Annals of Oncology* **2004**, *15*, 517.

(61) Riviere, K.; Huang, Z.; Jerger, K.; Macaraeg, N.; Szoka, F. C., Jr. *J Drug Target* **2011**, *19*, 14.

(62) Xie, Y.; Ye, L.; Zhang, X.; Cui, W.; Lou, J.; Nagai, T.; Hou, X. *J. Controlled Release* **2005**, *105*, 106.

(63) Klibanov, A. L.; Maruyama, K.; Torchilin, V. P.; Huang, L. *FEBS Lett* **1990**, *268*, 235.

(64) Papahadjopoulos, D.; Allen, T. M.; Gabizon, A.; Mayhew, E.; Matthay, K.; Huang, S. K.; Lee, K. D.; Woodle, M. C.; Lasic, D. D.; Redemann, C. *Proc. Natl. Acad. Sci. U.S.A.* **1991**, *88*, 11460.

(65) Allen, T. M.; Hansen, C.; Martin, F.; Redemann, C.; Yau-Young, A. *Biochim Biophys Acta* **1991**, *1066*, 29.

(66) Zhang, Z.; Zhang, X.; Xu, X.; Li, Y.; Li, Y.; Zhong, D.; He, Y.; Gu, Z. *Advanced Functional Materials* **2015**, *25*, 5250.

(67) Stewart, J. C. *Anal. Biochem.* **1980**, *104*, 10.

Chapter 4:

Length Matters: Linker Structure–Uptake Relationship for Guanidinylated Neomycin Molecular Transporters

4.1 Introduction

Guanidinium-rich transporters have been used extensively to enable or enhance the cellular uptake of poorly bioavailable drugs, probes, and biomolecules.[1,2] Guanidinium-rich peptides,[3] peptoids,[3] dendrimers,[4] and carbohydrates[5] are among the many scaffolds that have been shown to exhibit high water solubility and effective entry into mammalian cells. The unique and versatile ability of guanidinium groups to facilitate cellular uptake has been linked with their ability to form favorable interactions with negatively-charged cell-surface components such as phospholipids and proteoglycans.[6-9] However, the precise mechanism by which guanidinium-rich transporters are internalized is complex, most likely involves multiple pathways, and varies between transporters.[6,10] Additionally, the uptake pathways utilized can be dependent on several other factors including the size and charge of the cargo, cell type, incubation time, and linker amongst others.[9,11-17]

In 2003, we found that converting the ammonium groups of aminoglycosides into guanidinium groups enhances their cellular uptake.[5] Since then, guanidinoglycosides, and in particular guanidinoneomycin (GNeo), have been used to deliver high molecular weight proteins,[18-21] quantum dots,[22] active enzymes,[22] and liposomes[23] into mammalian cells. Unlike other guanidinium-rich transporters, GNeo delivers cargo at low nanomolar concentrations and has consistently shown uptake through endocytosis mechanisms that rely exclusively on cell-surface heparan sulfate proteoglycans.[18-20,22]

Although cell-penetrating peptides and guanidinium-rich transporters have been well studied, the linkers used to attach the transporter to different cargos are often overlooked and considered unconnected to cellular uptake properties. However, slight structural modifications to the transporter could result in different physicochemical properties that affect conjugation and translocation efficiencies; therefore, we hypothesized that modifying the length and hydrophobicity of the linker connecting a GNeo transporter to its cargo could alter the conjugation patterns as well as impact the interactions with the cell surface that facilitate uptake. Herein, we prepared GNeo-biotin derivatives with linkers of varying length composed of a hydrocarbon chain, an ethylene glycol chain, or a combination of both (Figure 4.1). The guanidinium-rich transporters were then evaluated using HPLC to determine hydrophobicity, FPLC to examine transporter-protein conjugation, and flow cytometry to evaluate cellular uptake. Streptavidin was used as a model protein to evaluate conjugation and uptake differences between the new transporters. Intriguingly, the derivatives with shorter, hydrophilic linkers exhibit higher levels of cellular uptake than the carriers with longer linkers. Additionally, higher levels of uptake do not necessarily correlate with enhanced protein conjugation. These observations illustrate the implication that modifications of the linker can have on uptake and the attention that should be applied when designing a novel molecular transporter and using model cargo to investigate the uptake properties. An excellent transporter could be discarded if the wrong linker, or no linker, is initially used to evaluate uptake.

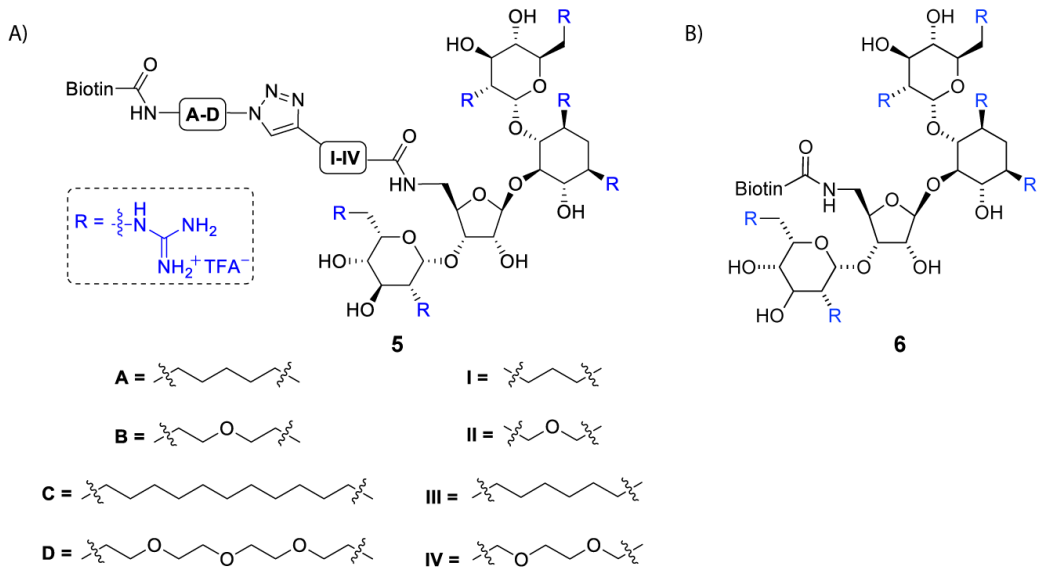

Figure 4.1. Structures of biotinylated-GNeo transporters A) General structure of biotinylated guanidinoneomycin (GNeo) carriers and linker components. B) Biotin-GNeo with no linker.

4.2 Results and Discussion

In order to investigate how subtle changes in linker structure might affect uptake, GNeo transporters were synthesized with sixteen different linkers connecting the 5" carbon of the GNeo core to a biotin moiety (Figure 4.1). The small library was prepared by peptide coupling four different alkyne-terminated linkers to **1**, yielding **2 I-IV** (Scheme 4.1). The compounds were then deprotected using trifluoroacetic acid to yield **3 I-IV** and subsequent guanidinylation providing intermediates **4 I-IV**. The alkyne intermediates could then undergo a copper-catalyzed 1,3-dipolar cycloaddition with different azide-extended biotin fragments (**A-D**) followed by TFA deprotection. Reversed-phase HPLC (RP-HPLC) purification on a C18 column provided **5 I-IV** (Scheme 4.1). For reference, **1** was coupled to biotin, with no additional linker, followed by guanidinylation and deprotection to yield compound **6** (Figure 4.1, Scheme 4.9).

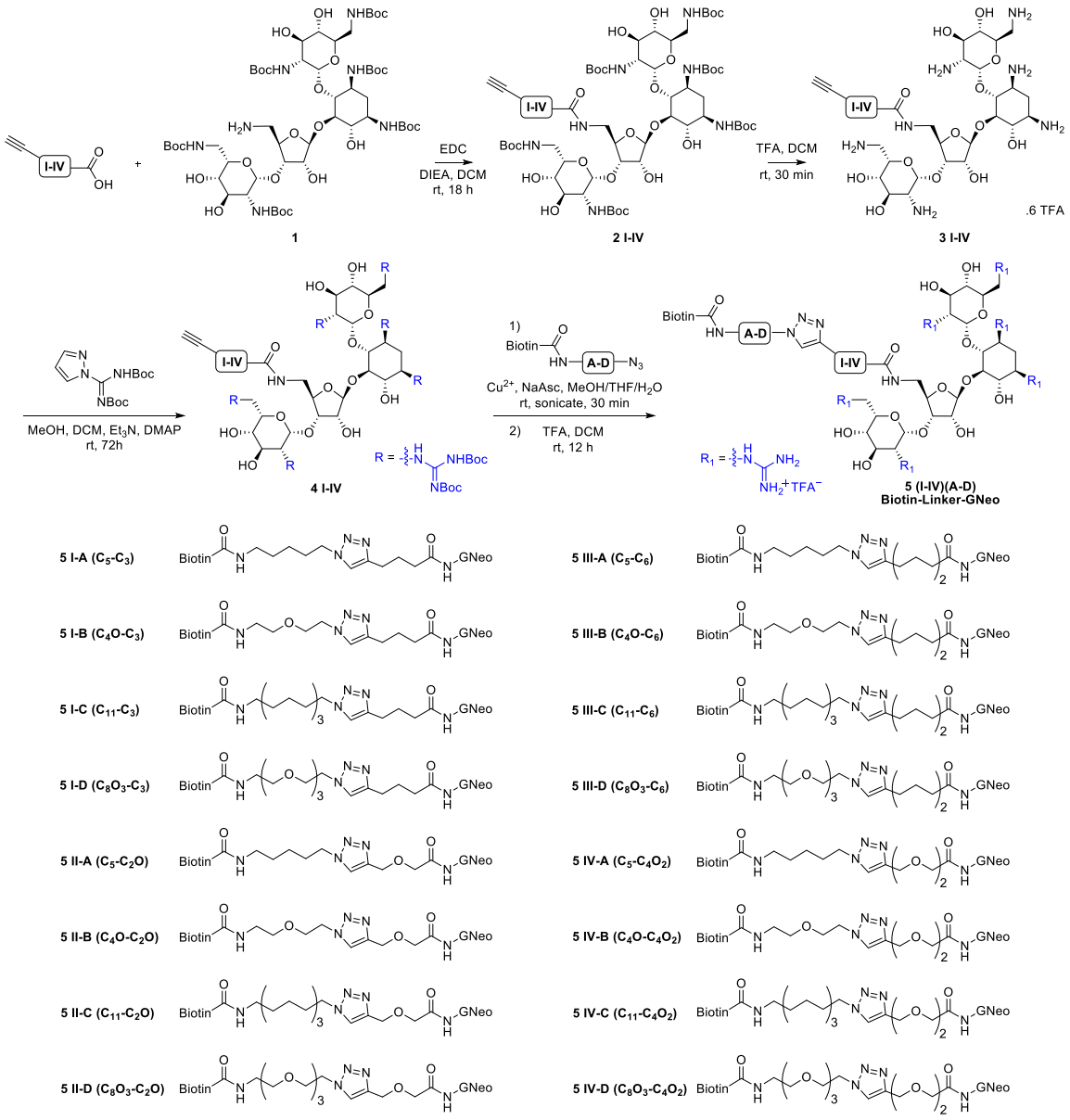

Scheme 4.1. Combinatorial synthesis of biotinylated-GNeo carriers. Detailed synthetic conditions are given in the experimental section.

RP-HPLC also provided some indication of the hydrophobicity of the transporters (Figure 4.2). As expected, compounds containing the long hydrophobic biotin linker C (C_{11}-) had the longest retention times, indicating a higher hydrophobicity. Interestingly, GNeo derivatives with the long, hydrophilic biotin linker D (C_8O_3-) were not the most polar

and showed similar retention times to compounds containing the C5 biotin linker A. A possible explanation is the ability of the triethylene glycol linker to complex with hydronium ions, thus enhancing its binding interactions with the C18 column. Derivatives containing the shorter, hydrophilic biotin linker B (C_4O-) were the most polar. On the other hand, the longer, hydrophilic linker IV (C_4O_2-) between GNeo and the triazole resulted in slightly more hydrophilic compounds then the two short linkers I (C_3-) and II (C_2O-). The long, hydrophobic linker III (C_6-) resulted in less polar derivatives with longer retention times.

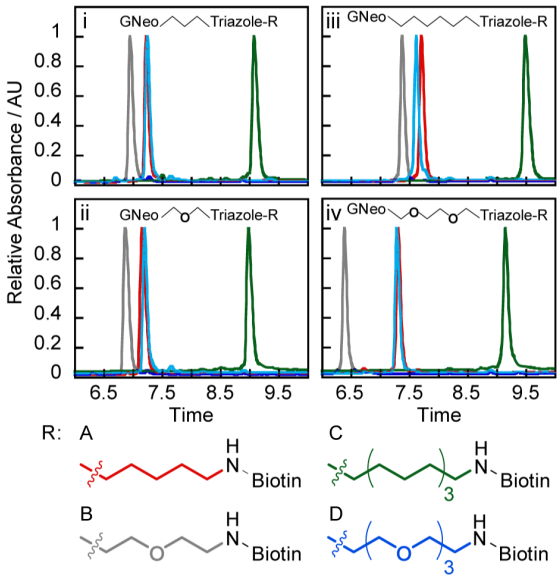

Figure 4.2. HPLC traces of biotinylated-GNeo transporters**.** GNeo-biotin derivatives were analyzed by RP-HPLC on a C18 column (5-30% ACN (0.1% TFA) in H_2O (0.1% TFA) over 10 min) to confirm purity and to observe differences in hydrophobicity.

To determine if the transporters form similar complexes with streptavidin, the biotinylated compounds were incubated with streptavidin in a 5:1 molar ratio for 20 min at room temperature. Conjugates were then diluted to 1 mL in phosphate buffered saline (PBS) and analyzed by FPLC on a heparin-Sepharose column. Streptavidin alone did not

bind to the resin and eluted with 0.14 M NaCl. Following incubation with biotin-GNeo, the streptavidin-GNeo conjugates required 0.7-1.7 M NaCl to elute from the column. Streptavidin is a tetramer and each subunit can bind biotin with femtomolar affinity. Based on the presence of multiple peaks in the FPLC chromatograms (Figure 4.5), two of the biotin-GNeo derivatives, **5 I-C** and **5 III-D**, form a mixture of monovalent, divalent, trivalent, and tetravalent conjugates. Additionally, compounds **5 II-B**, **5 III-C**, and **6** resulted in a high amount of unconjugated streptavidin remaining, whereas, **5 III-A**, **5 III-B**, **5 IV-B**, and **5 IV-D** formed only the tetravalent complex with streptavidin. The contribution of each conjugate, tetravalent, trivalent, divalent, monovalent, and unconjugated streptavidin, are presented in Figure 4.3. While no clear trend can be assigned to the complex formation, the linker clearly has an effect on the formation of protein-transporter complexes.

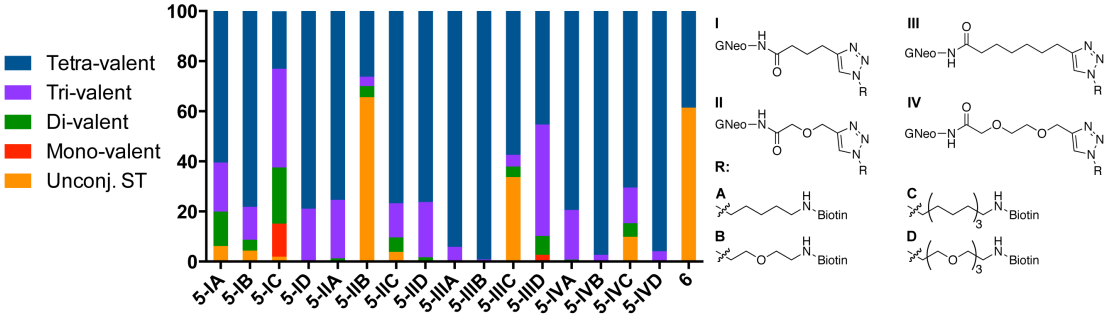

Figure 4.3. FPLC integrations of GNeo-biotin-ST conjugates**.** GNeo-biotin (225 μM) was incubated with streptavidin (45 μM) for 20 min at room temperature. The reaction was diluted to 1 mL with PBS and injected onto a Heparin-Sepharose column. The area under each peak was measured and normalized.

In order to investigate whether the different linkers have an effect on cellular uptake, fluorescent Cy5-streptavidin was used. Conjugates were again formed by incubating the biotin-transporter with Cy5-streptavidin in a 1:5 molar ratio for 20 min at

room temperature. The conjugates were then diluted with cell-culture medium to a final concentration of 2 nM streptavidin-Cy5. Wild-type Chinese hamster ovary cells (CHO-K1) were incubated with the conjugates for one hour at 37 °C, washed, harvested with trypsin/EDTA, and analyzed by flow cytometry. As shown in Figure 4.4, all transporters with linkers were able to internalize the fluorescent cargo. Transporter **6** with no linker, however, did not enable uptake of ST-Cy5. This suggests that a spacer between the cargo and the transporter is necessary in order for GNeo to interact with the cell surface and facilitate uptake. Additionally, uptake efficiency was dependent on linker length and polarity. Shorter biotin linkers A and B outperformed the longer biotin linkers C and D, with linker B being the best in each series. Additionally, the shorter GNeo linkers I and II outperformed the longer GNeo linkers III and IV, with linker II being the best. Overall, it appears that a shorter linker between transporter and cargo confers better uptake, and the more hydrophilic linkers are slightly better than their hydrophobic counterparts. However, as linker length increases, the more hydrophobic linkers outperform the hydrophilic linkers. Furthermore, cellular uptake does not correlate with formation of tetravalent streptavidin complexes. While compound **5 II-B** exhibited poor conjugation to streptavidin, it showed the highest uptake. Similarly, transporter **5 IV-D** showed only formation of a streptavidin tetravalent conjugate but demonstrated the lowest uptake activity.

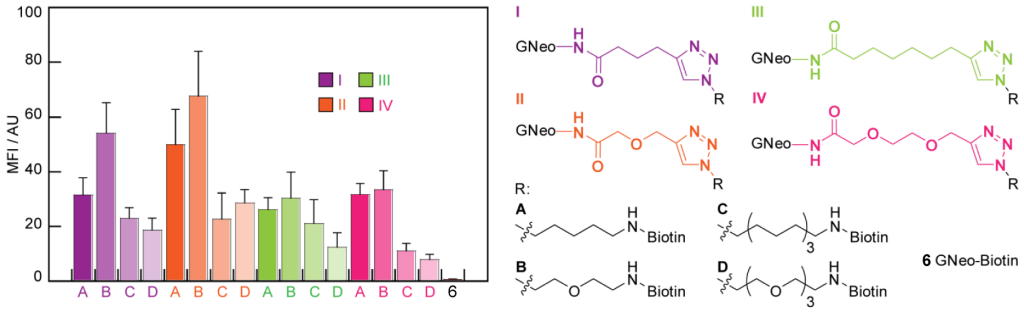

Figure 4.4. Cellular uptake of GNeo-biotin-ST conjugates**.** Cellular uptake of conjugates made from ST-Cy5 (2 nM) and biotin transporter molecules (10 nM). CHO-K1 cells were incubated with the conjugates at 37 °C for 1 h and lifted with EDTA/trypsin. The mean fluorescence intensity was measured by flow cytometry. The background signal from untreated cells was subtracted.

4.3 Conclusions

In conclusion, further understanding the properties that influence cellular uptake of guanidinium-rich molecular transporters is critical for maximizing the potential of these transporters for intracellular applications. Therefore, we synthesized a series of GNeo transporters with various spacer units between the transporter and the cargo in order to evaluate the role linker length and hydrophobicity play on conjugation and overall cellular uptake. Both conjugation to the model protein streptavidin and cellular uptake were responsive to the physicochemical properties of the linker. Streptavidin alone, or streptavidin conjugated to biotin-GNeo with no linker, resulted in no cellular uptake at low concentrations. In this particular system, the shortest linker with two oxyetheylene spacers had the most effective cellular uptake. Our results clearly demonstrate the importance of considering the properties of the linker when designing new molecular transporters.

4.4 Experimental

Materials

Materials obtained from commercial suppliers were used without further purification. All other chemicals and reagents were purchased from Sigma Aldrich.

Deuterated NMR solvents were purchased from Cambridge Isotope Laboratories. PBS (Dulbecco's phosphate buffered saline), F-12 Nutrient Mixture (Ham), Dulbecco's Modified Eagle Medium (DMEM), streptavidin, and streptavidin-Cy5 were purchased from Thermo Fisher. Trypsin/EDTA was purchased from VWR. Costar 3524 (Corning) 24-well plates were used.

Instrumentation

NMR spectra were recorded on a Varian VX 500 MHz spectrometer or a Varian 400 MHz spectrometer. Mass spectra were recorded at UCSD Chemistry and Biochemistry Mass Spectrometry Facility utilizing an Agilent 6230 HR-ESI-TOF mass spectrometer. Reverse-phase HPLC purification (CLIPEUS, C18, 5μm, 10x250 mm, Higgins analytical) and analysis (Eclipse, XDB-C18, 5μm, 4.6x150 mm) were carried out on an Agilent 1200 series instrument or Beckman Coulter System Gold 127P Solvent Module. FPLC was carried out on a Bio-Rad BioLogic DuoFlow system using a GE HiTrap Heparin HP column. Flow cytometry studies were performed on a BD FACSCalibur.

General synthesis of biotin-N_3 linkers

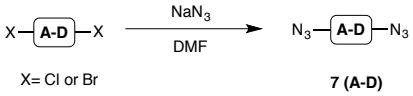

Scheme 4.2. Synthesis of diazide linker intermediates.

NaN_3 (0.5g, 7.7 mmol) was added to a solution of the dichloro- (linkers B and D) or dibromo- (linkers A and C) compound (2.2 mmol) in DMF (10 mL). The mixture was stirred at 60°C for 12h. The reaction was diluted into water and extracted with ether. The

organic layer was washed with water and brine before being concentrated under reduced pressure and used without further purification. **7A-D** have been previously reported.[24,25]

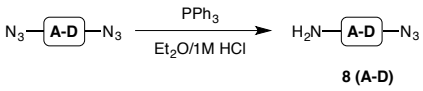

Scheme 4.3. Synthesis of azide-amino linker intermediates.

The diazide (**7**, 1.28 mmol) and triphenylphosphine (0.328g, 1.25 mmol) were treated with diethyl ether (2 mL) (linkers B and D) or 1:1 diethyl ether and hexanes (2 mL) (linkers A and C) followed by 1M HCl (2 mL). The mixture was stirred overnight at room temperature. The reaction was diluted with ether and washed with 1M HCl. The combined aqueous layers washed three times with dichloromethane. The combined aqueous phases were concentrated under reduced pressure. **8A**, **8B**, and **8D** have been previously reported.[19,26,27]

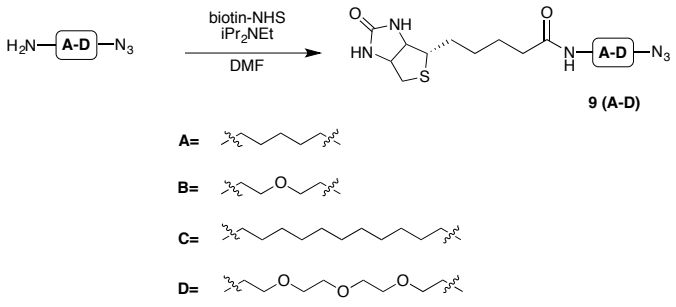

Scheme 4.4. Synthesis of biotin-linkers.

Biotin-NHS (218 mg, 0.64 mmol) and *N,N*-diisopropylethylamine (111 μL, 0.64 mmol) were added to a solution of the azidoamine (0.58 mmol) in DMF (800 μL). The reaction was stirred overnight at room temperature. The solvent was concentrated in vacuo then dissolved in CH_2Cl_2 and washed with water and brine. The compound was purified on silica gel using methanol and CH_2Cl_2.

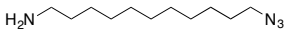

8C. ^{1}H NMR (500 MHz, $CDCl_3$): δ 3.25 (t, *J*=7.0 Hz, 2H), 2.97 (s, br, 2H), 1.76 (br, 2H), 1.57 (m, 2H), 1.35-1.20 (m, 16H). ^{13}C NMR (126 MHz, $CDCl_3$) δ: 51.46, 40.05, 29.42, 29.34, 29.15, 28.98, 28.84, 27.69, 26.71, 26.50. Yield: 33%. HRMS: $[M+H]^+$ 213.2073 (theoretical 213.2074).

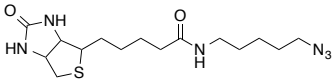

9A. ^{1}H NMR (500 MHz, CD_3OD): δ 4.51 (m, 1H), 4.32 (m, 1H), 3.23 (m, 2H), 3.18 (m, 3H), 2.92 (dd, *J*=5.3 Hz, 13.2 Hz, 1H), 2.74 (d, *J*=13.2 Hz, 1H), 2.22 (t, *J*=7.4 Hz, 2H), 1.69-1.39 (m, 12H). ^{13}C NMR (126 MHz, CD_3OD) δ: 174.62, 164.57, 62.09, 60.32, 55.64, 51.03, 39.83, 38.91, 35.50, 28.61, 28.42, 28.29, 28.09, 25.56, 23.83. Yield: 60%. HRMS: $[M+Na]^+$ 377.1730 (theoretical 377.1730).

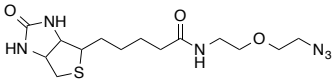

9B. ^{1}H NMR (500 MHz, CD_3OD): δ 4.51 (m, 1H), 4.35 (m, 1H), 3.67 (t, *J*=5.3 Hz, 2H), 3.58 (t, *J*=5.0 Hz, 2H), 3.50 (m, 2H), 3.39 (t, *J*=4.8 Hz, 2H), 3.24 (m, 1H), 2.95 (dd, *J*=4.9 Hz, 13.1 Hz, 1H), 2.81 (d, *J*=13.1 Hz, 1H), 2.24 (t, 2H, *J*=7.4 Hz), 1.81-1.4 (m, 6H). ^{13}C NMR (126 MHz, CD_3OD) δ: 176.21, 164.83, 70.89, 70.45, 63.37, 61.64, 56.99, 51.75, 41.04, 40.32, 36.72, 29.74, 29.48, 26.81. Yield: 67%. HRMS: $[M+Na]^+$ 379.1524 (theoretical 379.1523).

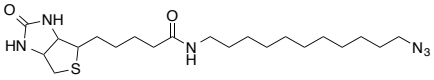

9C. ^{1}H NMR (500 MHz, CD_3OD): δ 4.51 (m, 1H), 4.32 (m, 1H), 3.32-3.17 (m, 5H), 2.93 (dd, *J*=5.0 Hz, 12.7 Hz, 1H), 2.72 (d, *J*=12.7 Hz, 1H), 2.21 (t, *J*=7.1 Hz, 2H),

1.80-1.22 (m, 24H). ^{13}C NMR (126 MHz, CD_3OD) δ: 174.53, 164.82, 61.96, 60.20, 55.61, 51.03, 39.63, 38.95, 35.41, 29.25, 29.22, 29.20, 29.02, 29.01, 28.87, 28.51, 28.37, 28.10, 26.59, 26.42, 25.55. Yield: 47%. HRMS: $[M+H]^+$ 439.2848 (theoretical 439.2850).

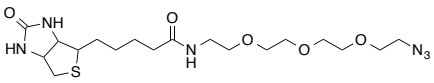

9D. Previously reported.[19]

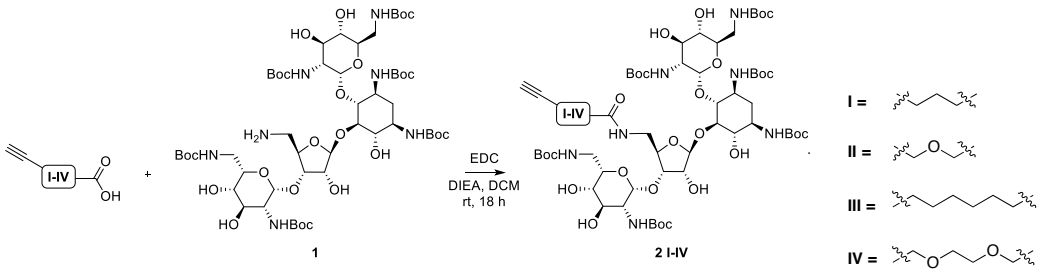

Scheme 4.5. Synthesis of BocNeo-alkyne intermediates.

Alkyne-acid linkers (I-IV). Linker **I** is commercially available (Sigma-Aldrich). Linkers **II**,[28] **III**,[29] and **IV**[30] were prepared as previously reported.

General synthesis of BocNeo-alkyne derivatives (2)

To a solution of alkyne-linker (3.2 eq) in DCM (0.6 ml/mmol) was added EDC (3.2 eq). The mixture was stirred for 30 min. A solution of **1** (1eq) in DCM (0.2 mol/L) and DIEA (3 eq) was then added dropwise. The mixture was then stirred for 48 h. The mixture was partitioned between DCM and 5% citric acid. The organic layer was separated and washed with sodium bicarbonate and brine. The organic layer was collected, dried over sodium sulfate, filtered off, and the filtrate was evaporated. Silica gel column chromatography (0-8% MeOH in DCM) afforded the desired product as a colorless amorphous.

2-I. Previously reported.[19]

2-II. ^{1}H NMR (500 MHz, CD_3OD): δ 6.59 (d, *J*=8.1 Hz, 1H), 5.37 (s, 1H), 5.11 (s, 1H), 4.35-4.30 (m, 4H), 4.18-4.11 (m, 3H), 3.96-3.89 (m, 3H), 3.75-3.36 (m, 15H), 3.19 (m, 3H), 2.97 (t, *J*=2.8 Hz, 1H), 1.96 (d, *J*=13.0, 1H), 1.47-1.43 (m, 54 H). ^{13}C NMR (126 MHz, CD_3OD) δ: 170.62, 157.66, 157.45, 157.13, 156.94, 156.60, 156.49, 109.94, 98.89, 97.58, 85.67, 79.29, 79.05, 78.95, 78.91, 78.77, 78.52, 75.95, 74.14, 73.83, 73.22, 71.83, 71.43, 71.25, 70.27, 67.88, 67.68, 57.94, 55.45, 52.10, 51.10, 49.96, 41.16, 40.69, 34.47, 27.55, 27.45, 27.43, 27.39, 27.34. Yield: 46%. HR-MS: $[M+Na]^+$ 1332.6529 (theoretical 1332.6532).

2-III. ^{1}H NMR (500 MHz, CD_3OD): δ 6.72 (s, 1H), 5.49 (s, 1H), 5.08 (s, 1H), 4.31 (s, 1H), 4.06-3.68 (m, 5H), 3.75 (m, 2H), 3.55-3.35 (m, 11H), 3.20 (m, 7H), 3.07(m, 3H), 2.35 (m, 2H), 2.17 (m, 3H), 1.95 (m, 1H), 1.65 (m, 2H), 1.47 (m, 54H). ^{13}C NMR (126 MHz, CD_3OD) δ: 157.17, 157.69, 157.47, 157.19, 156.64, 156.50, 110.79, 98.97, 97.37, 87.17, 83.63, 79.54, 79.27, 78.97, 78.91, 78.88, 78.79, 77.69, 74.77, 74.11, 72.97, 71.92, 71.21, 71.07, 70.28, 68.17, 67.59, 55.49, 52.13, 51.14, 49.92, 42.57, 41.25, 40.57, 35.55, 35.50, 34.33, 29.47, 28.26, 28.20, 27.61, 27.48 27.41, 27.38, 27.34, 25.76, 17.61. Yield: 61%. HR-MS: $[M+H]^+$ 1350.7391 (theoretical 1350.7389).

2-IV. ^{1}H NMR (500 MHz, CD_3OD): δ 5.34 (s, 1H), 5.12 (s, 1H), 4.86 (s, 1H), 4.28-4.05 (m, 8H), 3.98-3.69 (m, 4H), 3.78-3.69 (m, 9H), 3.57-3.47 (m, 10H), 3.37 (m, 2H), 3.20 (m, 1H), 2.92 (t, *J*=2.3 Hz, 1H), 1.96 (d, *J*=12.8 Hz, 1H), 1.47-1.44 (m, 54H). ^{13}C NMR (126 MHz, CD_3OD) δ: 171.58, 157.65, 157.46, 157.12, 156.85, 156.79, 156.48, 109.69, 99.05, 97.72, 85.72, 79.60, 79.31, 79.24, 79.14, 79.02, 78.96, 78.92, 78.77, 75.06, 74.18, 73.90, 73.20, 71.80, 71.46, 71.21, 70.28, 69.96, 68.72, 67.65, 57.68, 55.40, 52.11,

51.03, 50.01, 41.11, 40.67, 34.47, 27.57, 27.47, 27.44, 27.41, 27.35. Yield: 49%. HR-MS: $[M+Na]^+$ 1376.6777 (theoretical 1376.6794).

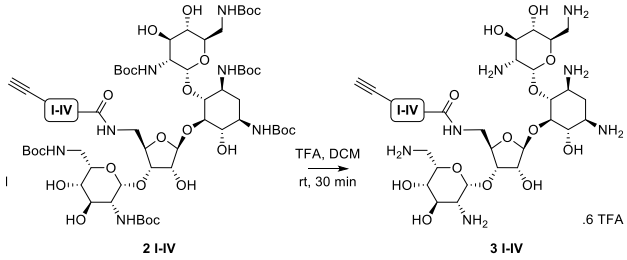

Scheme 4.6. Synthesis of Neo-alkyne intermediates.

General synthesis of Neo-alkyne derivatives (3)

To a solution of **2** (1 eq) and triisopropylsilane (6.0 eq) in DCM (6.1 ml/mmol) was added TFA (6.1 ml/mmol) at room temperature. The mixture was stirred for 2 hours. The reaction was azeotroped in toluene 3 times, and dissolved in water. The solution was washed with DCM (3 times) and lyophilized to give the desired product as a colorless amorphous.

3-I. Previously reported.[19]

3-II. ^{1}H NMR (500 MHz, D_2O): δ 5.79 (d, *J*=3.85 Hz, 1H), 5.19 (d, *J*=3.34 Hz, 1H), 5.08 (d, *J*=1.62 Hz, 1H). ^{13}C NMR (126 MHz, D_2O) δ: 172.41, 163.26, 162.98, 162.70, 162.42, 119.65, 117.33, 115.01, 112.69, 109.86, 95.19, 94.58, 84.94, 79.56, 78.40, 77.21, 76.63, 74.87, 73.06, 72.16, 70.11, 69.65, 68.23, 67.90, 67.37, 67.01, 58.41, 52.94, 50.67, 49.42, 48.30, 40.68, 40.19, 39.79, 27.72. Yield: 84%.

3-III. ^{1}H NMR (500 MHz, D_2O): δ 5.74 (s, 1H), 5.20 (s, 1H), 5.09 (s, 1H), 4.18 (m, 1H), 4.11 (m, 1H), 4.03 (m, 3H), 3.91 (t, *J*=9.0 Hz, 1H), 3.81 (t, *J*=8.7 Hz, 1H), 3.75 (m,

2H), 3.63 (s, 1H), 3.55-3.46 (m, 2H), 3.40-3.14 9 (m, 10H), 2.31 (d, *J*=10.4 Hz, 1H), 2.14-2.00 (m, 5H), 1.42 (m, 1H), 1.40 (m, 2H), 1.31 (m, 2H), 1.20 (m, 2H), 1.11 (m, 2H). ^{13}C NMR (126 MHz, D_2O) δ 177.65, 163.26, 162.97, 162.69, 162.41, 119.65, 117.33, 115.01, 112.69, 109.13, 95.67, 94.87, 86.26, 84.96, 80.64, 77.19, 74.95, 73.31, 72.22, 70.27, 69.98, 69.63, 68.94, 67.93, 67.44, 67.23, 53.05, 50.63, 49.33, 48.29, 40.83, 40.31, 39.86, 35.64, 27.74, 27.63, 27.44, 27.38, 25.15, 17.30. Yield: 90%. HR-MS: $[M+H]^+$ 750.4246 (theoretical 750.4244).

3-IV. ^{1}H NMR (500 MHz, D_2O): δ 5.99 (d, *J*=3.94 Hz, 1H), 5.39 (d, *J*=3.59 Hz, 1H), 5.27 (s, 1H), 4.45 (t, *J*=5.24 Hz, 1H), 4.28-4.22 (m, 6H), 4.13 (m, 3H), 4.00-3.92 (m, 3H), 3.82-3.69 (m, 7H), 3.59-3.34 (m, 10H), 2.92 (m, 1H), 2.51 (m, 1H), 1.91 (q, *J*=12.67 Hz, 1H). ^{13}C NMR (126 MHz, D_2O) δ: 175.49, 165.84, 165.56, 165.28, 164.99, 122.23, 119.90, 117.58, 115.27, 112.34, 97.87, 97.21, 87.50, 82.32, 81.62, 79.86, 78.60, 77.44, 75.68, 74.78, 72.64, 72.17, 71.97, 70.98, 70.50, 69.97, 69.61, 60.39, 55.56, 53.24, 51.99, 50.88, 43.40, 42.80, 42.39, 30.32. Yield: 74%. HR-MS: $[M+Na]^+$ 776.3649 (theoretical 776.3648).

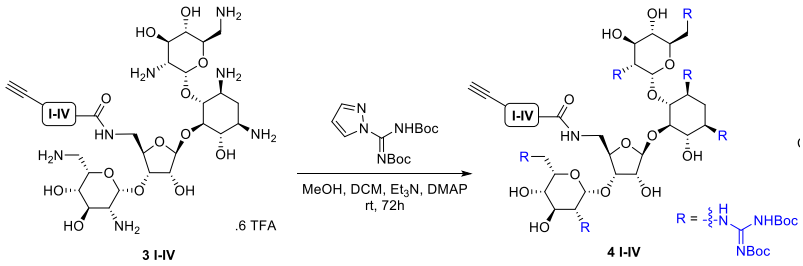

Scheme 4.7. Synthesis of BocGNeo-alkyne intermediates.

General synthesis of BocGNeo-alkyne derivatives (4)

To a solution of **3** (1 eq) in MeOH (0.12 mol/L) was added DCM (0.036 mol/L),), triethylamine (15 eq) and *N*,*N*′-Di-Boc-1*H*-pyrazole-1-carboxamidine (15 eq) and DMAP (1 eq) at ambient temperature. The mixture was stirred for 120 h. The mixture was partitioned between DCM and 5% citric acid. The organic layer was collected, dried over sodium sulfate, filtered off, and the filtrate was evaporated. Silica gel column chromatography (0-3% MeOH in DCM) afforded the desired product as a colorless amorphous.

4-I. Previously reported.[19]

4-II. ^{1}H NMR (500 MHz, CD_3OD): δ 5.85 (d, *J*=3.89 Hz, 1H), 5.08 (s, 1H), 5.02 (s, 1H), 4.58 (m, 1H), 4.39-4.32 (m, 3H), 4.28 (m, 1H), 4.16-4.08 (m, 3H), 3.92-3.85 (m, 4H), 3.77-3.69 (m, 3H), 3.54-3.48 (m, 2H), 3.22 (m, 1H), 2.25 (m, 1H), 1.59-1.4 (m, 108H). ^{13}C NMR (126 MHz, CD_3OD) δ: 170.55, 163.20, 162.92, 162.82, 162.76, 157.35, 156.57, 156.43, 156.13, 156.10, 153.29, 153.01, 152.78, 152.74, 152.60, 151.88, 151.79, 111.54, 97.92, 95.85, 87.30, 83.39, 83.31, 83.25, 83.22, 82.94, 82.66, 82.54, 81.58, 79.18, 79.13, 79.10, 79.08, 78.90, 78.84, 78.58, 78.39, 75.83, 75.65, 75.30, 74.19, 72.85, 72.19, 71.87, 70.58, 69.74, 68.13, 66.71, 58.24, 53.85, 51.59, 50.45, 48.76, 42.93, 41.34, 40.28, 33.85, 29.36, 27.44, 27.27, 27.16, 27.02, 26.97, 26.84, 26.81. Yield: 63%. HR-MS: $[M+2H]^{2+}$ 1082.0631 (theoretical 1082.0619).

4-III. ^{1}H NMR (500 MHz, CD_3OD): δ 5.69 (d, *J*=3.92 Hz, 1H), 5.04 (m, 2H), 4.58 (m, 1H), 4.39 (m, 1H), 4.29 (m, 3H), 4.14 (m, 1H), 3.99-3.68 (m, 9H), 3.55-3.49 (m, 4H), 3.22 (m, 2H), 2.36-2.16 (m, 6H), 1.59-1.43 (m, 116H). ^{13}C NMR (126 MHz, CD_3OD) δ: 174.78, 163.21, 163.17, 162.95, 162.92, 162.80, 162.74, 157.46, 156.58, 156.44, 156.11, 153.29, 153.01, 152.80, 152.76, 152.54, 151.84, 112.13, 104.19, 97.86, 95.68, 87.73,

83.62, 83.41, 83.35, 83.22, 83.18, 82.99, 82.61, 79.27, 79.13, 79.07, 78.95, 78.85, 75.56, 75.32, 73.97, 72.86, 71.88, 70.48, 69.68, 68.26, 66.70, 53.99, 51.54, 50.42, 43.04, 42.79, 40.37, 35.93, 33.90, 29.39, 28.67, 28.30, 28.20, 27.31, 27.26, 27.23, 27.14, 27.07, 26.97, 26.94, 26.82, 25.72, 17.64. Yield: 45%. HR-MS: $[M+2H]^{2+}$ 1102.0952 (theoretical 1102.0958).

4-IV. ^{1}H NMR (500 MHz, CD_3OD): δ 5.85 (d, *J*=3.59 Hz, 1H), 5.11 (s, 1H), 5.02 (s, 1H), 4.59 (m, 1H), 4.36 (m, 2H), 4.24-4.10 (m 6H), 4.04-3.85 (m, 6H), 3.79-3.68 (m, 8H), 3.50 (m, 3H), 3.37 (m, 1H), 2.26 (m, 1H), 1.59-1.46 (m, 110H). ^{13}C NMR (126 MHz, CD_3OD) δ: 171.41, 163.22, 163.20, 162.97, 162.92, 162.81, 162.71, 157.37, 156.64, 156.42, 156.38, 156.14, 156.12, 153.29, 153.01, 152.79, 152.66, 152.54, 151.86, 110.97, 98.21, 95.89, 87.36, 83.37, 83.29, 83.23, 83.20, 82.94, 82.63, 79.25, 79.16, 79.10, 79.09, 79.06, 78.93, 78.82, 78.46, 75.66, 75.11, 74.99, 74.41, 72.89, 72.24, 71.81, 70.57, 70.54, 70.16, 69.68, 68.80, 66.56, 57.78, 53.91, 51.60, 50.29, 48.03, 42.88, 40.65, 40.14, 33.90, 29.71, 27.32, 27.26, 27.24, 27.19, 27.17, 27.15, 27.01, 26.98, 26.96, 26.83. Yield: 66%. HR-MS: $[M+2H]^{2+}$ 1104.0745 (theoretical 1104.0751).

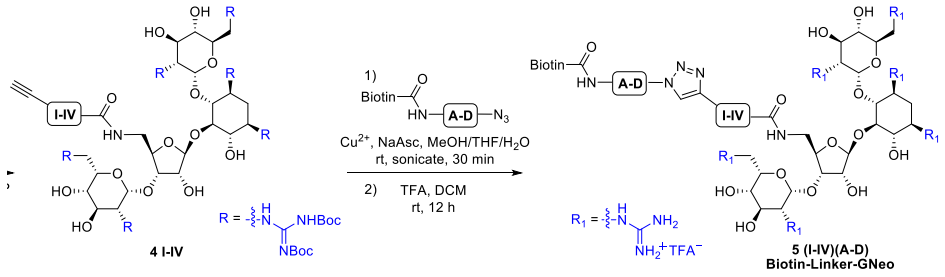

Scheme 4.8. Synthesis of biotin-linker-GNeo derivatives.

General synthesis of biotin-linker-GNeo (5)

4 (0.046 mmol), and biotin-azide linker (0.069 mmol) were dissolved in DMF (1ml). Cu(II) sulfate hydrate (0.01 mmol) and sodium ascorbate (0.01 mmol) were added as a solution in H_2O (150μL). The reaction was stirred overnight at room temperature under argon. The reaction was diluted into CH_2Cl_2 and washed with H_2O and brine. The organic layer was dried over Na_2SO_4 and concentrated in vacuo. The protected product was dissolved in CH_2Cl_2 (1 mL) and treated with trifluoroacetic acid (1 mL) and triisopropylsilane (10 μL) for 2 hours at room temperature. The reaction was evaporated and azeotroped with toluene (3x) and purified on C-18 reverse phase HPLC column (5-60% ACN (0.1% TFA) in H_2O (0.1% TFA) over 18 min).

5 I-A. ^{1}H NMR (500 MHz, D_2O): δ 7.75 (s, 1H), 5.69 (s, 1H), 5.07 (s, 1H), 5.01 (s, 1H), 4.55 (m, 1H), 4.35 (m, 3H), 4.29 (m, 2H), 4.09 (m, 2H), 3.96 (m, 1H), 3.75 (m, 2H), 3.66 (s, 1H), 3.58-3.51 (m, 5H), 3.50-3.35 (m, 9H), 3.25 (m, 1H), 3.10 (m, 2H), 2.94 (d, *J*=13 Hz, 1H), 2.69 (m, 3H), 2.28 (m, 2H), 2.16 (m, 2H), 1.86 (m, 4H), 1.69-1.46 (m, 8H) 1.38-1.15 (m, 4H). ^{13}C NMR: (126 MHz, D_2O) δ 176.42, 176.22, 165.20, 163.32, 163.04, 162.76, 162.48, 157.49, 157.27, 157.15, 157.03, 156.91, 156.32, 147.25, 123.01, 120.56, 119.67, 117.35, 115.03, 112.71, 110.69, 110.34, 98.31, 95.88, 84.89, 79.84, 78.53, 76.98, 74.38, 73.42, 72.49, 71.85, 70.71, 69.62, 69.41, 69.22, 68.93, 68.57, 66.49, 61.97, 60.13, 55.32, 53.35, 51.79, 50.42, 50.06, 41.57, 39.61, 38.64, 35.35, 35.20, 31.91, 28.84, 27.72, 27.58, 25.08, 24.06, 22.74. Yield: 37%. HRMS: $[M+2H]^{2+}$ 657.8473 (theoretical 657.8496).

5 I-B. ^{1}H NMR (500 MHz, D_2O): δ 7.81 (s, 1H), 5.72 (s, 1H), 5.10 (s, 1H), 5.03 (s, 1H), 5.46 (m, 3H), 4.37 (m, 1H), 4.32-4.29 (m, 2H), 4.11 (s, 2H), 3.98 (m, 1H), 3.90 (s, 2H), 3.78 (m, 3H), 3.68 (s, 1H), 3.60-3.40 (m, 15H), 3.29 (m, 3H), 2.93 (d, *J*=13.0 Hz,

1H), 2.72 (m, 3H), 2.31 (m, 2H), 2.17 (m, 2H), 1.94 (m, 2H), 1.69-1.42 (m, 5H), 1.35-1.15 (m, 3H). ^{13}C NMR: (126 MHz, D_2O) δ 176.64, 176.23, 165.25, 163.35, 163.07, 162.79, 162.50, 157.61, 157.40, 157.26, 157.17, 156.96, 156.43, 147.35, 123.51, 119.68, 117.43, 115.33, 112.79, 110.41, 98.43, 95.75, 84.95, 80.01, 78.74, 77.07, 74.58, 73.54, 72.65, 71.81, 70.86, 69.49, 69.07, 68.81, 68.52, 66.64, 62.02, 60.21, 55.53, 55.35, 53.35, 51.76, 50.33, 49.98, 41.81, 41.73, 40.95, 39.67, 38.72, 35.42, 35.24, 32.04, 27.83, 27.65, 25.14, 25.08, 24.16. Yield: 26%. HRMS: $[M+2Na]^{2+}$ 1281.1350 (theoretical 1281.1358).

5 I-C. ^{1}H NMR (500 MHz, D_2O): δ 7.73 (s, 1H) 5.67 (s, 1H), 5.04 (s, 1H), 4.98 (s, 1H), 4.52 (m, 1H), 4.31 (m, 3H), 4.25 (m, 1H), 4.06 (m, 2H), 3.94 (m, 1H), 3.73 (m, 3H), 3.63 (m, 1H), 3.60-3.32 (m, 12H), 3.24 (m, 1H), 3.10 (m, 2H), 2.90 (dd, *J*=4.9 Hz, 13.1 Hz, 1H), 2.68 (m, 3H), 2.33 (m, 1H), 2.25 (m, 2H), 2.16 (m, 2H), 1.88 (m, 2H), 1.79 (m, 2H), 1.70-1.45 (m, 7H), 1.44-1.25 (m, 5H), 1.24-1.08 (m, 14H). ^{13}C NMR: (126 MHz, D_2O) δ 176.40, 176.22, 171.50, 165.16, 157.49, 157.29, 157.16, 157.04, 156.92, 156.34, 147.26, 142.28, 123.09, 117.36, 115.04, 110.30, 108.46, 98.36, 95.86, 84.97, 79.95, 78.55, 76.95, 74.42, 73.48, 71.86, 70.71, 69.25, 68.94, 66.49, 61.93, 60.12, 55.34, 53.36, 51.76, 50.41, 50.26, 41.56, 40.51, 39.64, 39.08, 35.43, 35.23, 33.41, 33.30, 31.92, 29.11, 28.40, 28.11, 27.84, 27.70, 27.62, 25.81, 25.23, 25.18, 25.11, 24.04. Yield: 36%. HRMS: $[M+3H]^{3+}$ 466.9336 (theoretical 466.9335).

5 I-D. ^{1}H NMR (500 MHz, D_2O): δ 7.82 (s, 1H), 5.69 (s, 1H), 5.07 (s, 1H), 5.00 (s, 1H), 4.55 (m, 3H), 4.35 (m, 1H), 4.30 (m, 1H), 4.26 (m, 1H), 4.09 (s, 2H), 3.91 (m, 3H), 3.72 (m, 2H), 3.58 (s, 1H), 3.65-3.5 (m, 14H), 3.5-3.35 (m, 9H), 3.32 (m, 2H), 3.25 (m, 1H), 2.91 (d, *J*=13.0 Hz, 1H), 2.71 (m, 3H), 2.28 (t, *J*=6.6 Hz, 2H), 2.19 (m, 3H), 1.93 (m, 2H), 1.70-1.45 (m, 6H), 1.33 (m, 2H). ^{13}C NMR: (126 MHz, D_2O) δ 176.73, 176.14,

165.56, 165.20, 163.01, 162.72, 162.44, 157.50, 157.29, 157.15, 157.04, 156.91, 156.33, 147.15, 123.58, 119.65, 117.34, 117.33, 115.02, 112.69, 110.32, 98.23, 95.88, 84.88, 79.67, 78.53, 76.97, 74.35, 73.36, 72.49, 71.85, 70.71, 69.44, 69.29, 69.24, 68.93, 68.68, 68.61, 66.50, 61.94, 60.12, 55.40, 55.25, 53.35, 51.80, 50.42, 49.84, 41.58, 41.51, 40.68, 39.57, 38.76, 35.29, 35.16, 31.89, 27.76, 27.59, 25.04, 25.01, 23.96. Yield: 60%. HRMS: $[M+2Na]^{2+}$ 1325.1611 (theoretical 1325.1620).

5 II-A. ^{1}H NMR (500 MHz, D_2O): δ 8.01 (s, 1H), 5.69 (s, 1H), 5.05 (s, 1H), 4.99 (s, 1H), 4.54 (m, 1H), 4.39 (t, *J*=6.6 Hz, 2H), 4.33 (m, 2H), 4.29 (m, 1H), 4.06 (m, 4H), 3.99 (m, 1H), 3.73 (m, 3H), 3.64 (s, 1H), 3.56-3.35 (m, 13H), 3.25 (m, 1H), 3.09 (m, 2H), 2.93 (d, 1H, *J*=12.5 Hz), 2.71 (d, 1H, *J*=12.5 Hz), 2.15 (t, *J*=6.9 Hz, 3H), 1.85 (m, 2H), 1.71-1.50 (m, 8H), 1.30 (m, 2H), 1.19 (m, 3H). ^{13}C NMR: (126 MHz, D_2O) δ 176.51, 172.22, 165.26, 163.43, 162.99, 162.71, 162.43, 157.63, 157.36, 157.26, 157.10, 157.02, 156.43, 143.05, 125.07, 119.76, 117.45, 115.13, 112.81, 110.68, 98.17, 95.98, 85.03, 79.35, 78.41, 77.12, 74.48, 73.40, 72.57, 71.89, 70.85, 69.37, 69.04, 68.63, 66.66, 63.67, 62.04, 60.20, 55.43, 55.36, 53.44, 51.93, 50.51, 50.30, 41.68, 41.60, 40.34, 39.65, 38.77, 35.42, 31.97, 28.92, 27.79, 27.67, 27.63, 25.13, 22.84. Yield: 46%. HRMS: $[M+2H]^{2+}$ 658.8390 (theoretical 658.8393).

5 II-B. ^{1}H NMR (500 MHz, D_2O): δ 8.03 (s, 1H), 5.68 (s, 1H), 5.04 (s, 1H), 4.98 (s, 1H), 4.56 (m, 3H), 4.31 (m, 3H), 4.06 (m, 4H), 3.97 (m, 1H), 3.87 (m, 2H), 3.72 (m, 3H), 3.63 (s, 1H), 3.57-3.35 (m, 15H), 3.25 (m, 3H), 3.13 (m, 1H), 2.89 (d, *J*=13.0 Hz, 1H), 2.70 (d, *J*=12.9 Hz, 1H), 2.15 (m, 3H), 1.70-1.43 (m, 5H), 1.28 (m, 2H), 1.20 (m, 2H). ^{13}C NMR: (126 MHz, D_2O) δ 176.69, 172.21, 167.27, 157.63, 157.35, 157.25, 157.10, 156.99, 156.63, 156.41, 143.15, 125.52, 119.33, 117.44, 115.12, 112.79, 110.72,

98.28, 95.96, 85.01, 79.57, 78.56, 77.15, 74.46, 73.46, 72.57, 71.89, 70.86, 69.34, 69.04, 68.85, 68.69, 68.47, 67.86, 66.64, 66.52, 63.66, 62.03, 60.22, 55.45, 55.36, 53.44, 51.89, 50.49, 50.13, 46.63, 41.68, 41.60, 40.47, 39.67, 38.71, 35.41, 32.00, 28.92, 27.84, 27.67, 27.63, 25.10, 22.84. Yield: 55%. HRMS: $[M+2H]^{2+}$ 659.8267 (theoretical 659.8289).

5 II-C. ^{1}H NMR (500 MHz, D_2O): δ 8.00 (s, 1H), 5.67 (s, 1H), 5.03 (s, 1H), 4.97 (s, 1H), 4.51 (m, 1H), 4.36 (m, 2H), 4.30 (m, 1H), 4.26 (m, 1H), 4.06-4.03 (m, 4H), 3.97 (m, 1H), 3.72 (m, 3H), 3.62 (s, 1H), 3.57-3.50 (m, 4H), 3.47-3.35 (m, 9H), 3.23 (m, 1H), 3.10 (m, 2H), 2.90 (dd, *J*=4.9 Hz, 13.0 Hz, 1H), 2.68 (d, *J*=13.0 Hz, 1H), 2.16 (t, *J*=6.8 Hz, 2H), 1.81 (m, 2H), 1.65-1.46 (m, 7H), 1.41 (m, 3H), 1.31 (m, 3H), 1.25-1.10 (m, 15H). ^{13}C NMR: (126 MHz, D_2O) δ 172.14, 165.12, 163.28, 163.00, 162.71, 162.43, 157.46, 157.23, 157.13, 156.93, 156.86, 156.28, 142.86, 125.06, 119.61, 117.33, 115.01, 112.68, 110.58, 98.08, 95.89, 84.91, 79.22, 78.25, 77.01, 74.34, 73.26, 72.44, 71.77, 70.72, 69.21, 68.90, 68.41, 66.51, 63.51, 61.87, 60.07, 55.28, 53.33, 51.80, 50.37, 41.54, 40.06, 39.59, 39.03, 35.57, 31.89, 30.04, 29.39, 29.11, 28.40, 28.25, 28.13, 28.07, 27.73, 27.64, 27.55, 25.79, 25.23, 25.12. Yield: 32%. HRMS: $[M+2H]^{2+}$ 700.8868 (theoretical 700.8862).

5 II-D. ^{1}H NMR (500 MHz, D_2O): δ 8.07 (s, 1H), 5.69 (s, 1H), 5.05 (s, 1H), 4.98 (s, 1H), 4.59 (m, 2H), 4.53 (m, 1H), 4.33 (m, 2H), 4.29 (m, 1H), 4.05 (m, 4H), 3.99 (m, 1H), 3.92 (m, 2H), 3.73 (m, 3H), 3.63-3.50 (m, 17H), 3.50-3.35 (m, 9H), 3.30 (m, 2H), 3.25 (m, 1H), 2.92 (dd, *J*=3.4 Hz, 13.0 Hz), 2.70 (d, 1H, *J*=13.0 Hz), 2.18 (m, 3H), 1.69-1.43 (m, 6H), 1.32 (m, 2H). ^{13}C NMR: (126 MHz, D_2O) δ 176.75, 172.14, 165.20, 163.05, 162.76, 157.51, 157.25, 157.15, 156.97, 156.89, 156.31, 143.05, 125.49, 119.65, 117.33, 115.01, 112.68, 110.65, 98.11, 95.93, 84.89, 79.27, 78.38, 77.05, 74.34, 73.27, 72.47, 71.80, 70.74, 69.51, 69.40, 69.29, 69.24, 69.19, 69.09, 68.94, 68.66, 68.55, 66.53, 63.50,

62.28, 61.93, 60.11, 55.32, 55.25, 54.17, 53.36, 51.82, 50.40, 49.88, 41.57, 41.43, 40.23, 39.56, 38.73, 35.28, 35.14, 31.90, 27.75, 27.58, 25.03. Yield: 38%. HRMS: $[M+2H]^{2+}$ 703.8542 (theoretical 703.8551).

5 III-A. ^{1}H NMR (500 MHz, D_2O): δ 7.85 (s, 1H), 5.67 (s, 1H), 5.05 (s, 1H), 4.97 (s, 1H), 4.52 (m, 1H), 4.37 (m, 2H), 4.33(m, 1H), 4.25-4.18 (m, 2H), 4.06 (s, 2H), 3.91 (m, 1H), 3.72-3.62 (m, 4H), 3.55 (m, 3H), 3.50-3.35 (m, 9H), 3.22 (m, 1H), 3.07 (m, 2H), 2.89 (dd, *J*=4.9 Hz, 12.5 Hz, 1H), 2.66 (m, 3H), 2.20-2.10 (m, 4H), 1.84 (m, 2H), 1.68-1.38 (m, 13H), 1.25 (m, 7H), 1.16 (m, 2H). ^{13}C NMR: (126 MHz, D_2O) δ 177.09, 176.37, 165.15, 163.26, 162.98, 162.70, 162.42, 157.47, 157.25, 157.11, 157.02, 156.87, 156.29, 146.98, 123.88, 119.62, 117.30, 114.98, 112.66, 110.15, 98.29, 95.79, 85.14, 79.65, 78.49, 76.79, 74.48, 73.42, 72.50, 71.87, 70.65, 69.22, 68.88, 66.48, 61.94, 60.08, 55.39, 55.29, 53.31, 51.73, 50.84, 50.37, 41.59, 41.50, 40.53, 39.55, 38.61, 35.74, 35.30, 31.85, 28.53, 28.04, 27.89, 27.71, 27.53, 27.47, 25.13, 25.06, 23.70, 22.62. Yield: 38%. HRMS: $[M+2H]^{2+}$ 678.8733 (theoretical 678.8731).

5 III-B. ^{1}H NMR (500 MHz, D_2O): δ 7.86 (s, 1H), 5.67 (s, 1H), 5.05 (s, 1H), 4.97 (s, 1H), 4.55 (m, 3H), 4.31 (m, 1H), 4.23 (m, 2H), 4.06 (s, 2H), 3.92 (m, 1H), 3.86 (s, 2H), 3.75-3.60 (m, 4H), 3.56-3.35 (m, 15H), 3.23 (m, 3H), 2.90 (d, 1H, *J*=13.1 Hz), 2.69 (m, 3H), 2.18-2.10 (m, 5H), 1.63-1.40 (m, 9H), 1.27 (m, 6H). ^{13}C NMR: (126 MHz, D_2O) δ 177.06, 176.50, 165.15, 163.25, 162.97, 162.69, 162.40, 157.47, 157.26, 157.11, 157.01, 156.87, 156.29, 147.09, 124.25, 119.61, 117.29, 114.97, 112.65, 110.18, 104.99, 98.28, 95.80, 85.12, 79.63, 78.49, 76.81, 74.46, 73.42, 72.50, 71.86, 70.65, 69.22, 68.88, 68.73, 68.12, 66.48, 61.92, 60.09, 55.39, 55.28, 53.31, 51.74, 50.66, 50.37, 41.60, 41.50, 40.54,

39.56, 38.61, 36.75, 35.75, 35.30, 31.86, 30.04, 28.13, 27.95, 27.82, 27.76, 27.57, 25.14, 25.00, 23.83. Yield: 45%. HRMS: $[M+2H]^{2+}$ 679.8629 (theoretical 679.8627).

5 III-C. ^{1}H NMR (500 MHz, D_2O): δ 7.73 (s, 1H), 5.68 (s, 1H), 5.05 (s, 1H), 4.97 (s, 1H), 4.52 (m, 1H), 4.32 (m, 3H), 4.22 (m, 2H), 4.07 (m, 2H), 3.93 (m, 1H), 3.79-3.63 (m, 4H), 3.60-3.50 (m, 4H), 3.50-3.35 (m, 10H), 3.23 (m, 1H), 3.10 (t, *J*=6.0 Hz, 2H), 2.88 (dd, *J*=4.6Hz, 13.1 Hz), 2.63 (m, 3H), 2.17 (m, 5H), 1.80 (m, 2H), 1.68-1.46 (m, 8H), 1.41 (m, 2H), 1.35-1.05 (m, 23H). ^{13}C NMR: (126 MHz, D_2O) δ 177.07, 176.31, 166.83, 165.10, 163.32, 163.04, 162.76, 157.42, 157.25, 157.10, 156.99, 156.86, 156.27, 148.21, 123.06, 117.31, 114.99, 110.12, 98.46, 95.79, 85.25, 79.96, 78.47, 76.75, 74.54, 73.52, 71.87, 70.56, 69.16, 68.87, 66.45, 61.91, 60.07, 55.40, 55.33, 53.32, 51.66, 50.36, 50.14, 41.55, 41.47, 40.22, 39.61, 39.04, 35.80, 35.38, 31.91, 28.91, 28.47, 28.35, 28.18, 28.09, 28.05, 27.94, 27.69, 27.66, 27.62, 27.50, 25.80, 25.21, 25.17, 25.04, 24.24. Yield: 26%. HRMS: $[M+3H]^{3+}$ 480.9485 (theoretical 480.9491).

5 III-D. ^{1}H NMR (500 MHz, D_2O): δ 7.87 (s, 1H), 5.78 (s, 1H), 5.16 (s, 1H), 5.08 (s, 1H), 4.62 (m, 3H), 4.43 (m, 1H), 4.34 (m, 2H), 4.17 (s, 2H), 4.03 (m, 1H), 3.98 (s, 2H), 3.83-3.45 (m, 30H), 3.39 (m, 2H), 3.32 (m, 1H), 3.00 (d, *J*=13.0 Hz, 1H), 2.77 (m, 3H), 2.26 (m, 5H), 1.78-1.55 (m, 10H), 1.37 (m, 6H). ^{13}C NMR (126 MHz, D_2O): δ 177.17, 176.74, 165.26, 164.07, 163.04, 162.76, 162.48, 157.61, 157.39, 157.25, 157.16, 157.01, 156.43, 123.61, 119.76, 117.44, 115.12, 112.80, 110.30, 98.45, 95.91, 85.25, 79.92, 78.61, 76.94, 74.60, 73.61, 72.60, 71.99, 70.74, 69.60, 69.52, 69.40, 69.01, 68.79, 68.69, 66.62, 65.13, 62.02, 60.20, 55.52, 55.32, 53.44, 51.85, 50.51, 49.96, 48.27, 41.71, 41.61, 40.55, 39.65, 38.87, 35.87, 35.39, 32.52, 32.00, 28.53, 28.05, 27.95, 27.86, 27.68, 25.24, 25.12, 24.36. Yield: 15%. HRMS: $[M+2H]^{2+}$ 723.8897 (theoretical 723.8890).

5 IV-A. ^{1}H NMR (500 MHz, D_2O): δ 8.06 (s, 1H), 5.79 (s, 1H), 5.15 (s, 1H), 5.06 (s, 1H), 4.62 (m, 1H), 4.47 (m, 2H), 4.39 (m, 1H), 4.34 (m, 1H), 4.15 (m, 2H), 4.10 (m, 2H), 4.02 (m, 1H), 3.80 (m, 7H), 3.69-3.45 (m, 14H), 3.34 (m, 1H), 3.25-3.15 (m, 6H), 3.02 (d, *J*=13.0 Hz, 1H), 2.80 (d, *J*=13.0 Hz, 1H), 2.24 (m, 3H), 1.94 (m, 2H), 1.76-1.50 (m, 8H), 1.45-1.22 (m, 9H). ^{13}C NMR (126 MHz, D_2O): δ 176.52, 172.56, 165.27, 163.32, 163.04, 162.76, 162.47, 157.62, 157.35, 157.23, 157.12, 157.01, 156.43, 143.53, 125.00, 119.78, 117.46, 115.14, 112.82, 110.72, 98.10, 95.90, 85.19, 79.30, 78.61, 77.03, 74.59, 73.45, 72.57, 71.93, 70.85, 70.43, 69.36, 69.06, 68.70, 66.69, 63.02, 62.05, 60.20, 55.43, 55.37, 53.41, 51.89, 50.50, 50.26, 46.63, 41.75, 41.59, 40.59, 39.65, 38.77, 35.43, 31.97, 28.92, 27.79, 27.64, 25.15, 22.83. Yield: 26%. HRMS: $[M+2H]^{2+}$ 680.8528 (theoretical 680.8524).

5 IV-B. ^{1}H NMR (500 MHz, D_2O): δ 8.09 (s, 1H), 5.78 (s, 1H), 5.15 (s, 1H), 5.06 (s, 1H), 4.65 (m, 3H), 4.38 (m, 1H), 4.34 (m, 1H), 4.15 (m, 2H), 4.10 (s, 2H), 4.02 (m, 1H), 3.97 (s, 2H), 3.84-3.73 (m, 9H), 3.67-3.45 (m, 17H), 3.34 (m, 3H), 3.24 (dd, *J*=5.0 Hz, 13.2 Hz, 1H), 2.25 (m, 3H), 1.87 (m, 2H), 1.73-1.60 (m, 3H), 1.52 (m, 2H). ^{13}C NMR (126 MHz, D_2O): δ 176.54, 173.28, 172.62, 172.54, 163.50, 163.31, 163.03, 162.74, 162.46, 157.62, 157.34, 157.24, 157.12, 157.00, 156.42, 143.57, 125.43, 121.50, 117.44, 115.13, 112.80, 110.72, 104.99, 98.13, 95.88, 85.17, 79.35, 78.66, 77.03, 74.58, 73.46, 72.59, 71.91, 70.86, 70.40, 69.74, 69.36, 69.06, 68.73, 68.45, 66.68, 62.98, 57.20, 57.05, 55.43, 55.42, 51.89, 50.48, 50.07, 41.75, 41.59, 40.76, 40.65, 38.70, 35.26, 31.96, 26.20, 25.03, 24.78. Yield: 26%. HRMS: $[M+3H]^{3+}$ 454.8886 (theoretical 454.8971).

5 IV-C. ^{1}H NMR (500 MHz, D_2O): δ 8.07 (s, 1H), 5.79 (s, 1H), 5.16 (s, 1H), 5.06 (s, 1H), 4.61 (m, 1H), 4.46 (m, 3H), 4.38 (s, 1H), 4.34 (m, 1H), 4.15 (s, 2H), 4.09 (s, 2H),

4.02 (m, 1H), 3.84-3.70 (m, 9H), 3.69-3.44 (m, 14H), 3.33 (m, 1H), 3.19 (m, 2H), 3.00 (dd, *J*=4.7 Hz, 12.9 Hz, 1H), 2.79 (d, *J*=13.0 Hz, 1H), 2.27 (m, 3H), 1.91 (m, 2H), 1.79-1.57 (m, 5H), 1.51 (m, 2H), 1.41 (m, 2H), 1.32-1.15 (m, 17H). ^{13}C NMR (126 MHz, D_2O): δ 176.47, 172.56, 165.23, 163.35, 163.05, 162.77, 162.49, 157.62, 157.37 157.23, 157.12, 157.02, 156.44, 150.40, 143.54, 125.06, 119.78, 117.46, 115.14, 112.82, 110.70, 98.14, 95.91, 85.19, 79.35, 78.62, 77.04, 74.60, 73.46, 72.58, 71.94, 70.84, 70.45, 69.38, 69.07, 68.63, 66.69, 63.00, 61.99, 60.19, 55.45, 55.38, 53.43, 51.89, 50.45, 41.76, 41.61, 40.57, 39.69, 39.14, 35.50, 31.98, 29.18, 28.48, 28.30, 28.22, 28.18, 27.80, 27.76, 27.67, 25.88, 25.31, 25.22. Yield: 29%. HRMS: $[M+3H]^{3+}$ 482.2682 (theoretical 482.2686).

5 IV-D. ^{1}H NMR (500 MHz, D_2O): δ 8.13 (s, 1H), 5.80 (s, 1H), 5.16 (s, 1H), 5.07 (s, 1H), 4.68 (t, 2H), 4.62 (m, 1H), 4.44 (m, 1H), 4.40 (m, 1H), 4.35 (t, 1H), 4.17 (m, 2H), 4.11 (m, 2H), 4.01 (m, 3H), 3.81 (m, 7H), 3.75 (m, 1H), 3.70-3.60 (m, 15H), 3.60-3.46 (m, 9H), 3.40 (t, *J*=5.1 Hz, 2H), 3.34 (m, 1H), 3.00 (dd, *J*=4.9 Hz, 13.1 Hz, 1H), 2.80 (d, *J*=13.0 Hz, 1H), 2.28 (m, 3H), 1.80-1.52 (m, 6H), 1.48-1.35 (m, 2H). ^{13}C NMR (126 MHz, D_2O): δ 176.80, 172.56, 165.27, 163.32, 163.04, 162.76, 162.48, 157.62, 157.35, 157.23, 157.11, 157.01, 156.42, 143.58, 125.49, 119.75, 117.44, 115.11, 112.80, 110.72, 98.12, 95.93, 85.15, 80.03, 79.34, 78.63, 77.05, 74.57, 73.43, 72.57, 71.92, 70.84, 70.41, 69.54, 69.51, 69.39, 69.35, 69.06, 68.77, 68.72, 68.66, 66.67, 62.96, 62.01, 60.20, 55.43, 55.31, 53.44, 51.90, 50.51, 49.98, 46.63, 41.74, 41.56, 40.60, 39.64, 38.84, 35.39, 31.97, 27.83, 27.66, 25.10. Yield: 30%. HRMS: $[M+2H]^{2+}$ 725.8681 (theoretical 725.8682).

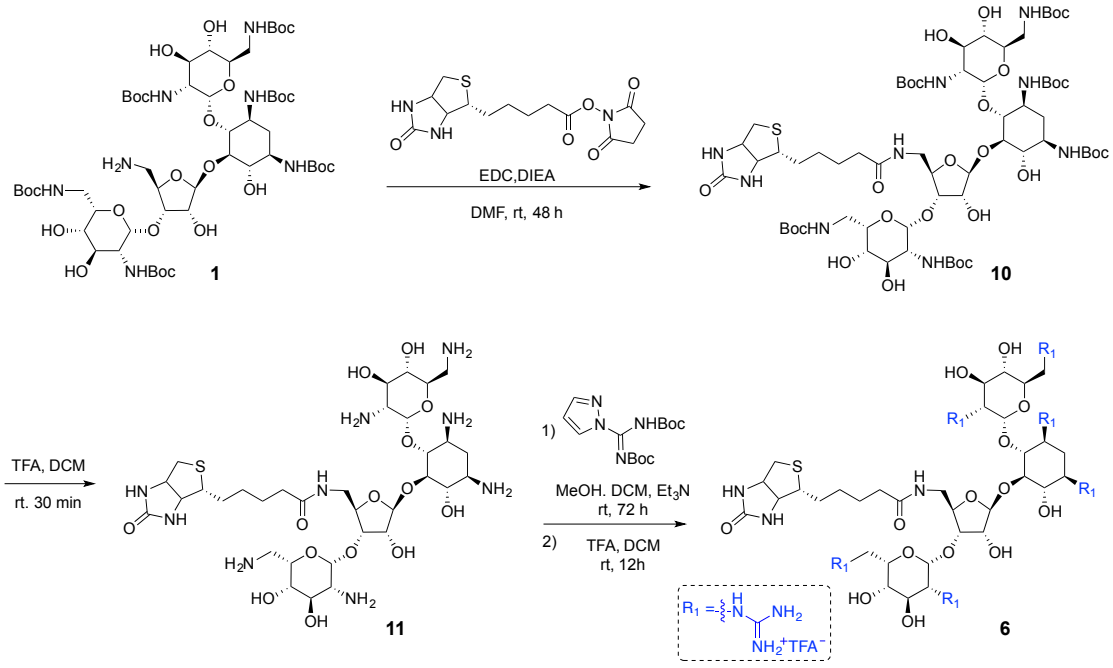

Scheme 4.9. Synthesis of GNeo-biotin with no linker.

10. To a solution of biotin-NHS (0.262 mmol, 3.2 eq) in DMF (9.4ml) was added EDC (0.261 mmol, 3.2 eq). The mixture was stirred for 30 min. A solution of **1** (0.082 mmol, 1 eq) in DMF (9.4ml) and DIEA (0.248 mmol, 3 eq) was then added dropwise. The mixture was then stirred for 48 h. The reaction was concentrated in vacuum and partitioned between DCM and 5% citric acid. The organic layer was separated and washed with sodium bicarbonate and brine. The organic layer was collected, dried over sodium sulfate, filtered off, and the filtrate was evaporated. Silica gel column chromatography (0-8% MeOH in DCM) afforded the desired product as a colorless amorphous (68mg, 55%). ^{1}H NMR (500 MHz, CD_3OD): δ 5.45 (s, 1H), 5.09 (s, 1H), 4.88 (s, 1H), 4.49 (m 2H), 4.32 (m, 2H), 3.90 (m, 3H), 3.75 (m, 3H), 3.53 (m, 6H), 3.24 (m, 3H), 2.95 (m, 1H), 2.86 (m, 1H), 2.70 (m, 1H), 2.35 (t, *J*=7.4 Hz, 2H), 1.96 (d, *J*=12.8 Hz, 1H), 1.73-1.60 (m, 6H), 1.48-1.43 (m, 54H). ^{13}C NMR (126 MHz, CD_3OD) δ: 175.08, 164.65, 157.68, 157.53, 157.17,

156.84, 156.53, 110.69, 99.16, 97.54, 87.01, 79.59, 79.42, 79.31, 79.27, 79.02, 78.90, 74.78, 74.17, 73.03, 72.01, 71.26, 70.28, 67.63, 62.09, 60.20, 55.58, 54.44, 53.39, 52.27, 51.18, 50.07, 42.64, 39.67, 35.31, 33.92, 28.99, 28.13, 27.64, 27.49, 27.45, 27.40, 27.35, 25.64, 23.82, 22.83. HR-MS: $[M+Na]^+$ 1462.7068 (theoretical 1462.7063)

11. To a solution of **10** (1 eq) and triisopropylsilane (6.0 eq) in DCM (6.1 ml/mmol) was added TFA (6.1 ml/mmol) at room temperature. The mixture was stirred for 2 hours. The reaction was azeotroped in toluene 3 times, and dissolved in water. The solution was washed with DCM (3 times) and lyophilized to give the desired product as a colorless amorphous. ^{1}H NMR (500 MHz, D_2O): δ 5.75 (d, *J*=2.71 Hz, 1H), 5.20 (d, *J*=2.98 Hz, 1H), 5.11 (s, 1H), 4.42 (m, 1H), 4.22 (m, 1H), 4.17 (m, 1H), 4.13 (m, 1H), 4.04 (m, 3H), 3.93 (t, *J*=9.14 Hz, 1H), 3.82-3.73 (m, 3H), 3.64 (s, 1H), 3.52 (t, *J*=9.19 Hz, 1H), 3.46 (m, 1H), 3.41-3.13 (m, 11H), 2.79 (m, 1H), 2.61 (d, *J*=11.86 Hz, 1H), 2.30 (m, 1H), 2.12 (m, 2H), 1.72 (q, *J*=12.42 Hz, 1H), 1.54-1.37 (m, 4H), 1.21 (m, 2H), 1.14 (m, 1H), 1.02 (m, 2H). ^{13}C NMR (126 MHz, D_2O) δ: 177.27, 165.26, 163.26, 162.98, 162.70, 162.41, 151.80, 148.81, 123.00, 119.66, 117.34, 115.02, 112.70, 109.12, 95.63, 94.94, 84.84, 80.61, 76.99, 75.11, 73.32, 72.21, 70.24, 69.95, 69.70, 67.98, 67.46, 67.30, 62.02, 60.18, 55.38, 53.08, 50.64, 49.46, 48.36, 40.80, 40.36, 39.86, 39.54, 35.30, 33.54, 29.30, 27.90, 27.75, 27.64, 25.10, 23.71, 22.74. HR-MS: $[M+Na]^+$ 862.3953 (theoretical 862.3951).

6. To a solution of **11** (1 eq) in MeOH (0.12 mol/L) was added DCM (0.036 mol/L), trimethylamine (15 eq) and guanidinylating reagent (15 eq) and DMAP (1 eq) at ambient temperature. The mixture was stirred for 120 h. The mixture was partitioned between DCM and 5% citric acid. The organic layer was collected, dried over sodium sulfate, filtered off, and the filtrate was evaporated off. The protected product was dissolved in CH_2Cl_2 (1 mL)

and treated with trifluoroacetic acid (1 mL) and triisopropylsilane (10 μL) for 2 hours at room temperature. The reaction was evaporated and azeotroped with toluene (3x) and purified on C-18 reverse phase HPLC column (5-60% ACN (0.1% TFA) in H_2O (0.1% TFA) over 18 min). ^{1}H NMR (500 MHz, D_2O): δ 5.70 (s, 1H), 5.07 (s, 1H), 5.04 (s, 1H), 4.56 (m, 1H), 4.35 (m, 1H), 4.23 (m, 2H), 4.14 (m, 1H), 4.08 (s, 1H), 3.95 (m, 1H), 3.74 (m, 3H), 3.65 (s, 1H), 3.57-3.38 (m, 14H), 3.26 (m, 1H), 2.93 (d, *J*=12.92 Hz, 1H), 2.74 (d, *J*=12.95 Hz, 1H), 2.22 (m, 3H), 1.67-1.32 (m, 8H). ^{13}C NMR (126 MHz, D_2O) δ: 176.79, 165.17, 163.31, 163.03, 162.74, 162.46, 157.49, 157.27, 157.13, 157.04, 156.88, 156.32, 119.65, 117.33, 115.00, 112.69, 110.05, 98.16, 95.77, 85.07, 79.71, 78.23, 76.67, 74.44, 73.52, 72.49, 71.88, 70.66, 69.16, 68.89, 66.49, 62.02, 60.21, 55.43, 53.31, 51.81, 50.41, 41.59, 41.47, 40.08, 39.48, 35.45, 31.79, 28.10, 27.83, 25.07. HR-MS: $[M+2H]^{2+}$ 546.7755 (theoretical 546.7756).

FPLC

The GNeo derivatives (225 μM in PBS) were incubated with ST (45 μM in PBS) for 20 min at ambient temperature then diluted to 1 mL PBS. The conjugates were analysed by automated FPLC using a HiTrap Heparin HP column equilibrated with PBS (Dulbecco's Phosphate Buffered Saline, Life Technologies) and a gradient of NaCl from 0.14 – 2 M. Absorbance of the flow-through was measured at 280 nm.

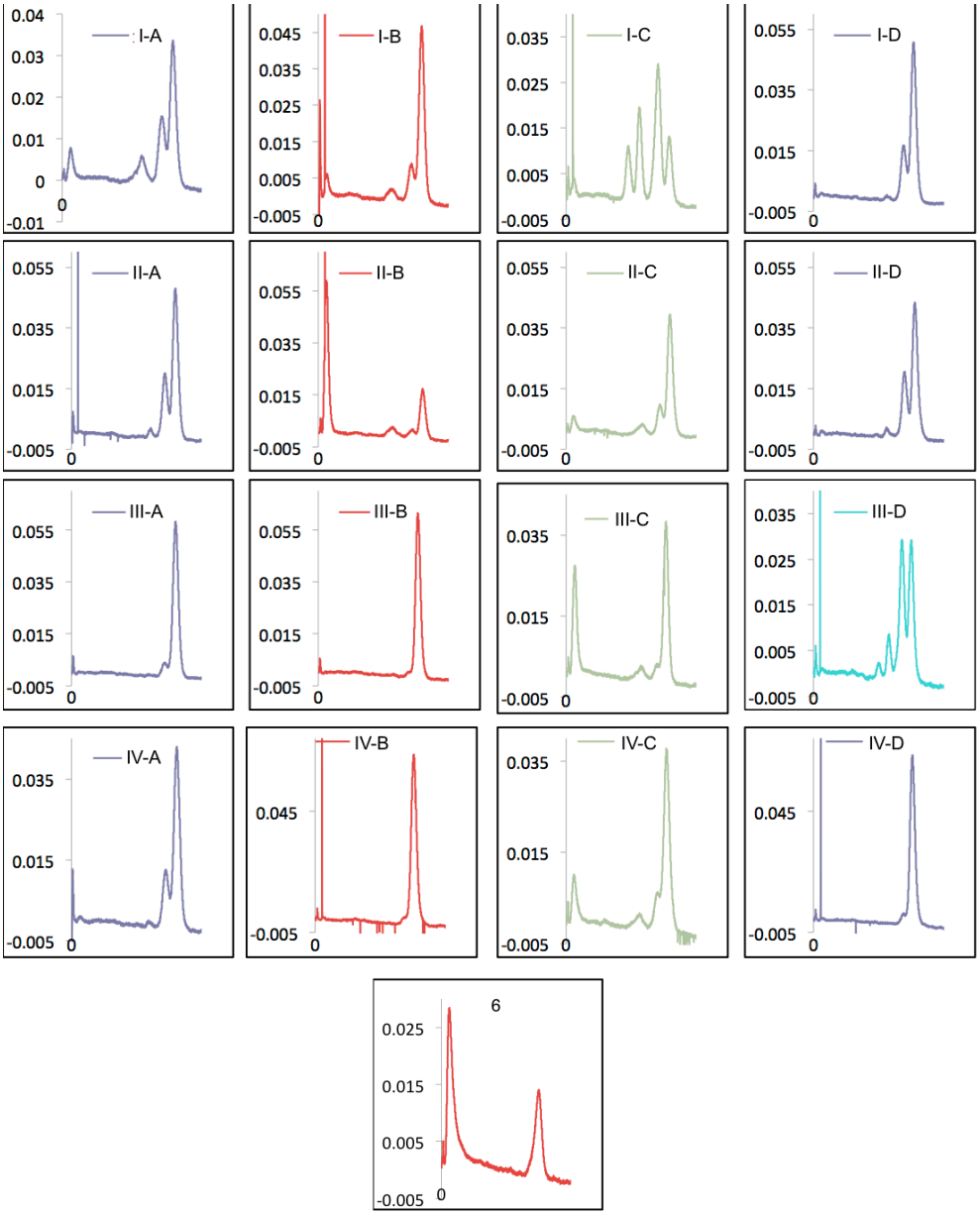

Figure 4.5. FPLC chromatograms of GNeo-biotin-ST conjugates. Conjugates were loaded onto a heparin-sepharose column and a gradient of 0.14 – 2 M NaCl in PBS. Absorbance was measured at 280 nm.

Cell culture

Wild-type Chinese hamster ovary cells (CHO-K1) were obtained from the American Type Culture Collection (CCL-61) were grown under an atmosphere of 5% CO_2 in air and 100% relative humidity. CHO-K1 were grown in F-12 medium

supplemented with fetal bovine serum (10% v/v) and penicillin/streptomycin solution (1% v/v).

Quantifying cellular uptake/binding

The GNeo derivatives (2.5 μM in DMEM) were incubated with ST-Cy5 (0.5 μM in DMEM) for 20 min at ambient temperature then diluted with DMEM cell culture medium to give final conjugate solutions (final ST-Cy5 concentration of 2 nM).

Cells were plated onto 24-well plates (100 000 cells/well) and grown for 24 h to about 80% confluence. Cells were washed with PBS and incubated with 300 μL of the corresponding conjugate for 1 h at 37 °C under an atmosphere of 5% CO2. Cells were washed twice with PBS, detached with 50 μL of trypsin-EDTA, diluted with PBS containing 0.1% BSA, and analyzed by FACS. Cellular uptake was quantified by the mean fluorescence intensity; raw data was interpreted by using FlowJo v8.8.6.

Acknowledgements

Chapter 4 is in full currently being prepared for publication: Hamill, K.M.; Wexselblatt, E.; Hadidi, K.; Esko, J. E.; Tor, Y. The dissertation author is the co-main author and researcher of this work.

4.5 References

(1) Stanzl, E. G.; Trantow, B. M.; Vargas, J. R.; Wender, P. A. *Acc. Chem. Res.* **2013**, *46*, 2944.

(2) Wexselblatt, E.; Esko, J. D.; Tor, Y. *J. Org. Chem.* **2014**, *79*, 6766.

(3) Wender, P. A.; Mitchell, D. J.; Pattabiraman, K.; Pelkey, E. T.; Steinman, L.; Rothbard, J. B. *Proc. Natl. Acad. Sci. U.S.A.* **2000**, *97*, 13003.

(4) Chung, H. H.; Harms, G.; Seong, C. M.; Choi, B. H.; Min, C.; Taulane, J. P.; Goodman, M. *Biopolymers* **2004**, *76*, 83.

(5) Luedtke, N. W.; Carmichael, P.; Tor, Y. *J. Am. Chem. Soc.* **2003**, *125*, 12374.

(6) Wender, P. A.; Galliher, W. C.; Goun, E. A.; Jones, L. R.; Pillow, T. H. *Adv. Drug Delivery Rev.* **2008**, *60*, 452.

(7) Fromm, J. R.; Hileman, R. E.; Caldwell, E. E.; Weiler, J. M.; Linhardt, R. J. *Arch. Biochem. Biophys.* **1995**, *323*, 279.

(8) Rothbard, J. B.; Jessop, T. C.; Lewis, R. S.; Murray, B. A.; Wender, P. A. *J. Am. Chem. Soc.* **2004**, *126*, 9506.

(9) Walrant, A.; Bechara, C.; Alves, I. D.; Sagan, S. *Nanomedicine* **2011**, *7*, 133.

(10) Schmidt, N.; Mishra, A.; Lai, G. H.; Wong, G. C. L. *FEBS Lett.* **2010**, *584*, 1806.

(11) El-Andaloussi, S.; Järver, P.; Johansson, Henrik J.; Langel, Ü. *Biochem. J.* **2007**, *407*, 285.

(12) Jiao, C.-Y.; Delaroche, D.; Burlina, F.; Alves, I. D.; Chassaing, G.; Sagan, S. *J. Biol. Chem.* **2009**, *284*, 33957.

(13) Khalil, I. A.; Kogure, K.; Futaki, S.; Harashima, H. *J. Biol. Chem.* **2006**, *281*, 3544.

(14) Maiti, K. K.; Jeon, O.-Y.; Lee, W. S.; Kim, D.-C.; Kim, K.-T.; Takeuchi, T.; Futaki, S.; Chung, S.-K. *Angew. Chem. Int. Ed.* **2006**, *45*, 2907.

(15) Biswas, G.; Jeon, O.-Y.; Lee, W. S.; Kim, D.-C.; Kim, K.-T.; Lee, S.; Chang, S.; Chung, S.-K. *Chem. – Eur. J.* **2008**, *14*, 9161.

(16) Lee, W. S.; Im, C. N.; Teng, Q. Y.; Chang, Y. T.; Kim, D. C.; Kim, K. T.; Chung, S. K. *Mol Biosyst* **2009**, *5*, 822.

(17) Wender, P. A.; Kreider, E.; Pelkey, E. T.; Rothbard, J.; VanDeusen, C. L. *Org. Lett.* **2005**, *7*, 4815.

(18) Elson-Schwab, L.; Garner, O. B.; Schuksz, M.; Crawford, B. E.; Esko, J. D.; Tor, Y. *J. Biol. Chem.* **2007**, *282*, 13585.

(19) Dix, A. V.; Fischer, L.; Sarrazin, S.; Redgate, C. P. H.; Esko, J. D.; Tor, Y. *Chembiochem* **2010**, *11*, 2302.

(20) Inoue, M.; Tong, W.; Esko, J. D.; Tor, Y. *ACS Chem. Biol.* **2013**, *8*, 1383.

(21) Inoue, M.; Wexselblatt, E.; Esko, J. D.; Tor, Y. *ChemBioChem* **2014**, *15*, 676.

(22) Sarrazin, S.; Wilson, B.; Sly, W. S.; Tor, Y.; Esko, J. D. *Mol Ther* **2010**, *18*, 1268.

(23) Wexselblatt, E.; Esko, J. D.; Tor, Y. *ACS Nano* **2015**, *9*, 3961.

(24) Thomas, J. R.; Liu, X.; Hergenrother, P. J. *J. Am. Chem. Soc.* **2005**, *127*, 12434.

(25) Lüning, U.; Baumstark, R.; Peters, K.; von Schnering, H. G. *Liebigs Ann. Chem.* **1990**, *1990*, 129.

(26) Wieland, M.; Mieusset, J.-L.; Brinker, U. H. *Tetrahedron Lett.* **2012**, *53*, 4351.

(27) Chouhan, G.; James, K. *Org. Lett.* **2011**, *13*, 2754.

(28) Morimoto, N.; Hirano, S.; Takahashi, H.; Loethen, S.; Thompson, D. H.; Akiyoshi, K. *Biomacromolecules* **2013**, *14*, 56.

(29) Lumbroso, A.; Abermil, N.; Breit, B. *Chem. Sci.* **2012**, *3*, 789.

(30) Holaday, J. W.; Magistro, P.; QRxPharma Ltd., Australia . 2012, p 75.

Chapter 5:

Synthesis of Cell-Penetrating Guanidinylated Neomycin Oligomers via ROMP

5.1 Introduction

High molecular weight and highly-charged biomolecules are emerging as a new class of drugs with high selectivity and efficacy; however, new delivery strategies are needed to improve their efficiency and targeted delivery in biological systems. [1-3] One method to address this problem is the conjugation or association of the biologic with a molecular transporter.[4,5] Inspired by proteins, such as HIV-Tat, with cellular translocation abilities,[6-8] numerous guanidinium-rich molecular transporters have been synthesized from a diverse range of nonpeptidic scaffolds such as peptoids,[8] carbamates,[9] carbohydrates,[10,11] and dendrimers.[12-14]

The discovery that a diverse range of scaffolds can be decorated with guanidinium groups to enhance cellular uptake, led to the development of new synthetic methods to construct novel guanidinium-rich transporters more efficiently and with unique backbone structures.[15,16] In particular, an oligomerization-based strategy has been utilized to reduce the number of synthetic steps and provide easy access to transporters of varying lengths and compositions.

Living polymerization reactions provide access to polymers with well-defined architectures and low polydispersities.[17] Additionally, these methods allow the incorporation of different monomers to generate well-defined block copolymers[18] and the molecular weight or degree of polymerization can easily be controlled by adjusting the

ratio of initiator to monomer.[19] This approach also allows for control over end groups and a variety of functionalities can be incorporated at the polymer termini. In 2008, the Kiessling group applied this strategy to synthesize cell-penetrating polymers by ring-opening metathesis polymerization (ROMP) of a reactive norbornene monomer.[16,20] The polymer was post-modified with guanidinium moieties to enable cellular uptake. Similarly, the Tew lab synthesized guanidinium-rich poly(oxanorbornene)s using ROMP and a monomer unit containing a protected guanidinium group.[21-24] Methacrylate,[25,26] cyclic carbonates,[27,28] disulfides,[21,29] and phospholanes[30] have also been used as monomers to synthesize guanidinium-rich oligomers for cellular transport. These cell-penetrating oligomers have been shown to efficiently deliver covalently attached small molecules and drugs,[16,27,30] as well as non-covalently associated cargo such as siRNA.[28,31,32]

Guanidinoglycosides are a non-oligomeric, multivalent family of low molecular weight carriers derived from aminoglycoside antibiotics in which the ammonium groups are converted to guanidinium groups.[10,33] Unlike other cell-penetrating peptides and guanidinium-rich carriers which may use multiple mechanisms for internalization, the uptake of guanidinoglycosides at low nanomolar concentrations depends exclusively on cell surface heparan sulfate proteoglycans.[33-36] Additional investigation into the uptake of guanidinylated neomycin (GNeo) using a cell-surface FRET analysis indicated clustering of heparan sulfate proteoglycans on the cell surface is a key step for the endocytosis of these carriers.[35] This is consistent with the cooperative cell surface binding observed for dimeric guanidinoglycosides compared to their monomeric counterparts in cells expressing undersulfated heparan sulfate.[34] We hypothesized that expanding the valency of GNeo

could enhance its binding to the cell surface through multivalent interactions with heparan sulfate. The higher valency could promote interactions between multiple heparan sulfate chains attached to the same or different core proteins leading to enhanced heparan sulfate proteoglycan (HSPG) aggregation. Access to multivalent GNeo derivatives could result in an improved delivery system or as a tool to further study GNeo and HSPG interactions.

Here we report the synthesis of a guanidinoneomcyin(GNeo)-norbornene monomer that can undergo ring-opening metathesis polymerization in the presence of a ruthenium catalyst to yield oligomeric GNeo transporters. This method provides a single-step route to oligomers of various lengths by simply adjusting the monomer to initiator ratio, thus allowing us to further probe the role of valency in the uptake of GNeo, investigate multivalent interactions with heparan sulfate, and potentially determine an optimum transporter length. Additionally, the oligomers can be terminated with a variety of functional groups, such as a biotin or a fluorophore. Preliminary results from cellular uptake in wild-type and heparan sulfate-deficient Chinese hamster ovary (CHO) cells are also presented.

5.2 Results and Discussion

To access multivalent GNeo-oligomers, we decided to use norbornene as the polymerizable group that could undergo ring-opening metathesis polymerization (ROMP) using a ruthenium-based initiator. Ruthenium-catalyzed ROMP has high functional group tolerance and generally produces polymers with low polydispersity.[37] A monomer consisting of a norbornene linker attached to GNeo that could undergo ROMP was designed using a synthetic approach that included “clicking” GNeo containing an azide-terminated linker to an alkyne-functionalized norbornene. The norbornene was

functionalized with the alkyne after previous reports showed azides react with the highly strained norbornene double bond and lead to inactive monomers.[38] The details of the monomer synthesis are outlined in the Experimental Section and Scheme 1. Briefly, the primary 5" alcohol on Boc-protected neomycin was converted to an amine (**5.2**) and coupled to a bifunctional triethylene glycol containing a carboxylic acid and an azide (**5.3**). Deprotection of **5.4** and subsequent Boc-guanidinylation yielded azide-BocGNeo (**5.5**). A copper-catalyzed 1,3-dipolar cycloaddition of **5.5** with a norbornene-alkyne derivatve (**5.6**) provided compound **5.7**, the BocGNeo-norbornene monomer.

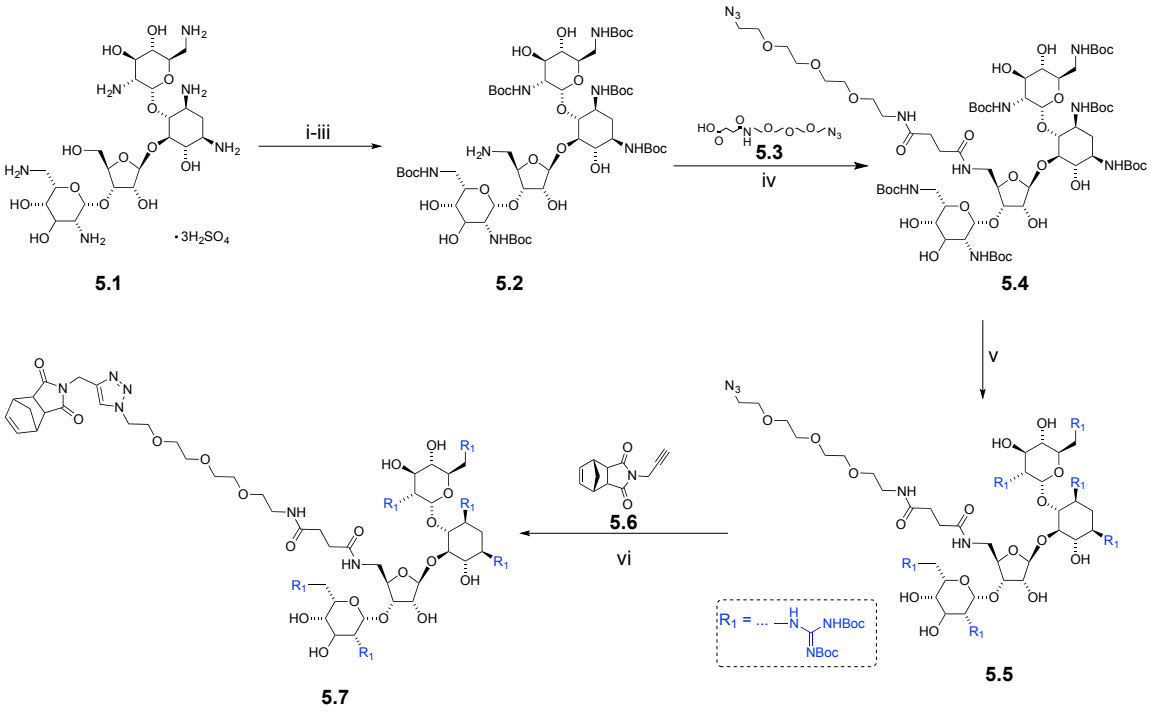

Scheme 5.1. Synthesis of norbornene-BocGNeo monomer. Reagents and conditions: (i) Boc_2O, Et_3N, H_2O/DMF; (ii) TIBSCl, pyridine; (iii) NH_3, CH_3OH, 80 °C; (iv) EDC, Et_3N, CH_2Cl_2; (v) 1. TFA, triisopropylsilane, CH_2Cl_2; 2. *N,N'*-Di-Boc-1*H*-pyrazole-1-carboxamidine, NEt_3, CH_2Cl_2/CH_3OH; (vi) $Cu(II)SO_4{\cdot}4H_2O$; sodium ascorbate, DMF/H_2O.

To investigate their cellular uptake properties, the oligomeric GNeo derivatives need to be functionalized with a fluorophore or reactive group. One strategy for

incorporating functional groups or probes at the terminus of a ROMP polymer is to synthesize custom initiators; however, this method requires a new catalyst be made for each new chain-end functionality, which can be challenging and low yielding.[39,40] Another, more common method when ruthenium carbenes are used as initiators, is the use of functionalized vinyl ethers or *cis*-olefins.[41,42] These compounds can be added at the end of a growing polymer chain to simultaneously introduce a new functionality to the terminus and deactivate the metathesis catalyst. We chose to functionalize oligo-GNeo using *cis*-olefins and a direct end capping method described by the Grubbs group.[43] To obtain a variety of functionalized terminating agents, *cis*-1,4-dichloro-2-butene (Scheme 5.2) or *cis*-2-butene-1,4-diol (Scheme 5.3) could be readily modified to contain biotin, different fluorophores, or various reactive functional groups. The previously reported symmetrical diamine **5.11** could be coupled to biotin, fluorescein isothiocyanate (FITC), or BODIPY to yield **5.12**, **5.13**, and **5.15** respectively (Scheme 5.2).[43] The dibromo terminating agent **5.16** could be substituted with NaN_3 to yield **5.17** or *N*-Boc-hydroxylamine to provide **5.19** (Scheme 5.3). Additionally, **5.16** can be clicked to an alkyne-Cy3 to afford **5.20** or potentially other alkyne-functionalized probes.

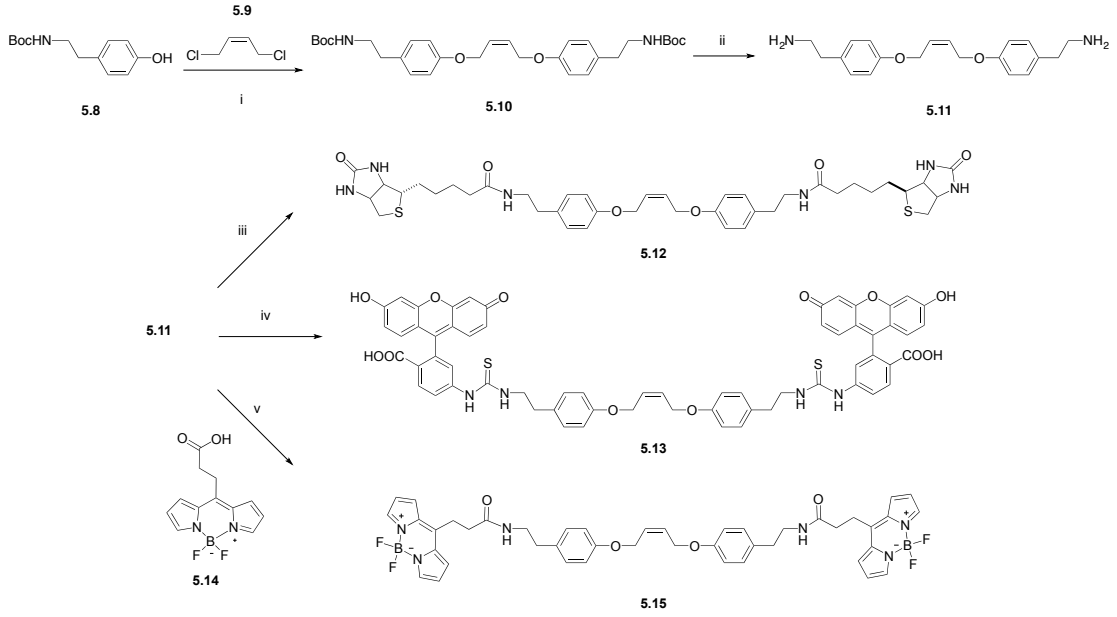

Scheme 5.2. Synthesis of biotin, FITC, and BODIPY-containing terminating agents. Reagents and conditions: (i) K_2CO_3, DMF, 90 °C; (ii) TFA, CH_2Cl_2; (iii) biotin, EDC, HOBt DMF; (iv) FITC, DMF; (v) BODIPY-acid, EDC, HOBt, DMF.

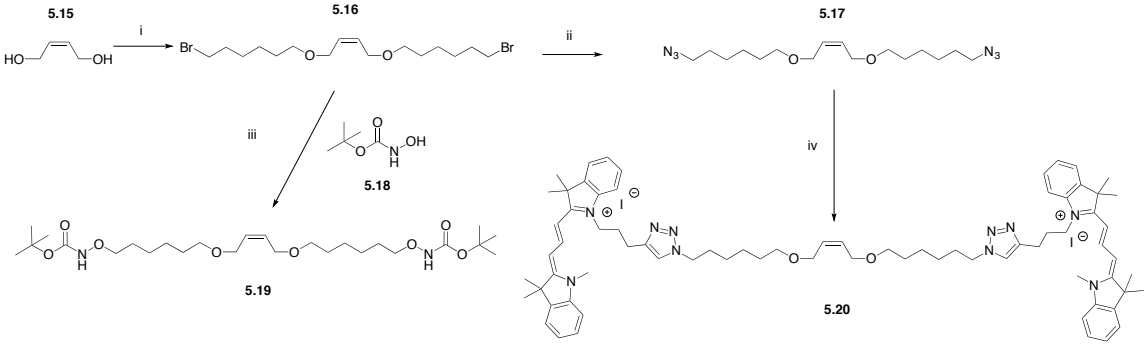

Scheme 5.3. Synthesis of azide, boc-hydroxylamine, and Cy3-containing terminating agents. Reagents and conditions: (i) 1,6-dibromohexane, NaH, DMF; (ii) NaN_3, DMF; (iv) DBU, DMF; (iv) alkyne-Cy3, $Cu(II)SO_4 \cdot 4H_2O$; sodium ascorbate, DMF/H_2O.

Oligomerization of the GNeo-monomer **5.7** was initiated with a 3rd generation Grubbs' ruthenium catalyst (Scheme 5.4).[37] The degree of polymerization was controlled by the ratio of the ruthenium initiator to monomer (5:1 or 10:1). After 24 hours, the monomer is completely consumed (monitored by TLC), at which point one of the functionalized terminating agents is added to afford the protected oligo-BocGNeo. The

Boc groups were then removed with TFA to give oligo-GNeo. ^{1}H NMR was used to confirm reaction completion and also to determine the degree of oligomerization by comparing the integrated signal of the distinct end-group protons (δ 7.15 ppm) to the integrated signals of monomer protons (δ 7.88 and 5.63) (Figure 1 and Table 1). The average molecular weights corresponded well with the predicted oligomer lengths (Table 1). Terminating agents **5.15** and **5.20** were not stable to TFA deprotection; therefore, only biotin and fluorescein terminated oligomers were evaluated for cellular uptake.

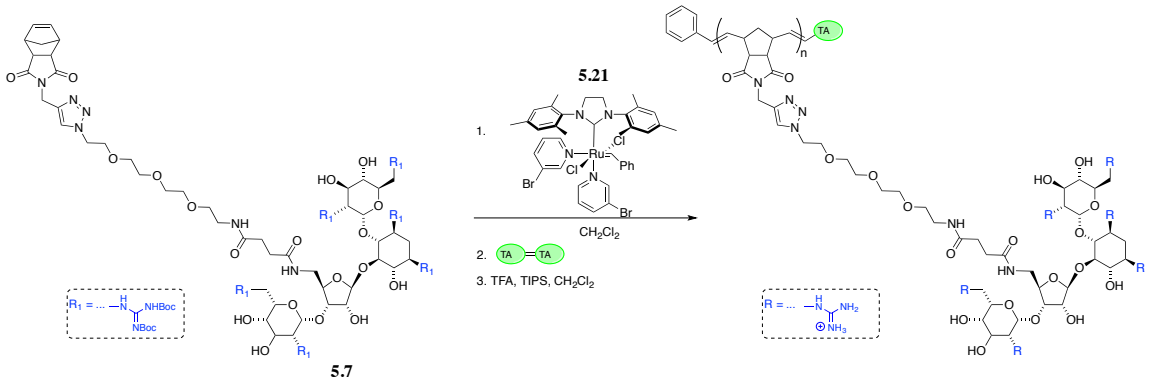

Scheme 5.4. General synthesis of GNeo-oligomers. TA represents one of the symmetrical functionalized terminating agents described previously.

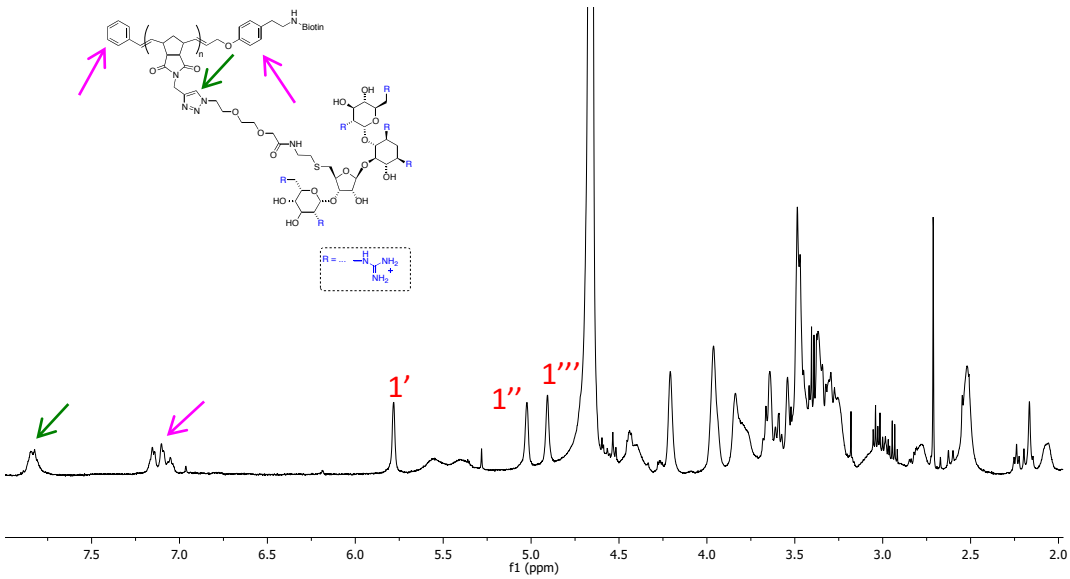

Figure 5.1. ^{1}H NMR (500 MHz) of biotin-oligoGNeo in D_2O. Arrows point to protons used to determine average length and molecular weight of oligomers.

Table 5.1. ^{1}H NMR characteristics of GNeo-oligomers. Synthesized GNeo oligomers with biotin or fluorescein terminating agents.

	Monomer:catalyst (molar ratio)	Terminating Agent Used	End group (aromatic) integration	Triazole C-*H* integration	1' C-*H* integration	Degree of Oligomer-ization
5.22	5:1	biotin	9	4	4	4
5.23	10:1	biotin	9	8	8	8
5.24	5:1	fluorescein	5	4	4	4

The cellular uptake of oligo-GNeo **5.22** terminated with biotin was evaluated in both wild-type and glycosaminoglycan deficient CHO cells (pgsA) and compared to GNeo-biotin **5.25** (Figures 5.2, 5.3). The tetravalent biotin-streptavidin conjugates were formed by incubating the biotin-compound with PE-Cy5-streptavidin in a 1:5 molar ratio for 20 min at room temperature. The conjugates were then diluted with cell-culture medium to the indicated final concentrations and incubated with cells for 1 h at 37 °C, washed,

harvested with trypsin/EDTA, and analyzed by flow cytometry. As shown in Figure 5.3a, oligomerization of GNeo did not enhance cellular uptake in wild-type CHO cells when compared to a previously described GNeo-biotin monomer (Figure 5.2). Oligo-GNeo did, however, retain heparan sulfate-dependent uptake (Figure 5.3b). To examine cell surface binding only, cells were incubated with the fluorescent conjugate at 4 °C, in which no uptake occurs, and lifted with EDTA, which does not cleave cell-surface bound material. In this case, higher binding was observed for GNeo-oligomer-ST complex than for GNeo-monomer-ST complex (Figure 5.3c). Additional experiments need to be performed to determine if the kinetics of uptake for oligoGNeo–conjugates are slower, which could explain the observed higher binding but similar uptake.

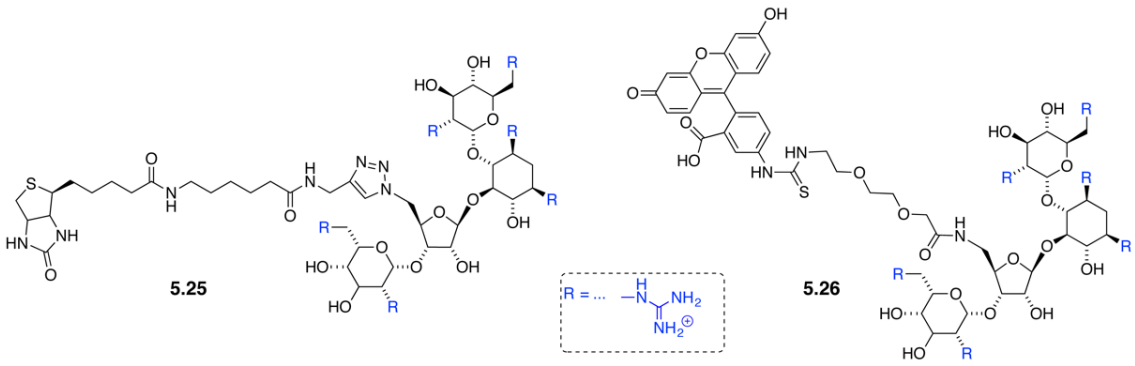

Figure 5.2. Structures of GNeo-monomers. Biotin- and fluorescein-functionalized mono-GNeo structures used for uptake and binding comparison.

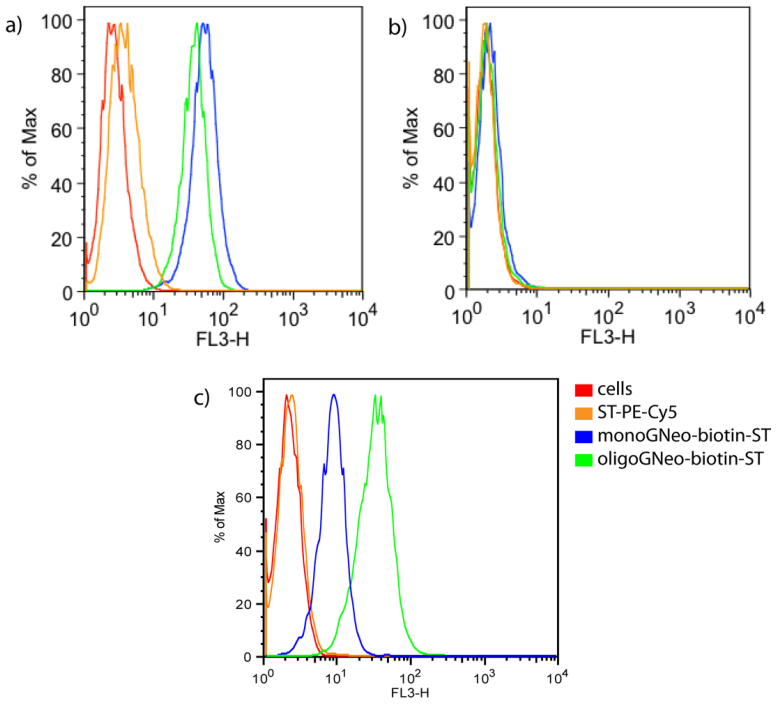

Figure 5.3. Cellular uptake and binding of biotin-GNeo monomer and oligomer. Representative histograms from cellular uptake and binding for biotin-GNeo monomer and oligomer. Background fluorescence of cells only are shown in red. (a) Cellular uptake of biotinylated monoGNeo (blue line) and oligoGNeo (green line) conjugated to ST-PE-Cy5. CHO-K1 cells were incubated with the conjugates (2 nM ST-PE-Cy5 and 10 nM compound) for 1 h at 37 °C. Uptake of ST-PE-Cy5 (2 nM) was used as a control (orange line). (b) Cellular uptake of biotinylated monoGNeo (blue line) and oligoGNeo (green line) conjugated to ST-PE-Cy5. pgsA cells were incubated with the conjugates (2 nM ST-PE-Cy5 and 10 nM compound) for 1 h at 37 °C. (c) Binding of biotinylated monoGNeo (blue line) and oligoGNeo (green line) conjugated to ST-PE-Cy5 to the surface of CHO-K1 cells. Cells were incubated with the conjugates (2 nM ST-PE-Cy5 and 10 nM compound) for 0.5 h at 4 °C. Binding of ST-PE-Cy5 (2 nM) was used as a control (orange line).

The cellular uptake and binding of oligo-GNeo terminated with fluorescein (**5.24**) were also evaluated in both wild-type and glycosaminoglycan deficient CHO-pgsA cells and compared to a GNeo-monomer terminated with fluorescein (**5.26,** Figure 5.2). No difference in uptake between oligo-GNeo and mono-GNeo is observed (Figure 5.4) at the highest concentrations; however, mono-GNeo shows a concentration dependence whereas oligo-GNeo does not. Additionally, uptake in this case was very close to background. This could be attributed to quenching of the acid-sensitive fluorescein probe if the transporter is

delivering to the lysosomes, which has been seen for previous GNeo transporters.[36] Again, the uptake of monomeric- and oligomeric-GNeo appears to be dependent on the presence of cell-surface glycosaminoglycans (Figure 5.4c,d). When the compounds were analyzed for binding, higher binding was observed for oligoGNeo-FITC than monoGNeo-FITC in wild-type CHO cells (Figure 5.5). Moreover, a higher fluorescence signal was observed for binding than for uptake. This further suggests that upon internalization, the transporter resides in an acidic environment causing the fluorophore to be quenched.

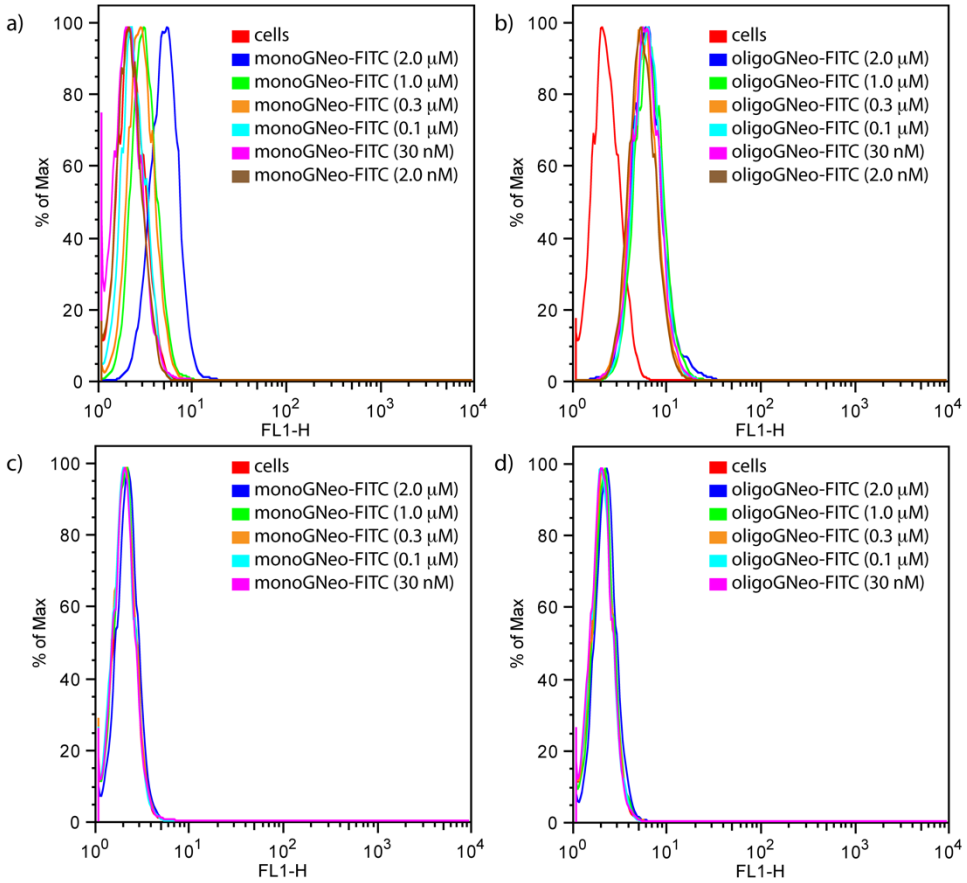

Figure 5.4. Cellular uptake of fluorescein-GNeo monomer and oligomer. Representative histograms from cellular uptake of mono- and oligo-FITC-GNeo in wild-type CHO-K1 cells (a & b) and in pgsA cells (c & d). Cells were incubated with the compound at various concentrations for 1 h at 37 °C. Cells only are represented by the red line.

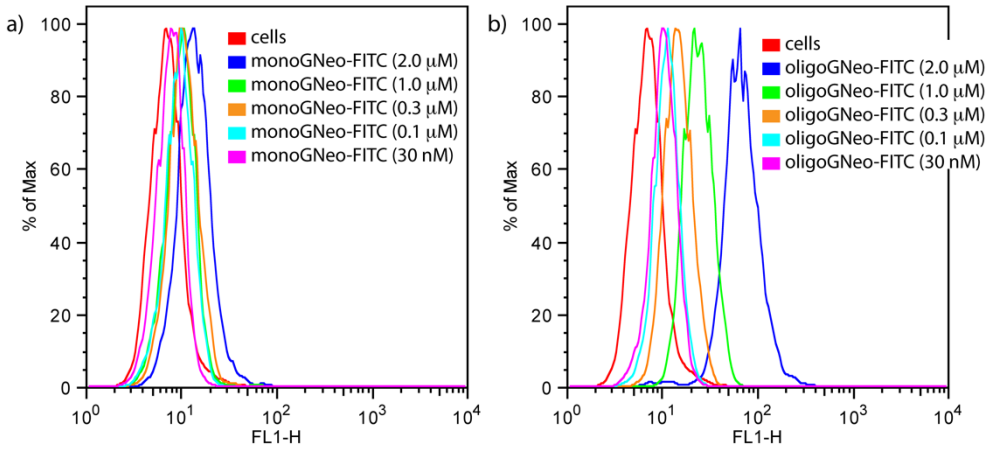

Figure 5.5. Cellular binding of fluorescein-GNeo monomer and oligomer. Representative histograms from cellular binding of mono-FITC-GNeo (a) and oligo-FITC-GNeo (b) in wild-type CHO-K1 cells. Cells were incubated with the compound at various concentrations for 1 h at 37 °C. Cells only are represented by the red line.

5.3 Conclusions and Outlook

In summary, a GNeo-substituted norbornene oligomer has been synthesized using ROMP. This strategy allows for the direct end-capping of the oligomer with various functional groups or probes and access to GNeo oligomers of varying lengths. Preliminary cellular uptake experiments suggest oligo-GNeo has enhanced binding to the cell surface.

Moving forward, the oligomer products need to be further characterized by gel permeation chromatography (GPC) to determine polydispersity, which cannot be obtained from the NMR, as well as a better idea of the molecular weight. Additionally, the oligomerization needs to be optimized to ensure oligomers of different lengths can be obtained and to determine the maximum length accessible. Ideally, we will be able to separate the different length products using ion exchange or size exclusion chromatography in order to evaluate multivalent effects and examine the differences length has on uptake and heparan sulfate selectivity.

The synthesis of additional terminating agents will also be critical for evaluating the uptake properties of oligomeric GNeo derivatives. One option is to terminate the oligomers with an azide, such as **5.17**, which can be clicked to alkyne-functionalized fluorophores. Post-polymerization of an azide-terminated oligomer, as well as other functional groups, has been demonstrated by the Kiessling group.[44] Furthermore, oligomers terminated with the oxy-amine terminating agent **5.19** could potentially be used to singly modify proteins at the N-terminus without modifying their lysine residues.[45] Previous protein modification with GNeo required accessible lysines that could be modified with an NHS-ester derivative. Therefore, the number of available lysines will affect the conjugation efficiency, which can alter the cellular uptake. Additionally, conjugation to multiple amino acids can interfere with the protein's function. By modifying the N-terminus only, a variety of proteins, such as enzymes or antibodies, can be conjugated without relying on accessible amines or interfering with function. The use of GNeo-oligomers, as oppose to a monomer, will be important to maintain high uptake efficiencies.

In addition to improving the intracellular delivery of proteins, cationic oligomers are known to complex and delver negatively charged cargo, such as siRNA.[28,31,32,46-49] GNeo-oligomers would be less susceptible to proteases than oligo-arginine and other cell-penetrating peptides. Furthermore, the living polymerization synthesis of oligo-GNeo allows for the incorporation of hydrophobic side chains or other chemical compositions that can be easily tuned to improve delivery.

5.4 Experimental Section

Materials

Materials obtained from commercial suppliers were used without further purification. cis-5-Norbornene-exo-2,3-dicarboxylic anhydride was purchased from VWR. *N,N'*-Di-boc-1*H*-pyrazole-1-carboxamidine was purchased from Fisher. All other chemicals and reagents were purchased from Sigma Aldrich. Deuterated NMR solvents were purchased from Cambridge Isotope Laboratories. PBS (Dulbecco's phosphate buffered saline) and F-12 Nutrient Mixture (Ham) were purchased from Gibco Thermo Fisher. Trypsin/EDTA was purchased from VWR. Steptavidin-PE-Cy5 was purchased from Biolegend.

Instrumentation

NMR spectra were recorded on a Varian VX 500 MHz spectrometer or a Varian 400 MHz spectrometer. Mass spectra were recorded at UCSD Chemistry and Biochemistry Mass Spectrometry Facility utilizing an Agilent 6230 Accurate-Mass TOFMS or a Bruker Biflex IV MALDI-TOFMS. Reverse-phase HPLC purification (CLIPEUS, C18, 5μm, 10x250 mm, Higgins analytical) and analysis (Eclipse, XDB-C18, 5μm, 4.6x150 mm) were carried out on an Agilent 1200 series instrument or Beckman Coulter System Gold 127P Solvent Module. Flow cytometry studies were performed on a BD FACSCalibur.

Synthesis

Synthesis of compounds **5.2**, **5.3**, and **5.6** have been previously reported.[10,34]

N_3-BocNeo (5.4). 5.2 (200 mg, 0.165 mmol) was dissolved in CH_2Cl_2 (1 mL) and Et_3N (28 μL, 0.198 mmol) and added to a solution of **5.3** (63mg, 0.198 mmol) and *N*-(3-

dimethylaminopropyl)-*N*'-ethylcarbodiimide HCl (EDC, 38mg, 0.198 mmol) in CH_2Cl_2 (1 mL) and the reaction was stirred at room temperature for 24 h. The reaction was diluted with CH_2Cl_2 and washed with saturated $NaHCO_3$, water, and brine. The organic layer was dried over Na_2SO_4, filtered, and evaporated under reduced pressure. The product was isolated by automated flash chromatography (0–10% MeOH in CH_2Cl_2) to afford a white solid (167 mg, 0.11 mmol, 57% yield). ^{1}H NMR (500 MHz, CD_3OD) δ 5.40 (s, 1H), 5.10 (s, 1H), 4.89 (s, 1H), 4.82 (s, 1H), 4.28 (m, 1H), 4.06 (m, 1H), 3.91 (m, 4H), 3.75 (m, 2H), 3.69–3.66 (m, 8H), 3.64–3.62 (m, 3H), 3.58 (m, 2H), 3.55 (m, 3H), 3.51 (s, 1H), 3.49 (s, 1H), 3.47 (m, 2H), 3.40–3.36 (m, 6H), 3.29 (m, 1H), 3.22 (m, 1H), 2.60 (t, J = 6.6 Hz, 2H), 2.54 (t, J = 6.7 Hz, 2H), 1.96 (m, 1H), 1.47–1.43 (m, 56H). ^{13}C NMR (126 MHz, CD_3OD) δ 173.43, 173.28, 157.60, 157.48, 157.12, 157.02, 156.79, 156.44, 110.47, 99.25, 97.76, 86.62, 79.82, 79.28, 79.05, 78.90, 78.81, 74.59, 74.11, 73.08, 71.96, 71.40, 71.33, 70.25, 70.22, 70.12, 69.89, 69.73, 69.17, 67.66, 55.53, 52.17, 51.06, 50.37, 50.08, 42.12, 41.27, 40.60, 39.06, 34.39, 31.21, 31.06, 27.60, 27.49, 27.46, 27.44, 27.40, 27.35. HR-ESI-MS calculated for $C_{65}H_{115}N_{11}O_{29}$ $[M+Na]^+$ 1536.7754, found 1536.7757.

N_3-BocGNeo (5.5). To a solution of **5.4** (167 mg, 0.11 mmol) in CH_2Cl_2 (1 mL), triisopropylsilane (10 μL) and trifluoroacetic acid (1 mL) were added. The reaction was stirred for 2 h at room temperature then diluted in toluene and evaporated under reduced pressure. The residue was dissolved in methanol (250 μL) and triethylamine. *N*,*N*′-Di-Boc-1*H*-pyrazole-1-carboxamidine (410 mg, 1.32 mmol) was added as a solution in CH_2Cl_2 and the reaction was stirred for 3 days at room temperature. The reaction was diluted with CH_2Cl_2 and washed with saturated $NaHCO_3$. The organic layer was dried over Na_2SO_4,

filtered, and evaporated under reduced pressure. The product was isolated by automated flash chromatography (0–5% MeOH in CH_2Cl_2) to afford a while solid (161 mg, 0.068 mmol, 62% yield). ^{1}H NMR (500 MHz, CD_3OD) δ 5.91 (d, *J* = 3.93 Hz, 1H), 5.05 (d, *J* = 2.01 Hz, 1H), 5.01 (d, *J* = 1.91 Hz, 1H), 4.59 (m, 1H), 4.38 (m, 1H), 4.26 (m, 3H), 4.15 (m, 1H), 3.98 (m, 2H), 3.91–3.84 (m, 3H), 3.77–3.62 (m, 15H), 3.56–3.45 (m, 7H), 3.38 (m, 6H), 3.26 (m, 2H), 2.58–2.50 (m, 4H), 2.26 (m, 1H), 1.58–1.44 (m, 108H). ^{13}C NMR (126 MHz, CD_3OD) δ 173.38, 173.29, 173.04, 163.23, 163.19, 162.95, 162.91, 162.86, 162.73, 157.37, 156.61, 156.41, 156.39, 156.07, 153.28, 153.02, 152.75, 152.59, 151.91, 111.84, 104.16, 98.20, 95.63, 87.77, 83.39, 83.29, 83.24, 83.22, 83.01, 82.69, 79.15, 79.12, 79.09, 79.07, 78.92, 78.85, 75.64, 75.27, 74.20, 72.81, 72.13, 71.94, 70.50, 70.26, 70.23, 70.13, 69.86, 69.75, 69.67, 69.26, 66.64, 54.10, 51.61, 50.38, 47.99, 42.98, 42.58, 40.22, 39.05, 33.91, 31.20, 27.35, 27.31, 27.27, 27.23, 27.20, 27.17, 27.16, 27.03, 27.00, 26.97, 26.84. HR-ESI-MS calculated for $C_{101}H_{175}N_{23}O_{41}$ $[M+2H]^{2+}$ 1184.1231, found 1184.1216.

Norbornene-BocGNeo (5.7). 5.5 (90 mg, 0.038 mmol) and **5.6** (15.2 mg, 0.076 mmol) were dissolved in DMF (1 mL) and purged with argon. $Cu(II)SO_4 \cdot 5H_2O$ (0.0076 mmol) and sodium ascorbate (0.0076 mmol) were added as solutions in water. The reaction was stirred overnight at room temperature then evaporated under reduced pressure. The resulting residue was diluted in CH_2Cl_2 and washed with aqueous KCN and EDTA. The organic layer was dried over Na_2SO_4, filtered, and evaporated under reduced pressure. The reaction was isolated by automated flash chromatography (0–5% CH_3OH in CH_2Cl_2) to afford the product as a white solid (72mg, 0.028 mmol, 74% yield). ^{1}H NMR (500 MHz, CD_3OD) δ 7.96 (s, 1H), 6.32 (m, 2H), 5.91 (d, *J* = 3.90 Hz, 1H), 5.04 (d, *J* = 2.13 Hz, 1H),

5.02 (d, J = 1.92 Hz, 1H), 4.83 (s, 2H), 4.55 (m, 3H), 4.37 (m, 1H), 4.26–4.20 (m, 3H), 3.98 (m, 2H), 3.90–3.85 (m, 6H), 3.72 (m, 4H), 3.59 (m, 9H), 3.52–3.48 (m, 7H), 3.35 (m, 4H), 3.18 (m, 2H), 2.75 (s, 2H), 2.54–2.47 (m, 4H), 2.26 (m, 1H), 1.60–1.45 (m, 110 H). ^{13}C NMR NMR (126 MHz, CD_3OD) δ 177.71, 173.36, 173.28, 173.03, 163.23, 163.19, 162.95, 162.91, 162.86, 162.72, 157.36, 156.60, 156.40, 156.37, 156.06, 153.28, 153.01, 152.76, 152.74, 152.57, 151.90, 141.89, 137.62, 124.26, 111.85, 98.24, 95.62, 87.82, 83.39, 83.29, 83.25, 83.22, 83.01, 82.69, 79.15, 79.13, 79.09, 79.06, 78.93, 78.84, 75.64, 75.26, 74.22, 72.80, 72.14, 71.94, 70.50, 70.15, 70.09, 70.04, 69.85, 69.66, 69.24, 68.94, 66.62, 54.11, 51.61, 50.36, 50.05, 48.73, 45.08, 42.19, 39.04, 32.94, 31.22, 27.35, 27.31, 27.27, 27.24, 27.20, 27.18, 27.17, 27.03, 27.01, 26.97, 26.84. HR-ESI-MS calculated for $C_{113}H_{186}N_{24}O_{43}$ $[M+2H]^{2+}$ 1284.6626, found 1284.6627.

Synthesis of compounds **5.8 – 5.14** have been previously reported.[43,50]

BODIPY-containing Terminating Agent (5.14). BODIPY-acid (24 mg, 0.09 mmol), EDC (14 mg, 0.09 mmol), and HOBt (1 mg, 0.009 mmol) were dissolved in DMF (1 mL). **5.11** (12 mg, 0.037 mmol) was added as a solution in DMF (1 mL) and the reaction was stirred at room temperature under argon overnight. The reaction was concentrated under reduced pressure. The resulting residue was dissolved in CH_2Cl_2 and washed with H_2O and brine. The organic phase was dried over Na_2SO_4, filtered, and evaporated under reduced pressure. The product was isolated by automated column chromatography (0–3% CH_3OH in CH_2Cl_2; 14 mg, 0.017 mmol, 46%). LR-ESI-MS calculated for $C_{44}H_{44}B_2F_4N_6O_4$ $[M+Na]^+$ 841.35, found 841.32. ^{1}H NMR (500 MHz, CD_3OD) δ 7.82 (s, 2H), 7.48 (d, J = 4.25 Hz, 2H), 6.96 (d, J = 8.61 Hz, 2H), 6.81 (d, J = 8.62 Hz, 2H), 6.56 (dd, J = 1.61 Hz,

4.24 Hz, 2H), 5.82 (t, *J* = 3.43 Hz, 1H), 4.62 (d, *J* = 4.01 Hz, 2H), 3.25 (m, 4H), 2.55 (m, 4H).

Br-Terminating Agent (5.16). NaH (0.545 g, 22.7 mmol, 60% in mineral oil) was added to cis-2-butene-1,4-diol (0.5 g, 5.6 mmol) dissolved in DMF (12 mL). After 10 minutes, 1,6-dibromohexane was added (5.53 g, 22.7 mmol) and the reaction stirred for 1.5h at room temperature. The reaction was quenched with 15 mL H_2O and diluted with 75 mL hexane. The organic layer was washed with brine, dried over Na_2SO_4, filtered, and evaporated under reduced pressure. The product was isolated by automated flash column chromatography (0–30% EtOAc in hexanes; 743 mg, 1.79 mmol, 32%). LR-ESI-MS calculated for $C_{16}H_{30}Br_2O_2$ $[M+Na]^+$ 435.06, found 435.13. ^{1}H NMR (300 MHz, $CDCl_3$) δ 5.70 (m, 1H), 4.02 (d, *J* = 3.70, 2H), 3.40 (m, 4H), 1.86 (m, 2H), 1.58 (m, 2H), 1.41 (m, 4H).

N_3-Terminating Agent (5.17). NaN_3 (94 mg, 1.45 mmol) was added to **5.16** (200 mg, 0.48 mmol) dissolved in DMF (2 mL). The reaction was stirred overnight at 40 °C. The reaction was concentrated under reduced pressure then diluted in hexanes and washed with H_2O and brine. The organic layer was dried over Na_2SO_4, filtered, and evaporated under reduced pressure to afford the product with no further purification (160 mg, 0.47 mmol, 98%). LR-ESI-MS calculated for $C_{16}H_{30}N_6O_2$ $[M+H]^+$ 339.25, found 339.40. ^{1}H NMR (300 MHz, $CDCl_3$) δ 5.73 (t, *J* = 3.90 Hz, 1H), 4.05 (d, *J* = 4.61 Hz, 2H), 3.44 (t, *J* = 6.48 Hz, 2H), 3.29 (t, *J* = 6.90 Hz, 2H), 1.63 (m, 4H), 1.41 (m, 4H). ^{13}C NMR (126 MHz, CD_3OD) δ 129.42, 70.30, 66.51, 51.39, 29.62, 28.79, 26.57, 25.80.

Boc-hydroxylamine Terminating Agent (5.19). *N*-Boc-hydroxylamine (257 mg, 1.93 mmol) was dissolved in DMF (2 mL). DBU (294 mg, 1.93 mmol) was added followed by **5.16** (200 mg, 0.483) as a solution in DMF (2 mL). The reaction was stirred overnight at room temperature and then concentrated under reduced pressure. The resulting residue was diluted in CH_2Cl_2 and washed with 1M HCl and brine. The organic layer was dried over Na_2SO_4, filtered, and evaporated under reduced pressure. The product was isolated by automated column chromatography (0–100% EtOAc in hexanes; 105 mg, 0.20 mmol, 42%). LR-ESI-MS calculate for $C_{26}H_{50}N_2O_8$ $[M+Na]^+$ 541.36, found 541.27. ^{1}H NMR (500 MHz, $CDCl_3$) δ 5.70 (t, J = 3.90 Hz, 1H), 4.02 (d, J = 4.61 Hz, 2H), 3.84 (m, 2H), 3.40 (m, 2H), 1.56 (m, 4H), 1.47 (m, 9H), 1.37 (m, 4H).

Cy3-Terminating Agent (5.20). 5.17 (20 mg, 0.06 mmol) and Cy3-alkyne (64 mg. 0.12 mmol) were dissolved in DMF (1.5 mL) and purged with argon. $Cu(II)SO_4 \cdot 5H_2O$ (0.012 mmol) and sodium ascorbate (0.012 mmol) were added as solutions in water. The reaction was stirred overnight at room temperature then evaporated under reduced pressure. The resulting residue was diluted in CH_2Cl_2 and washed with aqueous KCN and EDTA. The organic layer was dried over Na_2SO_4, filtered, and evaporated under reduced pressure. The reaction was isolated by automated flash chromatography (0–20% CH_3OH in CH_2Cl_2; 20 mg, 0.014 mmol, 24%). HR-ESI-MS calculated for $C_{74}H_{96}N_{10}O_2$ $[M+2H]^{2+}$ 578.3853, found 578.3855. ^{1}H NMR (500 MHz, CD_3OD) δ 8.54 (t, J = 13.45 Hz, 1H), 7.99 (s, 1H), 7.86 (s, 1H), 7.54 (t, J = 6.41 Hz, 2H), 4.44 (m, 3H), 7.38 (m, 1H), 7.32 (m, 2H), 6.49 (m, 2H), 5.61 (m, 1H), 4.39 (t, J = 7.01 Hz, 2H), 4.23 (t, J = 7.46 Hz, 2H), 3.99 (d, J =4.09 Hz, 2H), 3.72 (s, 3H), 3.00 (s, 3H), 2.93 (t, J = 7.38 Hz, 2H), 2.87 (s, 2H), 2.25 (m, 2H), 1.90

(m, 2H), 1.77 (m, 12H), 1.53 (m, 3H), 1.41–1.30 (m, 8H). ^{13}C NMR (126 MHz, CD_3OD) δ 175.33, 174.40, 163.43, 150.69, 164.14, 142.63, 141.90, 140.70, 128.94, 128.56, 125.43, 125.27, 122.34, 122.13, 121.99, 110.94, 102.73, 102.42, 69.83, 65.99, 53.39, 49.87, 49.23, 49.16, 48.45, 43.18, 35.57, 30.64, 30.26, 29.84, 29.11, 27.79, 26.97, 26.79, 26.43, 25.88, 25.27, 22.09.

Synthesis of GNeo Oliogmers (general procedure):

A solution of **5.7** (n equiv) in CH_2Cl_2 was added to a dried round bottom flask under argon. The ruthenium catalyst (**5.21**, 1 equiv) in CH_2Cl_2 was added to the monomer solution and the reaction mixture was stirred for 24 hours. The consumption of monomer was monitored on TLC (10% CH_3OH in CH_2Cl_2, stained with ninhydrin). On completion of the reaction, the functionalized terminating agent (2 equiv) was added and stirred for an additional 5 hours before being quenched with excess vinyl ether for 1 h. The solvent was removed under reduced pressure. The protected oligomers were then redissolved in CH_2Cl_2 and treated with triisopropylsilane (10 μL) and trifluoroacetic acid (1 mL). The reaction was stirred for 3 h at room temperature then diluted in toluene and evaporated under reduced pressure. The GNeo-oligomers were purified by reverse-phase HPLC. The product containing fractions were collected, lyophilized, and analyzed by ^{1}H NMR.

Fluorescent Streptavidin-Biotin Conjugates

GNeo-oligomers terminated with biotin (2.5 μM in PBS) were incubated with ST-PE-Cy5 (0.5 μM in PBS) for 20 min at ambient temperature then diluted with F-12 cell culture medium to give final conjugate solutions.

Cell Culture

Wild-type Chinese hamster ovary cells (CHO-K1) were obtained from the American Type Culture Collection (CCL-61). Cells were cultured at 37 °C under of 5% CO_2 in F-12 medium supplemented with fetal bovine serum (10% v/v, Gemini Bio-Products) and penicillin/streptomycin solution (1% v/v).

Cellular Uptake and Binding Studies

Cells were plated onto 24-well plates (100 000 cells/well) and grown for 24 h to about 80% confluence. For uptake studies, cells were washed with PBS and incubated with 300 μL of the corresponding compound for 1 h at 37 °C under an atmosphere of 5% CO_2. Cells were washed twice with PBS, detached with 50 μL of trypsin-EDTA, diluted with PBS containing 0.1% BSA, and analyzed by FACS. For binding experiments, cells were treated with 300 μL of the conjugate and incubated for 0.5 h at 4 °C under an atmosphere of 5% CO_2. Cells were washed twice with cold PBS, detached with 100 μL Versene (EDTA), diluted with PBS containing 0.1% BSA, and analyzed by FACS. Cellular uptake was quantified by the mean fluorescence intensity; raw data was interpreted by using FlowJo v8.8.6.

5.5 References

(1) Carton, J. M.; Strohl, W. R. In *Introduction to Biological and Small Molecule Drug Research and Development*; Jefferis, S. R., Ed.; Elsevier: Oxford, 2013, p 127.

(2) Kling, J. *Nature biotechnology* **2012**, *30*, 128.

(3) Ho, R. J.; Chien, J. Y. *Journal of pharmaceutical sciences* **2012**, *101*, 2668.

(4) Stanzl, E. G.; Trantow, B. M.; Vargas, J. R.; Wender, P. A. *Acc. Chem. Res.* **2013**, *46*, 2944.

(5) Wexselblatt, E.; Esko, J. D.; Tor, Y. *The Journal of Organic Chemistry* **2014**, *79*, 6766.

(6) Frankel, A. D.; Pabo, C. O. *Cell* **1988**, *55*, 1189.

(7) Green, M.; Loewenstein, P. M. *Cell* **1988**, *55*, 1179.

(8) Wender, P. A.; Mitchell, D. J.; Pattabiraman, K.; Pelkey, E. T.; Steinman, L.; Rothbard, J. B. *Proceedings of the National Academy of Sciences* **2000**, *97*, 13003.

(9) Wender, P. A.; Rothbard, J. B.; Jessop, T. C.; Kreider, E. L.; Wylie, B. L. *Journal of the American Chemical Society* **2002**, *124*, 13382.

(10) Luedtke, N. W.; Carmichael, P.; Tor, Y. *Journal of the American Chemical Society* **2003**, *125*, 12374.

(11) Maiti, K. K.; Jeon, O.-Y.; Lee, W. S.; Kim, D.-C.; Kim, K.-T.; Takeuchi, T.; Futaki, S.; Chung, S.-K. *Angewandte Chemie International Edition* **2006**, *45*, 2907.

(12) Futaki, S.; Nakase, I.; Suzuki, T.; Zhang; Sugiura, Y. *Biochemistry* **2002**, *41*, 7925.

(13) Chung, H. H.; Harms, G.; Seong, C. M.; Choi, B. H.; Min, C.; Taulane, J. P.; Goodman, M. *Biopolymers* **2004**, *76*, 83.

(14) Wender, P. A.; Kreider, E.; Pelkey, E. T.; Rothbard, J.; VanDeusen, C. L. *Organic Letters* **2005**, *7*, 4815.

(15) Wender, P. A.; Jessop, T. C.; Pattabiraman, K.; Pelkey, E. T.; VanDeusen, C. L. *Organic Letters* **2001**, *3*, 3229.

(16) Kolonko, E. M.; Kiessling, L. L. *Journal of the American Chemical Society* **2008**, *130*, 5626.

(17) Szwarc, M. *Nature* **1956**, *178*, 1168.

(18) Szwarc, M.; Levy, M.; Milkovich, R. *J. Am. Chem. Soc.* **1956**, *78*, 2656.

(19) Waack, R.; Rembaum, A.; Coombes, J. D.; Szwarc, M. *J. Am. Chem. Soc.* **1957**, *79*, 2026.

(20) Kolonko, E. M.; Pontrello, J. K.; Mangold, S. L.; Kiessling, L. L. *Journal of the American Chemical Society* **2009**, *131*, 7327.

(21) Hennig, A.; Gabriel, G. J.; Tew, G. N.; Matile, S. *Journal of the American Chemical Society* **2008**, *130*, 10338.

(22) Lienkamp, K.; Tew, G. N. *Chemistry – A European Journal* **2009**, *15*, 11784.

(23) Tezgel, A. Ö.; Telfer, J. C.; Tew, G. N. *Biomacromolecules* **2011**, *12*, 3078.

(24) Gabriel, G. J.; Madkour, A. E.; Dabkowski, J. M.; Nelson, C. F.; Nüsslein, K.; Tew, G. N. *Biomacromolecules* **2008**, *9*, 2980.

(25) Treat, N. J.; Smith, D.; Teng, C.; Flores, J. D.; Abel, B. A.; York, A. W.; Huang, F.; McCormick, C. L. *ACS Macro Lett.* **2012**, *1*, 100.

(26) Kim, Y.; Binauld, S.; Stenzel, M. H. *Biomacromolecules* **2012**, *13*, 3418.

(27) Cooley, C. B.; Trantow, B. M.; Nederberg, F.; Kiesewetter, M. K.; Hedrick, J. L.; Waymouth, R. M.; Wender, P. A. *Journal of the American Chemical Society* **2009**, *131*, 16401.

(28) Wender, P. A.; Huttner, M. A.; Staveness, D.; Vargas, J. R.; Xu, A. F. *Molecular Pharmaceutics* **2015**, *12*, 742.

(29) Bang, E.-K.; Ward, S.; Gasparini, G.; Sakai, N.; Matile, S. *Polymer Chemistry* **2014**, *5*, 2433.

(30) McKinlay, C. J.; Waymouth, R. M.; Wender, P. A. *J Am Chem Soc* **2016**, *138*, 3510.

(31) Tezgel, A. O.; Gonzalez-Perez, G.; Telfer, J. C.; Osborne, B. A.; Minter, L. M.; Tew, G. N. *Mol Ther* **2013**, *21*, 201.

(32) Geihe, E. I.; Cooley, C. B.; Simon, J. R.; Kiesewetter, M. K.; Edward, J. A.; Hickerson, R. P.; Kaspar, R. L.; Hedrick, J. L.; Waymouth, R. M.; Wender, P. A. *Proceedings of the National Academy of Sciences* **2012**, *109*, 13171.

(33) Elson-Schwab, L.; Garner, O. B.; Schuksz, M.; Crawford, B. E.; Esko, J. D.; Tor, Y. *J Biol Chem* **2007**, *282*, 13585.

(34) Dix, A. V.; Fischer, L.; Sarrazin, S.; Redgate, C. P. H.; Esko, J. D.; Tor, Y. *Chembiochem* **2010**, *11*, 2302.

(35) Inoue, M.; Tong, W.; Esko, J. D.; Tor, Y. *ACS Chem. Biol.* **2013**, *8*, 1383.

(36) Sarrazin, S.; Wilson, B.; Sly, W. S.; Tor, Y.; Esko, J. D. *Mol Ther* **2010**, *18*, 1268.

(37) Choi, T. L.; Grubbs, R. H. *Angew. Chem., Int. Ed.* **2003**, *42*, 1743.

(38) Yang, S. K.; Weck, M. *Macromolecules* **2008**, *41*, 346.

(39) Burtscher, D.; Saf, R.; Slugovc, C. *Journal of Polymer Science Part A: Polymer Chemistry* **2006**, *44*, 6136.

(40) Ambade, A. V.; Yang, S. K.; Weck, M. *Angewandte Chemie International Edition* **2009**, *48*, 2894.

(41) Gordon, E. J.; Gestwicki, J. E.; Strong, L. E.; Kiessling, L. L. *Chemistry & Biology* **2000**, *7*, 9.

(42) Gibson, V. C.; Okada, T. *Macromolecules* **2000**, *33*, 655.

(43) Matson, J. B.; Grubbs, R. H. *Macromolecules* **2010**, *43*, 213.

(44) Mangold, S. L.; Carpenter, R. T.; Kiessling, L. L. *Organic Letters* **2008**, *10*, 2997.

(45) Gilmore, J. M.; Scheck, R. A.; Esser-Kahn, A. P.; Joshi, N. S.; Francis, M. B. *Angewandte Chemie International Edition* **2006**, *45*, 5307.

(46) Kim, S. H.; Jeong, J. H.; Ou, M.; Yockman, J. W.; Kim, S. W.; Bull, D. A. *Biomaterials* **2008**, *29*, 4439.

(47) Kim, S. H.; Jeong, J. H.; Kim, T.-i.; Kim, S. W.; Bull, D. A. *Molecular Pharmaceutics* **2009**, *6*, 718.

(48) Tabujew, I.; Freidel, C.; Krieg, B.; Helm, M.; Koynov, K.; Müllen, K.; Peneva, K. *Macromolecular Rapid Communications* **2014**, *35*, 1191.

(49) deRonde, B. M.; Torres, J. A.; Minter, L. M.; Tew, G. N. *Biomacromolecules* **2015**, *16*, 3172.

(50) Wang, D.; Fan, J.; Gao, X.; Wang, B.; Sun, S.; Peng, X. *The Journal of Organic Chemistry* **2009**, *74*, 7675.